1-1-1992

Phase behavior and transreaction studies of model polyester/ bisphenol-A-polycarbonate blends/

Jeffrey S. Kollodge
University of Massachusetts Amherst

PHASE BEHAVIOR AND TRANSREACTION STUDIES OF MODEL POLYESTER/BISPHENOL-A-POLYCARBONATE BLENDS

A Dissertation Presented

by

JEFFREY S. KOLLODGE

Submitted to the Graduate School of the
University of Massachusetts in partial fulfillment
of the requirements for the degree of

DOCTOR OF PHILOSOPHY

September 1992

Polymer Science and Engineering

PHASE BEHAVIOR AND TRANSREACTION STUDIES OF MODEL POLYESTER/BISPHENOL-A-POLYCARBONATE BLENDS

A Dissertation Presented

by

JEFFREY S. KOLLODGE

Approved as to style and content by:

Roger S. Porter, Chair

C. Peter Lillya, Member

William J. MacKnight, Member

William J. MacKnight, Department Head
Polymer Science and Engineering

DEDICATION

To Mom & Dad, Vicky, Steve, Dan, Mary and Ann;
all of you in your own way have inspired me.

ACKNOWLEDGMENTS

As I type these final words of this dissertation (the acknowledgements having been saved for last), it is hard to believe that nearly five years have past and another chapter of my life has come to a close. I came to graduate school with many expectations and many goals. Although these expectations and goals did not quite match what the real world has had to offer, my years at U-Mass have been one of the most enriching experiences of my life. During these years, I have grown much more as a person and as a student than I ever thought possible. Much of that growth is due to the students and faculty that I have had the privilege to be associated with. There are many "Thank yous!" due and I begin by thanking the faculty and staff.

I thank my advisor Dr. Porter for his scientific and personal support over these years. Most importantly, I thank him for giving me the freedom, flexibility and encouragement to pursue research in my own way. I also would like to thank my committee members Dr. Lillya and Dr. MacKnight for their helpful discussions, comments and suggestions during the course of my research. I owe a very special thanks both professionally and personally to Dr. Dickinson. He has inspired me to take a subject that I previously had no interest in (NMR spectroscopy) and make it the crux of my research. He has taught me much and has brought new meaning to the word "rich". I wish to thank Norm Page, John Domain and Jay Conway for coming to the rescue whenever equipment problems threatened to burst the "bubble of science". Their friendship has also been appreciated over the years. Thank you Chris, Carol and Sophie. Although your administrative efforts often occur behind the scenes, they have not gone unnoticed. The final staff member I would like to thank is Eleanor Thorpe. She has withstood my constant interruptions for computer time, pilfering of the candy dish, and the brunt of my taste for bad humor. She is a special friend.

The students I have met at U-Mass are one of the most diverse group of people I have ever been associated with. With that diversity comes a very unique synergy which makes the department special. There are many students who helped me reach this point. I would like to thank Howard Creel, Tim Bee and Brant Kolb for answering any and all chemistry questions I presented to them, teaching me proper chemistry techniques and training me to use various analytical equipment. Gregg Bennett and Scott Joslin deserve thanks for

providing help with questions/training on DuPont thermal analysis equipment. Past members of Dr. Porters group; Matt Muir, Kevin Schell, and Bob Karcha also helped train me in on various pieces of equipment and provided moral support during those difficult early cumes.

Perhaps the most important thing to come out of my time at U-Mass is the close friendships that developed and I thank all of you who helped me through the ups and downs of grad school. Some of you deserve special recognition and I will try to encapsulated many "moments" into a few sentences. Warren Nachlis is the only person I know who questions what he is doing with his life and why he is doing it , as much, if not more than I do. Our questioning of life often occurred with a fermented or distilled beverage in hand, hence, there were numerous mornings when I wished I had never met Warren. Two aspirins and a couple hours of extra sleep usually changed my disposition and helped me appreciate this unique friendship.

The Running Radicals intramural basketball team was also a source of many "moments". Howard Creel, Gregg Bennett, Tim Bee, Chris Haak, Kevin Schaffer and myself became a closely knit squad of highly talented hoop players who compiled a record of 11-2 in two seasons of intramural play (there is some truth to this statement, the 11-2 record). Most of the squad has accepted jobs at 3M, thus, U-MASS WEST will debut in the 92-93 intramural season. A special thanks to all you Running Radical fans, come catch us in Minnesota.

The squad also compiled quite a record at the poker table where we all seemed "Born to Run" up our gambling debt. Often joining us at the table were Mark and Jayne Dadmun. Perhaps the most dynamic couple I know (maybe it's the homebrew), I hope they give "The Great White North" a look see when they finish their D.C. experience. Scott Joslin and I became good friends in the confines of Mike's Billiards. I don't know if I'll ever be able to stop laughing the day Florida excepts at 3M. Other times stand out , golf games and lab reports with Howard, Mardi Gra with Gregg and Tony, the U-Mass post season hoop run ending in Madison Square Garden with the T.V. debut for many of us on ESPN, 1047 parties, "being stupid" as Elmer so eloquently put it, numerous Panda excursions, and harassment by the ladies of the 8th floor - Ann Jacob, Luisa Cabrera, Marianne Yarmey and Susan Dawson to be named specifically in the lawsuit. Thank you all for making U-Mass the experience it turned out to be. Marianne and Ann, thanks for all your help at the defense.

I thank my parents and family for the love and support they have given me throughout my life and during these past five years. I also want to thank my fiancée Ann, for all her love and encouragement during this these past 14 months. Hon, you're the "bestest!" Finally, I would like to thank God for giving me the talents and perseverance to complete this endeavor and for blessing me with what truly is a wonderful life.

ABSTRACT

PHASE BEHAVIOR AND TRANSREACTION STUDIES OF MODEL POLYESTER/BISPHENOL-A-POLYCARBONATE BLENDS

SEPTEMBER 1992

JEFFREY S. KOLLODGE, B.S., UNIVERSITY OF MINNESOTA

M.S., UNIVERSITY OF MASSACHUSETTS

Ph.D., UNIVERSITY OF MASSACHUSETTS

Directed by: Professor Roger S. Porter

The goal of this thesis is to quantitatively study the relationship between interchange reaction and blend phase behavior in polyester/bisphenol-A-polycarbonate (PC) blends. Before transreaction studies are conducted, equilibrium phase behavior prior to reaction is identified and used as a basis to judge the reacting blends. To facilitate all of these studies, poly(2-ethyl-2-methyl-1,3-propylene terephthalate) (PEMPT) has been selected as a model polyester for blends with PC. PEMPTs having M_ns from 4,100-37,500 g/mol were synthesized and fully characterized by a variety of elemental, spectroscopic and thermal analysis techniques. In addition, PEMPT was end capped to produce samples having heptafluorobutyrate (HFB) and benzylate (BNZ) end groups. These end capped samples exhibit different thermal characteristics compared to the hydroxyl (OH) terminated PEMPTs.

Blends of PEMPT with PCs having M_ns of 11,000 and 21,000 g/mol were prepared by solution casting techniques. Equilibrium phase behavior studies were conducted as a function of blend composition, molecular weight and end group type. In most cases, PEMPT/PC blends exhibited partial miscibility, which was monitored by the shifting of glass transition temperatures as measured by DSC. Blend composition had little effect on the phase behavior. Molecular weight reduction lead to improved intermixing between components for the OH and BNZ terminated PEMPTs. No improvement in the degree of intermixing was observed with decreasing M_n in the HFB terminated PEMPT/PC blends.

Detailed ^{1}H NMR spectroscopy enabled the identification of separate resonances corresponding to direct midchain and alcoholysis interchange reactions in PEMPT/PC non-stabilized blends. It was found that transreaction of

~ 4% of the terephthalate groups was required to shift the phase behavior from two phase to single phase in a PEMPT/PC 50/50 wt. % blend of high molecular weight. This reaction extent represented 2.8% alcoholysis and 1.2% direct midchain reaction. These results were in agreement with calculations based on simplified models of the reacting blend. Alcoholysis exchange reaction was also observed at varying degrees in stabilized blends. Complete alcoholysis lead to the formation of single phase blends at low PEMPT molecular weights.

TABLE OF CONTENTS

LIST OF TABLES

LIST OF FIGURES

CHAPTER 1

INTRODUCTION

1.1 Thesis Scope

This thesis presents research focusing on the phase behavior of polyester/polycarbonate blends. The motivation behind this work is centered on the ability of polyester/polycarbonate blends to undergo interchange reaction between the ester and carbonate functional groups. Interchange reaction, often called transreaction or exchange reaction, has pronounced effects on the phase behavior of these systems. Initially, transreaction leads to the formation of block copolymers. If reaction is extensive, random copolymers result from the original homopolymer pair. The homogenizing effect associated with the formation of these block/random copolymers transforms a two phase blend into a miscible system. The significance of this statement should not be overlooked. With the phase behavior of a blend system being a key factor in relation to its exhibited mechanical properties, any variable that can alter the degree of miscibility becomes critically important. Interchange reaction is thus a means of modifying the phase behavior and, hence, the overall properties of the blend.

With respect to their ability to transreact, blends containing bisphenol-A polycarbonate (PC), poly(ethylene terephthalate) (PET), poly(butylene terephthalate) (PBT) and polyarylate (PAr) have received much academic and industrial attention [1-23]. It is for this reason that polymers of this type have been chosen for study. From a qualitative perspective, blends of PET/PC, PBT/PC and PAr/PC and others of this nature have all been shown to undergo interchange reaction modifying their phase behavior [1-8]. However, no attempt has been made to obtain a quantitative understanding of the extent and type of transreaction and its effect on blend phase behavior. The thermodynamics of the reacting system have also largely been ignored. The goal of this thesis is to quantitatively relate exchange reaction to the observed phase behavior of the blend and to obtain a thermodynamic understanding of the blend system under investigation. Extensive studies are first carried out on non-reacted blends to gain this thermodynamic foundation and to obtain a basis on which to judge the

effect of interchange reactions. The role of end group structure on blend miscibility is also examined, as end capping techniques may be one method employed to prevent end group transreactions. Additionally, studies into the role of direct midchain reaction vs. end group reaction (alcoholysis) are conducted.

The above mentioned blends, which are all capable of transreaction, offer challenges uncommon to most other blend systems. Before one can study the effect of interchange reaction, knowledge of the phase behavior prior to reaction is required. Due to their ability to transreact, this information can only be obtained if exchange reaction is very slow relative to the equilibrium kinetics of phase separation. Often, the catalyst used in the synthesis of the polymers, particularly the polyester's, is capable of causing transreaction between blend components [9-11], making equilibrium phase behavior studies difficult. This problem can be circumvented by the addition of inhibitors to the blend system [9,11,24-27]. Other factors that can complicate the study of blends containing PET and PBT is the insolubility of these polyesters to most solvents caused by their ability to crystallize. Insolubility creates difficulties in blend preparation characterization and analysis. Crystallization often hinders the clear identification of the amorphous regions [6,8,28,29] and complicates the thermodynamics with the formation of this additional phase. These inherent difficulties point to the use of a model polyester to replace PET and PBT in blends with PC. It is this approach which is used to facilitate the transreaction studies presented herein.

The model polyester should have the following properties: Structural similarity to PET and PBT, amorphous or slow to crystallize, soluble in common solvents, glass transition temperature (T_g) well separated from that of PC, form a two phase system when blended with PC, and be thermally stable at the temperatures required for exchange reaction. After a screening study which examined four polyesters, the polyester which best fit the above requirements is poly(2-ethyl-2-methylpropylene terephthalate) (PEMPT). PEMPT is used in all subsequent polyester/PC blend studies.

With the selection of the polyester, this thesis proceeds in a straight-forward manner. Chapter 2 details the screening study mentioned above. Chapter 3 discusses the synthesis of PEMPT of varying molecular weights, end capping procedures and characterization of the polymers. Chapter 4 describes the equilibrium phase behavior studies with composition, molecular weight and

end group type as variables. Chapter 5 examines the effect of direct midchain and end group transreaction on phase behavior and provides a detailed proton NMR analysis of the transreacting systems. Chapter 6 concludes with an overall summary of results and a discussion of related future work.

1.2 References

1. Huang, Z.H.; Wang L.H. *Makromol. Chem., Rapid Commun.* **1986**, 7, 255.

2. Wang, L.H.; Huang, Z.; Hong, T.; Porter, R.S. *J. Macromol. Sci. Phys.* **1990**, B29, 155.

3. Kimura, M.; Porter, R.S. in *Analytical Calorimetry*; edited by P. Gill and J.F. Johnson, Plenum Press: New York, 1984.

4. Birley, A.W.; Chen, X.Y. *Br. Polym. J.* **1984**, 16, 77.

5. Kimura, M.; Porter, R.S. *J. Polym. Sci., Polym. Phys. Ed.* **1983**, 21, 367.

6. Kimura, M.; Salee, G.; Porter, R.S. *J. Appl. Polym. Sci.* **1984**, 29, 1629.

7. Suzuki, T.; Tanaka, H.; Nishi, T. *Polymer* **1989**, 30, 1287.

8. Robeson, L.M. *J. Appl. Polym. Sci.* **1985**, 30, 4081.

9. Devaux, J.; Godard, P.; Mercier, J.P. *Polym. Eng. Sci.* **1982**, 22, 229.

10. Devaux, J.; Godard, P.; Mercier, P., *J. Polym. Sci., Polym. Phys. Ed.* **1982**, 20, 1901.

11. Godard, P.; Dekoninck, J.M.; Devlesaver, V.; Devaux, J., *J. Polym. Sci., Polym. Chem.* **1986**, 24, 3315.

12. Golovoy, A.; Cheung, M.-F.; Carduner, K.R.; Rokosz, M.*J. Polym. Eng. Sci.* **1989**, 29, 1226.

13. Devaux, J.; Godard, P.; Mercier, P. *J. Polym. Sci., Polym. Phys. Ed.* **1982**, 20, 1875.

14. Devaux, J.; Godard, P.; Mercier, P.; Touillaux, R.; Dereppe, J.M. *J. Polym. Sci., Polym. Phys. Ed.* **1982**, 20, 1881.

15. Devaux, J.; Godard, P.; Mercier, P. *J. Polym. Sci., Polym. Phys. Ed.* **1982**, 20, 1895.

16. Pilati, F.; Marianucci, E.; Berti, C. *J. Appl. Polym. Sci.* **1985**, 30, 1267.

17. Godard, P.; Dekoninck, J.M.; Devlesaver, V.; Devaux, J. *J. Polym. Sci., Polym. Chem.* **1986**, 24, 3301.

18. Velden, G.v.d, Kolfschoten-Smitsmans, G.; Veermans, A. *Polym. Commun.* **1987**, 28, 169.

19. Valero, M.; Iruin, J.J.; Espinosa, E.; Fernandez-Berridi, M.J. *Polym. Commun.* **1990**, 31, 127.

20. Henrichs, P.M.; Tribone, J.; Massa, D.J.; Hewitt, J.M. *Macromolecules* **1988**, 21, 1282.

21. Golovoy, A.; Cheung, M.-F.; Van Oene, H. *Polym. Eng. Sci.* **1987**, 27, 1642.

22. Wang, L.H.; Lu, M.; Yang, X.; Porter, R.S. *J. Macromol. Sci. Phys.* **1990**, B29, 171.

23. Mondragon, I. J. *Appl. Polym. Sci.* **1986**, 32, 6191-6207.

24. Kurashiki Rayon Kabushiki Kaisha, Japanese Patent 1,060,401.

25. Carduner, K.R.; Carter III, R.O.; Cheung, M.-F.; Golovoy, A. *J. Appl. Polym. Sci.* **1990**, 40, 963-975.

26. Cheung, M.-F.; Carduner, K.R.; Golovoy, A.; Van Oene, H. *J. Appl. Polym.* Sci. **1990**, 40, 977-987.

27. Delimoy, D.; Bailly, C.; Devaux, J.; Legras, R. *Polym. Eng. Sci.* **1988**, 28, 104-112.

28. Hanrahan, B.D.; Angeli, S.R.; Runt, *J. Polym. Bull.* **1986**, 15, 455-463.

29. Yuan, L.; Williams, H.L. *J. Appl. Polym. Sci.* **1990**, 40, 1891-1902.

CHAPTER 2

SCREENING STUDY: SELECTION OF THE MODEL POLYESTER

2.1 Introduction

This chapter discusses the screening study conducted to select a polyester that best fits the criteria for the model polyester described in Chapter 1. The goal of this study is not to be a detailed analysis of many polyesters and their blends with PC. Hence, characterization of the polyesters and the analysis of the corresponding blends is minimal. Only the information required to make appropriate comparisons is determined. As a consequence, the opportunity arises to present a brief review of the role of transreaction in polyester synthesis.

2.2 Transreaction in Polyester Synthesis

The basic aspects of polyester synthesis can be found in most polymer textbooks or reviews [1-7], hence, all the generalities will not be presented here Instead, discussion will focus on specific aspects of transreaction during the synthesis of polyesters such as PET and PBT. These two polymers are often synthesized by a standard two stage polycondensation technique used in the production of a wide variety of polyesters [1-6]. This two stage polycondensation procedure employs transreaction in both steps. A typical example is shown in Figure 2.1a with the formation of bis(2-hydroxyethyl) terephthalate (BHET) from dimethyl terephthalate (DMT) and ethylene glycol (EG). This example typifies an alcoholysis transreaction with reaction occurring between the alcohol and ester functional groups. The equilibrium is shifted to the right by continuous removal of methanol. The reaction shown in Figure 2.1a is the first step in the two stage synthesis of PET. After all the methanol is removed, increasing the temperature and applying vacuum signifies the beginning of the second stage of polymerization.

During this step, Figure 2.1b, high molecular weight polymer is formed through the continuous alcoholysis reactions at the 2-hydroxyethylene

a)

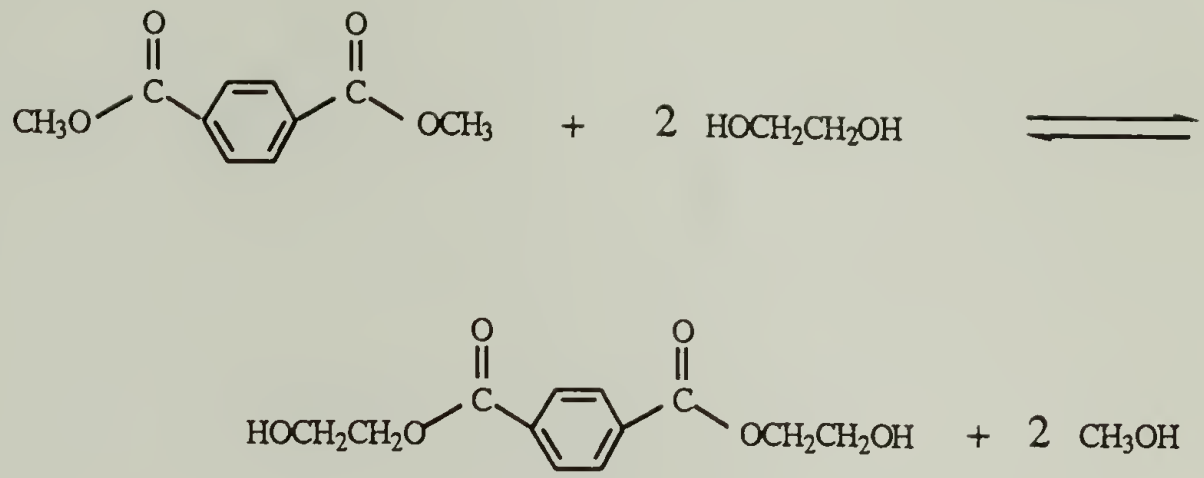

b)

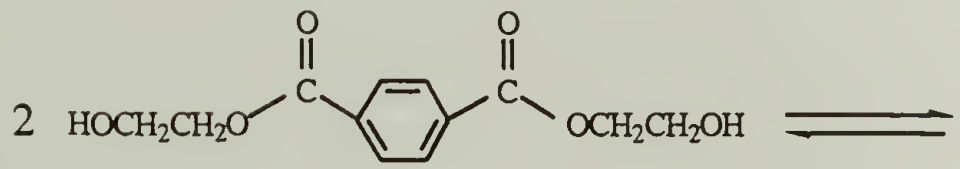

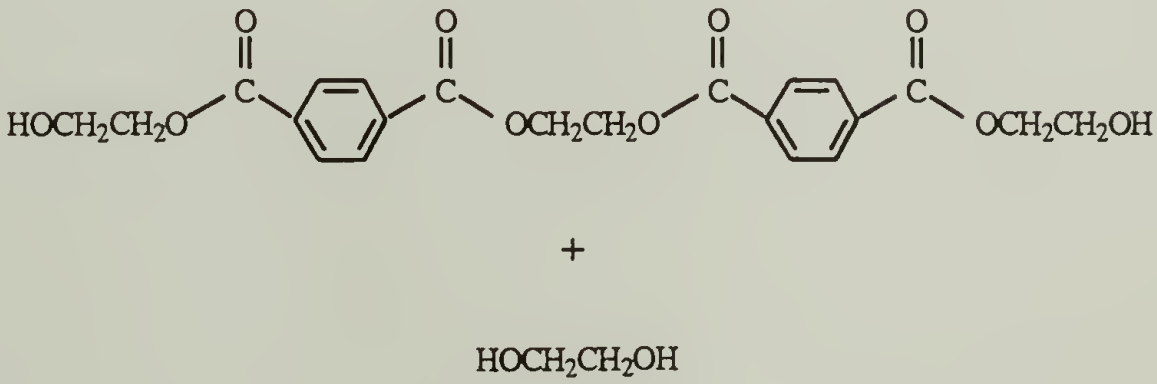

+

HOCH2CH2OH

Figure 2.1 Synthesis of PET a) 1st stage reaction, formation of BHET b) 2nd stage reaction, alcoholysis of 2-hydroxy ethylene terephthalate end.

terephthalate ends. It is important to note that high molecular weight polymer will only be formed if a volatile by-product can be removed, in this case ethylene glycol. Any alcoholysis reactions occurring at a midchain ester group or any direct midchain reaction between two ester groups will not produce a volatile leaving group. These type of interchange reactions merely "randomize" the mixture and do not cause an increase in the polymers molecular weight. In addition to direct midchain and alcoholysis, a third type of exchange reaction exists, acidolysis. Often during the polymerization of polyesters, trace amounts of moisture in the reaction mixture or decomposition reactions can lead to the formation of small amounts of acid end groups [8-13]. Acid end groups are also capable of undergoing interchange reactions [1,12,14]. Kotliar [7], has reviewed these important reactions; intermolecular acidolysis, intermolecular alcoholysis and direct midchain transreaction, schematically diagrammed in Figure 2.2a-c. It is these same exchange reactions that can "randomize" a blend system when both components are capable of transreaction.

Studies of the kinetics of polyester synthesis can be divided into two broad categories based on the two stages of the polymerization. Investigations on the first stage of reaction (Figure 2.1a) are often called "transreaction" studies and the catalysts employed "transreaction" or "transesterification" catalysts. Second stage reaction studies (Figure 2.1b) are usually termed "polycondensations" with associated "polycondensation" catalysts. This nomenclature is somewhat misleading with both reactions involved being transreactions, specifically alcoholysis exchange reactions. To avoid any confusion with later discussions on transreactions between blend components, the two synthesis reactions described above will simply be identified as "first stage" and "second stage", respectively.

Early studies on the kinetics of the first stage reaction are inconclusive in regards to the reaction order. Peebles and Wagner use a consecutive 2nd order reaction scheme (1st order in DMT and EG concentrations) to analyze the kinetics and found fair agreement [15]. Using the same data, analysis was carried out applying a first order reaction scheme. The experimental results were also in fair agreement with this model. Peebles and Wagner concluded that the high initial concentrations of EG used during their studies could lead to a pseudo first order reaction mechanism. Later studies by Fontana [16] and Tomita and Ida [17] identified the reaction as third order overall, 1st order with respect to DMT, EG and catalyst concentration. A coordination type mechanism

a)

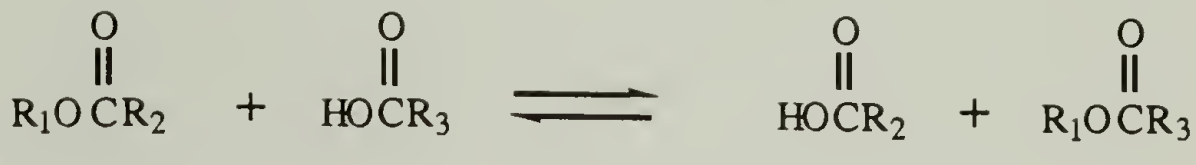

b)

c)

Figure 2.2 Schematic diagram of interchange reactions a) acidolysis b) alcoholysis and c) direct midchain transreaction.

between the catalyst and carbonyl, activating the carbonyl carbon for nucleophilic attack, has been proposed [18]. The ability of various metals to complex with a model carbonyl compound has been correlated to their observed catalytic activity during first stage synthesis [18], adding credibility to the coordination type mechanism.

In regards to catalyst activity, catalyst that function well in the first stage of reaction may not be adequate for the second stage of polymerization. Hovenkamp concluded that the metal acetate catalysts of Mn, Pb(II), PB(IV), Zn and Ca perform well in the environment with high hydroxyl concentration (1st stage), but their activity diminishes during the second stage of polymerization where they are deactivated by the small amount of acid end groups formed [19]. He also noted that antimony catalysts function poorly during the first stage of reaction (high hydroxyl concentration), but work well in the 2nd stage of reaction where the hydroxyl concentration is being continuously lowered. The antimony catalysts were uneffected by the presence of acid end groups. Use of combinations of these catalyst is necessary for optimum polymerization rates. Titanium catalysts have also been found to be excellent first stage reaction catalysts and have higher overall reaction rates compared to a commonly used catalyst, calcium acetate [20]. Between three Ti catalyst studied, titanium isopropoxide was found to be superior on the basis of having the highest overall reaction rate [20].

Several 2nd stage reaction studies have examined the principle of equal reactivity of the 2-hydroxylethylene terephthalate ends [16,19,21,22]. Conclusions of Challa [21] proposed that equal reactivity does not hold, with K_{eq} (of the reaction depicted in Figure 2.1b) increasing from approx. 0.4-1.1 with extent of reaction. Fontana has challenged this data, indicating that Challa did not account for the presence of acid end groups which would modify the calculation of the actual extent of reaction [16]. Fontana's studies have determine K_{eq} to be 0.5 (hydroxyl groups of EG twice as reactive as the 2-hydoxylethylene terephthalate end groups) and that equal reactivity of the 2-hydoxylethylene terephthalate end groups holds. Similar values for K_{eq} have been reported by Hovenkamp [19]. A recent study by Yu, et al., has again questioned the premise of equal reactivity in the PET system [22]. However, their molecular weight data is in full agreement with the Flory most probable distribution, seemingly contradicting their kinetic data. They reason that direct ester interchange or alcoholysis of midchain ester groups may lead to the most

probable distribution, even if the principle of equal reactivity does not hold. In the same study, Yu, et al., also examined a PBT system and found equal reactivity to hold.

Pilati, et al., have also conducted kinetic studies on the 2nd stage reaction of a PBT system using model compounds [23]. Making the assumption that the reaction is first order with respect to hydroxyl and ester concentration, they have identified the reaction order with respect to the titanium catalyst used. They found a reaction order of 0.9 which agrees with 1st stage reaction studies [16,17]. Their kinetic findings are also in agreement with a coordination type reaction mechanism between the catalyst and ester carbonyl. This model gave a 1st order dependence on catalyst. Another model which assumes basic catalysis (ionic mechanism) calculates the reaction order with respect to catalyst to be 0.5. The overall conclusion of the study is that the reaction is most likely to follow a coordination mechanism, but the ionic pathway can not be totally ruled out. In a study which examined the effect of varying catalyst type on the 2nd stage reaction of BHET, titanium isopropoxide was found to be superior in regards to minimizing the number of acid end groups formed compared to other Ti catalysts and Sb_2O_3 [20]. All the catalyst studied were found to produce nearly equivalent molecular weight PETs. One final point to be made about 2nd stage transreactions, most of the studies discussed above were carried out in the melt state. Solid state polymerizations to increase molecular weight have been reported in a catalyzed PBT system [24] and on a catalyst free PET [25]. The mechanism appears to be diffusion controlled reaction of the hydroxyl groups.

2.3 Synthesis and Characterization of PPT, PHT, PNT and PEMPT

Before the experimental aspects of the synthesis are detailed, the logic behind the selection of the four polyesters to be synthesized should be mentioned. Narrowing down the field of possible polyesters began with the requirement that only polyesters with similar structure to PET and PBT be considered. This immediately required an aliphatic-aromatic polymer. The terephthalate group is characteristic of both PET and PBT, thus, it was not modified. With this restriction, the only allowable structure changes occurred in the aliphatic sequence. It is well known that aliphatic-terephthalate polyesters with an odd number of main chain methylene groups (particularly those with 5

or greater) have improved solubility, and slower crystallization rates than their even numbered counterparts [6]. They also have T_gs well separated from PC [26,27]. The three polyesters, poly(1,5-pentylene terephthalate (PPT), poly(1,7-heptylene terephthalate (PHT) and poly(1,9-nonylene terephthalate) (PNT) appear to meet the initial requirements, thus, they were synthesized and studied in blends with PC. Additionally, poly(2-ethyl-2-methylpropylene terephthalate) (PEMPT) was synthesized and studied. With it's 2-ethyl-2-methyl substitution, PEMPT can form an atactic structure, assuming the propylene group is incorporated into the polymer in random fashion. The formation of an atactic structure yields an amorphous polyester and the corresponding absence of crystallinity produces improved solubility compared to PET and PBT.

2.3.1 Monomers and Catalyst

Diols; 1,5 pentanediol (Aldrich 97%), 1,7 heptanediol (Aldrich 95%), 1,9 nonanediol (Aldrich 98%) and 2-ethyl-2-methyl-1,3-propanediol (EMPD) (Aldrich 98%) for the synthesis of PPT, PHT, PNT, PEMPT were vacuum distilled prior to polymerization. Distillation temperatures were between 90-125°C and an applied vacuum between 0.5-2.0 mm Hg, depending on the diol. Due to its low purity level, PHT was dried over magnesium sulfate prior distillation. Dimethyl terephthalate (DMT) (Aldrich 99+%) was purified by a recrystallization procedure which will be described in detail in the proceeding chapter. With the benefits of being both a 1st and 2nd stage catalyst and the ability to minimize acid end group formation, titanium (IV) isopropoxide (Aldrich) was selected as catalyst. It was used as received for all the polymerizations.

2.3.2 Polymerization

The polymerization of the four polyesters followed the general procedure described in the synthesis of PBT [10,28]. The apparatus used and the specific procedure is described below. A 100 mL trap tube served as the reactor. During the first stage of polymerization, the reactor tube outlet was connected to a cold trap (dry ice/ethanol) for methanol collection. To aid in the removal of methanol during the first stage of reaction, the tube was continuously flushed with nitrogen, approx. 120 mL/min via the tube inlet. Stirring of the reaction mixture was achieved with an oval magnetic stir bar placed in the reactor tube.

A mineral oil bath and a hot plate were used for heating. The oil bath was contained in a 2000 mL beaker which had been cut down to 1800 mL. This allowed the majority of the reactor tube to be submersed while facilitating magnetic stirring inside the tube. The oil bath was fitted with mechanical stirring and a thermometer for monitoring the oil temperature. During the second stage of reaction, a heated vacuum line at 70°C was connected to the trap outlet. The heated line was required to prevent diol from crystallizing in the outlet. A cold trap (dry ice/ethanol) was connected between the vacuum line and the vacuum pump.

All polymerizations started with 4-7 g DMT and the appropriate amount of diol (50% mol excess) being placed in the reactor. The tube was then sealed and flushed with nitrogen for 10 min followed by submersion into the oil bath preheated to 200°C. When both components had melted and were thoroughly mixed, the nitrogen line was removed briefly and the appropriate amount of catalyst was injected into the mixture via a 10 µL syringe. Titanium (IV) isopropoxide was used at a 0.001 g/1 g catalyst/DMT ratio. First stage reactions were conducted for 1 1/2 h at temperatures from 195-205°C. At the end of this time, the temperature was gradually raised to approx. 250°C. The nitrogen line was removed and the inlet plugged. Vacuum was applied marking the beginning of the second stage of reaction. Second stage reactions were conducted under vacuum, 0.6-1.0 mm Hg, at temperatures ranging from 247-253°C, for two hours. When the end of the reaction was reached, the reactor tube was removed from the oil bath and placed under cold water. Excess EMPD and oligomers that had crystallized on the tube walls were removed by rinsing with 10 mL of chloroform (Fisher, spec. grade).

The polyesters were removed from the reactor tube by dissolving them into 75 mL of chloroform. The solution was filtered through a 25-50 µm fritted glass funnel. The polymers were precipitated dropwise into 350-400 mL of vigorously mixed methanol. The recovered samples were washed with 2 x 100 mL aliquots of fresh methanol followed by drying under vacuum for several days at 75°C.

2.3.3 Characterization

Characterization consisted of thermal analysis, specifically, differential scanning calorimetry (DSC) and thermogravimetric analysis (TGA). A Perkin-

Elmer DSC-4 with a System 4 Thermal Analysis Microprocessor Controller and a Thermal Analysis Data Station was used to determine the T_gs and crystallization data. A dry ice/ethanol slurry was used for subambiant cooling. Indium was the calibration standard and scanning auto zero (SAZ) was used during the actual runs. Sample size was 6-8 mg and reported T_gs are midpoint values determined from a single heating run. The thermal program was as follows: load samples at 20°C, heat @ 100°C/min to 200°C, quench to -40°C, scan @ 20°C/min to 200°C. The rapid quenching from 200°C to -40 °C simulated the expected quench to be used during blend studies. Phase behavior identification requires clear, distinguishable T_gs and the rapid quench should prevent/minimize crystallization.

Thermogravimetric analysis was carried out in a Perkin-Elmer TGS-2 with a System 4 Thermal Analysis Microprocessor Controller and a Thermal Analysis Data Station. Nitrogen at ~ 45 mL/min was used as a purge gas. Calibration was conducted using four ferromagnetic standards; Alumel, Nickel, Nicoseat and Perkalloy. All heating scans were conducted at 20°C/min A sample size of approx. 5 mg was used. The reported decomposition temperature, T_d, represents the temperature at which the maximum rate of weight loss occurred.

2.3.4 Results and Discussion

Table 2.1 summarizes the DSC and TGA data of the polyesters. The T_gs of PPT, PHT and PNT agree with those reported by Smith, et. al [26]. It is observed that the three polyesters with linear aliphatic sequences were all able to crystallize to some extent even with the rapid quench. Some of this crystallization occurred during the actual heating scan once the temperature was above the polyester T_g. In general, the reported melting temperatures, which are peak temperatures, are slightly lower than those reported by Smith [26]. However, during the current experiment, the goal was to minimize the crystallization. No attempt was made to enhance the amount of crystallization obtained or improve crystal perfection. These factors are most likely responsible for the discrepancies and the current data should be examined within this context. It is slightly disappointing that all the linear aliphatic polyesters crystallized to some extent under these minimizing conditions.

Table 2.1 Thermal Analysis Data of PPT, PHT, PNT and PEMPT

Polyester	T_g (°C)	T_m (°C)	ΔH_f (cal/g)	T_d* (°C)
PPT	14	129	7.5	421
PHT	4	88, 95	0.3	422
PNT	-1	90, 96	10.9	422
PEMPT	63	-	-	461

* Temperature of the maximum rate of thermal decomposition.

However, it is seen that PEMPT exhibited a T_g at 63°C and appears to be completely amorphous. This point will be discussed further in Chapter 3.

The TGA data shows marked differences in the maximum rate of decomposition, T_d, between the linear aliphatic polyesters and PEMPT. Comparing the T_d of PEMPT to that of PPT, PHT and PNT, a 40°C increase in the decomposition temperature of PEMPT is observed. The removal of all beta hydrogens in PEMPT eliminates a common mechanism of decomposition of aliphatic-aromatic esters similar to the Chugaev reaction [29,30]. This mechanism involves the formation of a cyclic intermediate incorporating the beta hydrogens and the carbonyl, followed by decomposition to acid and alkene end groups. The stability of esters has been shown to decrease as the number of β-hydrogens increases [31]. Thus, the replacement of the beta hydrogens in PEMPT by ethyl-methyl substitution has produced a more thermally stable polyester. With the thermal characterization completed, the remaining criteria to be evaluated is the phase behavior of the polyesters with PC.

2.4 Blends of PPT, PHT, PNT and PEMPT with PC

2.4.1 Blend Preparation

The polymers used for the blend study are the four polyesters described above and a bisphenol-A polycarbonate, PC2. The polycarbonate was obtained from the General Electric Company. It contained no additives. Presently, the only necessary characterization data of PC2 is its glass transition temperature at the previously used scanning rate. This was measured to be 149.3°C. Characterization of PC2 is discussed in Chapter 3.

Blend preparation followed two techniques. One was a codissolution/precipitation procedure. One half gram of polyester and polycarbonate were dissolved in chloroform (5% w/v). After mixing, they were recovered by dropwise precipitation into 100 mL of vigorously stirred methanol. The recovered polymers were washed with 2 x 25 mL of fresh methanol followed by vacuum drying @ 70°C for 12 h. The other preparation method was a solution casting technique. One half gram of polyester and polycarbonate were dissolved in chloroform (5% w/v). The chloroform contained a small amount of dioctadecyl phosphite (DNOP) such that it was in a theoretical 5/1

mol ratio of DNOP/Ti catalyst. DNOP is known to be a good transreaction inhibitor for the catalyst used in the polymerization of PEMPT [32,33]. It should be mentioned that the precipitation procedure used to recover the polyesters could also remove some of the Ti catalyst, thus the exact ratio of DNOP/Ti catalyst is not specifically known. After mixing, these solutions were cast into crystallization dishes and the solvent was removed by vacuum drying, ~ 300 mm Hg, at 50°C. After all the solvent was removed, these blends were dried under full vacuum for 12 h at 70°C. All blends were stored in a vacuum desiccator over calcium sulphate prior to study. The two blend preparation procedures were used so that a comparison in the observed phase behavior between stabilized and non-stabilized blends could be made.

2.4.2 Characterization: Analysis

Phase behavior was determined by the appearance of either one or two glass transition temperatures in a DSC heating scan. Thermal analysis to determine T_gs was conducted in the DSC described above. SAZ was also employed during all heating scans. The thermal program used for annealing and scanning are shown below.

Annealing	Scanning
Load @ 50°C.	Start Temp. -38°C.
Heat @ 100°C/ min to 280°C.	Scan @ 20°C/min to 202°C.
Quench to 240°C, hold 2 min.	quench to 50°C.
Quench to -40°C.	

The thermal ramp to 280°C was required to melt PC crystals that formed in the solution cast blends. No crystallization of the PC component was observed in the solution precipitated blends. The identical temperature program was followed for consistency.

2.4.3 Results and Discussion

Table 2.2 identifies the phase behavior of the four blends with respect to the two preparation methods. Blends that were cast and stabilized with DNOP all exhibited two phase behavior. The T_gs of the PC rich phase being shifted

Table 2.2 Phase Behavior of Polyester/PC2 Blends

Blend	Preparation Technique	
	Cast/DNOP Stab.	Soln. Precip./Non-Stab.
PPT/PC2	Partially Miscible T_{g1} = 16°C, T_{g2} = 103°C	Miscible T_g = 63°C
PHT/PC2	Partially Miscible T_{g1} = 3°C, T_{g2} = 107°C	Miscible T_g = 56°C
PNT/PC2	Partially Miscible T_{g1} = -4°C, T_{g2} = 100°C	Miscible T_g = 41°C
PEMPT/PC2	Partially Miscible T_{g1} = 60°C, T_{g2} = 117°C	Miscible T_g = 94°C

considerably lower, implying some level of miscibility of PEMPT in this phase. The T_gs of the polyester rich phase were nearly identical to the pure component values. It was noticed that several of these T_gs are actually slightly lower than their pure component values. The drying period for the samples was only 12 h. For the relatively thick cast samples, this may not have been an adequate enough time to remove all the residual solvent which could act as a plasticizer. Later blend studies (Chapter 4) employ a considerably longer drying period and this behavior was not observed. In contrast, blends that had been prepared by codissolution/precipitation showed single phase behavior. The T_gs fall between the two pure component values, being somewhat biased toward the lower glass transition temperature. The most interesting result was the contrast in the observed phase behavior between the two preparation techniques. In DNOP stabilized samples, transreaction does indeed appear to be inhibited allowing the identification of the two phase nature of these blends. In the non-stabilized blends, enough reaction has occurred during the short annealing time in the DSC to create a miscible, single phase system.

One additional point to be discussed is the ability of PPT, PHT and PNT to crystallize in the blend system. Figure 2.3 shows the DSC heating scans for the PPT/PC, PHT/PC and PEMPT/PC blends. Crystallization peaks were observed in both the PPT/PC (127°C) and PHT/PC (93°C) blends (this also occurred in the PNT/PC system). The appearance of these crystallization endotherms very near the T_gs makes precise determination of the T_gs difficult. The PEMPT/PC blend exhibited no crystallization endotherm and two very distinct T_gs are observed.

2.5 Conclusions

On the basis of the requirements previously set forth for the model polyester, PEMPT matches all the criteria. With its atactic structure, PEMPT appears amorphous with a T_g well removed from that of PC. PEMPT is soluble in a common solvent which will facilitate blend preparation, characterization and analysis. Removal of the β-hydrogens has produced a polyester that is thermally more stable than its linear aliphatic-aromatic counterparts. Finally, PEMPT/PC blends appear to be two phase and initial blend studies indicate that transreaction may be occurring in non-stabilized systems.

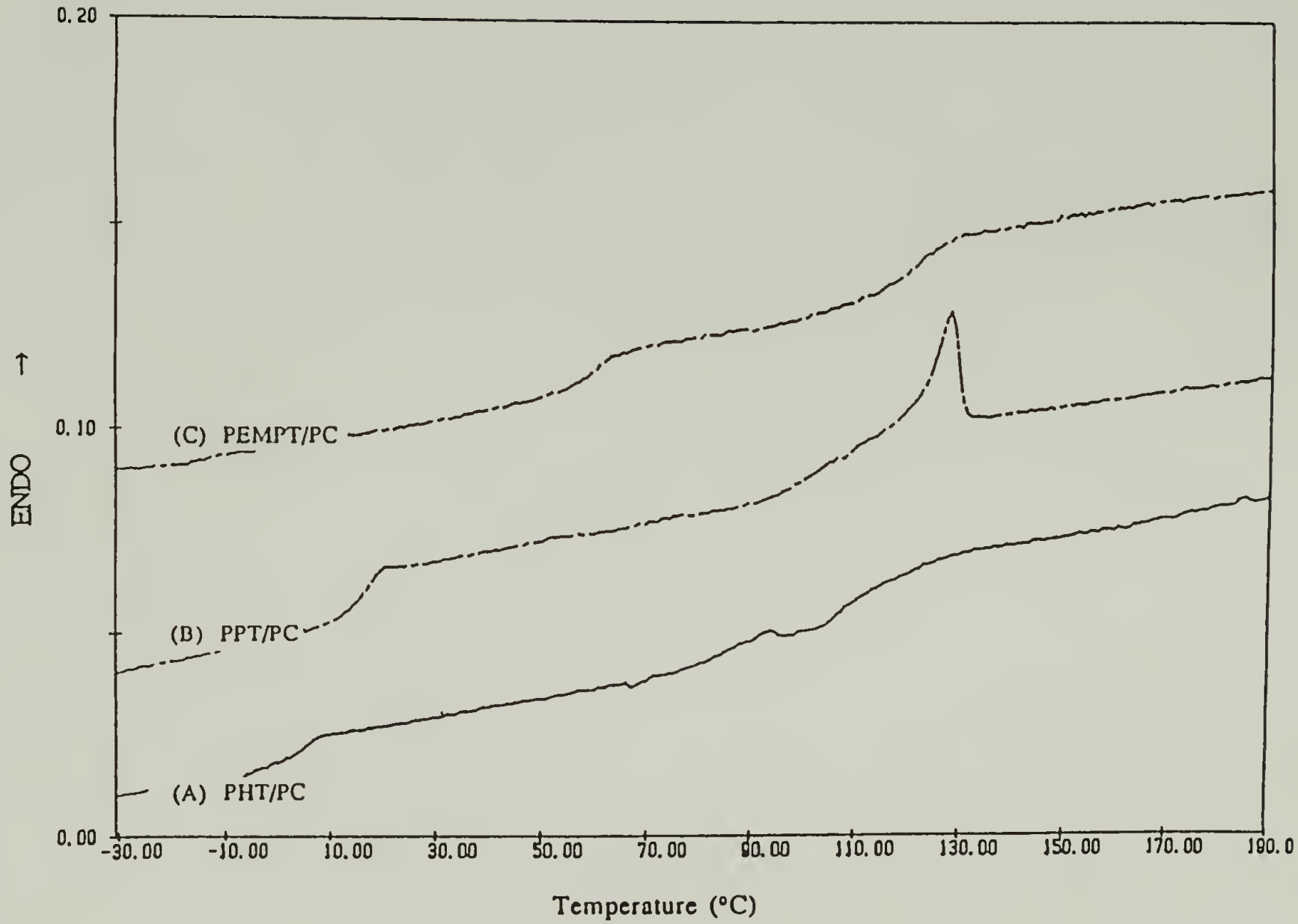

Figure 2.3 DSC heating scans of the indicated 50/50 wt. % polyester/PC2 blends.

2.6 References

1. Flory, P.J. *Principles of Polymer Chemistry*; Cornell University Press: Ithica,1953.

2. Billmeyer Jr., F.W. *Textbook of Polymer Science*; Wiley-Interscience, New York, 1971.

3. Bovey, F.A.; Winslow, F.H., Eds. *Macromolecules, An Introduction to Polymer Science*; Academic Press, New York, 1979.

4. Odian, G. *Principles of Polymerization*; Wiley-Interscience, New York, 1981.

5. Young, R.J. *Introduction to Polymers*; Chapman and Hall, Ltd.: New York, 1981.

6. Goodman, I. in *The Encyclopedia of Polymer Science and Engineering, Vol. 12, 2nd Ed.* ; Wiley: New York,1988.

7. Kotliar, A.M. *Macromol. Rev.*, **1981**, 16, 367.

8. Sommers, E.E.; Crowell, T.I. *J. Chem. Soc.* **1955**, 5443.

9. Iengar, H.V.R.; Ritchie, P.D. *J. Chem. Soc.* **1956**, 3563.

10. Allan, R.J.; Iengar, H.V.R.; Ritchie, P.D. *J. Chem. Soc.* **1957**, 2107.

11. Passalacqua, V.; Pilati, F.; Zamboni, V.; Fortunato, B.; Manaresi,P. *Polymer* **1976**, 17, 1044.

12. Zimmerman, H.; Kim, N.T. *Polym. Eng. Sci.* **1980**, 20, 680.

13. Pilati, F.; Manaresi, P.; Fortunato, B.; Munari, A.; Passalacqua, V. *Polymer* **1981**, 22, 1566.

14. Reimschuessel, H.K. *Ind. Chem. Res. Dev.* **1980**, 19, 117.

15. Peebles, L.H.; Wagner, W.S. *J. Phys. Chem.* **1959**, 63, 1206.

16. Fontana, C.M. *J. Polym. Sci.: A-1* **1968**, 6, 2343.

17. Tomita, K.; Hiroaki, I. *Polymer* **1973**, 14, 55.

18. Tomita, K.; Hiroaki, I. *Polymer* **1975**, 16, 185.

19. Hovenkamp, S.G. *J. Polym. Sci.: A-1* **1971**, 9, 3617.

20. Sivaram, S.; Upadhyay, V.K.; Bhardwaj, I.S. *Polym. Bull.* **1981**, 5, 159.

21. Challa, G. *Makromol. Chem.* **1960**, 38, 105.

22. Yu, T.-Y.; Fu, S.-K.; J, C.-Y.; Cheng, W.-Z.; Xu, R.-Y. *Polymer* **1986**, 27, 1111.

23. Pilati, F.; Manaresi, P.; Fortunato, B.; Munari, A.; Passalacqua, V., *Polymer* **1981**, 22, 799.

24. Fortunato, B.; Pilati, F.; Manaresi, P., *Polymer* **1981**, 22 655.

25. Droscher, M.; Wagner, G., *Polymer* **1978**, 19, 43.

26. Smith, J.G; Kibler, C.J.; Sublett, B.J. *J. Polym. Sci.: A-1* **1966**, 4, 1851.

27. *Encyclopedia of Polymer Science and Engineering, Vol. 11, Second Ed.*; Wiley, New York, 1988, p. 681.

28. Boreman, W.F.H. *J. Appl. Polym. Sci.* **1978**, 22, 2119.

29. O'Connor, G.L; Nace, H.R. *J. Amer. Chem Soc.* **1952**, 74, 5454.

30. O'Connor, G.L; Nace, H.R. *J. Amer. Chem Soc.* **1953**, 75, 2118.

31. Hurd, C.D.; Blunk, F.H. *J. Amer. Chem Soc.* **1938**, 60, 2419.

32. Devaux, J.; Godard, P.; Mercier, J.P. *Polym. Eng. Sci.* **1982**, 22, 229.

33. Godard, P.; Dekoninck, J.M.; Devlesaver, V.; Devaux, J., *J. Polym. Sci., Polym. Chem.* **1986**, 24, 3315.

CHAPTER 3

SYNTHESIS, END CAPPING AND CHARACTERIZATION OF A MODEL POLYESTER: POLY(2-ETHYL-2-METHYLPROPYLENE TEREPHTHALATE)

3.1 Introduction

With the background information on polyester synthesis presented in Chapter 2, discussion of the experimental details of the synthesis and characterization of PEMPT can begin. This chapter is divided into four major sections. The first two present the synthesis of PEMPT and its characterization. Two slightly different synthesis procedures were used. Both followed the general two stage polycondensation procedure described in Chapter 2. One polymerization was a bulk synthesis of PEMPT (~ 200 g of polymer). The second procedure was used to make several PEMPT samples of varying molecular weight. It involved a considerably smaller scale (6-10 g of polymer per sample), using prepolymer from the first stage of the bulk synthesis as a starting material. The characterization of the polycarbonates to be used in blend studies is also presented in this section. The two polycarbonates, designated PC1 and PC2, were obtained from the General Electric Company and have been stated to have absolute weight average molecular weights (determined from GPC applying a universal calibration) of 11,300 and 21,200, respectively. They contain no additives. The second two sections of this chapter detail the end capping of PEMPT and the subsequent characterization of these modified polymers.

3.2 Synthesis

3.2.1 Purification of Monomers

Dimethyl terephthalate (DMT) (Aldrich 99+%) was purified by a recrystallization procedure. In a 2000 mL beaker, 254 g, 1.31 mol of DMT were added to 520 mL of chloroform (Aldrich, HPLC grade). The beaker was covered with aluminum foil. The solution was heated on a hot plate to 70°C while

applying magnetic stirring. When all the DMT had dissolved, 780 mL of hot, 90°C, n-heptane (Fisher, HPLC grade) was added to the DMT/chloroform solution. Vigorous stirring was conducted for 10-15 min while the solution temperature was raised to 90°C. The beaker was then cooled to room temperature and left for 72 h. At this time, the solvents were decanted and the short, needle like, white crystals were dried under vacuum at 72°C for 24 h.

418 g, 3.54 mol of 2-ethyl-2-methyl-1,3-propanediol (EMPD) (Aldrich 98%) was purified by drying at 52°C over 24 g, .2 mol of magnesium sulfate (Mallinckrodt, Anhydrous powder-Analytical reagent grade). The solution was filtered, followed by vacuum distillation at 94°C (~ 1.5 mm Hg). The condenser of the vacuum distillation column was connected to a Neslab Endocal refrigerated circulating bath operated in the heating mode. This allowed the condenser water to be continually heated to 55°C which prevented EMPD from crystallizing in the column. The monomer was stored under nitrogen until use.

3.2.2 Polymerization

3.2.2.1 Polymerization of PEMPT: Bulk

To a 500 mL reactor kettle, 204 g, 1.05 mol of DMT and 219 g, 1.85 mol EMPD were added. The kettle was equipped with a bearing sleeve for mechanical stirring, a thermometer, septa/nitrogen inlet and a distillation adapter. When the reactor was sealed, nitrogen at ~ 300 mL/min was purged through for 10 min. Power to a heating mantle was initiated and stirring was begun. When both monomers had melted (~ 140°C), 210 mL of titanium (IV) isopropoxide (Aldrich 97%) was injected into the reactor mixture. The temperature of the mixture was raised to 202°C which marked the beginning of the first stage of reaction. Within minutes, methanol began to condense out and was collected in a 100 mL R.B. flask. Nitrogen was continually flushed through the reactor to assist in methanol removal. During the first stage of reaction, the temperature of the reaction mixture gradually increased to 218°C. When the first stage of reaction was nearly complete (~ 2 1/2 h), the temperature of the mixture was raised to 242°C to drive off any remaining methanol. After a total reaction time of 2 h 40 min., 98 wt. % of the theoretical amount of methanol had been collected.

At this time, the distillation adapter was removed. Using a 25 mL glass pipet, 8-18 mL aliquots of prepolymer were removed from the kettle. During this procedure, nitrogen was continually flushed through the reactor. The clear, colorless prepolymer samples were placed in 26 mL vials which were capped and placed in a desiccator. These prepolymer samples were required for the synthesis of PEMPT samples varying in molecular weight. After all eight aliquots had been removed, the septa/nitrogen inlet was replaced by a plug and the distillation adapter was replaced by a vacuum adapter. A heated vacuum line hose at 55°C was connected to the vacuum adapter and, on the opposite end, to a cold trap (dry ice/ethanol). The temperature of the reactor was raised to 245°C, vacuum was applied to the system and stirring was resumed. This marked the beginning of the second stage of reaction. Throughout the course of the polymerization the temperature of the reacting mixture was maintained at 245 ± 1°C. The vacuum was measured with a Sargent-Welch vacuum gauge and remained between 1.2 ± .2 mm Hg during the polymerization. After 2 h, the vacuum was removed and the reactor kettle was opened to the atmosphere. The clear, colorless polymer was placed into a large petri dish and stored in a vacuum desiccator.

3.2.2.2 Polymerization of PEMPT: Varying Molecular Weights

By varying the second stage reaction time, the prepolymer samples removed at the end of the first stage of the bulk reaction were polymerized to obtain PEMPT varying in molecular weight. The apparatus used for the syntheses of Chapter 2 was also employed here. In addition, a separate hot plate and mineral oil bath (500 mL Erlenmeyer flask with magnetic stir bar) equipped with a thermocouple was used for preheating the prepolymer and reaction tube. Six reactions were carried out with the appropriate conditions for each described in Table 3.1 (samples PEMPT1-OH15 through PEMPT6-OH15). A typical second stage polymerization is described below. A 26 mL vial containing prepolymer was capped with a septa and flushed with nitrogen at ~ 50 mL/min. The vial was heated in a water bath at 70°C for 15 min while continuing nitrogen purge. The PEMPT oligomer was poured into the reaction tube which was then sealed with the trap top. The reaction tube was purged with nitrogen (200 mL/min) for 5 min. The tube was placed in the preheat oil bath at 250°C for 5 min while nitrogen purging continued. The reactor tube was

Table 3.1 2nd Stage Synthesis Conditions and Elemental Analysis

Polyester	Synthesis			Analysis			
	Time (min)	Temp. (°C)	Vacuum (mm Hg)	% C (Meas.)	% C (Theor.)	% H (Meas.)	% H (Theor.)
PEMPT1-OH15	10	250	0.55	67.78	67.63	6.84	6.77
PEMPT2-OH15	20	245	0.46	68.01	67.50	6.75	6.65
PEMPT3-OH15	60	250	0.37	68.09	67.56	6.78	6.60
PEMPT4-OH15	90	250	0.42	68.29	67.61	6.61	6.58
PEMPT5-OH15	130	250	0.41	68.34	67.65	6.67	6.55
PEMPT6-OH15	180	250	0.43	68.22	67.69	6.69	6.52
PEMPT-B	120	245	1.2	67.72	67.65	6.53	6.55

then placed into the main oil bath and connected to the heated vacuum line. The nitrogen line was removed, stirring begun and vacuum applied to the system. This marked the beginning of the second stage of reaction. The mixture was allowed to react for the appropriate time (see Table 3.1). When the specified time was reached, the reactor tube was removed from the oil bath and placed under cold water. A small amount of excess EMPD and oligomer crystallized out on the tube walls. Chloroform (Fisher, spec. grade), 20 mL, was flushed around the tube walls to remove this material. The chloroform was subsequently decanted.

3.2.3 Purification and Drying

3.2.3.1 PEMPT: Bulk Synthesized

20 g of bulk synthesized PEMPT was dissolved in 100 mL of chloroform. The solution was filtered through a 4-8 μm fritted glass funnel. The polymer was recovered by dropwise precipitation into 1000 mL of methanol (fisher spec. grade) under vigorous mixing. The recovered sample was washed with 2 x 200 mL aliquots of fresh methanol. The polymer was placed in a petri dish and dried in a oven at 90-100°C for 48 h. This single precipitated polymer from the bulk synthesis will be designated PEMPTB.

3.2.3.2 PEMPT: Varying Molecular Weight

50 mL of chloroform was placed in the reactor tube containing the polymer. The tube was covered and the polymer was allowed to dissolve. The polymer solution was then filtered through a 4-8 μm fritted glass funnel. The polymer was recovered by dropwise precipitation into 500 mL of methanol (Fisher spec. grade) with vigorous mixing. The recovered sample was washed with 2 x 100 mL aliquots of fresh methanol. The single precipitated samples were stored in teflon film lined petri dish and dried for several hours by placing in a vacuum desiccator and pulling a slight vacuum using an aspirator. Further drying was conducted in a oven at 90-100°C for 48 h.

It was noticed in some initial GPC runs that the PEMPTs polymerized for short reaction times appeared to have a low molecular weight tail. Due to this fact, each of the precipitated and dried polymers above were reprecipitated.

Three grams of each polymer were redissolved (20 mL chloroform) and reprecipitated (200 mL methanol). The twice precipitated polymers were placed in teflon film lined petri dishes and dried 1 h at 100°C in a vacuum oven using an aspirator for vacuum. The temperature of the oven was lowered to 78°C and the polymers were dried under full vacuum for four days. These samples that had been twice precipitated were identified as PEMPT-OH15. The "OH" designates that the polyester has hydroxyl end groups while the "15" designates that it was precipitated from a 15% polymer/chloroform solution. All the PEMPT samples, including PEMPTB were stored in a vacuum desiccator over calcium sulphate.

3.3 Characterization: Analysis

Characterization involving the bulk polymerized polymer was conducted on the once precipitated and dried PEMPTB. Unless otherwise stated, all samples used to characterize the polyesters of varying molecular weight were samples that had been twice precipitated, PEMPT1-OH15 through PEMPT6-OH15.

3.3.1 Elemental Analysis: Carbon and Hydrogen

Elemental analysis was conducted at the University of Massachusetts Microanalysis Laboratory. A Control Equipment Corp. Elemental Analyzer employing a modified Pregl-Dumas technique was used for Carbon and hydrogen analysis.

3.3.2 Molecular Weight

3.3.2.1 End capping

Number average molecular weights (M_ns) were determined by end capping with heptafluorobutyryl chloride followed by determination of end group concentrations by weight analysis of fluorine. The end capping procedure is described later in this chapter. It should be noted that all the values for the measured wt % fluorine have been increased by 11%, corresponding to the measured % conversion of hydroxyl end groups, which was not quite

quantitative (see section 3.6.1). The end capping procedure is one of the few instances where PEMPT-OH15 samples were not analyzed directly. End capping started with the single precipitated, varying molecular weight PEMPTs that had been recovered from the reaction tube. The end capping was carried out in a 2% (w/v) solution and the samples were recovered by precipitation. It is these samples recovered from a 2% solution that were actually analyzed. GPC results indicate little difference between the polyesters recovered from 2% and 15 % solutions. Results are presented here for comparison with M_ns determined from proton NMR. Four samples each of PEMPT2 and PEMPT6 were analyzed to obtain an average value for the weight % fluorine while two samples of each of the remaining polyesters were used.

End group concentrations were also adjusted for the presence of acid end groups. Acid end group content was determined on PEMPT-OH15 samples following a procedure similar to that of Pilati, et al [1]. All titrations were conducted under nitrogen with a 2.310×10^{-3} M KOH/methanol solution which had been standardized using a 5.005×10^{-3} M potassium hydrogen phthalate solution. Several drops of a 1% phenolphthalene/ethanol solution were used as an indicator.

3.3.2.2 ^{1}H NMR

Number average molecular weights were also determined by proton NMR. The resonances used in these calculation will be discussed in conjunction with the end capping experiments later in this chapter. It should be mentioned that the close proximity of the end group resonance relative the main chain resonance used for comparison prevented instrumental integration. Integration was carried out by cutting and weighing. To minimize the error introduced by dividing the peaks, six photo copies were made of each samples spectra which were then used to calculate peak areas and an average value for the molecular weight. The specifics of the spectrometer operation are described in section 3.3.3.

3.3.2.3 GPC

GPC was conducted using a Waters Model 590 pump combined with a Waters WISP Auto Injector Model 710B. The detector was a Perkin-Elmer

Model LC90 variable wave length u.v. detector operated at 254 nm. Three Waters Ultra Styragel columns of 10^5, 10^4 and 103 Å were employed. Chloroform at 1 mL/min was used as the solvent. A Nelson Analytical data collection system with series 2600 software was used to collect and analyze the data. Narrow molecular weight polystyrene (PS) standards were used for calibration. Unless otherwise stated, reported molecular weights are relative to these PS standards.

3.3.3 NMR: ^1H and ^{13}C

Proton NMR was conducted on a Varian 300-XL spectrometer (300 MHz). Samples solutions were approximately 1% (w/v) with deuterated chloroform as solvent and TMS used as an internal reference. The pulse width was 7.0 µs (9.3 µs equivalent to 90° pulse width) with an acquisition time of 3.725 s and a delay time between pulses of 7.0 s. Sixty-four scans per sample were recorded.

Carbon-13 NMR was conducted on a Varian 200-XL spectrometer (200 MHz). The sample, PEMPTB, was dissolved in deuterated chloroform (9.5% w/v). Several drops of TMS (Aldrich 99.9+% NMR grade) were added as an internal reference. The number of scans was 2048 with proton decoupling applied.

A carbon-hydrogen HETCOR (heterogeneous correlation) experiment was also conducted on the Varian 200-XL spectrometer. The PEMPTB sample prepared for ^{13}C experiment above was used in this experiment. The full carbon and hydrogen spectral widths of the polyester were scanned.

3.3.4 Infrared Spectroscopy

Infrared spectroscopy was conducted on a IBM 38 FTIR under nitrogen at room temperature. The frequency range was 400-4000 cm^{-1} with 4 cm^{-1} resolution. One hundred scans were recorded on samples that had been cast from chloroform solution (approx. 1% w/v) onto NaCl plates and annealed 24 h under vacuum at 76°C. Samples were stored in a vacuum desiccator over calcium sulfate prior to scanning.

3.3.5 Thermal Analysis

Glass transition temperatures were determined from DSC using a Perkin-Elmer DSC-7. Nitrogen was used as a purge gas and ice water bath was used for subambient cooling. Indium and recrystallized dimethyl isophthalate were used for calibration standards. All scans were conducted at 20°C/min. Sample size was ~ 6 mg. Reported T_gs are midpoint values determined from heating runs. Values are averages of 3 separate runs per sample.

Thermogravimetric analysis was carried out on the identical instrument under the identical conditions as described in Chapter 2. The reported decomposition temperature, T_d, once again represents the temperature at which the maximum rate of weight loss occurred. Also reported is the % wt loss at 300°C. Samples PEMPT-1, PEMPT-3 and PEMPT-5 were run twice while PEMPT-2, PEMPT-4 , PEMPT-6 were run once.

3.3.6 Density

Density measurements were carried out in a density gradient column at 23.1°C. The column was composed of a sodium bromide (Fisher Scientific Company) deionized, degassed aqueous solution. Beads of known density, ranging from 1.0600-1.2700 g/cm^3, were used for calibration. Reported values are averages of 3-5 samples per polyester. Samples were allowed to equilibrate 12 h in the column prior to measurement.

3.3.7 Solubility of PEMPTB

The solubility of PEMPTB was determined for a variety of solvents at room temperature. All solvents were 99% pure or greater, except for 1,1,2,2-tetrachloroethane which was 98%. To a 2 mL vial, ~ 0.020 g of polymer and 1.0 mL of solvent were added. The vials were covered with teflon tape and then capped. The solubility of the polyester was identified after 25 h and 75 h in solution.

3.4 Characterization: Results and Discussion

3.4.1 Synthesis Conditions and Elemental Analysis

Table 3.1 displays the synthesis conditions for the second stage polymerization of samples PEMPT1-OH15 through PEMPT6-OH15 and PEMPTB. Table 3.1 includes the reaction time, temperature and applied vacuum, as well as, the carbon-hydrogen elemental analysis of the synthesized polymers. All but one of the six PEMPT samples polymerized in the reaction tube were synthesized at an oil bath temperature of 250°C. PEMPT2-OH5 and PEMPTB were polymerized at 245°C. Carbon-hydrogen elemental analysis is seen to be in good agreement with estimates. However, the experimentally determined carbon and hydrogen content are both slightly higher than the theoretical calculations. Initially, it was thought that this may be due to residual methanol remaining from the precipitation procedure. In calculations including 1% methanol, the theoretical amount of percent carbon and hydrogen would both be lowered, increasing the difference with the experimentally determined values. Thus, insufficient drying of the samples does not appear to be the cause of the discrepancies.

3.4.2 Molecular Weight Determination

Table 3.2 displays the end group data used for the number average molecular weight calculation. As expected, the measured wt % fluorine systematically decreases with increasing polymerization time. Included is the standard deviation for the measured wt % fluorine for each sample. These deviations include error from the actual measurement of fluorine content and the adjustment in the fluorine content due to incomplete reaction conversion. The corresponding number average molecular weights, determined from the calculated number of hydroxyl end groups and corrected for acid end group content, are seen to range from 4,100-37,500 g/mol. The percent error in these measurements increases with increasing M_n due to the decrease in the measured fluorine content with increasing molecular weight of the polyester.

The M_ns determined from ^1H NMR are systematically higher than those determined from the end capping techniques. The discrepancy most likely results from a systematic error in resolving the two resonances used for the

Table 3.2 End Group Analysis and Number Average Molecular Weight Data

Polyester	Wt. % Fluorine	$\frac{\text{Moles OH}}{\text{g Polymer}}$ (x 10^{-4})	$\frac{\text{Moles COOH}}{\text{g Polymer}}$ (x 10^{-4})	M_n (End Group) (g/mol)	M_n (NMR) (g/mol)
PEMPT1	5.91 ± 0.21	4.87	0.0093	4,100 ± 150	5,800 ± 1,800
PEMPT2	4.07 ± 0.15	3.26	0.0141	6100 ± 250	7,400 ± 2,200
PEMPT3	2.68 ± 0.11	2.10	0.0112	9,500 ± 400	13,600 ± 4,100
PEMPT4	2.22 ± 0.10	1.73	0.0174	11,500 ± 500	17,500 ± 5,300
PEMPT5	1.41 ± 0.08	1.08	0.0115	18,200 ± 1,100	25,700 ± 7,700
PEMPT6	0.66 ± 0.07	0.50	0.0314	37,500 ± 3,800	39,200 ± 11,800
PEMPTB	1.44 ± 0.08	1.11	0.0245	17,700 ± 1,000	21,000 ± 6,300

analysis. The results from NMR follow the general trend of increasing M_ns with increasing reaction time. The two sets of data are within ~ 30% of one another which is approximately the error in the corresponding NMR measurements. Table 3.3 displays molecular weight results from GPC analysis. All values are relative to the PS calibration standards. Once again the general trend of increasing molecular weight with increasing reaction time is observed. Further discussion of this data will be included with the discussion of GPC data of end capped PEMPTs (section 3.6.2).

Table 3.3 also contains the molecular weight data for PC1 and PC2. The values displayed here are the absolute molecular weights based on the absolute weight average molecular weights provided by the General Electric Co. The M_ns and M_zs of the two PCs were subsequently determined from the appropriate polydispersities measured by GPC.

3.4.3 NMR: ^1H and ^{13}C

Figures 3.1 and 3.2 show the 300 MHz proton and 200 MHz carbon spectra of PEMPTB, respectively. Included above each spectra is the chemical structure of PEMPT with the corresponding coded hydrogens and carbons, respectively. It should be noted that in the proton spectrum the peak at 7.266 ppm is associated with chloroform and that at 1.595 ppm is that of water. Similarly, in the carbon spectrum, the triplet centered at 77.08 ppm is that of chloroform. Proton assignments were unambiguous due to chemical shift and splitting considerations. The Hetcor experiment (Figure 3.3) was used to assign carbon atoms a, d, e, g and h. Carbon c (the ester functional group) was assigned to the peak at 165.49 ppm [3], hence, carbon b is assigned to the final resonance characteristic of an aromatic group, 133.95 ppm. The remaining resonance, 37.88 ppm, corresponds to the quaternary carbon, f. Table 3.4 summarizes the peak assignments. The hydrogen and carbon resonances of the terephthalate ring and the methylene sequences adjacent to the carbonyl in PEMPT are in good agreement with literature values of similar compounds [4-9].

3.4.4 Infrared Spectroscopy

Infrared spectroscopy will be used in this dissertation in a qualitative fashion, thus, a detailed analysis of the resonances, as conducted above for

Table 3.3 Molecular Weight Data from GPC Analysis*

Polymer	M_n (g/mol)	M_w (g/mol)	M_z (g/mol)	M_w/M_n	M_z/M_w
PEMPT1-OH15	3,150	7,310	11,700	2.321	1.601
PEMPT2-OH15	4,610	11,940	18,510	2.588	1.551
PEMPT3-OH15	11,550	21,000	31,700	1.821	1.508
PEMPT4-OH15	13,530	25,190	38,070	1.863	1.511
PEMPT5-OH15	17,840	34,510	52,490	1.934	1.521
PEMPT6-OH15	21,360	42,640	65,400	1.996	1.534
PC1	11,330	17,190	23,860	1.517	1.388
PC2	21,200	30,640	41,660	1.445	1.360

* Polyester molecular weights are relative to polystyrene standards, while PC molecular weights represent absolute values.

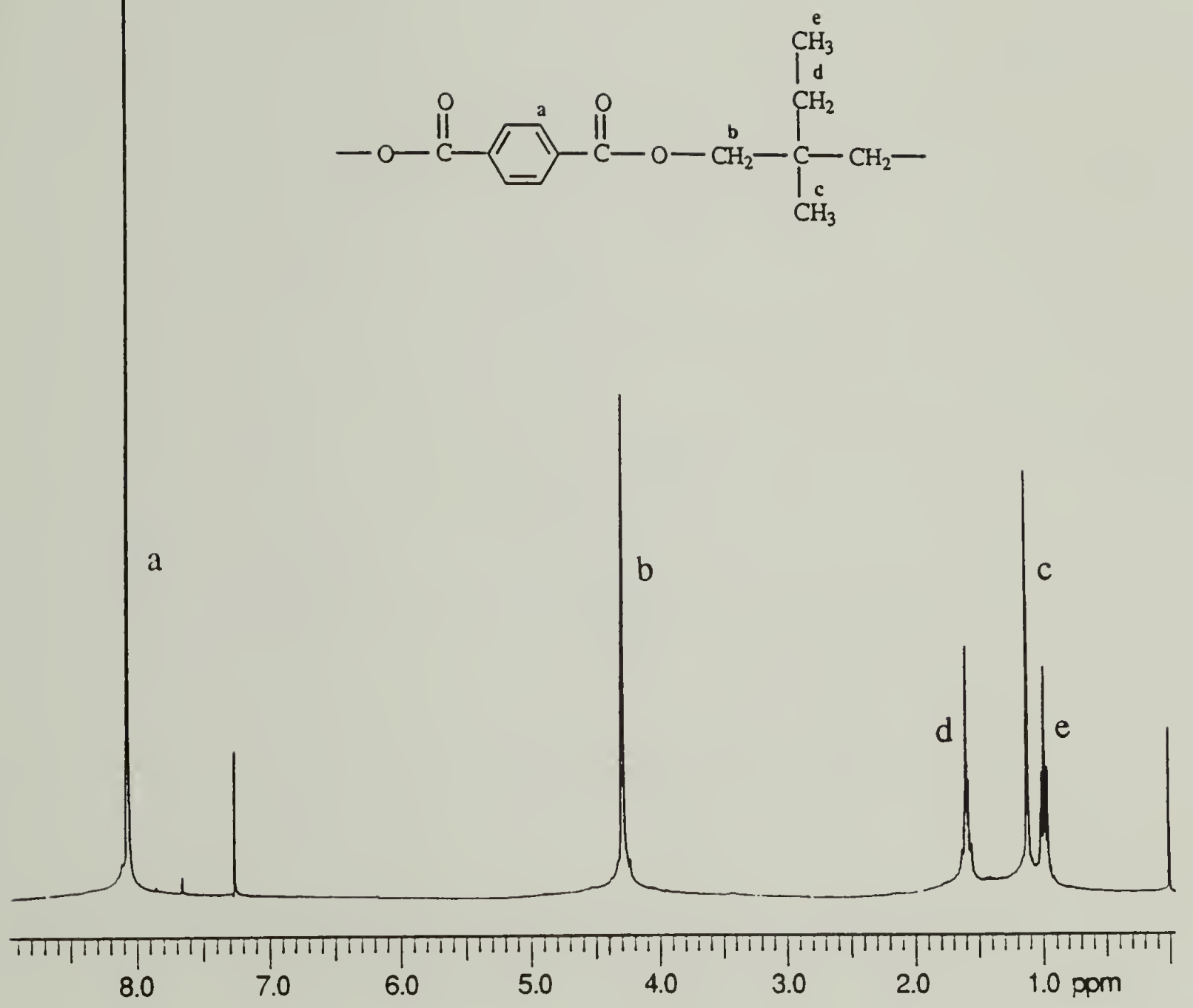

Figure 3.1 300 MHz ^{1}H NMR spectrum of PEMPTB. Also shown is the chemical structure of PEMPT and the corresponding coded hydrogens.

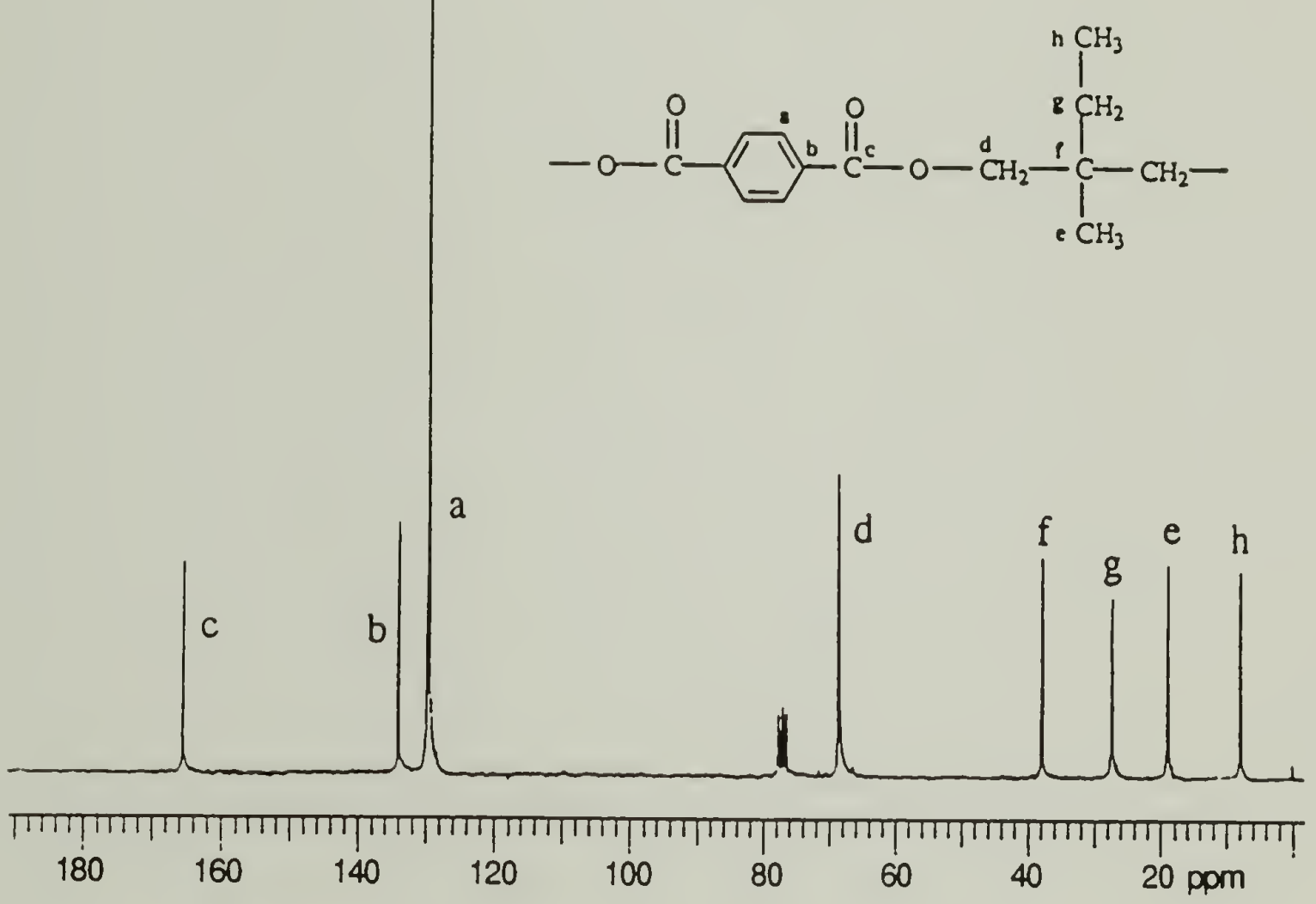

Figure 3.2 200 MHz ^{13}C NMR spectrum of PEMPTB. Also shown is the chemical structure of PEMPT and the corresponding coded carbons.

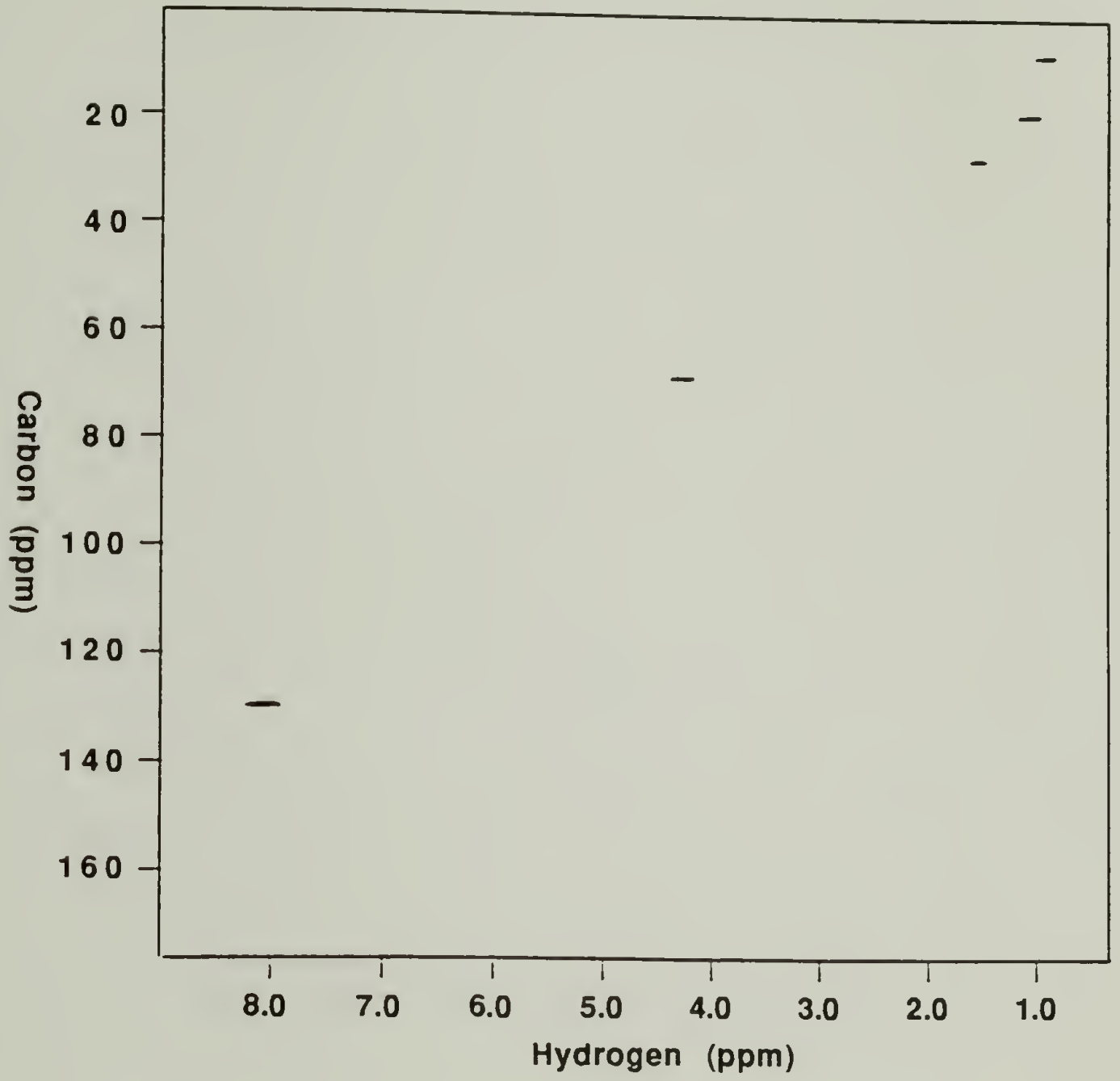

Figure 3.3 200 MHz ^{1}H-^{13}C hetcor spectrum of PEMPTB.

Table 3.4 NMR Peak Assignments of PEMPT

Hydrogen*	δ (ppm)	Carbon**	δ (ppm)
a	8.081 (s)	a	129.616
b	4.290 (s)	d	68.503
c	1.118 (s)	e	18.847
d	1.591 (q)	g	27.289
e	0.979 (t)	h	7.708
-	-	b	133.953
-	-	c	165.492
-	-	f	37.880

* See Figure 3.1 for hydrogen coding.
** See Figure 3.2 for carbon coding.

proton and carbon NMR, will not be done. Instead, features that are of specific interest are noted. Figure 3.4 shows the infrared spectrum of PEMPT5-OH15. The general aspects of the spectrum are in agreement with literature values of similar polymers [10-13]. Of particular interest is the ability of the polyester to hydrogen bond. Figure 3.5a,b show the I.R. spectra in the region of 2800-3800 cm^{-1} of PEMPT1-OH15 and PEMPT5-OH15. As is plainly observed, the broad hydrogen bonding resonances at 3430 cm^{-1} and 3550 cm^{-1} are much more apparent in the lower molecular weight polyester. A sharper peak is observed in sample PEMPT5-OH15 at 3585 cm^{-1}. This peak is not apparent in the low molecular weight sample, although it could be obscured by the broad 3550 cm^{-1} peak. Self associated hydrogen bonds have been observed in pure phenoxy to occur as broad peaks at 3450 cm^{-1} while the free hydroxyl is found at 3570 cm^{-1} [14]. In the current samples, the sharp resonance at 3585 cm^{-1} is assigned to the unassociated hydrogens, while the broad resonance at 3430 cm^{-1} is assigned to the self associated hydroxyl-hydroxyl interaction. The remaining broad peak at 3550 cm^{-1} is assigned to a hydroxyl-carbonyl hydrogen bond. A resonance in this frequency region has been assigned to this interaction in a phenoxy/poly(ε-caprolactone) blend [14].

3.4.5 Thermal Analysis

Figure 3.6 is a DSC scan of PEMPTB from 30-250°C. A single sharp T_g is observed at 62.3°C. With its 2-ethyl-2-methyl substitution on the propyl group, PEMPT has the potential to form an atactic structure and would be expected to exhibit the behavior of an amorphous polymer. However, if long enough sequences of a regular crystallizable structure had been formed, the melting point would likely be no greater than that of poly(propylene terephthalate) (PPrT), 227°C [15]. With no other transitions observed in the above temperature range, it can be concluded that PEMPT is indeed amorphous.

Table 3.5 summarizes the DSC and TGA data of all the polyesters. Examining the data for the varying molecular weight PEMPT samples, the T_g varies with the molecular weight of the polyester. Fox and Flory [16,17] have shown using free volume arguments that the observed T_g should increase with increasing molecular weight according to the functional form,

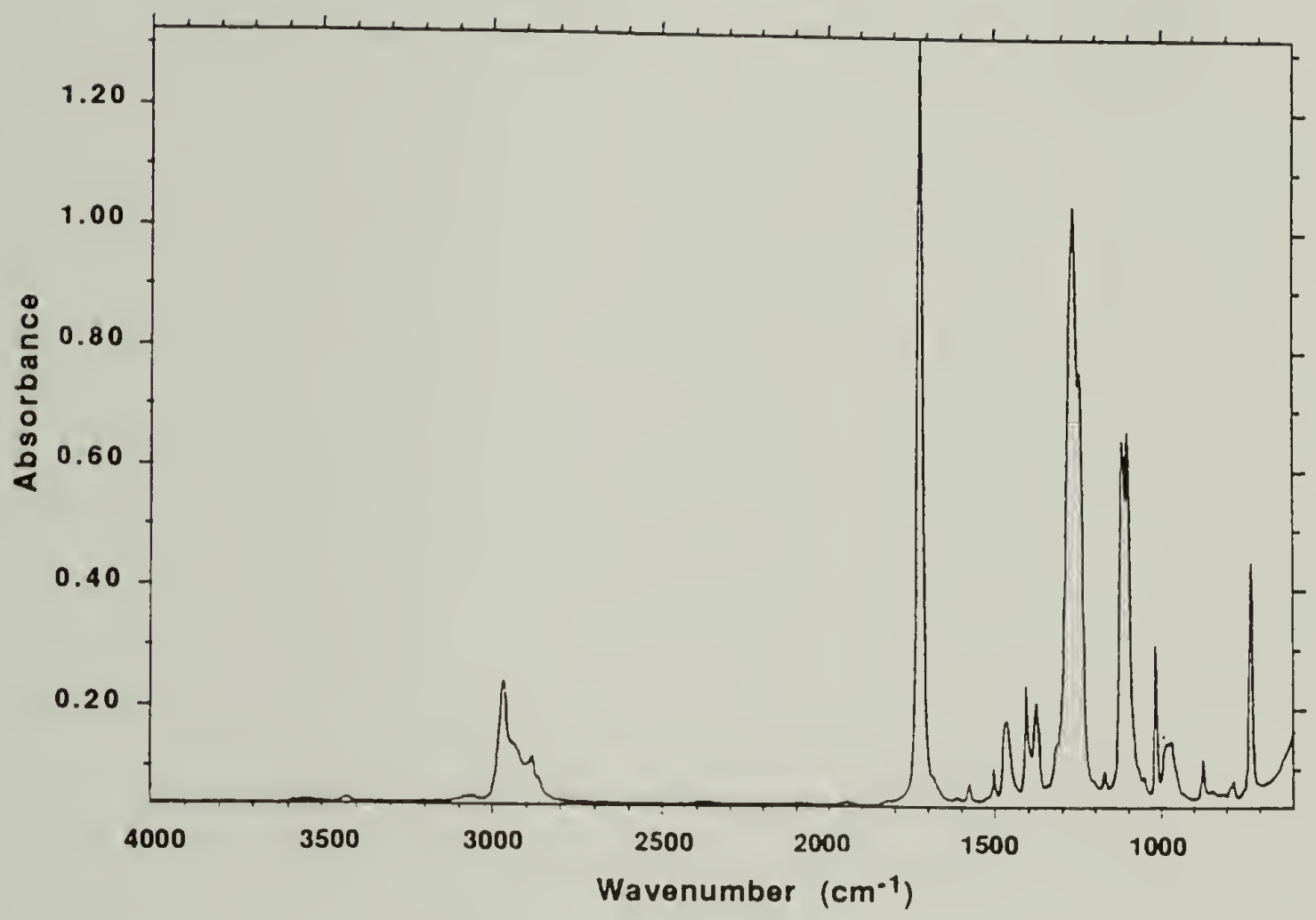

Figure 3.4 FTIR spectrum of PEMPT5-OH15.

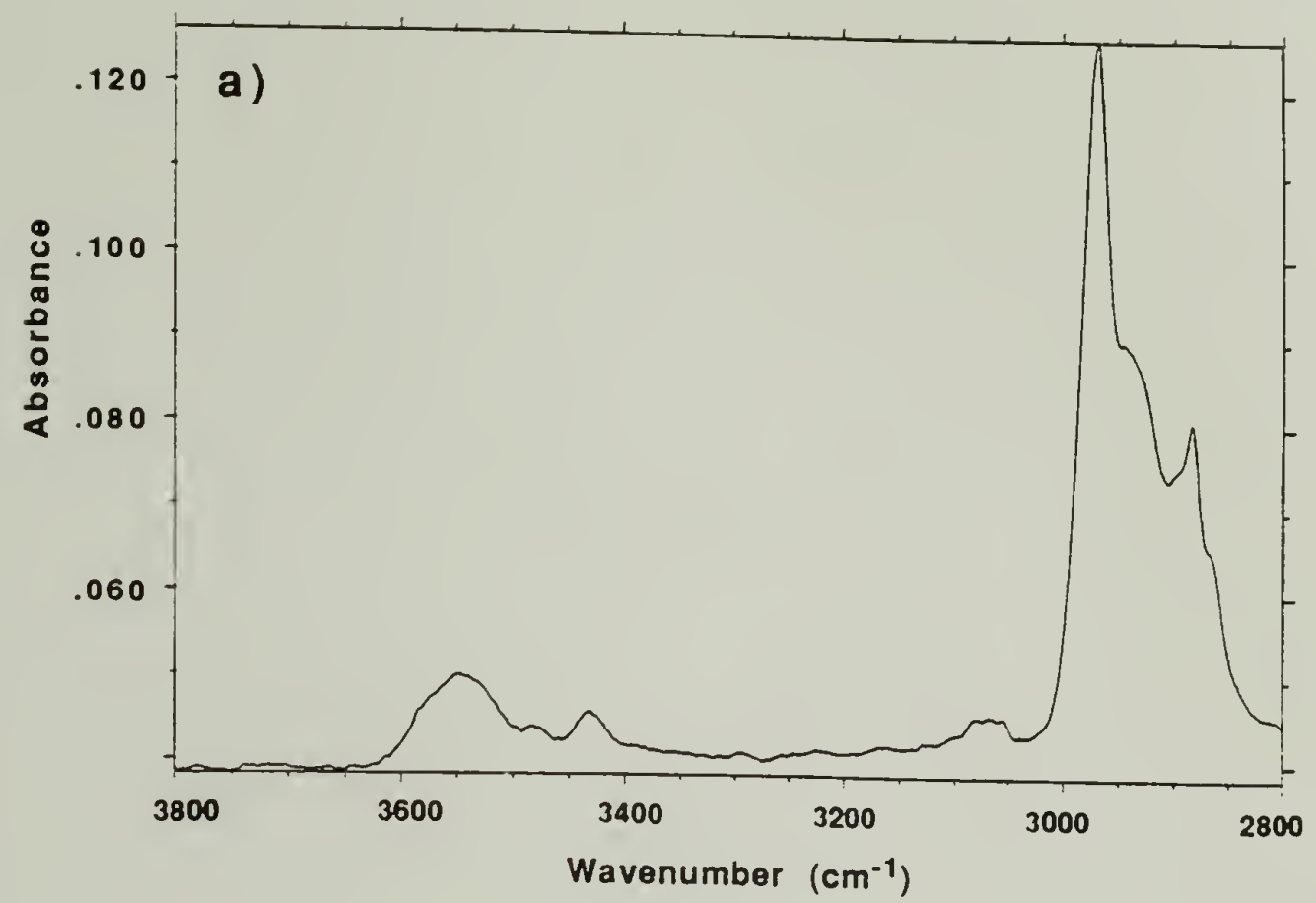

Figure 3.5 FTIR spectrum displaying the hydrogen bonding region of a) PEMPT1-OH15 and b) PEMPT5-OH15.

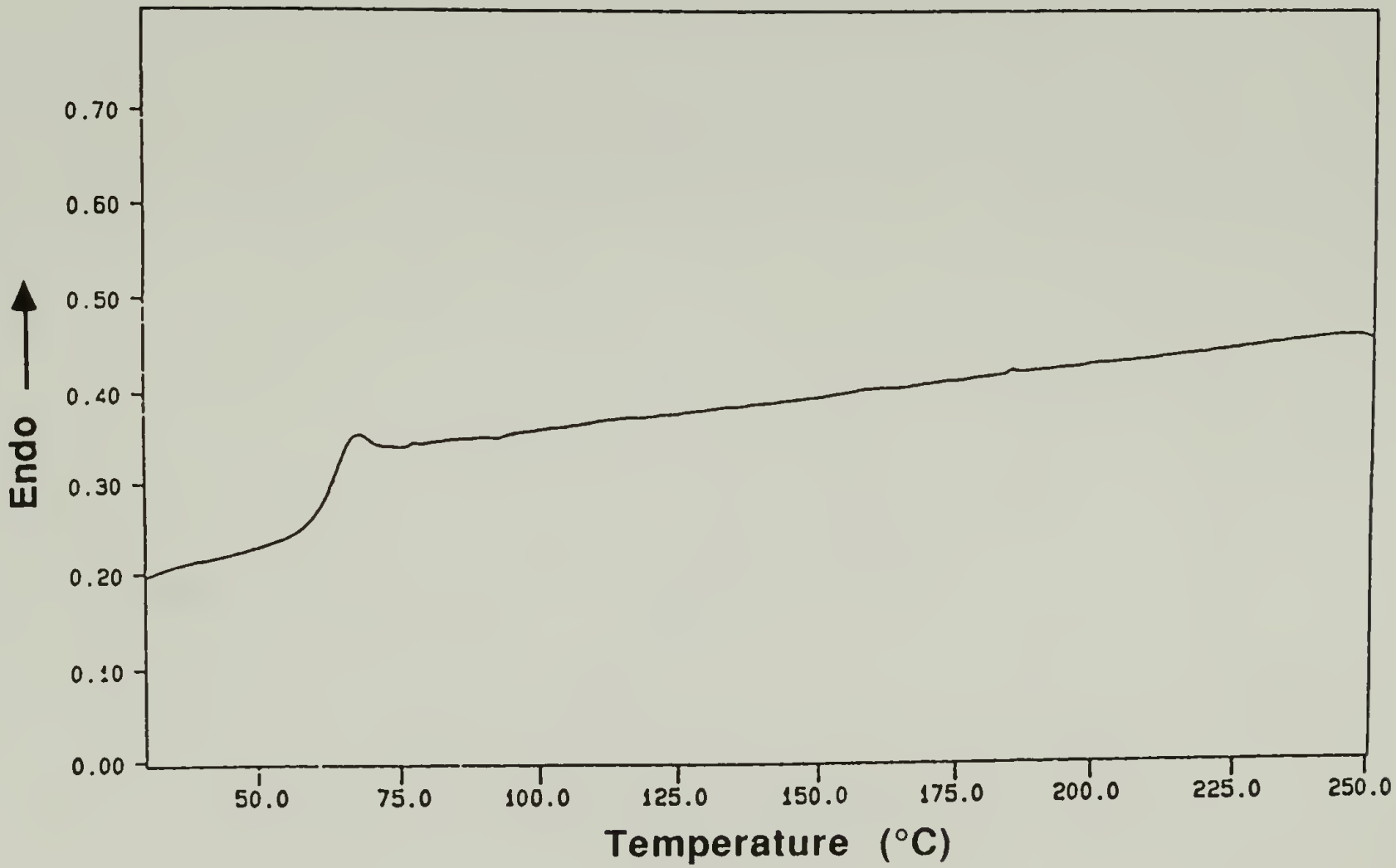

Figure 3.6 DSC heating scan of PEMPTB.

Table 3.5 Thermal Analysis and Density Data

Polyester	T_g (°C)	ΔC_p (J/g °C)	T_d^* (°C)	% wt. loss @ 300°C	Density (g/cm^3)
PEMPT1	55.2	.256	470	1.11	1.190
PEMPT2	58.3	.262	470	0.90	1.190
PEMPT3	60.7	.245	470	0.76	1.192
PEMPT4	62.2	.279	470	0.28	1.190
PEMPT5	64.2	.242	467	0.48	1.194
PEMPT6	65.4	.253	466	0.12	1.194
PEMPTB	62.0	-	-	-	1.190
PC1	145.4	.253	-	-	1.20**
PC2	149.3	.251	-	-	1.20**

* Temperature of the maximum rate of thermal decomposition.
** From reference [20].

$$T_g = T_{g,\infty} - \frac{K}{M_n} \qquad (3.1)$$

T_g: Observed glass transition temperature.
$T_{g,\infty}$: Glass transition temperature at infinite molecular weight.
M_n: Number average molecular weight.
K: Constant related to the thermal expansion coefficients of the glassy and rubbery states.

Figure 3.7 is a plot of the T_g vs. the inverse M_n for samples PEMPT1-OH15 through PEMPT6-OH15. The data fits the above functional form well with the $T_{g,\infty}$ equal to 66.3°C and the constant K equal to 8.85 x 10^4 °C g/mol. It should be noted that the above values were calculated for T_gs determined at a heating rate of 20°C/min. and that no extrapolations to zero scanning rate were made. It is seen that an order of magnitude increase in M_n leads to a 10°C increase in the glass transition temperature of the polyester.

Polyesters used for industrial applications have molecular weights generally in the range of 15,000-30,000. In the case of PEMPT, this corresponds to a range in the T_g of 62-66°C. Using this range, the effect of the ethyl-methyl substitution on T_g will be examined. Smith, et al. [18], report the T_g of PPrT as 35°C from a DTA experiment, while Wick, et al. [15], report the T_g of Poly(2,2-dimethyl-1,3-propylene terephthalate) (PDMPT) to be 70.9°C as measured by DSC at a 10°C/min scanning rate. Due to the dimethyl substitution, the T_g of PDMPT is seen to be increased 35°C over that of PPrT. The ethyl-methyl substitution of PEMPT also leads to a T_g increase of 25-30°C over that of PPrT. However, the increase is lower than that observed for PDMPT. This type of behavior has been observed in a previous study on substituted PETs [19].

Fagerburg reports an increase from 78°C to 95°C in the T_g of poly(1,2-propylene terephthalate) compared to that of PET [19]. Upon lengthening of the substituent from methyl in poly(1,2-propylene terephthalate) through the series ethyl, propyl and butyl, the T_g of the substituted PETs was shown to systematically decrease; 80°C, 67°C, 58°C. The overall behavior has been described in terms of two competing factors effecting T_g. One is that initial methyl substitution increases the energy barrier to rotation of the main chain carbons, stiffening the polymer chain and thus raising the T_g. The second is

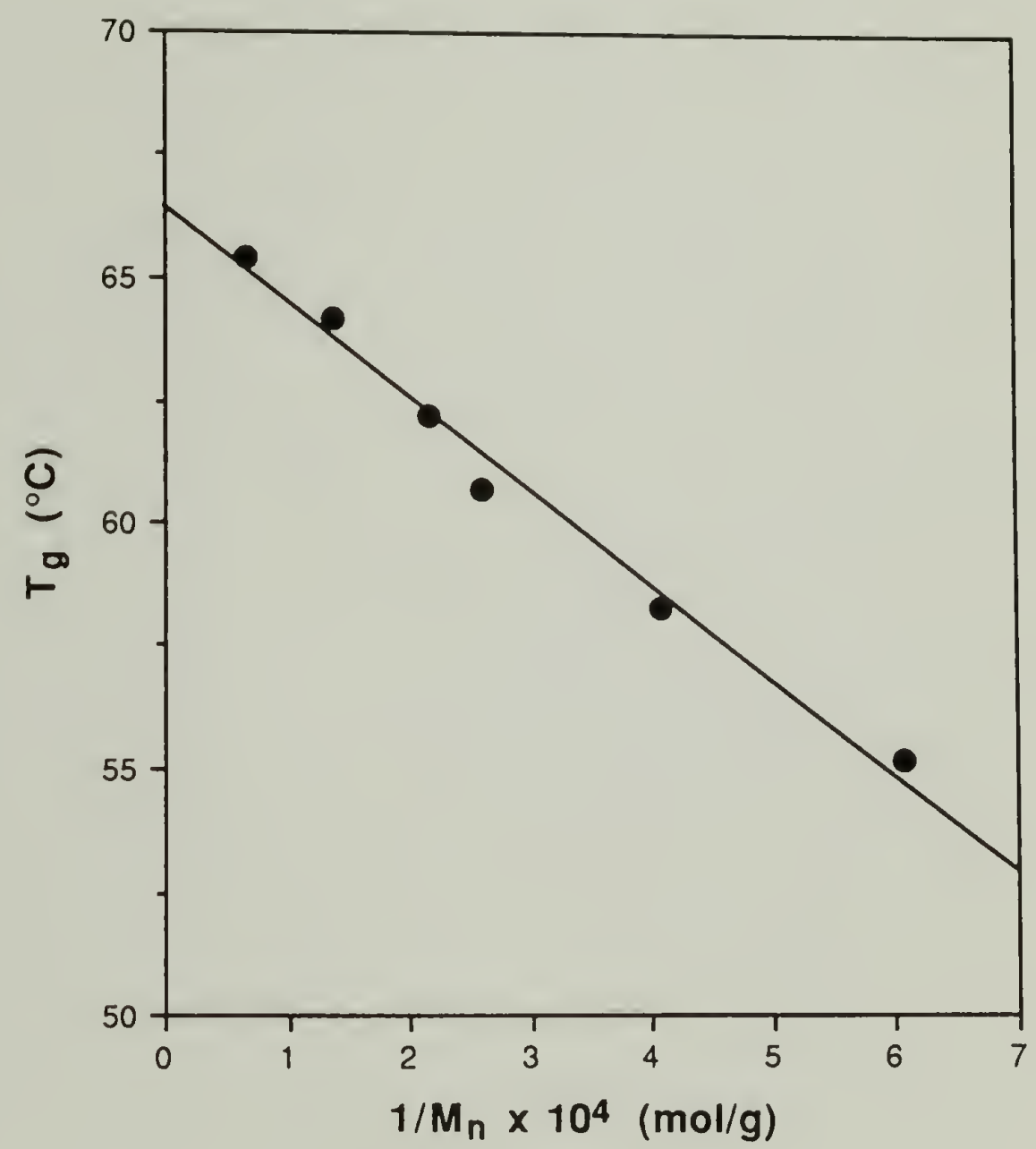

Figure 3.7 T_g vs. $1/M_n$ of PEMPT1-OH15 through PEMPT6-OH15 samples.

that upon increasing the substituted group's length, the packing efficiency of the chains is decreased. This can be thought of as an increase in the free volume of the polymer which will consequently decrease the T_g. In the case of both PDMPT and PEMPT, the energy barrier to rotation-stiffening effect is dominating the substituent length-free volume effect and a large increase in the T_g is observed compared to that of PPrT. The lengthening-free volume effect is also seen, with a decrease in T_g observed upon going from methyl-methyl to ethyl-methyl substitution.

Table 3.5 also displays the T_gs and ΔC_ps of PC1 and PC2. The T_g of PC1 is observed to be slightly lower than that of PC2. This is in conjunction with the lower molecular weight of PC1 relative to PC2.

The TGA data of Table 3.5 shows several features including that the temperature of the maximum rate of decomposition, T_d, is relatively insensitive to changes in the molecular weight. The average value for the entire molecular weight population being 468°C. This value is in agreement with the previously measured value identified during the screening study. Also reported for the PEMPT-OH15 samples is the % wt. loss at 300°C. It is observed that there is a general increase in the weight loss with decreasing molecular weight. This fact is most likely caused by the greater percentage of low molecular weight polymer that must be present in the molecular weight distribution of the PEMPT samples having smaller M_ns. At 300°C some of the oligomeric type species that make up the distribution may indeed be volatile or more prone to thermal degradation and lead to the observed weight loss.

3.4.6 Density

Since variations in T_gs can be described in terms of free volume effects associated with varying molecular weight polyesters, one might anticipate a systematic change in density among the polyesters. Table 3.5 also contains density data for the PEMPT samples. Indeed, a slight increase in density is observed with increasing molecular weight. However, the span is only $\pm$ 0.002 g/cm^3, which is within experimental error. On this basis, the densities are equivalent. The population as a whole has a density of 1.191 $\pm$ 0.003 g/cm^3. This value agrees with the reported densities of aliphatic side-chain substituted PET's, poly(1,2 pentylene terephthalate) and poly(1,2 hexylene terephthalate),

reported by Fagerburg [19]. The literature value for the density of PC is also listed [20].

3.4.7 Solubility of PEMPTB

With its amorphous structure, the solubility of PEMPT is expected to be increased over its crystallizable counterparts PET and PBT. Table 3.6 identifies the solubility of PEMPTB in a variety of solvents. The table is divided by solvent type including: aliphatic, alcoholic, aromatic and chlorinated. In addition, some other commonly used solvents were also tested. Included in Table 3.6 is the solubility parameter of each solvent [21].

PEMPTB is completely insoluble in both aliphatic and alcoholic type solvents. The solubility parameters of these solvents are characterized as being on the upper and lower end of those tested. PEMPTB is insoluble in dimethyl sulfoxide, another high solubility parameter solvent. On the other hand, PEMPTB is completely soluble in all the aromatic and chlorinated solvents tested. These solvents have solubility parameters in the range of 8.5-10.5 $(cal/cm^3)^{1/2}$. In addition, PEMPTB is soluble in THF and methyl ethyl ketone, both having solubility parameters in the above range. PEMPTB is partially soluble in three other polar aprotic solvents; n,n-dimethylformamide, acetonitrile, and acetone. These three solvents have solubility parameters just inside or slightly above the upper limit listed above.

The average solubility parameter of the ten solvents that PEMPTB is completely soluble in will be taken as a rough approximation for the solubility parameter of PEMPT itself. This value is 9.4 ± 0.6 $(cal/cm^3)^{1/2}$. Using the molar attraction constants of Van Krevelen [22], a solubility parameter of 9.44 $(cal/cm^3)^{1/2}$ is calculated from group contributions. This value is in agreement with the experimental observations. As anticipated, PEMPT, due to its amorphous structure, is soluble in a considerably wide variety of solvents compared to PET and PBT. At room temperature, PET and PBT are only soluble in phenols, phenol-chlorohydrocarbon mixtures and trihalogenoacetic acids [23].

Table 3.6 Solubility of PEMPTB

Solvent	δ ([cal/cm^3]$^{1/2}$)	Solubility (25 h)	Solubility (75 h)
Hexane	7.3	I	I
Heptane	7.45	I	I
Decane	7.75	I	I
Cyclohexane	8.2	I	I
Methanol	14.5	I	I
Ethanol	12.7	I	I
1-Propanol	11.9	I	I
1-Butanol	11.4	I	I
Benzene	9.15	S	S
Toluene	8.9	S	S
P-Xylene	8.8	S	S
Dichloromethane	9.7	S	S
Chloroform	9.3	S	S
Carbon Tetrachloride	8.6	S	S
1, 2-Dichloroethane	9.8	S	S
1,1,2,2-Tetrachloroethane	10.4	S	S
Dimethyl Sulfoxide	13.4	I	I
N, N-Dimethylformamide	12.1	P	P
Acetonitrile	11.9	P	P
Acetone	10.0	P	P
Tetrahydrofuran	9.9	S	S
Methyl Ethyl Ketone	9.3	S	S

I: Insoluble.
S: Soluble.
P: Partially soluble, solvent plasticized PEMPT.

3.5 End Capping of PEMPT

3.5.1 Introduction

The end capping of PEMPT is conducted for two reasons. One, which has been previously discussed, is for the determination of the polyester's M_ns. The second is to identify the effect of end group type on the phase behavior of PEMPT/PC blends. End capping is one possible method of preventing end group transreaction. The study of how these end groups may effect blend phase behavior is thus important. PEMPT samples will be end capped with two different acid chlorides, heptafluorobutyryl chloride and benzoyl chloride.

Original end capping experiments follow a standard procedure used for the determination of polyester M_ns [24]. In particular, the molecular weight of poly(butylene terephthalate) (PBT) and other aromatic-aliphatic polyesters has been determined by reacting the hydroxyl groups with succinic anhydride creating an acid end group [1,25]. A quantitative measure of the number of end groups (and hence, the number of polymer molecules) per gram of sample may then be obtained from a simple titration.

Following the procedure of Pilati, et al. [1], acylation of PEMPT with succinic anhydride in refluxing 1,1,2,2-tetrachloroethane with pyridine as the acylation catalyst led to coloration of the initially clear, colorless solution. This color varied from yellow to dark brown as the reaction progressed. The precipitated polymer, which had been washed repeatedly with methanol followed by vacuum drying, remained grey-brown in color. When redissolved in chloroform, the polymer once again formed a dark, brown solution. Determination of the number of acid end groups; by titration with a standardized, basic alcohol solution using phenol red as an indicator was impossible due to this dark, brown color. Repeated attempts at the acylation reaction yielded similar results.

With these disappointing results, a different approach was consequently taken to determine the hydroxyl end group content of the polyester. Alcohols are known to react with acid chlorides to very high yields under relatively mild conditions [26]. Perfluorinated acid chlorides are particularly reactive due to the strong electron withdrawing ability of the fluorines alpha to the carbonyl. Additionally, elemental analysis of fluorine is well developed [27-30] with detection limits on the order of 10^{-6} M [27]. Reaction of the hydroxyl end groups

of PEMPT with heptafluorobutyryl chloride (HFBC) produces a fluorine rich ester end group. At molecular weights of about 40,000 g/mol, the fluorine content is approximately 0.6 wt % which is measurable to within 10 % by standard analytical techniques. At molecular weights of 4,000 g/mol the precision is about 1 % and the relatively high fraction of end groups enables one to monitor the progress of the end capping reaction by NMR. This technique offers the additional advantage of small sample size (2-5 mg) required for analysis compared to that for common titration procedures (~0.5 g). However, this procedure does not account for the presence of the small amount of acid end groups which remain after the initial polyesterification. Corrections to the molecular weight due to these moieties were described earlier.

3.5.2 Materials

The PEMPT samples varying in molecular weight that had been recovered from the reaction tube (single precipitated) and PEMPTB were used for the end capping procedure. Heptafluorobutyryl chloride (HFBCl) (Aldrich 98%) was distilled trap-to-trap and stored under nitrogen prior to use. Benzoyl chloride (BZCl) (Aldrich 99 +%) and pyridine (Aldrich 99+%, anhydrous) were used as received. Chloroform (Aldrich, HPLC grade) was distilled under nitrogen from P_2O_5 and stored under nitrogen.

3.5.3 Procedure

The HFBCl end capping procedure is described below. Variations to the procedure for the BZCl end capping follow this description. Chloroform (40 mL) was transferred via cannula to a nitrogen-purged 100 mL round bottom flask containing 0.8 g of PEMPT and a magnetic stir bar. Three hours were allowed for the the polymer to dissolve at ambient temperature. HFBCl (0.65 mL, 4.4 mmol) was then added via syringe while the solution was vigorously stirred. Two samples for each molecular weight PEMPT were prepared in this manner. After all samples had been prepared, the 100 mL R.B. flasks were placed in a Lab-Line, Orbit Environ-Shaker operating at approx. 60 rpm. All reactions were carried out at room temperature with one set of samples removed after 18 h while the other set was removed after 94 h of reaction.

The polymers were recovered by a precipitation procedure which terminated the end capping reaction. The solutions were added dropwise to 400 mL methanol under rigorous mixing. The precipitated polymers were then rigorously washed with 3 x 40 mL aliquots of fresh methanol followed by drying under vacuum at 80 °C for 5 days. The other set of samples was recovered and dried in a similar fashion after 94 h of reaction at ambient temperature.

Variations to the procedure for BZCl end capping included the use of smaller sample sizes ~ 0.2 g. The volume of chloroform was subsequently decreased to 10 mL. BZCl (0.37 mL, 3.2 mmol) was added along with pyridine (0.26 mL, 3.2 mmol) as catalyst. These reactions were carried out at ambient temperature for 48 h. The samples were precipitated into 100 mL methanol, followed by washing with 3 x 10 mL fresh methanol. The polyesters were dried as described above. In addition to these samples, control samples of PEMPT varying in molecular weight were also prepared. These samples followed the procedure for the BZCl end capped PEMPTs, except no BZCl or pyridine was added to the solution. The three sets of samples, HFBCl end capped, BZCl end capped and the controls are designated as PEMPT-HFB, PEMPT-BNZ and PEMPT-OH2, respectfully. The "OH" once again represents the hydroxyl end group and the "2" signifies that these polyesters were recovered from a 2 % w/v PEMPT/chloroform solution. The corresponding three end groups structures are shown in Figure 3.8.

3.6 Characterization of End Capped PEMPTs: Results and Discussion

Fluoride analysis was conducted at the University of Massachusetts Microanalysis Laboratory. The procedure involves combustion of the sample utilizing the Schoniger oxygen-flask technique with capture of the fluoride ions in an aqueous solution [30]. Fluoride concentration is then determined using a calibrated, fluoride selective electrode. The M_ns determined from the fluoride analysis were discussed in Section 3.4.2 and will not be reiterated here. One point which directly effected the M_n calculation, extent of hydroxyl conversion in the PEMPT-HFB samples, is presented here. The reason for delaying discussion of this point is that % conversion was determined from ^1H NMR and it is felt that NMR analysis would be better understood in the context of this section on end capping. Proton NMR, GPC and DSC were conducted as

a)

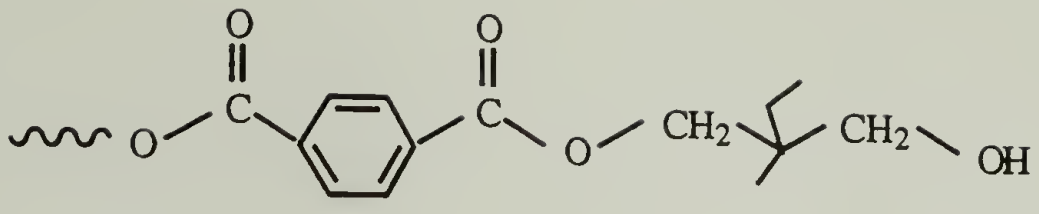

b)

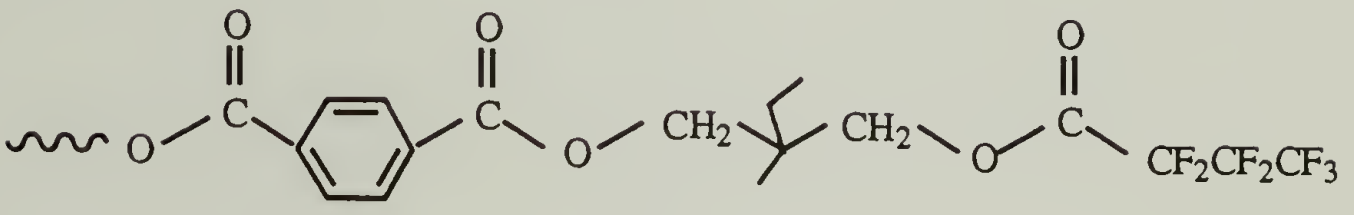

c)

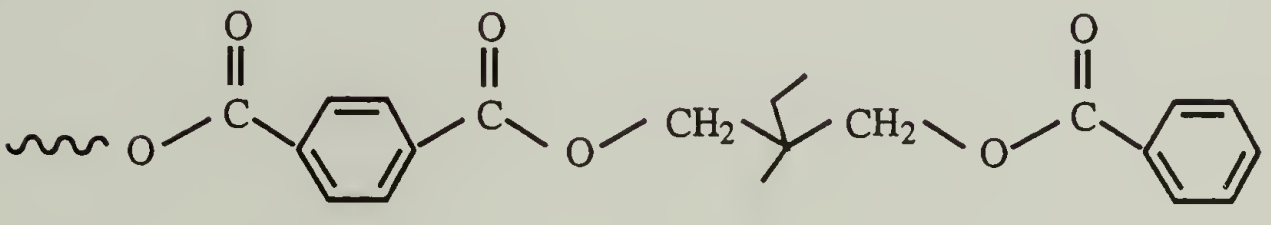

Figure 3.8 End group structures of PEMPT a) PEMPT-OH b) PEMPT-HFB and c) PEMPT-BNZ.

previously described in this chapter. The exception being that DSC data is the average of two separate runs per polyester.

3.6.1 ^{1}H NMR

End capping reactions allow the identification and confirmation of resonances associated with the hydroxyl end groups in the as synthesized (hydroxyl terminated) PEMPT. Thus, what follows is an intermixed discussion of the NMR of the end capped samples, as well as, that of the original polyesters. Figure 3.9a,b shows the substitutions on the propylene group of PEMPT including dual aromatic ester and aromatic ester/hydroxyl, respectfully. The protons have been alphabetically coded (note: the coding does not correspond to that of section 3.4.3). The ^{1}H NMR spectra of PEMPT-OH15 with molecular weights varying from 4,100-37,500 g/mol (reaction times varying from 10-180 min) are shown in Figure 3.10. The region displayed corresponds to the backbone methylene protons of the propylene group (protons **a**, **b** and **c** in Figure 3.9a,b). The large singlet at 4.290 ppm has previously been assigned to the methylene protons with dual aromatic ester substitution, protons **a**. Two additional resonances, a singlet at 4.231 ppm and a multiplet centered at 3.423 ppm, decrease with increasing molecular weight (increasing polymerization time). With the number of end groups expected to decrease with increasing second stage reaction time (increasing M_n), these resonances are tentatively assigned to the methylene protons of a hydroxyl terminated propylene group, **b** and **c**, respectively.

Upon formation of the hydroxyl end group (Figure 3.9b), the resonance associated with the methylene protons adjacent to the remaining aromatic ester, protons **b**, are expected to remain a singlet and be shifted slightly upfield. This is caused by the removal of the other deshielding aromatic ester. The resonance at 4.231 ppm is assigned to these methylene protons. Methylene protons adjacent to a hydroxyl groups are known to be multiplets due to splitting associated with the adjacent hydroxyl proton [26]. This fact, combined with the large upfield shift expected with the removal of the aromatic ester, enables the multiplet at 3.423 ppm to be assigned to the methylene protons adjacent to the hydroxyl end group, protons **c**. The relative shift of proton **b** downfield from proton **c** is in general agreement with the shifts seen in model compounds studied by Judas, et al. [4]. It should be noted that the resonance of the hydroxyl

a)

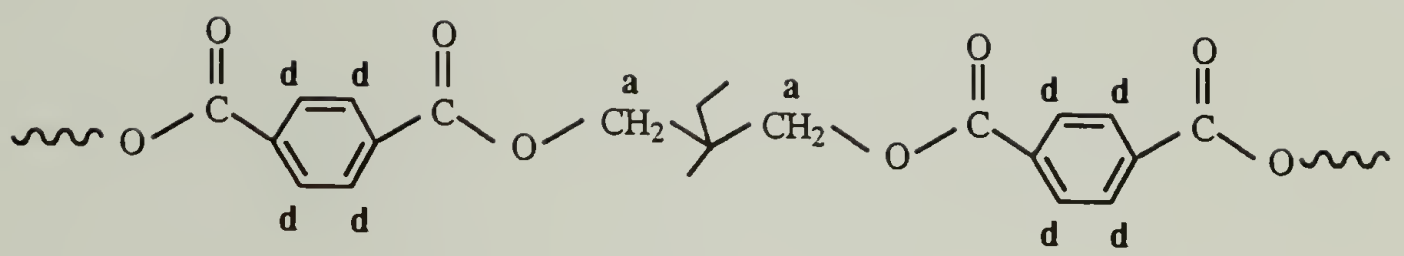

b)

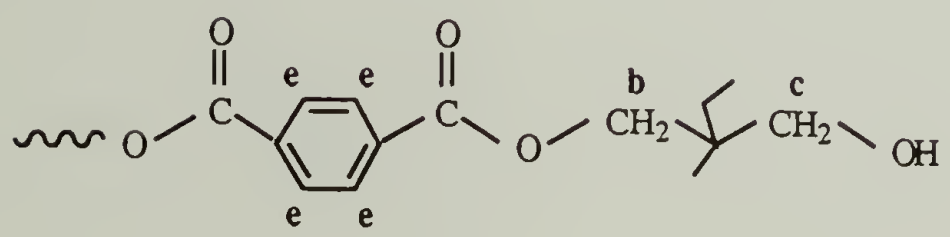

Figure 3.9 Substitution of the propylene group of PEMPT a) dual aromatic ester and b) aromatic ester/hydroxyl.

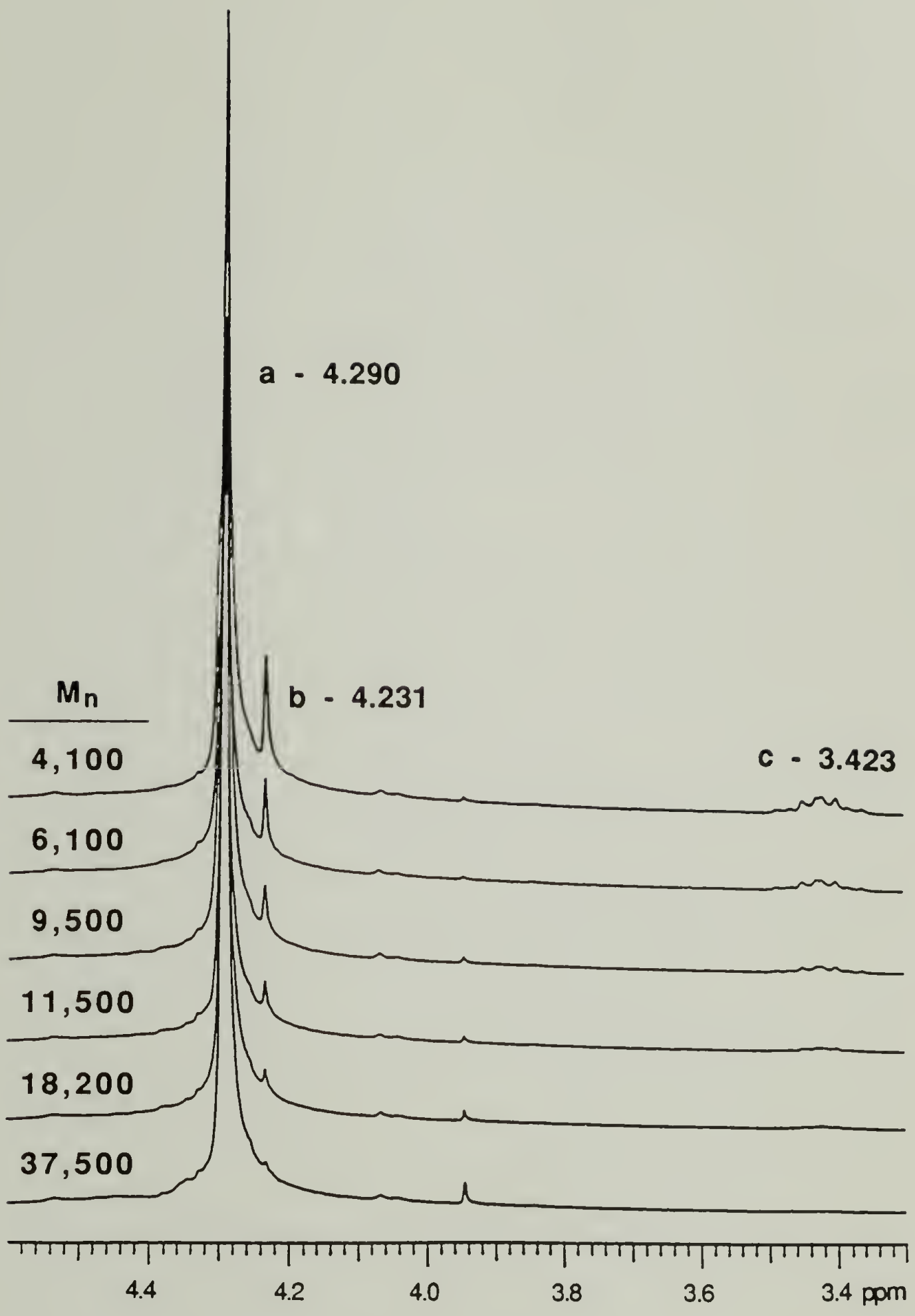

Figure 3.10 300 MHz ^{1}H NMR spectra displaying the backbone methylene region of PEMPT at the indicated molecular weights.

proton is observed as a triplet at 2.174 ppm. This fact has been varified by the addition of deuterium oxide to the NMR sample solution. A decrease in intensity of the 2.174 ppm resonance, as well as, a collapse of the multiplet at 3.423 ppm to a quartet is observed, Figure 3.11a,b. This behavior is expected for hydrogen-deuterium exchange of an alcohol, providing additional confirmation for the above peak assignments. Additional evidence that these two resonances are associated with hydroxyl terminated propylene end groups is contained in the ^{1}H NMR spectra of the HFBC end capped PEMPT samples.

Figure 3.12a-c shows the identical region of the ^{1}H spectra corresponding to PEMPT2 reacted with HFBC for 0, 18, and 94 h., respectively. Both the resonances at 4.231 ppm and 3.423 ppm are seen to decrease in intensity with increasing end capping time. The decrease in intensity of these two resonances with increased end capping time, representing the conversion of the hydroxyl groups to heptafluorobutyrate esters, confirms that these resonances correspond to the methylene protons of the hydroxyl terminated propylene group. Similarly, Figure 3.13 shows the same region of the spectra for the PEMPT2 after reaction with BZCl. Both the 4.231 and 3.423 ppm resonances are gone, reaffirming the assignments.

Similarly, Figure 3.14 displays the aromatic region associated with the ^{1}H NMR of the non-end capped PEMPT samples. The large resonance at 8.081 ppm has previously been assigned to the protons of a terephthalate ring with dual aliphatic-aromatic ester substitution (protons **d** in Figure 3.9a). The smaller resonance at 8.065 ppm decreases with increasing M_n. This peak will be assigned to the protons of a terephthalate ring with aliphatic-aromatic ester/aliphatic-hydroxyl substitution (protons **e** in Figure 3.9b). This assignment is confirmed once again by examining the proton spectra of the HFBC end capped samples. Figure 3.15a-c displays the aromatic region corresponding to the proton NMR of PEMPT2 reacted with HFBC for 0, 18 and 94 h. It is observed that as end capping reaction time increases, the resonance at 8.065 ppm decreases. The decrease in intensity of this peak with increased end capping time once again corresponds to the conversion of the hydroxyl groups to heptafluorobutyrate groups and varifies the assignment of this resonance. Additionally, the proton NMR of the aromatic region of PEMPT2-BNZ, Figure 3.16, shows complete disappearance of this resonance and a new resonance at 8.070 ppm. It is apparent from this discussion that the terephthalate group adjacent to the terminal propylene group is magnetically non-equivalent to the

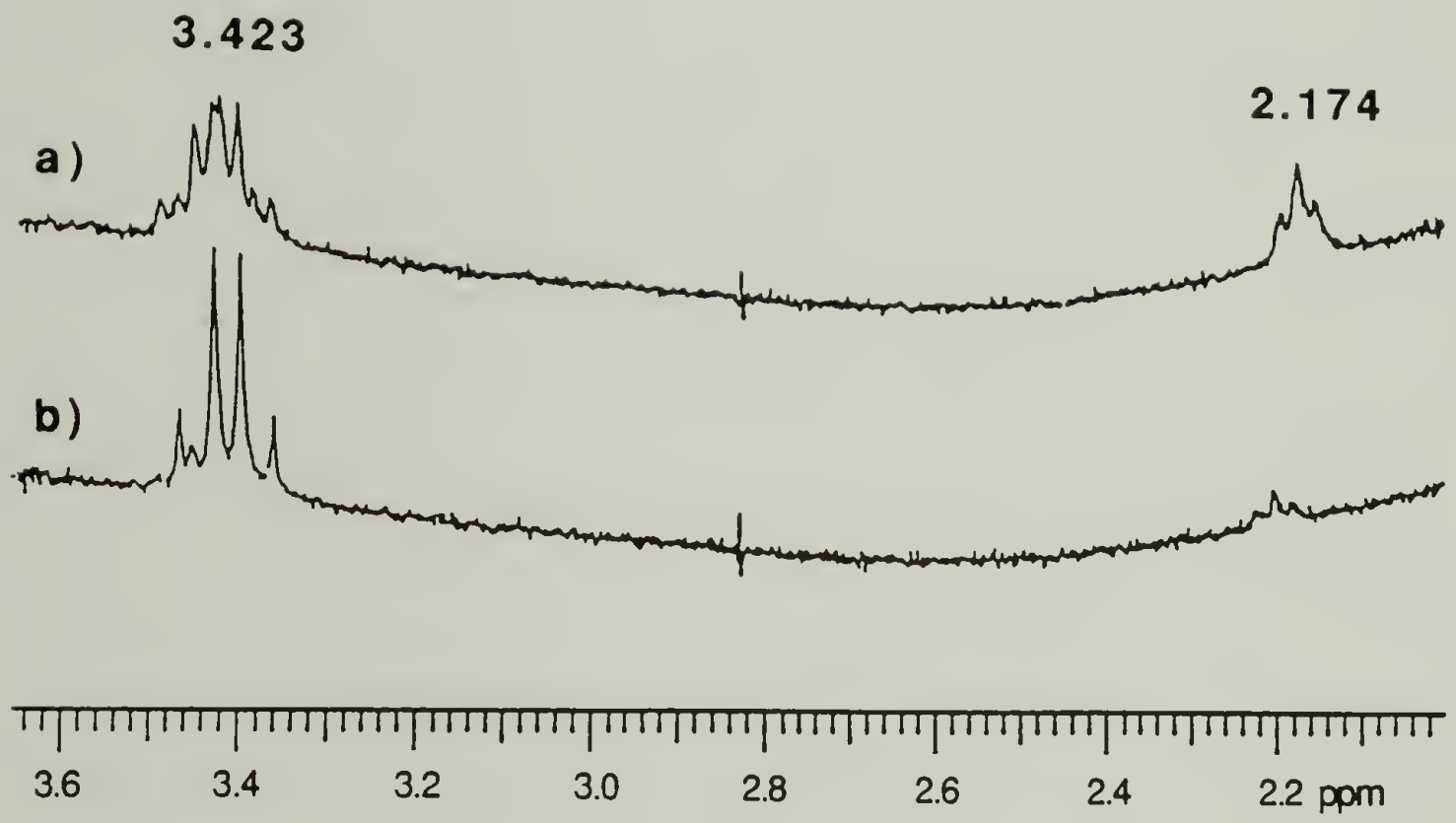

Figure 3.11 300 MHz ^{1}H NMR spectra displaying the backbone methylene and the hydroxyl region of PEMPT a) before and b) after D_2O wash.

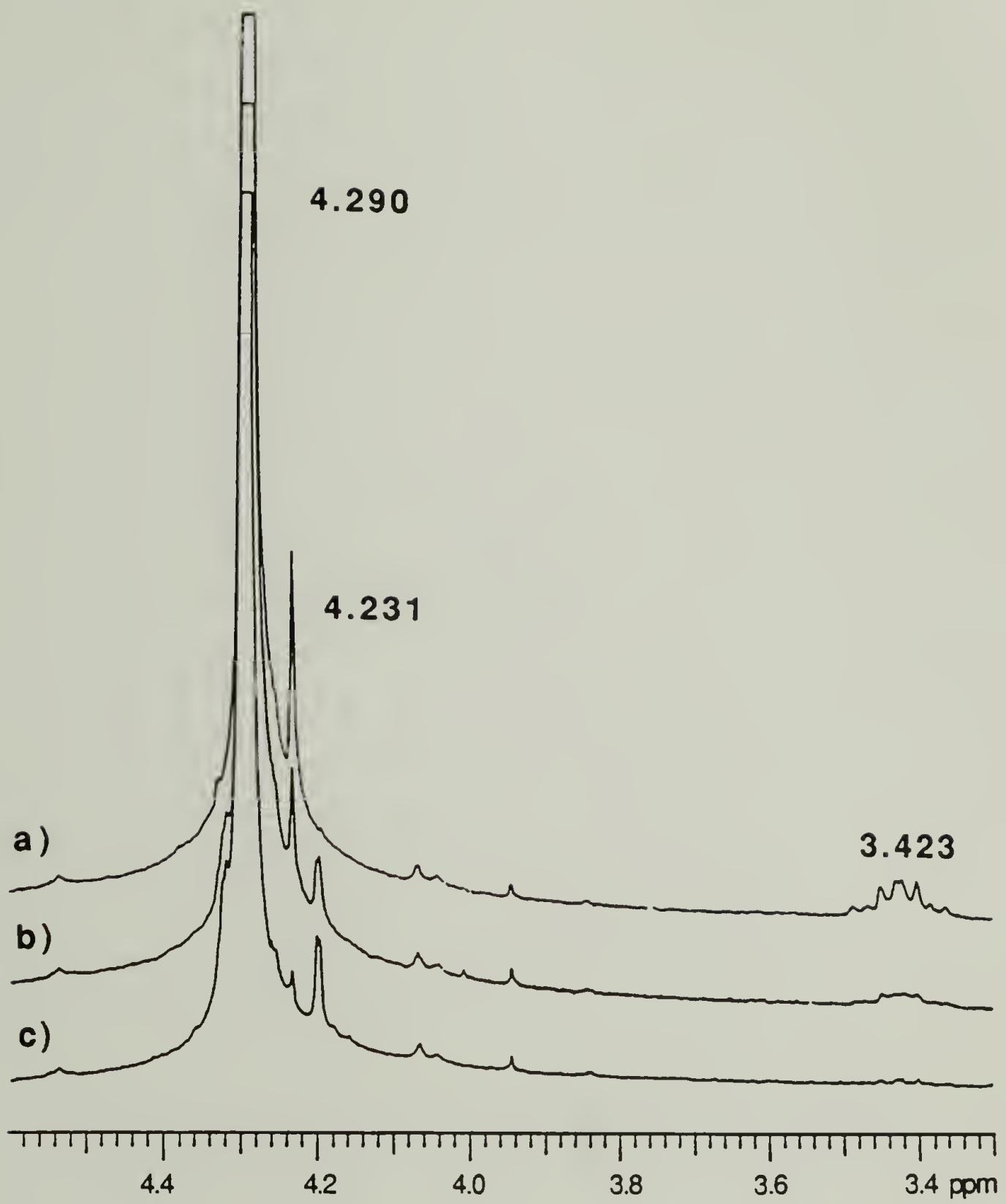

Figure 3.12 300 MHz ^{1}H NMR spectra displaying the backbone methylene region of PEMPT2. End capping reaction times with HFBCl of a) 0 b) 18 c) 94 h.

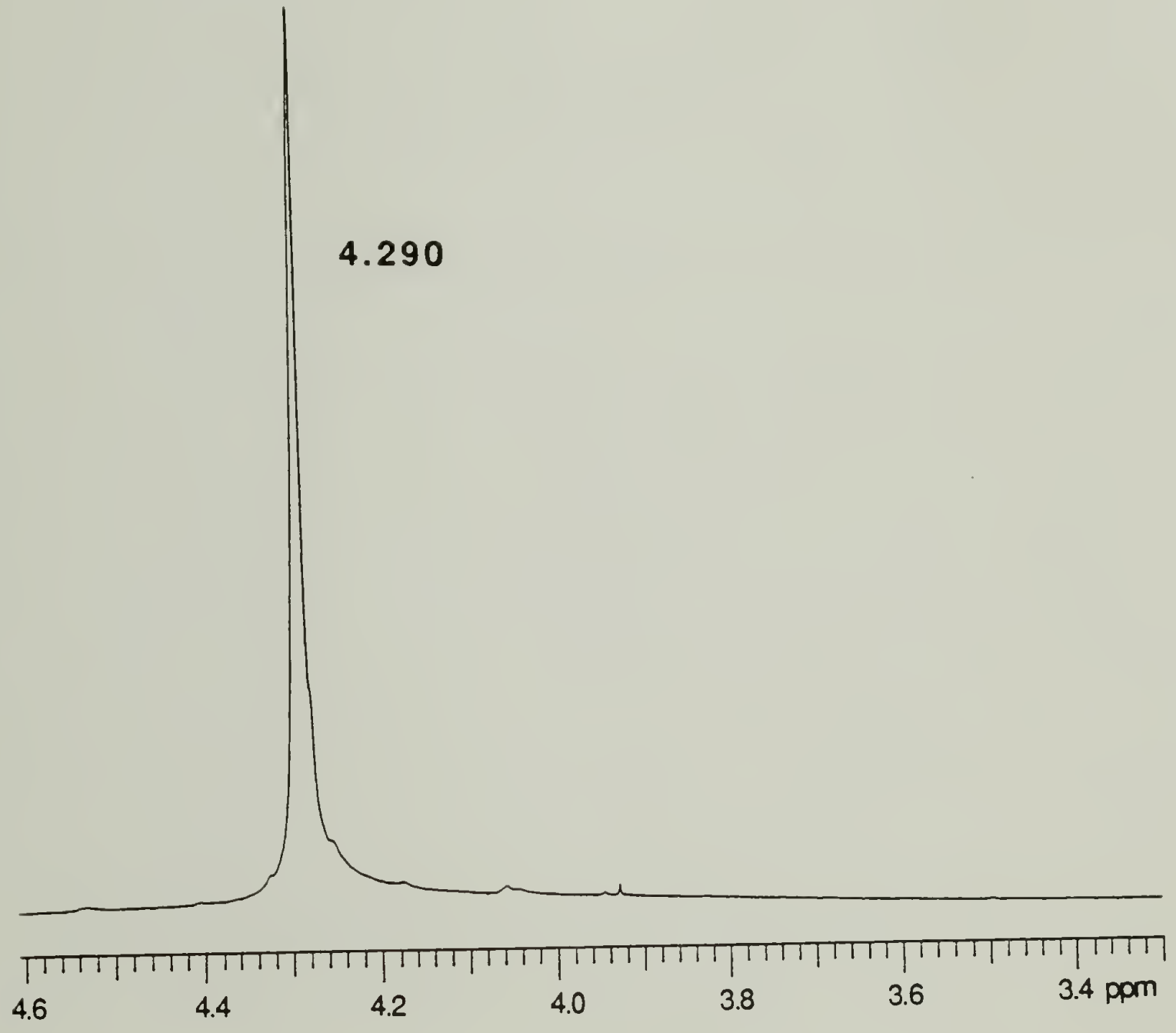

Figure 3.13 300 MHz ^{1}H NMR spectrum displaying the methylene backbone region of PEMPT2 after end capping with BZCl.

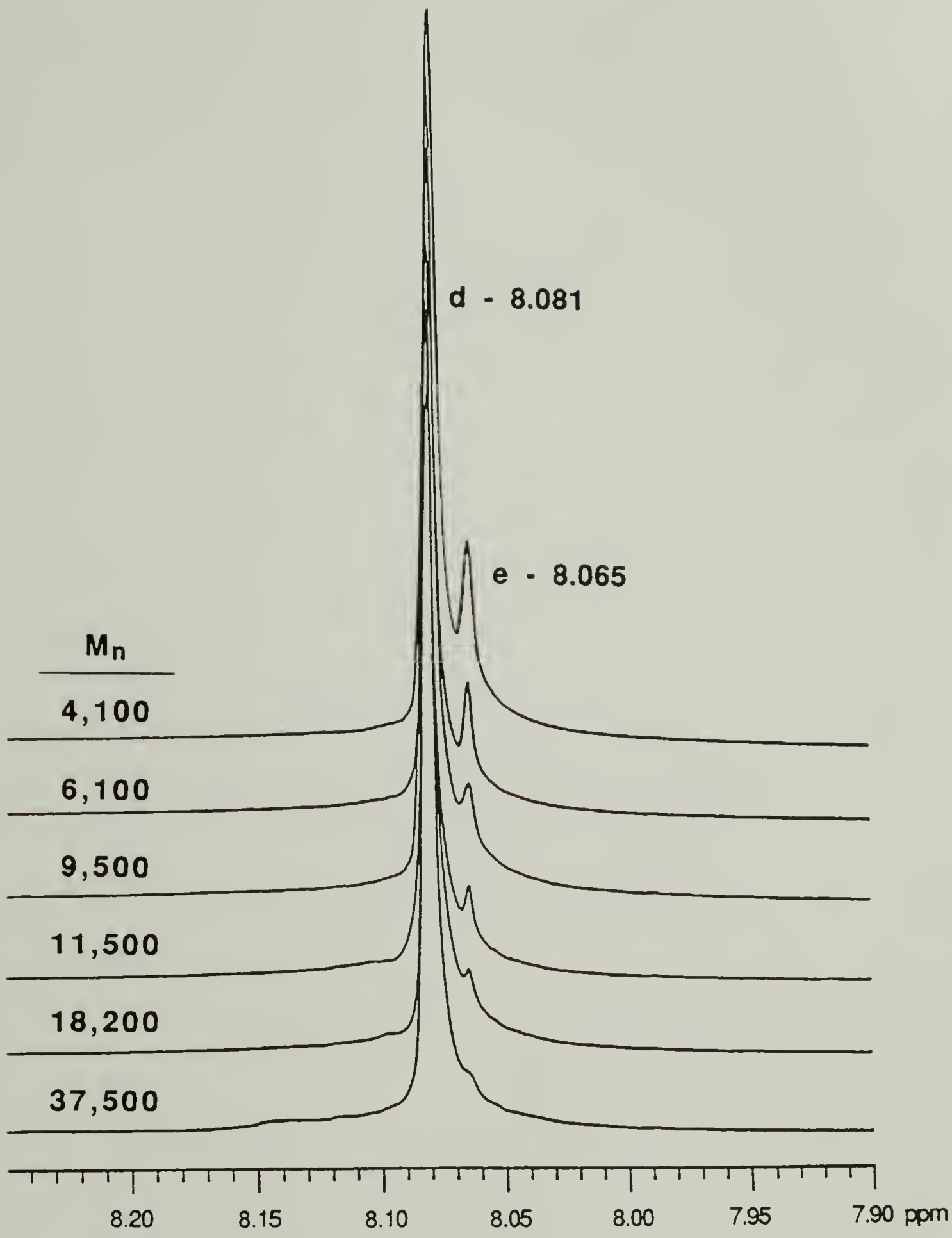

Figure 3.14 300 MHz ^{1}H NMR spectra displaying the aromatic region of PEMPT at the indicated molecular weights.

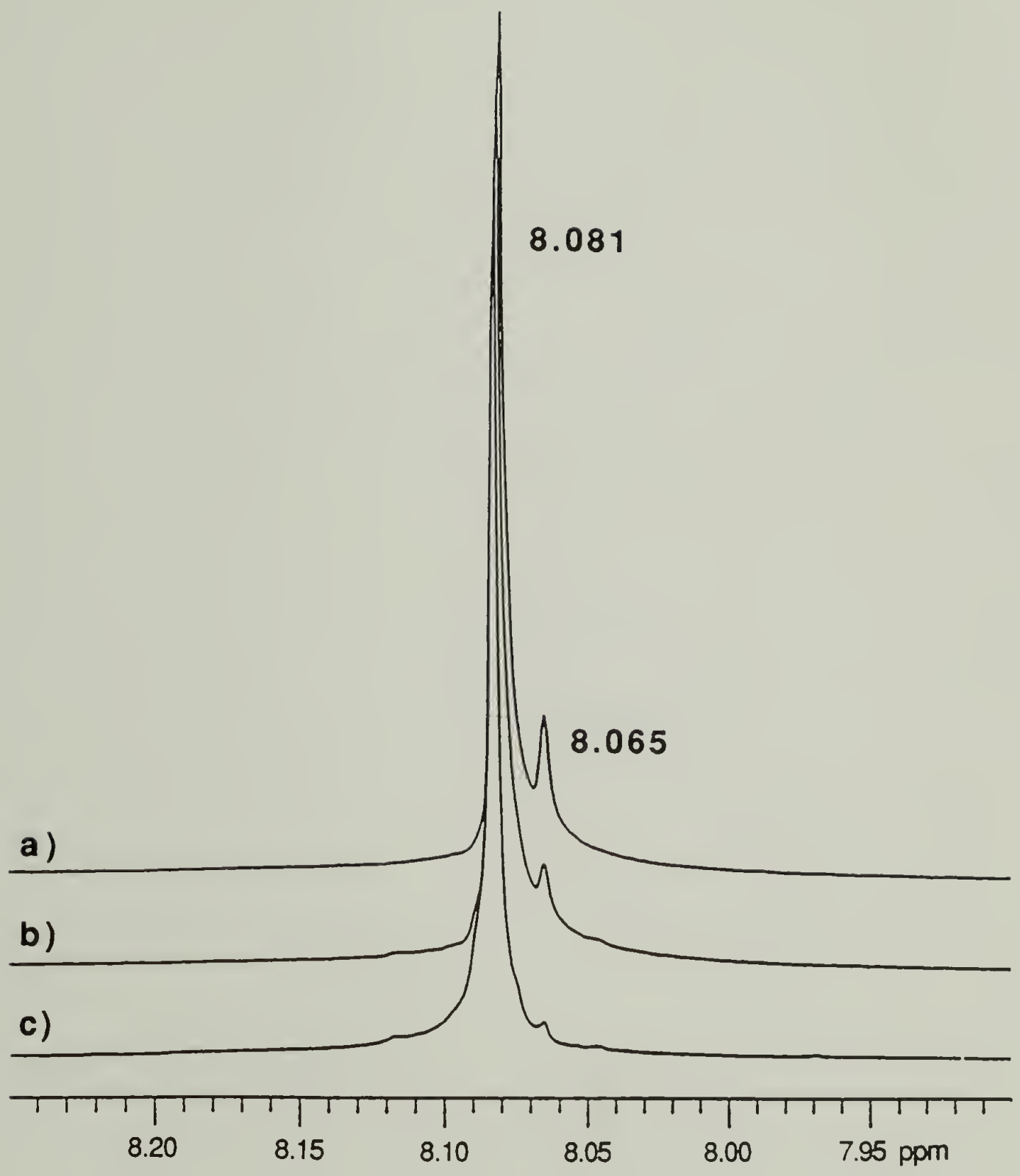

Figure 3.15 300 MHz ^{1}H NMR spectra displaying the aromatic region of PEMPT2. End capping reaction times with HFBCl of a) 0 b) 18 and c) 94 h.

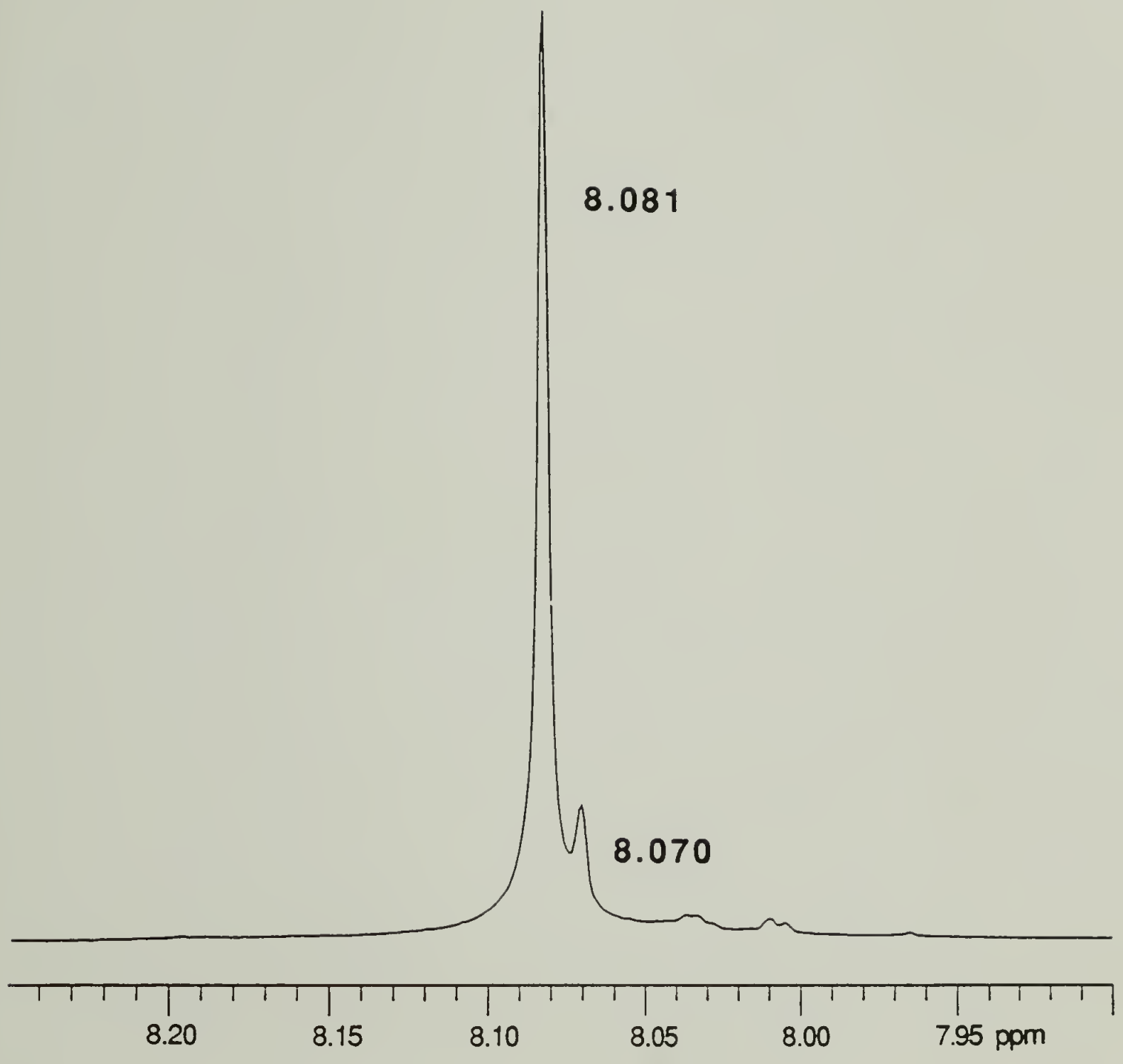

Figure 3.16 300 MHz ^{1}H NMR spectrum displaying the aromatic region of PEMPT2 after end capping with BZCl.

terephthalic groups with dual aliphatic-aromatic substitution (hydrogens **d** in Figure 3.9a). It should be mentioned, that it was these two resonances, 8.081 and 8.065 ppm, that were used to calculate M_ns from ^1H NMR (Table 3.2)

Figures 3.13 and 3.16 indicate complete conversion of hydroxyl groups to benzylate end groups. In contrast, it is observed in Figures 3.12 and 3.15, that the resonances associated with the propylene-hydroxyl end group, 4.231, 3.423 and 8.065 ppm, are still observable after 94 h of reaction. This indicates that the end capping with HFBCl was not completely quantitative. Using the resonance at 8.065 ppm, it is estimated from the ^1H NMR spectra of end capped and non-end capped PEMPT1-OH15 and PEMPT2-OH15 samples that 10 ± 3% of the hydroxyl groups remained after end capping. In order to obtain an accurate measure of the number average molecular weight, it is required that the measured wt % fluoride be adjusted accordingly. It is this adjustment that was previously mentioned in section 3.3.2.1.

3.6.2 Molecular Weights: GPC

Table 3.7 displays the molecular weight data obtained from GPC for PEMPT-OH2, PEMPT-HFB and PEMPT-BNZ. The values for PEMPT-HFB and PEMPT-BNZ are in good agreement . At the high molecular weights, the polydispersity (M_w/M_n) approaches a value of 2, which is the theoretical prediction for polyesters synthesized by a step growth mechanism [31]. It is noticed that as the molecular weight decreases for these two end capped polymers, the polydispersity decreases. This behavior is thought to be associated with the precipitation procedure used to recover the polyesters. It must be assumed that polymers/oligomers below a certain low molecular weight will be soluble in the solvent used for recovery, especially at the low polymer concentrations employed during recovery. As the molecular weight decreases, the fraction of low molecular weight species increases, thus, a greater fraction of these low molecular weight species are removed. The consequence of this behavior is that as the polyester molecular weight is lowered, the polydispersity is also decreased. Deviations from this behavior are observed in the samples of PEMPT-OH15 and PEMPT-OH2 (Tables 3.3 and 3.7).

Comparing the M_ns of these two hydroxyl terminated polyesters, the values are in good agreement with one another, indicating that the original

Table 3.7 Molecular Weights of End Capped PEMPTs from GPC Analysis

Polyester	M_n (g/mol)	M_w (g/mol)	M_z (g/mol)	M_w/M_n	M_z/M_w
PEMPT1-OH2	3,440	8,070	12,170	2.343	1.508
PEMPT2-OH2	5,559	13,310	20,540	2.395	1.543
PEMPT3-OH2	10,180	21,210	33,020	2.085	1.557
PEMPT4-OH2	12,230	25,410	39,500	2.077	1.555
PEMPT5-OH2	17,100	34,100	52,690	1.994	1.545
PEMPT6-OH2	21,070	42,260	65,230	2.006	1.544
PEMPT1-HFB	6,310	8,751	11,934	1.387	1.364
PEMPT2-HFB	8,840	13,370	19,090	1.513	1.428
PEMPT3-HFB	12,500	21,280	31,992	1.703	1.503
PEMPT4-HFB	14,430	25,450	38,643	1.764	1.518
PEMPT5-HFB	18,370	34,170	52,290	1.860	1.530
PEMPT6-HFB	21,820	42,410	65,340	1.944	1.507
PEMPT1-BNZ	5,549	8,010	11,240	1.443	1.404
PEMPT2-BNZ	8,620	13,190	18,950	1.530	1.436
PEMPT3-BNZ	11,530	20,280	30,820	1.759	1.520
PEMPT4-BNZ	13,550	24,460	37,280	1.805	1.524
PEMPT5-BNZ	17,990	33,650	51,240	1.871	1.523
PEMPT6-BNZ	21,670	41,990	64,200	1.938	1.529

PEMPT/chloroform ratio (2% and 15%) did not significantly alter the molecular weights/distributions of these two sets of polyesters. It should be mentioned that the chloroform/methanol ratio used during precipitation was identical for the two hydroxyl terminated polyesters and for the end capped samples as well. This ratio is perhaps more important if low molecular weight species are soluble in the recovery solvent.

Comparing these M_ns with the values for PEMPT-HFB and PEMPT-BNZ, significant differences are observed between the hydroxyl and end capped polyesters. This difference is most prominent at the two lowest molecular weights. The higher molecular weights, however, are observed to be in good agreement with the end capped samples. It is also noticed that the decrease in the polydispersity with decreasing molecular weights is not observed in the hydroxyl terminated samples. The two lowest molecular weights have polydispersities significantly greater than that predicted from theory. Thus it appears that at the low molecular weights, high hydroxyl content, PEMPT-OH2 and PEMPT-OH15 are interacting with the GPC columns. Interaction with the columns would be expected to slow the travel of the polyesters, making the calculated M_ns lower and the polydispersity greater, as is observed. It should also be pointed out that the molecular weight averages that are less dependent on low molecular weight species, M_w and M_z, are in much better agreement with the end capped samples at all molecular weights. This would also indicate that the lowest molecular weight species are indeed interacting with the column.

3.6.3 Thermal Analysis

Table 3.8 displays the thermal data obtained from DSC. As expected, all three sets of data show decreasing T_gs as the M_n (determined from HFBC end capping and corrected for acid end groups) decreases. The interesting characteristic of this data is that the end capped samples have T_gs that are lower than the hydroxyl terminated polyesters. Figure 3.17 shows a plot of T_g vs. $1/M_n$ for PEMPT-OH2, PEMPT-HFB, and PEMPT-BNZ. The T_gs of the end capped samples are nearly identical, while the deviations between the hydroxyl and capped T_gs increases with decreasing M_n. The extrapolation to infinite molecular weight all approach a similar value in the range of 66-68°C.

It appears that the ability of the PEMPT-OH samples to hydrogen bond is altering the physical properties of these samples. Hydrogen bonding would act

Table 3.8 Thermal Analysis Data of End Capped PEMPTs

M_n (g/mol)	PEMPT-OH2		PEMPT-HFB		PEMPT-BNZ	
	T_g (°C)	ΔC_p (J/g °C)	T_g (°C)	ΔC_p (J/g °C)	T_g (°C)	ΔC_p (J/g °C)
4,100	56.5	0.250	48.2	0.219	47.4	0.230
6,100	61.1	0.254	54.3	0.244	54.5	0.263
9,500	63.1	0.250	58.7	0.264	57.9	0.258
11,500	64.2	0.257	60.7	0.262	59.5	0.279
18,200	65.5	0.243	63.1	0.266	62.4	0.257
37,500	65.9	0.237	65.1	0.263	64.1	0.258

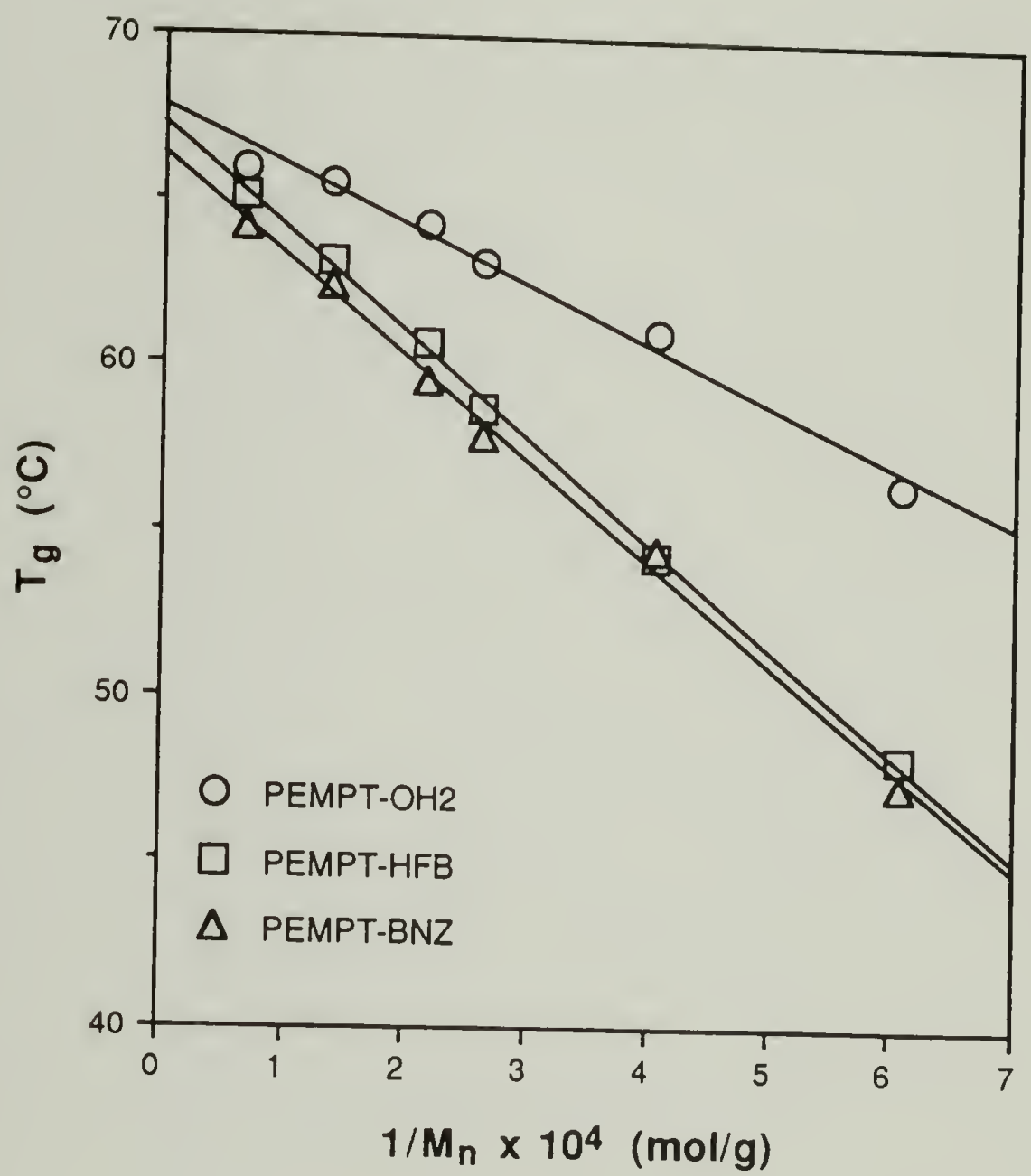

Figure 3.17 T_g vs. $1/M_n$ of the indicated end capped PEMPTs.

to stiffen the chain and increase T_g. At low molecular weights, where the greatest concentration of OH groups exist and the greatest level of hydrogen bonding is anticipated (see Section 3.4.4), the interaction should be the highest. It is also expected that the effect would decrease as the concentration of end groups decreased (increasing molecular weight). The current observations are in agreement with these two statements. One additional point to be made about the thermal analysis of PEMPT-OH2 and PEMPT-OH15 blends is that the T_gs of PEMPT-OH15 samples are slightly lower than those of PEMPT-OH2 samples. The average difference is 1.7°C. The reason for the discrepancy is not apparent.

3.7 Conclusions

The synthesis, purification and characterization of the model polyester, PEMPT, was carried out using standard two stage polycondensation techniques with titanium (IV) isopropoxide as catalyst. Characterization included the following: carbon and hydrogen elemental analysis, end group analysis, molecular weight and distribution (end group, NMR and GPC analysis), ^1H and ^{13}C NMR spectroscopy, infrared spectroscopy, thermal analysis (DSC and TGA), density and solubility studies. Elemental analysis was in agreement with calculated values. Number average molecular weights were determined from a novel end capping technique which involved reacting the hydroxyl ends of PEMPT with HFBCl followed by the analysis of the wt % fluorine. M_ns ranging from 4,100 to 37,500 g/mol were calculated. The M_ns obtained from end capping were in agreement with the values calculated from ^1H NMR.

All of the main chain proton and carbon resonances of PEMPT were identified and assigned. They were in general agreement with literature values of similar compounds. Infrared spectroscopy was used in a qualitative sense to identify hydrogen bonding of the hydroxyl end groups. As expected, the 4,100 g/mol PEMPT exhibited a much greater level of hydrogen bonding compared to a 18,000 g/mol sample. DSC analysis exhibited only a single T_g, confirming the anticipated amorphous structure of PEMPT. The T_g of PEMPT varied with varying molecular weight, following the inverse function of molecular weight as predicted by Fox and Flory. T_gs ranged from 55.2°C-65.4°C as the molecular weight ranged from 4,100-37,500 g/mol. TGA analysis agreed with the earlier results of Chapter 2. The maximum rate of decomposition showed no molecular

weight dependence. The weight loss at 300°C increased slightly as molecular weight was lowered. The density of PEMPT was 1.191 g/cm^3, being relatively insensitive to molecular weight variations. This value agrees with the density of polyesters with similar structure. Due to its amorphous structure PEMPT displayed improved solubility compared to PET and PBT which are capable of crystallization. PEMPT was soluble in solvents that had solubility parameters in the range of 8.8-10.4 (cal/cm^3)$^{1/2}$.

In addition to this, the end capping of PEMPT with HFBCl and BZCl was described in detail. Characterization of these samples included ^{1}H NMR, GPC, and DSC. Comparison of the NMR analysis of these samples and the previously mentioned hydroxyl terminated polyesters allowed the unambiguous assignment of resonances corresponding to the hydroxyl end groups in PEMPT. These resonances can now be used to identify alcoholysis interchange reaction between the hydroxyl groups of PEMPT and the carbonate groups of PC. The resonances were also used to monitor the two end capping reactions.

GPC results on the end capped samples agree with one another across the entire polyester molecular weight range examined. In general, the molecular weight distribution narrowed as the molecular weight of the polyester was lowered. This is thought to be caused by selective fractionation of the low molecular weight species during the recovery/purification of the polyesters. At high molecular weights, the measured polydispersity agreed with the theoretical value of two. GPC results on the hydroxyl terminated polyesters indicated that the polyesters of low molecular weight were interacting with the columns.

Within experimental error, the T_gs of the end capped PEMPTs were identical across the entire range of molecular weights analyzed. However, the T_gs of the HFB and BNZ end capped PEMPTs were not in agreement with the values determined for the hydroxyl terminated PEMPTs. In general, the T_gs of the hydroxyl terminated samples were greater than those of the HFB or BNZ terminated polyesters. The deviation increased as the molecular weight of the polyesters was lowered. This phenomenon was explained in terms of the hydrogen bonding capabilities of the hydroxyl terminated PEMPTs which could lead to a stiffer, higher T_g polyester. The T_gs of all three PEMPTs; OH, BNZ and HFB; extrapolated to the same value at infinite molecular weight.

3.8 References

1. Pilati, F.; Munari, A.; Manaresi, P.; Milani, G.; Bonora, V. *Eur. Polym. J.* **1987**, 23, 265.

2. Jonza, J.M., Ph. D. Dissertation, University of Massachusetts at Amherst, 1985.

3. Bovey, F.A.; Jelinski, L; and Mirau, P.A. *Nuclear Magnetic Resonance Spectroscopy*; Academic Press, Inc.: San Diego, California, 1988.

4. Judas, D.; Fradet, A.; Marechal, E. *Makromol. Chem.* **1983**, 184, 1129.

5. Godard, P.; Dekoninck, J.M.; Devlesaver, V.; Devaux, J., *J. Polym. Sci., Polym. Chem.* **1986**, 24, 3301.

6. Devaux, J.; Godard, P.; Mercier, P.; Touillaux, R.; Dereppe, J.M., *J. Polym. Sci., Polym. Phys. Ed.* **1982**, 20, 1881.

7. Murano, M.; Yamadera, R. *Polymer J.* **1971**, 2, 8.

8. Yamadera, R.; Murano, M. *J. Polym. Sci., A-1* **1967**, 5, 2259.

9. Chen, M.S.; Chang, S.J.; Chang, R.S.; Kuo, W.F.; Tsai, H.B. *J. Appl. Polym. Sci.* **1990**, 40, 1053.

10. Stokr, J.; Schneider, B.; Doskocilova, D.; Lovy, J.; Sedlacek, P. *Polymer* **1982**, 23, 714.

11. Ward, I.M.; Wilding, M.A. *Polymer* **1977**, 18, 327.

12. Addleman, R.L.; Zichy, V.J.I. *Polymer* **1972**, 13, 391.

13. Devaux, J.; Godard, P.; Mercier, J.P. *Polym. Eng. Sci.* **1982**, 22, 229.

14. Coleman, M.; Painter, P.C. *Appl. Spectr. Rev.* **1984**, 20, 255.

15. Wick, G.; Zeitler, H. *Die Angew. Macromol. Chem.* **1983**, 112, 59.

16. Fox Jr., T.G.; Flory, P.J. *J. Appl. Phys.* **1950**, 21, 581.

17. Fox Jr., T.G.; Flory, P.J. *J. Polym. Sci.* **1954**, 14, 315.

18. Smith, J.G; Kibler, C.J.; Sublett, B.J. J. *Polym. Sci.: A-1* **1966**, 4, 1851.

19. Fagerburg, D.R. *J. Appl. Polym. Sci.* **1985**, 30, 889.

20. Freitag, D.; Grigo, U.; Muller, P.R. in *The Encyclopedia of Polymer Science and Engineering, Vol. 11, 2nd Ed.*; Wiley: New York, 1988.

21. Gardon, J.L. *J. Paint Technol.* **1966**, 38, 43.

22. Van Krevelen, D.W. *Properties of Polymers Their Estimation and Correlation with Chemical Structure*; Elsevier/North Holland, Inc.: New York, 1972.

23. Goodman, I. in *The Encyclopedia of Polymer Science and Engineering, Vol. 12, 2nd Ed.*; Wiley: New York,1988.

24. Pohl, H.A. *Analyt. Chem.* **1954**, 26, 1614.

25. Boreman, W.F.H. J. *Appl. Polym. Sci.* **1978**, 22, 2119.

26. Streitwiesser Jr., A.; Heathcock, C.H. *Introduction to Organic Chemistry Second Edition*; Macmillian Publishing Co., Inc.: New York, 1981.

27. Edgerton, H.E *Science* **1966**, 154, 1553.

28. Macdonald, A.M.G. *Org. Microchem. Appl.* **1971**, 8, 12.

29. Pavel, J.; Kuebler, R.; Wagner, H. *Microchem. J.* **1970**, 15, 192.

30. Shearer, D.A.; Morris, G.F. *Microchem. J.* **1970**, 15, 199.

31. Flory, P.J. *Principles of Polymer Chemistry*; Cornell University Press: Ithica,1953.

CHAPTER 4

PHASE BEHAVIOR: COMPOSITION, MOLECULAR WEIGHT AND END GROUP EFFECTS

4.1 Introduction

Before the effects of interchange reaction on blend phase behavior can be examined, the equilibrium phase behavior prior to transreaction must be established. This information serves as the basis upon which the transreacting blends are judged. Variations in the blend phase behavior is determined as a function of three variables, composition ratio, molecular weight and end group type. Phase behavior studies are conducted as a function of the composition ratio to identify the magnitude this variable has on the observed level of intermixing. Studies examining varying molecular weight yield information useful in several ways. First, by applying appropriate theories, some insight into the thermodynamics of the blend are obtained. In particular, this data allows an estimation of the interaction parameter. Later, this parameter is used to interpret the phase behavior results of transreacting blends. Second, the degree of polymerization (critical molecular weights) required to form a single phase blend are determined. This data is also used to help interpret the thermodynamic aspects of transreacting blends.

The role of end group type relative to the observed phase behavior is also examined. Of particular interest is the effect the hydroxyl end group has on the resulting phase behavior, i.e., whether or not end group hydrogen bonding is important. Of equal interest is to identify the concentration of end groups (molecular weight of the polyester) at which significant changes in the phase behavior are observed. Before presenting the details of these studies, background information is discussed. Appropriate thermodynamic aspects of polymer blends is presented followed by a literature review of the phase behavior of PBT/PC and PET/PC blends. The importance of identifying the equilibrium phase behavior prior to exchange reaction is illustrated in this review.

4.2 Background

4.2.1 Thermodynamics of Polymer Blends

The thermodynamics of solutions are governed by the free energy of mixing, ΔG_m, composed of an entropic and an enthalpic contribution [1-3]. For polymer solutions, Flory [4] and Huggins [5] were the first to modify the entropic contribution to the free energy to account for the decrease in configurational entropy associated with the macromolecular chains. Both authors later extended this derivation to include an enthalpic term producing an equation for the free energy of mixing a polymer and a solvent [6,7]. This lattice model served as the basis for many of the models latter developed to improve the original Flory-Huggins equation. Further refinement by Flory [8] and Scott and Magat [9] lead to the derivation of ΔG_m for the mixing of a polydisperse polymer and a solvent . Scott later derived the free energy of mixing for a pair of monodisperse polymers [10]. The result, Equation 1, represents a general expression for the free energy of mixing per lattice site of a monodisperse binary blend composed of $N_1X_1 + N_2X_2$ sites, where the subscripts indicate components 1 and 2.

$$\Delta G_m = kT\left[\frac{\phi_1 \ln\phi_1}{X_1} + \frac{\phi_2 \ln\phi_2}{X_2} + \chi_{12}\phi_1\phi_2\right] \qquad (4.1)$$

N_i: number of polymer molecules of component i.
X_i: relative chain length of component i (based on reference molar volume V_r).
ϕ_i: volume fraction of component i.
χ_{12}: interaction parameter.
k: Boltzmann constant.
T: Absolute temperature.

The importance of Equation 1 lies in its ability to qualitatively/semi-quantitatively predict the effect of varying composition and chain length on the free energy of mixing. The temperature dependence of the free energy is often manifested in the temperature dependence of χ_{12}. In the absence of specific interactions between the two components, χ_{12} is described as having an

inverse relationship with temperature [11]. This fact is associated with the observation that the heat of mixing is often endothermic and leads to the prediction of an upper critical solution temperature (UCST) in polymer blends. Using equations such as Equation 1, the binodal and spinodal curves can be calculated by applying the appropriate stability conditions [12, 13]. For a binary polymer blend, the binodal is calculated by determining the chemical potentials with respect to each component in each phase and setting the respective pairs of potentials equal to one another, Equations 2a and b.

$$\Delta\mu_1' = \Delta\mu_1'' \tag{4.2a}$$

$$\Delta\mu_2' = \Delta\mu_2'' \tag{4.2b}$$

$\Delta\mu_i'$: Chemical potential with respect to component i in phase 1.
$\Delta\mu_i''$: Chemical potential with respect to component i in phase 2.

The equations for the chemical potentials are usually complex, containing logarithmic and quadratic terms in ϕ_i. Thus, the calculation of the binodal is difficult and is rarely done. The spinodal is more amendable to exact calculation being determined from the condition (at constant temperature and pressure),

$$\frac{\partial^2 \Delta G_m}{\partial \phi_i^2} = 0 \tag{4.3}$$

yielding,

$$\chi_{12s} = 1/2 \left[\frac{1}{X_1 \phi_{1s}} + \frac{1}{X_2 \phi_{2s}} \right] \tag{4.4}$$

The critical conditions at constant temperature and pressure are determined from Equation 1 by setting the 2nd and 3rd derivatives of ΔG_m with respect to an independent composition variable equal to one another, Equation 5.

$$\frac{\partial^2 \Delta G_m}{\partial \phi_i^2} = \frac{\partial^3 \Delta G_m}{\partial \phi_i^3} \tag{4.5}$$

The interaction parameter and compositions at the critical point can then be determined by Equations 6 and 7, respectively [11].

$$\chi_{12c} = 1/2 \left[\frac{1}{(X_1)^{1/2}} + \frac{1}{(X_2)^{1/2}} \right]^2 \tag{4.6}$$

$$\phi_{1c} = \frac{1}{1 + (X_1/X_2)^{1/2}} \tag{4.7}$$

The effect of varying molecular weight on the blend phase behavior is of particular interest. A representation of the binodal surface as a function of temperature, composition and the molecular weight of one component (the other assumed constant) as described by Equations 1-7 is shown in Figure 4.1. The surface shown represents the boundary between the single phase region (outside the surface) and two phase region (enclosed by the surface). At constant molecular weight, represented by dissecting the molecular weight axis with plane P1 (perpendicular to axis M_n), a typical temperature vs composition phase diagram depicting UCST behavior is observed, curve acb. Molecular weight effects at constant temperature, on the other hand, are represented by a perpendicular slice through the temperature axis, plane P2. Curve dce represents the "phase diagram" developed by treating molecular weight as the independent variable. Phase diagrams of this nature will be constructed during the course of this study. In addition, point c represents the critical point and designates the appropriate critical temperature, composition and molecular weight at constant pressure. It should be mentioned that the term "phase diagram" is normally associated with a temperature vs. composition plot (curve acb). In order to avoid confusion with this nomenclature, the molecular weight vs. composition diagrams will be designated as "miscibility maps".

Mixtures composed of two polydisperse macromolecules have also been discussed [14,15]. The corresponding thermodynamic equations for these quasi-binary systems are shown below.

$$\Delta G_m = kT\left[\sum_i \frac{\phi_{1i} \ln \phi_{1i}}{X_{1i}} + \sum_j \frac{\phi_{2j} \ln \phi_{2j}}{X_{2j}} + \chi_{12}\phi_1\phi_2 \right] \tag{4.8}$$

X_{1i}: chain length of species i of component 1.

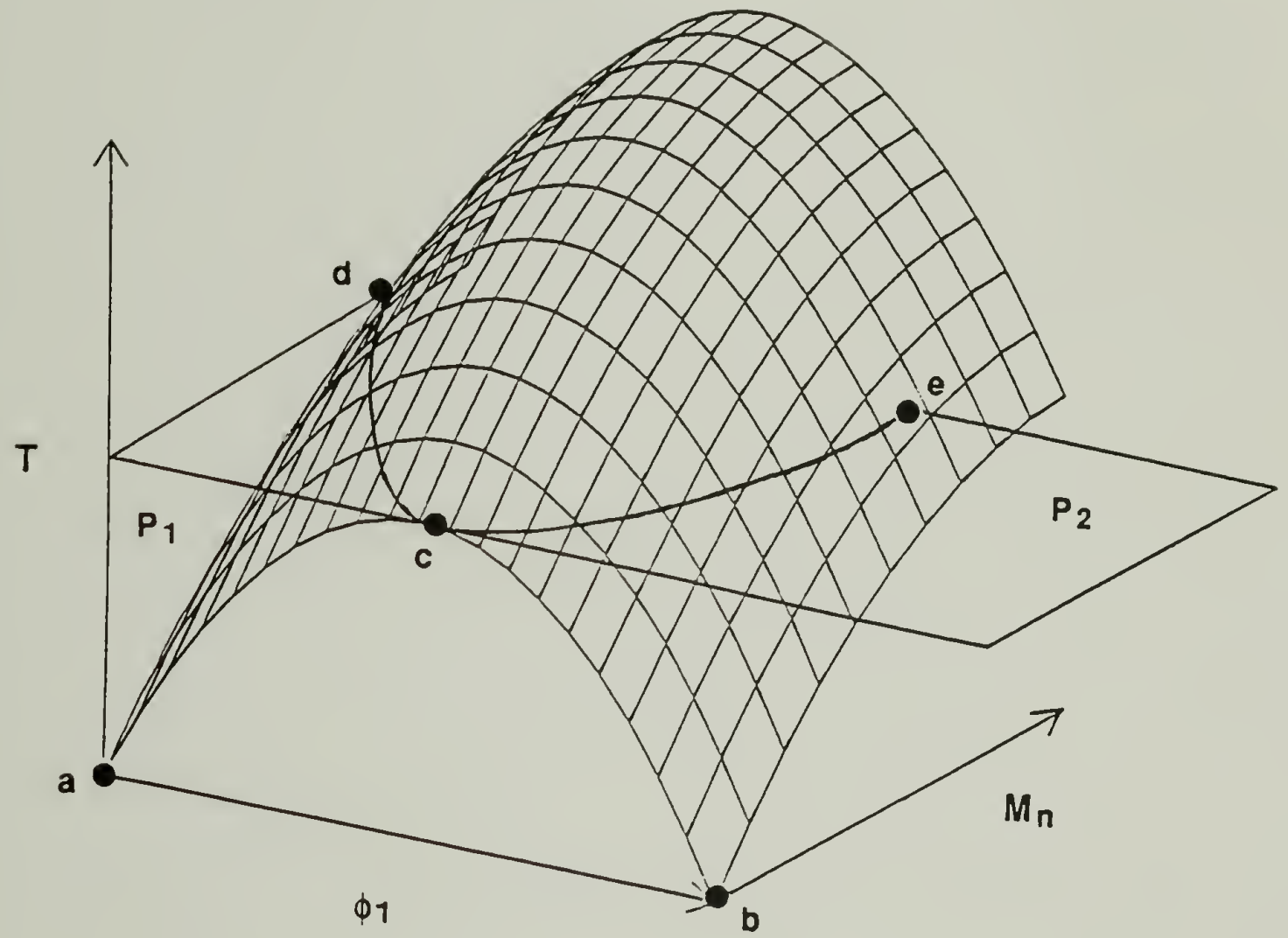

Figure 4.1 Three dimensional phase behavior diagram.

ϕ_{1i}: volume fraction of species i of component 1.

χ_{12}: interaction parameter (assumed to be independent of chain length).

$$\phi_{1i} = \frac{N_{1i}X_{1i}}{\sum_i N_{1i}X_{1i} + \sum_j N_{2j}X_{2j}} \qquad (4.9a)$$

$$\phi_1 = \frac{\sum_i N_{1i}X_{1i}}{\sum_i N_{1i}X_{1i} + \sum_j N_{2j}X_{2j}} \qquad (4.9b)$$

N_{1i}: number of polymer molecules of chain length i of component 1.

$$\chi_{12s} = 1/2 \left[\frac{1}{X_{w1}\phi_{1s}} + \frac{1}{X_{w2}\phi_{2s}} \right] \qquad (4.10)$$

X_{w1}: weight average chain length of component 1.

$$\phi_{1c} = \frac{1}{\left[1 + \frac{X_{w1}\, X_{z2}{}^{1/2}}{X_{w2}\, X_{z1}{}^{1/2}} \right]} \qquad (4.11)$$

X_{z1}: z- average chain length of component 1.

The above equations will be used to interpret the observed phase behavior of the PEMPT/PC blends under investigation and also to calculate the interaction parameter between these two components.

4.2.2 Phase Behavior of PBT/PC and PET/PC Blends

Numerous phase behavior studies have been conducted on polyester and polyester/polycarbonate blends. Discussion will focus once again on the PBT/PC and PET/PC blends that the current system was developed to model. In general, the literature is inconsistent with respect to the identification of phase behavior in these blends. The ability of polyester/PC blends to undergo exchange reactions is the most likely single reason leading to the observed discrepancies. Other factors, such as, different molecular weights and different

extents to which true equilibrium phase behavior was reached also likely contribute to the inconsistencies.

Wahrmund [16] showed evidence of partial miscibility in a PC/PBT system indicated by shifting of the T_g in DTA and DMTA measurements. Samples had been melt blended in a Brabender Plasticorder at 250°C for 10 min. Hanrahan [17] in an effort to minimize exposure to high temperatures, prepared PC/PBT blends by solution casting. DSC measurements were conducted on as-cast and on samples that had been quenched from 257°C in the DSC. Results showed nearly complete immiscibility. In a study on melt and solution cast PC/PBT blends, Hobbs [18] reported that solvent induced phase separation causes behavior associated with complete immiscibility, as observed by Hanarahan. In melt blended samples, a large Tg drop was observed for the PC phase. Upon solution casting of this partially miscible melt blend, the Tg shifted back to within a few degrees of the Tg of pure PC. From these observations, Hobbs concluded that the PC/PBT blend is partially miscible, with solvent effects causing the apparent immiscible behavior. However, Hobbs results could be equally well explained as a diffusion problem, insufficient time being allowed for complete phase separation in the melt blended sample. Other studies [19-21] show evidence of partial miscibility in this system, however, they were conducted on commercial melt blends where transesterification and/or mixing/demixing effects could alter phase behavior. Morphological and diffusion studies [22-25], employing TEM to examine structure, support the argument for partial miscibility in this system. In particular, PBT fibrils growing across a sharp interface into a pure PC phase provides convincing evidence for partial miscibility [25]. Recent studies by Kim and Burns [26] also supports partial miscibility.

The studies on PC/PET blend systems are equally conflicting. Several papers report complete miscibility in melt blended systems containing greater than 60%-70% PET [27,28], with partial miscibility in compositions containing less PET. Others report immiscibility over the entire composition range with some evidence of partial miscibility as observed by Tg shifts away from the pure component values [29-31]. These reports include studies on melt blended, as well as, solution cast samples. It should be mentioned that interchange reaction has been observed in the two blends by a variety of techniques including; IR [31-35], DRIFT [36], ^{1}H and ^{13}C solution NMR [36,37] and solid state ^{13}C NMR [36,37]. However, in all of the above phase behavior studies, none of these

direct measures was employed to prove the presence or absence of exchange reaction.

The ability of these blends to transreact presents an interesting problem which undoubtedly has lead to some of the inconsistencies described above. In order to obtain equilibrium phase behavior data, a sample should be annealed at temperatures significantly above the T_gs and T_ms of the component polymers to facilitate the diffusion process. However, for the case of PBT/PC and PET/PC blends, this requires temperatures in excess of 260°C. At these temperatures, interchange reaction can also proceed at an appreciable rate modifying the phase behavior. In the current model system, the T_g of PC is the limiting transition temperature. Thus, temperatures higher than 150°C are required for the phase behavior studies. At these temperatures, transreactions can also occur. To obtain equilibrium phase behavior data, the kinetics of phase separation must be considerably faster than the rate of exchange reactions. To insure that this is true, dioctadecyl phosphite (DNOP), which is known to inhibit interchange reactions in PBT/PC blends containing Ti catalyst, was used in the current blends. An initial study was conducted to determine the required concentration of DNOP. This concentration was then used in all subsequent blends.

4.3 Blend Preparation

All blends were prepared by a solution casting procedure similar to that described in Chapter 2. Prior to the precipitation procedures used for purification of the polyesters (Section 3.2.3.2), all PEMPT samples contained a ca 2.71×10^{-6} mol Ti catalyst/g polymer. This value is used as the basis for the determination of DNOP/Ti ratios to be studied. For the study examining varying DNOP concentration, equal amounts by weight of PEMPTB and PC2 were dissolved in a 7.12×10^{-7} M DNOP/chloroform solution. Three separate blends were made with the amount of DNOP/chloroform solution varied to obtain theoretical DNOP/Ti ratios of 1.5/1, 2.5/1 and 5/1. Pure chlorform was added to each sample to produce a final polymer/chloroform ratio of 10% (w/v). The samples were dried in a vacuum oven 350 mm Hg at 75-80°C for several hours. Full vacuum was not applied at this time to prevent rapid boiling of the solutions. When all the solvent had been removed, the samples were placed under full vacuum and allowed to dry an additional 24 h.

Blends for phase behavior studies were prepared similarly to that described above. A 5/1 DNOP/Ti ratio was used for all samples. Longer drying times under full vacuum, 8-14 days, was the only significant variation to the blending procedure. The polyesters used were the twice precipitated PEMPTs of varying molecular weight (PEMPT-OH15 and PEMPT-OH2 series) and the polyesters that had been end capped (PEMPT-HFB and PEMPT-BNZ series). The PCs used were the twice precipitated PC1 and PC2. Initial phase behavior studies examined PEMPT-OH15/PC blends at composition ratios of 15/85, 30/70, 50/50, 70/30, 85/15 (w/w). For the PEMPT-OH2, PEMPT-HFB and PEMPT-BNZ/PC blends only 50/50 ratios were prepared. Samples were stored in a vacuum desiccator under calcium sulphate prior to thermal analysis.

4.4 Analysis

Thermal analysis for the varying DNOP/Ti ratio study was conducted in a Perkin-Elmer DSC-4 as described in Chapter 2. The annealing and scanning temperature ramps used for this study are shown below.

Annealing
Load @ 20°C.
Heat @ 100°C/ min to 280°C.
Hold .2 min.
Cool @ 100°C/min to 240°C.
Annealing time: variable.
Cool @ 50°C/min to 20°C.

Scanning
Load @ 20°C.
1st Scan, 20°C/min to 200°C.
Cool @ 50°C/min to 20°C.

Once again the short annealing period at 280°C was used to melt the PC crystals that had formed during the casting procedure.

Thermal analysis for the actual phase behavior studies was conducted in a DSC-7 as described in the previous chapter. During these studies, a Perkin-Elmer Intercooler II was used for subambiant cooling. The annealing and scanning programs are described below.

Annealing
Load @ 20°C.
Heat @ 100°C/ min to 280°C.

Scanning
Load @ 20°C.
1st Scan, 20°C/min to 200°C.

Hold .2 min.
Cool @ 100°C/min to 200°C.
Anneal 60 min
Cool @ 50°C/min to 20°C.
Cool @ 50°C/min to 20°C.
Hold 2 min.
2nd Scan, 20°C/min to 200°C.
Cool @ 50°C/min to 20°C.

The first systems examined were the PEMPT-OH15/PC2 blends at varying composition ratios. Only a single heating scan was run for these blends. It was found that in some cases, particularly samples containing low molecular weight PEMPTs, T_g identification was complicated by a particularly large endothermic overshoot. In these instances, second heating scans were run. To insure uniform heat treatments, all remaining blends were scanned twice, with the second heating scan used for T_g identification. In most cases, agreement between T_gs identified from 1st and 2nd heating scans was good.

Proton NMR was conducted identically to that described in Chapter 3. Following DSC runs, the sample pans were opened and the blends removed for NMR analysis.

4.5 Results and Discussion

4.5.1 Identification of the Optimum DNOP/Ti Ratio.

Figure 4.2 shows a plot of the T_g vs. annealing time for blends containing varying DNOP/Ti ratios. Considerable shifts in the T_gs of the 1.5/1 and 2.5/1 blends are observed as annealing time increases, indicating some level of phase behavior modification due to transreaction. Both the upper and lower T_gs of the 5/1 DNOP/Ti ratio blend appear stable as annealing time increases. T_g shifts of only 2-3°C are observed after annealing 120 min at 240°C implying little or no interchange reaction. Figure 4.3 is the 300 MHz proton NMR of a 5/1 ratio PEMPTB/PC2 blend after annealing 60 min @ 200°C (identical to the thermal program used for phase behavior studies). The terephthalate region of the spectrum is displayed. Interchange reaction in PBT/PC blends has previously been identified by the appearance of new resonances shifted 0.1-0.3 ppm downfield from the main terephthalate resonance [32]. Figure 4.3 shows no evidence of any new resonances in this region confirming the absence of interchange reaction.

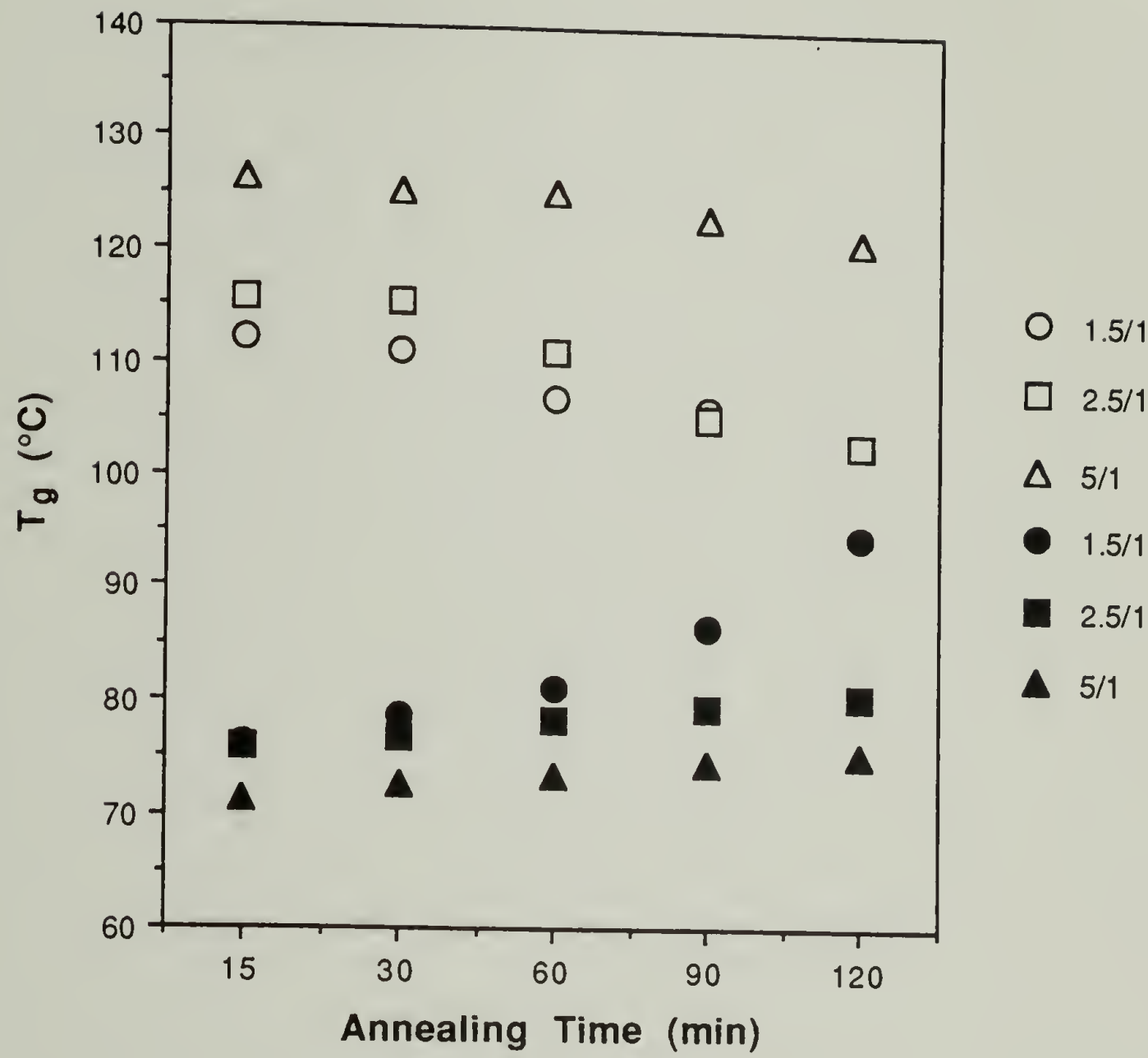

Figure 4.2 T_g vs. annealing time @ 240°C for PEMPTB/PC2 blends at the indicated DNOP/Ti ratio (open symbols: PC rich phase, filled symbols: PEMPT rich phase).

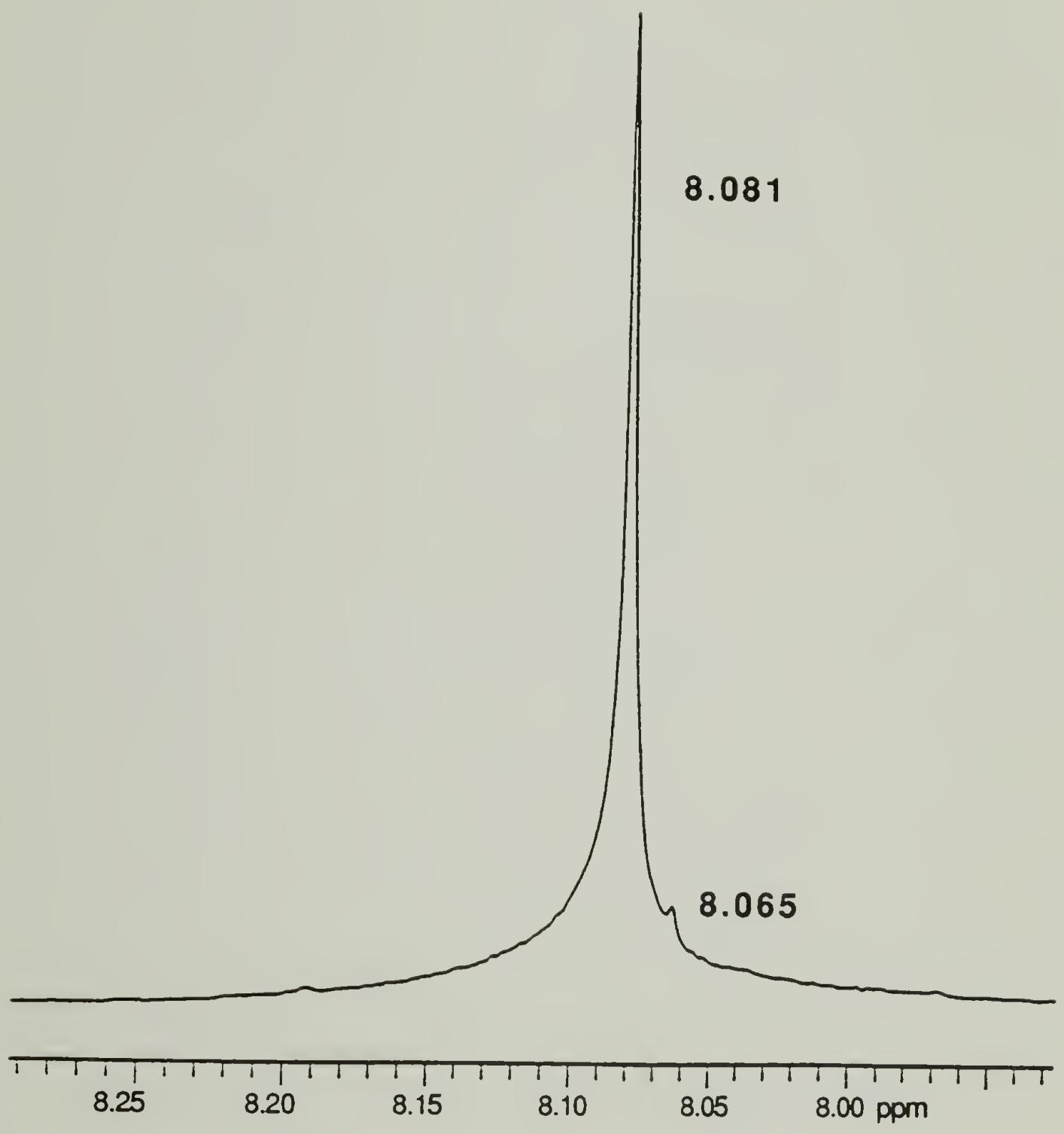

Figure 4.3 300 MHz ^{1}H NMR of PEMPTB/PC2 blend containing a 5/1 DNOP/Ti ratio after annealing 60 min @ 200°C. Terephthalate region of PEMPT is displayed.

As previously mentioned, in order to identify the equilibrium phase behavior, the rate of interchange reaction must be slow relative to the kinetics of diffusion. It appears from this study that the 5/1 DNOP/Ti ratio significantly inhibits interchange reaction satisfying this requirement. On the basis of these results, all other DNOP stabilized blends were prepared using a 5/1 theoretical DNOP/Ti mol ratio (section 4.3). It should also be mentioned that during the actual phase behavior studies, considerably milder annealing conditions were employed compared to the annealing conditions discussed here. This should further reduce the rate of interchange reaction.

4.5.2 Phase Behavior Studies

Before discussing the equilibrium phase behavior results, the criterion for establishing that equilibrium had been reached should be mentioned. The criterion for equilibrium is based on the phase behavior of a transreacting system. It was determined from phase behavior results on PEMPTB/PC2 non-DNOP stabilized blends that a single broad T_g was observed after 64 min of annealing at 200°C (Chapter 5). This result indicates that diffusion of the polymer chains occurs at a rate significant enough to produce a single phase blend from an initially two phase system after annealing ~ 1 h at 200°C. These results not only reflect a diffusion effect, but also represent a kinetic effect associated with the rate of interchange reaction. This kinetic factor is expected to limit the diffusion of the polymer chains. Additionally, the majority of blends studied contained polyesters that have molecular weights lower than that used in this transreaction study, enhancing chain mobility and decreasing the time required to reach equilibrium. Thus, an annealing time of 60 min at 200°C should produce blends at or very near equilibrium. It was for this reason that all samples were annealed 1 h at 200°C prior to the heating scans.

4.5.2.1 PEMPT-0H15/PC Blends

Figures 4.4 and 4.5 show the DSC scans for PEMPT-OH15/PC1 and PEMPT-OH15/PC2 50/50 blends with varying polyester molecular weight, respectively. As molecular weight of the polyester is lowered, a shift in the T_gs of the polymers is observed. Examining the T_gs of the PEMPT rich phases, only a slight shift is observed for all but the lowest molecular weights. In contrast to

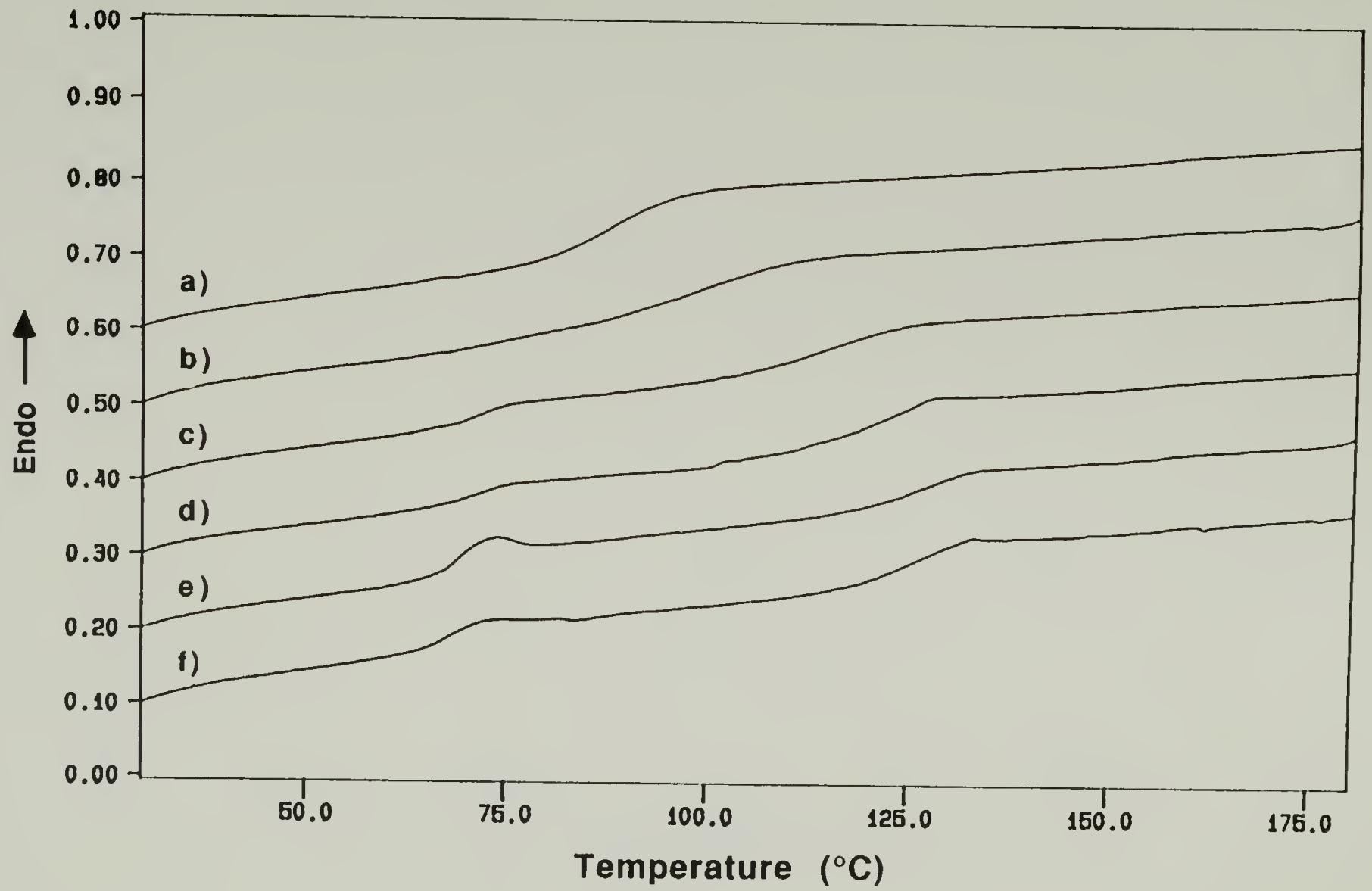

Figure 4.4 DSC scans of PEMPT-OH15/PC1 blends at PEMPT M_ns of a) 4,100 b) 6,100 c) 9,500 d) 11,500 e) 18,200 and f) 37,500 g/mol.

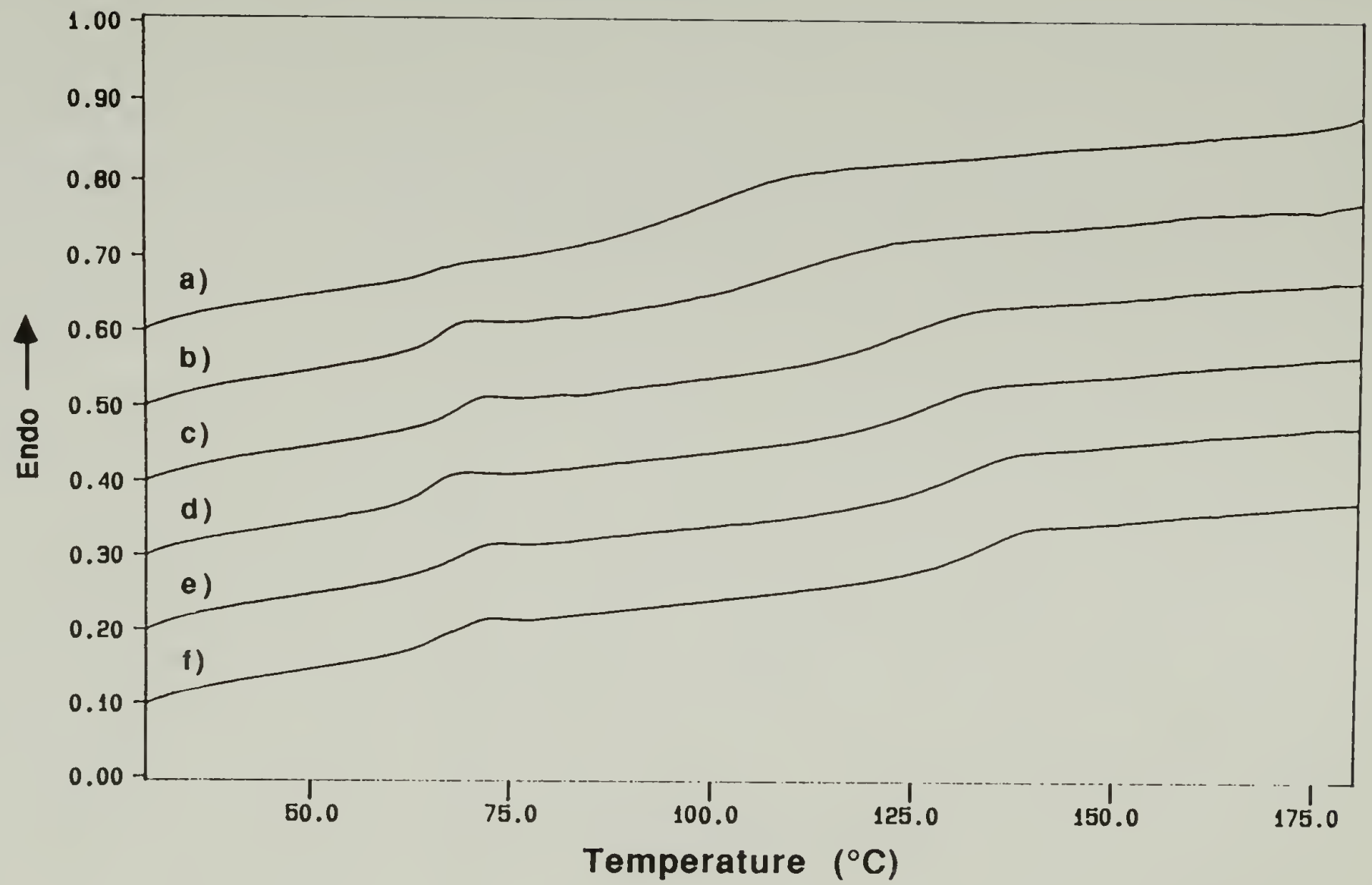

Figure 4.5 DSC scans of PEMPT-OH15/PC2 blends at PEMPT M_ns of a) 4,100 b) 6,100 c) 9,500 d) 11,500 e) 18,200 and f) 37,500 g/mol.

this, a shift in the T_g of the PC1 and PC2 rich phases is increasingly evident as the molecular weight of PEMPT is lowered. This improved level of intermixing of PEMPT in the PC rich phase is the result of a change in the entropic contribution to the free energy of mixing (Equations 1 and 8). As the PEMPT molecular weight is lowered, the entropic portion of ΔG_m decreases (greater negative value), decreasing ΔG_m and leads to enhanced mixing. In general, the PEMPT-OH15/PC1 systems show a greater degree of intermixing of the two phases than the PEMPT-OH15/PC2 blends (greater T_g shifts). This is also related to a decrease in the entropic contribution to the free energy of mixing associated with the lower molecular weight of PC1 relative to PC2. It should also be mentioned that one of these blends,PEMPT1-OH15/PC1, was observed to be miscible (miscibility being defined as the observation of a single T_g). Additional phase behavior studies were conducted on the PEMPT-OH15/PC1 and PEMPT-OH15/PC2 blends as a function of molecular weight at PEMPT/PC wt ratios of 15/85, 30/70, 70/30 and 85/15. Eleven additional blends were found to be miscible (see Table 4.1).

As previously mentioned, it is desired to construct miscibility maps (X_1 vs. ϕ_1) for these blends. In order to do so, a measure of the volume fraction (ϕ_1', ϕ_1'', ϕ_2' and ϕ_2'') of each component in the PEMPT rich phase (lower T_g or "prime" phase) and PC rich phase (upper T_g or "double prime" phase) is required. PEMPT is designated as component 1. The Couchman equation [38] with $\Delta C_{p2}/\Delta C_{p1} = 0.7$ was used to calculate these volume fractions. It should be noted that the Couchman equation is normally used to calculate the weight fractions of the components. However, in this blend with the density of PEMPT being nearly identical to the density of PC, weight fractions and volume fractions are equivalent. The value for $\Delta C_{p2}/\Delta C_{p1}$ was determined by fitting the calculated volume fractions to the known volume fractions of the previously identified twelve miscible blends. For the miscible blends, the volume fractions are equivalent to the initial blend composition. It is observed from the data in Table 4.1 that the value for $\phi_{2,actual}$ is in good agreement with the calculated value across the entire composition range. The absolute value of the difference between $\phi_{2,actual}$ and $\phi_{2,calculated}$ is shown in the last column of Table 4.1. The largest deviation is only 0.054 with the average deviation being 0.024.

Using the Couchman equation along with the appropriate pure component T_gs (Table 3.5) and the T_gs determined from the DSC scans of the blends, the volume fractions, ϕ_1', ϕ_1'', ϕ_2' and ϕ_2'' were calculated. Tables 4.2

Table 4.1 Couchman Equation Fit ($\Delta C_{p2}/\Delta C_{p1} = 0.7$)

Blend	$\phi_{2,actual}$	$\phi_{2,calculated}$	$\lvert \Delta\phi_2 \rvert$
PEMPT1-OH15/PC1 15/85	0.85	0.850	0.000
PEMPT2-OH15/PC1 15/85	0.85	0.819	0.031
PEMPT1-OH15/PC2 15/85	0.85	0.834	0.026
PEMPT1-OH15/PC1 30/70	0.70	0.679	0.021
PEMPT2-OH15/PC1 30/70	0.70	0.677	0.023
PEMPT1-OH15/PC2 30/70	0.70	0.646	0.054
PEMPT1-OH15/PC1 50/50	0.50	0.473	0.027
PEMPT1-OH15/PC1 70/30	0.30	0.283	0.017
PEMPT1-OH15/PC2 70/30	0.30	0.264	0.036
PEMPT1-OH15/PC1 85/15	0.15	0.177	0.027
PEMPT2-OH15/PC1 85/15	0.15	0.142	0.008
PEMPT1-OH15/PC2 85/15	0.15	0.162	0.012

and 4.3 display the T_gs of the PEMPT rich phase and PC rich phase along with the calculated volume fractions associated with the DSC scans of Figures 4.4 and 4.5. The only additional data required to construct the miscibility maps is the number average relative chain lengths, X_i, of PEMPT and PC. These were calculated from the molecular weight data of Tables 3.2 and 3.3 using the molar volume of the repeat unit of PEMPT, ca 208.4 cm^3/mol repeat, as the reference volume (Table 4.4).

Figure 4.6 is a plot of X_1 vs. ϕ_1 for the PEMPT-OH15/PC1 and PEMPT-OH15/PC2 50/50 blends. The general trends previously discussed in conjunction with the DSC plots of these blends (Figures 4.4 and 4.5) are also observed in this figure. Additional data on PEMPT/PC blends with weight ratios of 15/85, 30/70, 70/30 and 85/15 are displayed in Tables 4.5-4.12. Figures 4.7 and 4.8 (pp. 98 & 99) show plots X_1 vs. ϕ_1 for the PEMPT-OH15/PC1 and PEMPT-OH15/PC2 blends, respectively, at composition ratios of 15/85, 30/70, 50/50 and 70/30. Examining the PEMPT rich phase, it is observed that the degree of intermixing of PC in the PEMPT phase is relatively independent of composition ratio in both figures. It is also observed that the amount of PC1 intermixed in the PEMPT rich phase varies from is 6 -30% as X_1 varies from 151-24.6. Similarly, for blends containing PC2, 3 -18% PC2 is present in the PEMPT rich phase as X_1 varies from 151-16.5.

Focusing now on the PC rich phase, the degree of intermixing of PEMPT in the PC rich phase appears to have some dependence on blend composition. In general, as the composition of PEMPT in the blend increases, the level of intermixing increases. For the blend compositions plotted, there is an increase of intermixing corresponding to ~ 0.10-0.20 volume fraction units. Overall, intermixing of PEMPT in the PC1 rich phase ranges from 10-42% as X_1 varies from 151-24.6. The intermixing of PEMPT in PC2 rich phase ranges from 10-45% as X_1 varies from 151-16.5. For blends containing high molecular weight PEMPT, the levels of intermixing are in agreement with the values reported by Kim and Burns in their studies of PBT/PC and PET/PC blends [26,39]. Similar to the present study, Kim and Burns report an increase in the level of intermixing of the polyester in the PC rich phase as polyester composition increases. They also report an increased degree of intermixing of PC in the polyester rich phase as the polyester composition increases, contrary to the current observations.

Although a small compositional dependence exists, the miscibility maps of Figures 4.7 and 4.8 show that the same general trends are observed at all

Table 4.2 T_g and ϕ_i Data for PEMPT-OH15/PC1 50/50 Wt. % Blends

Polyester	T_g' (°K)	T_g'' (°K)	ϕ_1'	ϕ_2'	ϕ_1''	ϕ_2''
PEMPT-1	360.7	-	0.527	0.473	-	-
PEMPT-2	350.8	372.4	0.688	0.312	0.414	0.586
PEMPT-3	344.0	386.9	0.823	0.177	0.273	0.727
PEMPT-4	344.1	391.6	0.844	0.156	0.233	0.767
PEMPT-5	343.0	399.8	0.896	0.104	0.160	0.840
PEMPT-6	342.1	397.2	0.934	0.066	0.188	0.812

Table 4.3 T_g and ϕ_i Data for PEMPT-OH15/PC2 50/50 Wt. % Blends

Polyester	T_g' (°K)	T_g'' (°K)	ϕ_1'	ϕ_2'	ϕ_1''	ϕ_2''
PEMPT-1	339.1	371.1	0.829	0.171	0.427	0.573
PEMPT-2	339.8	382.9	0.862	0.138	0.324	0.676
PEMPT-3	341.1	395.9	0.877	0.123	0.212	0.788
PEMPT-4	338.7	398.3	0.942	0.058	0.195	0.805
PEMPT-5	341.7	402.3	0.923	0.077	0.164	0.836
PEMPT-6	339.8	405.3	0.989	0.021	0.140	0.860

Single "prime" denotes PEMPT rich phase, "double prime" PC rich phase.
PEMPT is designated as component 1.

Table 4.4 Number Average Relative Chain Lengths of PEMPT and PC

Polymer	M_n (g/mol)	X_n
PEMPT1	4,100	16.5
PEMPT2	6,100	24.6
PEMPT3	9,500	38.3
PEMPT4	11,500	46.4
PEMPT5	18,200	73.4
PEMPT6	37,500	151
PC1	11,300	45.2
PC2	21,200	84.8

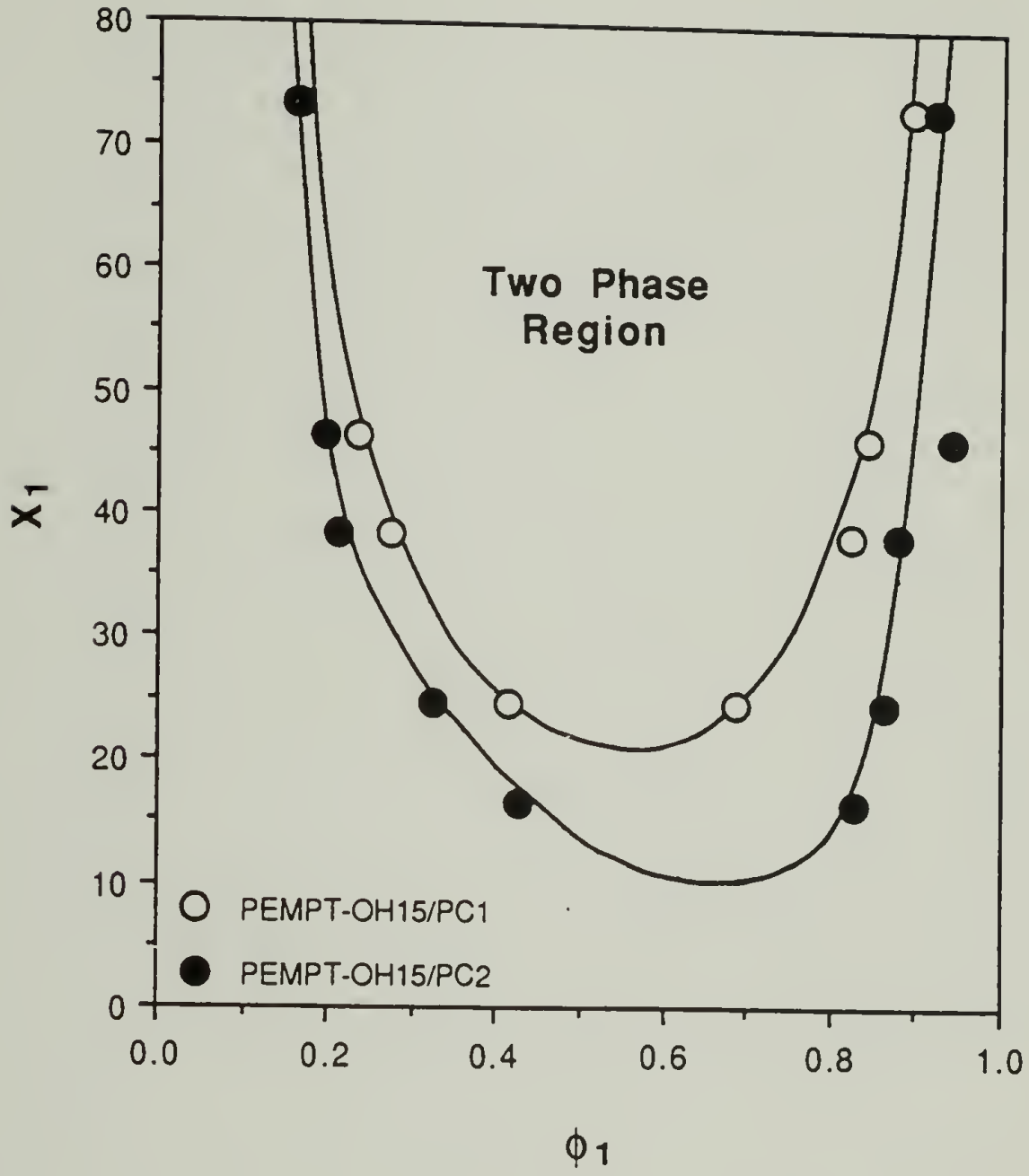

Figure 4.6 Miscibility maps of PEMPT-OH15/PC1 and PEMPT-OH15/PC2 50/50 wt. % blends.

Table 4.5 T_g and ϕ_i Data for PEMPT-OH15/PC1 15/85 Wt. % Blends

Polyester	T_g' (°K)	T_g'' (°K)	ϕ_1'	ϕ_2'	ϕ_1''	ϕ_2''
PEMPT-1	398.7	-	0.150	0.850	-	-
PEMPT-2	395.9	-	0.181	0.819	-	-
PEMPT-3	340.8	398.7	0.877	0.123	0.162	0.838
PEMPT-4	343.0	403.1	0.863	0.137	0.126	0.874
PEMPT-5	343.0	405.9	0.896	0.104	0.105	0.895
PEMPT-6	341.3	407.0	0.949	0.051	0.107	0.903

Table 4.6 T_g and ϕ_i Data for PEMPT-OH15/PC2 15/85 Wt. % Blends

Polyester	T_g' (°K)	T_g'' (°K)	ϕ_1'	ϕ_2'	ϕ_1''	ϕ_2''
PEMPT-1	399.7	-	0.166	0.834	-	-
PEMPT-2	338.3	401.4	0.886	0.114	0.159	0.841
PEMPT-3	337.0	408.8	0.947	0.053	0.103	0.897
PEMPT-4	342.5	412.3	0.887	0.123	0.077	0.923
PEMPT-5	340.7	414.2	0.941	0.059	0.064	0.936
PEMPT-6	341.5	412.9	0.948	0.052	0.076	0.924

Single "prime" denotes PEMPT rich phase, "double prime" PC rich phase. PEMPT is designated as component 1.

Table 4.7 T_g and ϕ_i Data for PEMPT-OH15/PC1 30/70 Wt. % Blends

Polyester	T_g' (°K)	T_g'' (°K)	ϕ_1'	ϕ_2'	ϕ_1''	ϕ_2''
PEMPT-1	379.7	-	0.321	0.679	-	-
PEMPT-2	380.9	-	0.323	0.677	-	-
PEMPT-3	343.6	391.0	0.830	0.170	0.233	0.767
PEMPT-4	344.4	398.4	0.839	0.161	0.168	0.832
PEMPT-5	344.7	401.0	0.866	0.134	0.149	0.851
PEMPT-6	342.4	404.0	0.928	0.072	0.124	0.876

Table 4.8 T_g and ϕ_i Data for PEMPT-OH15/PC2 30/70 Wt. % Blends

Polyester	T_g' (°K)	T_g'' (°K)	ϕ_1'	ϕ_2'	ϕ_1''	ϕ_2''
PEMPT-1	378.4	-	0.354	0.646	-	-
PEMPT-2	339.6	393.7	0.865	0.135	0.224	0.776
PEMPT-3	339.0	401.8	0.912	0.088	0.160	0.840
PEMPT-4	342.5	405.3	0.877	0.123	0.134	0.866
PEMPT-5	340.8	407.4	0.939	0.061	0.120	0.880
PEMPT-6	340.2	410.0	0.972	0.028	0.100	0.900

Single "prime" denotes PEMPT rich phase, "double prime" PC rich phase.
PEMPT is designated as component 1.

Table 4.9 T_g and ϕ_i Data for PEMPT-OH15/PC1 70/30 Wt. % Blends

Polyester	T_g' (°K)	T_g'' (°K)	ϕ_1'	ϕ_2'	ϕ_1''	ϕ_2''
PEMPT-1	346.2	-	0.717	0.283	-	-
PEMPT-2	344.1	373.9	0.788	0.212	0.398	0.602
PEMPT-3	343.4	392.0	0.833	0.167	0.224	0.776
PEMPT-4	343.0	396.5	0.863	0.137	0.186	0.814
PEMPT-5	340.2	396.3	0.948	0.052	0.193	0.807
PEMPT-6	341.3	399.3	0.949	0.051	0.168	0.832

Table 4.10 T_g and ϕ_i Data for PEMPT-OH15/PC2 70/30 Wt. % Blends

Polyester	T_g' (°K)	T_g'' (°K)	ϕ_1'	ϕ_2'	ϕ_1''	ϕ_2''
PEMPT-1	345.5	-	0.736	0.264	-	-
PEMPT-2	343.0	383.1	0.812	0.188	0.322	0.678
PEMPT-3	340.7	395.9	0.884	0.116	0.212	0.788
PEMPT-4	340.3	391.4	0.914	0.086	0.258	0.742
PEMPT-5	342.8	403.1	0.904	0.096	0.157	0.843
PEMPT-6	340.8	401.0	0.961	0.039	0.179	0.821

Single "prime" denotes PEMPT rich phase, "double prime" PC rich phase. PEMPT is designated as component 1.

Table 4.11 T_g and ϕ_i Data for PEMPT-OH15/PC1 85/15 Wt. % Blends

polyester	T_g' (°K)	T_g'' (°K)	ϕ_1'	ϕ_2'	ϕ_1''	ϕ_2''
PEMPT-1	339.1	-	0.823	0.177	-	-
PEMPT-2	339.7	-	0.858	0.142	-	-
PEMPT-3	342.5	-	0.848	0.152	-	-
PEMPT-4	341.7	-	0.886	0.114	-	-
PEMPT-5	344.7	404.4	0.866	0.134	0.119	0.881
PEMPT-6	340.8	404.8	0.959	0.041	0.117	0.883

Table 4.12 T_g and ϕ_i Data for PEMPT-OH15/PC2 85/15 Wt. % Blends

Polyester	T_g' (°K)	T_g'' (°K)	ϕ_1'	ϕ_2'	ϕ_1''	ϕ_2''
PEMPT-1	338.5	-	0.838	0.162	-	-
PEMPT-2	339.6	-	0.865	0.135	-	-
PEMPT-3	340.8	398.0	0.882	0.118	0.193	0.807
PEMPT-4	342.1	399.5	0.884	0.116	0.084	0.816
PEMPT-5	344.0	409.1	0.883	0.117	0.106	0.894
PEMPT-6	341.4	408.0	0.950	0.050	0.117	0.883

Single "prime" denotes PEMPT rich phase, "double prime" PC rich phase.
PEMPT is designated as component 1.

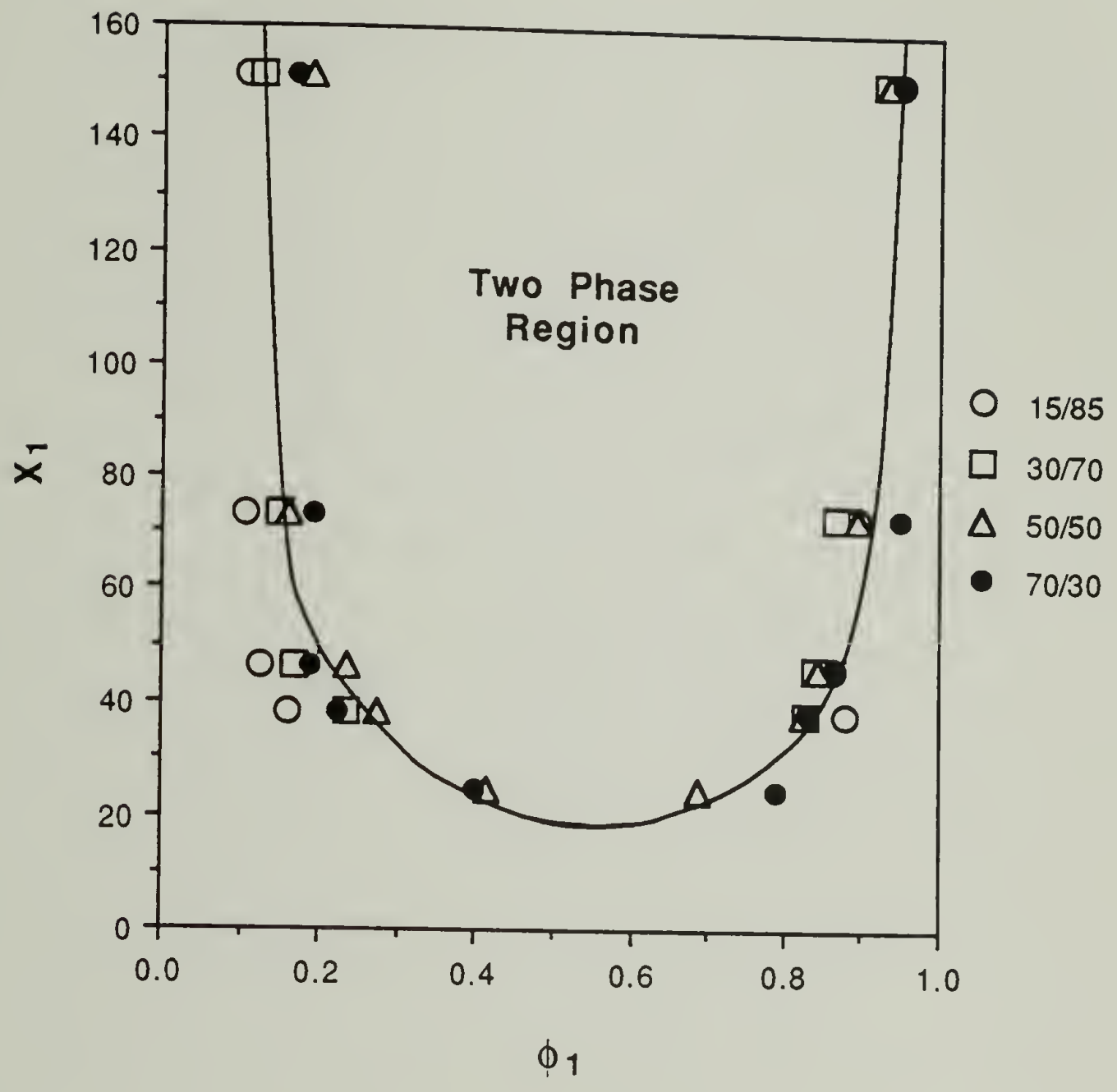

Figure 4.7 Miscibility maps of PEMPT-OH15/PC1 blends at the indicated blend composition ratios.

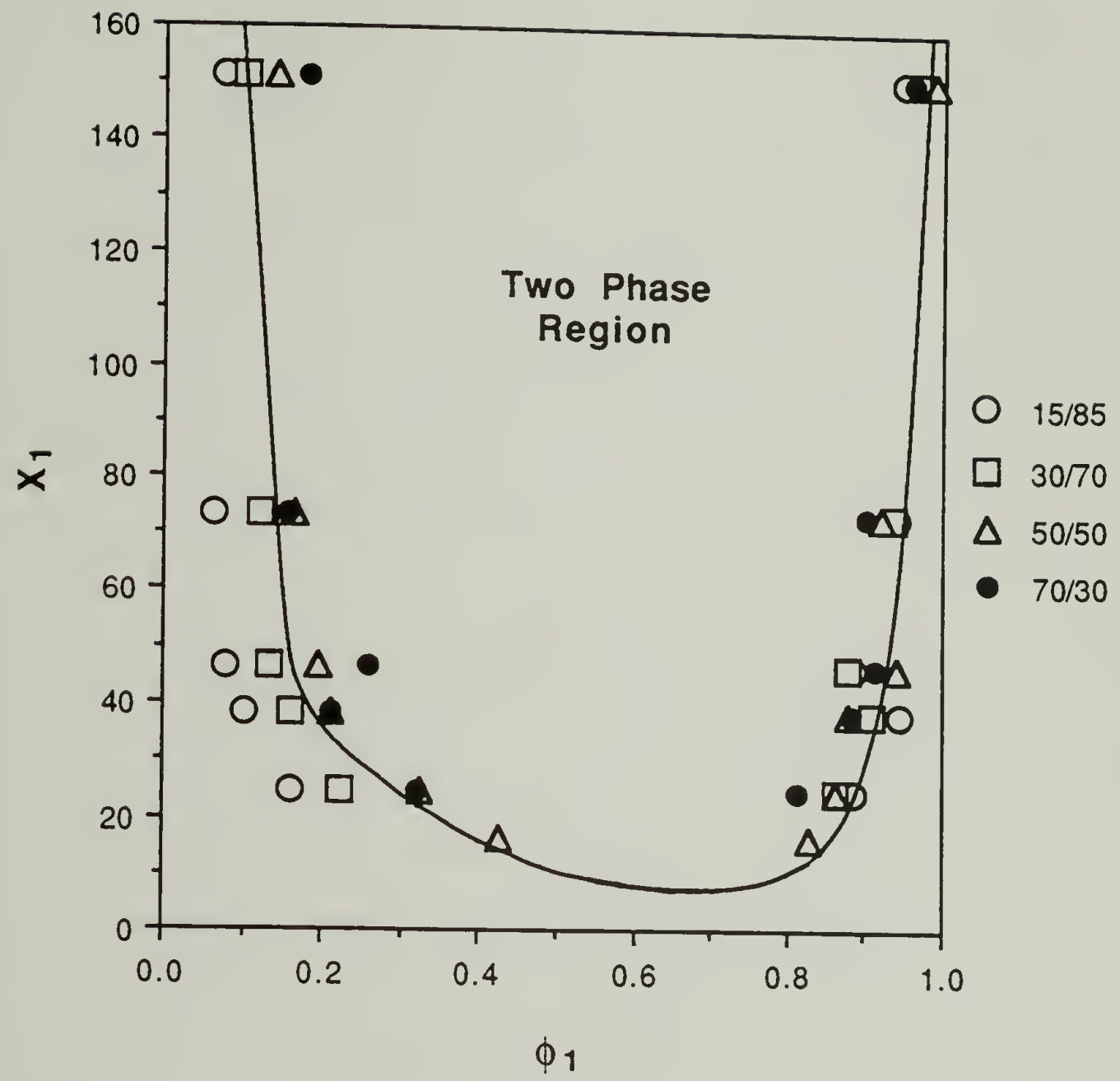

Figure 4.8 Miscibility maps of PEMPT-OH15/PC2 blends at the indicated blend composition ratios.

PEMPT/PC compositions. Thus, in order to facilitate further studies, the miscibility map at a single blend composition will be assumed to be an adequate representation of the phase behavior across the entire composition range. A PEMPT/PC ratio of 50/50 was selected for this purpose. Due to the nearly identical volume fractions of the components, the identification of the T_gs is most accurately obtained at this composition ratio. One additional point should be made about the PEMPT-OH15/PC blends. It will be shown in Chapter 5 that in spite of all the precautions taken to eliminate/minimize interchange reaction, a small percentage, ~ 16%, of the hydroxyl end groups of PEMPT reacted via an alcoholysis type exchange reaction. Their was no evidence to indicate that any direct midchain transreaction had occurred. From extrapolations (Section 5.3.1), it is estimated that this level of reaction increased the intermixing in both the PEMPT and PC rich phases by ~ 0.02-0.04 volume fraction units. Figure 4.9 shows the miscibility map of PEMPT-OH-0%/PC1 and PEMPT-OH-0%/PC2 blends. These curves are the extrapolations corresponding to 0% hydroxyl exchange reaction (Section 5.3.3.1). These miscibility maps closely follow those of the blends with 16% hydroxyl group reaction, thus, the results discussed above apply to the unreacted blends as well.

4.5.2.2 PEMPT-OH2/PC Blends

Tables 4.13 and 4.14 list the T_g and ϕ_i data for the PEMPT-OH2/PC 50/50 wt. % blends. It was found that complete alcoholysis interchange reaction occurred in these blends. Thus, these results are discussed within the contents of Chapter 5 which focuses on the transreacting blends.

4.5.2.3 PEMPT-BNZ/PC Blends

T_g and ϕ_i data for PEMPT-BNZ/PC 50/50 wt. % blends is contained in Tables 4.15 and 4.16. Figure 4.10 shows the corresponding miscibility maps for the PEMPT-BNZ/PC1 and PEMPT-BNZ/PC2 50/50 wt. % blends. The range of the ordinate axis has been decreased to emphasize the low molecular weight portion of the miscibility map. The miscibility map of Figure 4.10 is very similar to that previously observed for the hydroxyl terminated PEMPT/PC blends. PEMPT1-HFB/PC1 and PEMPT1-HFB/PC2 blends were both single phase.

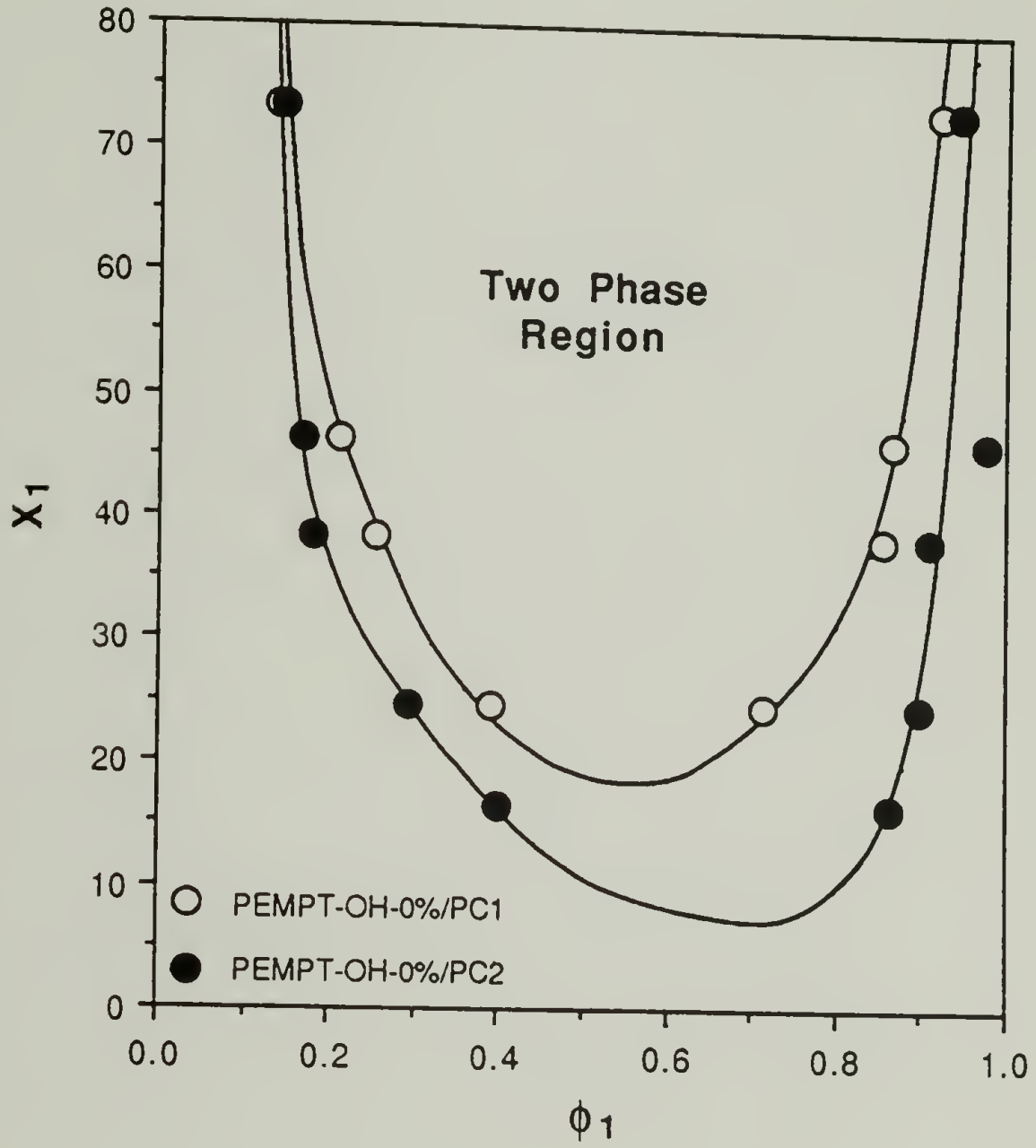

Figure 4.9 Miscibility maps of PEMPT-OH-0%/PC1 and PEMPT-OH-0%/PC2 50/50 wt. % blends.

Table 4.13 T_g and ϕ_i Data for PEMPT-OH2/PC1 50/50 Wt. % Blends

polyester	T_g' (°K)	T_g'' (°K)	ϕ_1'	ϕ_2'	ϕ_1''	ϕ_2''
PEMPT-1	360.2	-	0.544	0.456	-	-
PEMPT-2	367.5	-	0.492	0.508	-	-
PEMPT-3	356.7	377.7	0.657	0.343	0.384	0.616
PEMPT-4	353.1	381.2	0.725	0.275	0.350	0.650
PEMPT-5	351.7	387.2	0.766	0.234	0.291	0.709
PEMPT-6	347.5	394.0	0.844	0.156	0.221	0.779

Table 4.14 T_g and ϕ_i Data for PEMPT-OH2/PC2 50/50 Wt. % Blends

Polyester	T_g' (°K)	T_g'' (°K)	ϕ_1'	ϕ_2'	ϕ_1''	ϕ_2''
PEMPT-1	368.1	-	0.468	0.532	-	-
PEMPT-2	371.3	-	0.464	0.536	-	-
PEMPT-3	354.9	379.3	0.695	0.305	0.387	0.613
PEMPT-4	351.5	384.3	0.760	0.240	0.339	0.661
PEMPT-5	349.4	392.6	0.812	0.188	0.259	0.741
PEMPT-6	343.7	399.7	0.917	0.083	0.192	0.808

Single "prime" denotes PEMPT rich phase, "double prime" PC rich phase.
PEMPT is designated as component 1.

Table 4.15 T_g and ϕ_i Data for PEMPT-BNZ/PC1 50/50 Wt. % Blends

polyester	T_g' (°K)	T_g'' (°K)	ϕ_1'	ϕ_2'	ϕ_1''	ϕ_2''
PEMPT-1	356.0	-	0.492	0.508	-	-
PEMPT-2	340.7	370.3	0.796	0.204	0.414	0.586
PEMPT-3	341.9	385.2	0.817	0.183	0.279	0.721
PEMPT-4	341.0	389.8	0.855	0.145	0.241	0.759
PEMPT-5	340.9	397.4	0.903	0.097	0.178	0.822
PEMPT-6	342.0	401.3	0.913	0.087	0.146	0.854

Table 4.16 T_g and ϕ_i Data for PEMPT-BNZ/PC2 50/50 Wt. % Blends

Polyester	T_g' (°K)	T_g'' (°K)	ϕ_1'	ϕ_2'	ϕ_1''	ϕ_2''
PEMPT-1	361.3	-	0.481	0.519	-	-
PEMPT-2	331.8	378.9	0.933	0.067	0.345	0.655
PEMPT-3	334.5	391.9	0.943	0.057	0.239	0.761
PEMPT-4	334.8	395.7	0.965	0.035	0.210	0.790
PEMPT-5	339.1	405.1	0.939	0.061	0.136	0.864
PEMPT-6	339.3	407.7	0.965	0.035	0.117	0.883

Single "prime" denotes PEMPT rich phase, "double prime" PC rich phase.
PEMPT is designated as component 1.

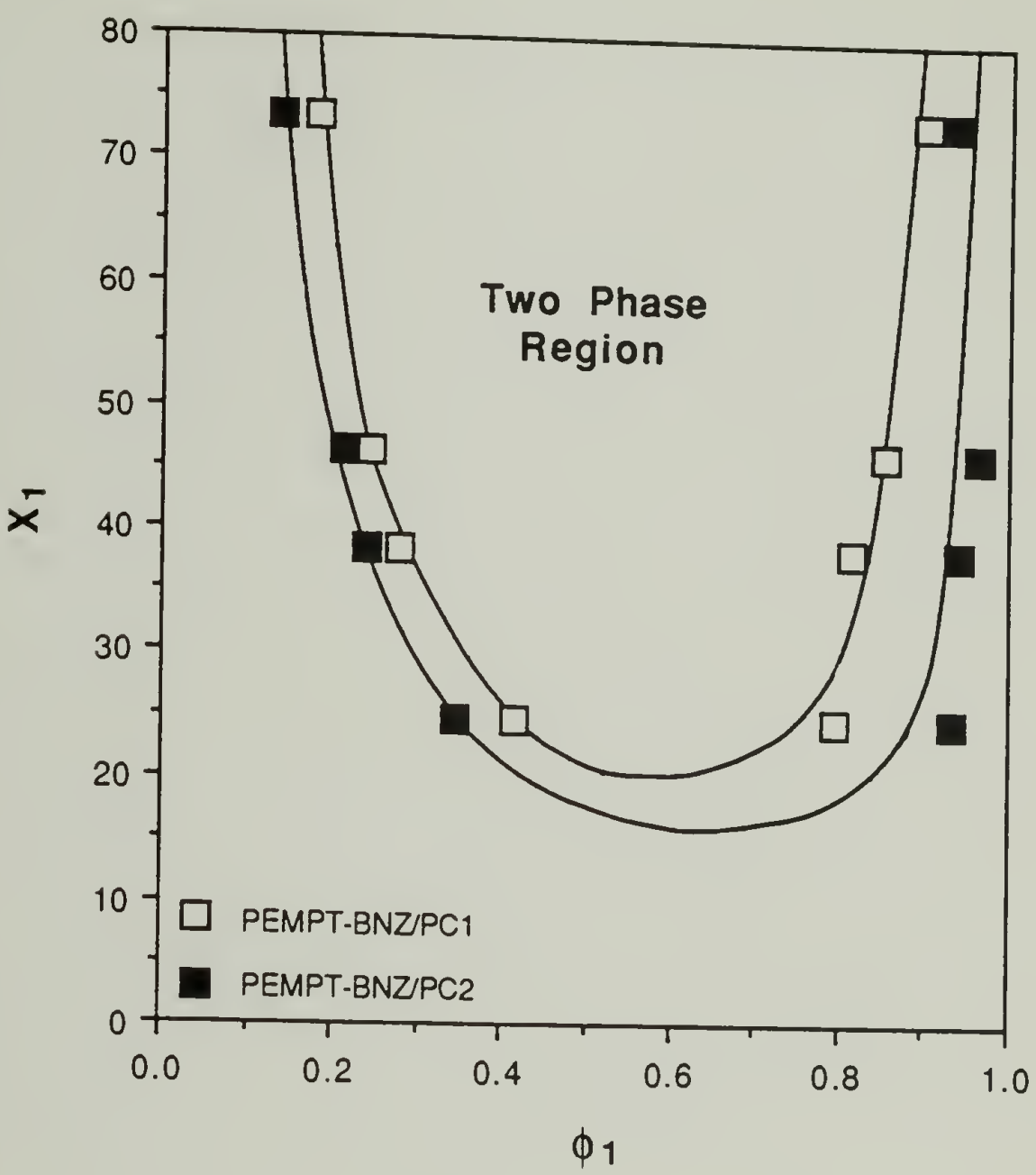

Figure 4.10 Miscibility maps of PEMPT-BNZ/PC1 and PEMPT-BNZ/PC2 50/50 wt. % blends.

However, it should be noted that the single T_g of PEMPT1-HFB/PC2 blend was somewhat broader than that observed for the PEMPT1-HFB/PC1 blend, indicating this system was near the edge of the immiscible/miscible window. The improvement in intermixing between the two phases as both the PEMPT and PC molecular weights are lowered is once again observed, conforming to theoretical entropic considerations. To insure that improved intermixing was not a result of interchange reaction, ^1H NMR was run on the PEMPT1-BNZ/PC2 blend. Figure 4.11 shows the terephthalate region of the spectrum. If interchange reaction had occurred, additional resonances in the region of 8.1-8.3 ppm are expected. No evidence of these resonances are seen and the conclusion is drawn that no transreaction has occurred. Due to the fact that the PEMPT1-BNZ/PC2 blend was single phase, there was a greater probability of contact between the two functional groups (compared to phase separated blends), hence, this blend was expected to have the greatest probability of exchange reaction. With no evidence to support transreaction, it is concluded that transreaction in blends containing higher molecular weight PEMPT-BNZ is most unlikely.

Figure 4.12 and 4.13 compare the miscibility maps of the hydroxyl terminated (extrapolated to 0% alcoholysis transreaction) and benzylate terminated PEMPT/PC1 and PEMPT/PC2 blends, respectively. The miscibility maps of the PEMPT/PC1 blends show little difference in the level of intermixing. Blends containing the hydroxyl terminated PEMPTs are slightly more phase separated than those containing the benzylate terminated. The PEMPT/PC2 blends of Figure 4.13 show a more pronounced difference, with the PEMPT-OH blends showing less intermixing among the two phases than the PEMPT-BNZ blends. This effect is more prominent at the lower molecular weights where the concentration of end groups is high. Comparing the PEMPT1/PC2 blends, the hydroxyl system was two phase while the benzylate end capped system was single phase. This data indicates that the end group type can cause variations in the phase behavior of the blend. However, the effect is only significant at the lowest molecular weights where the end groups concentrations are ~ 8-12%. Overall, the fact that PEMPT-OH-0%/PC and PEMPT-BNZ/PC blends exhibited very similar phase behavior indicates that hydrogen bonding is not a dominating driving force for phase separation.

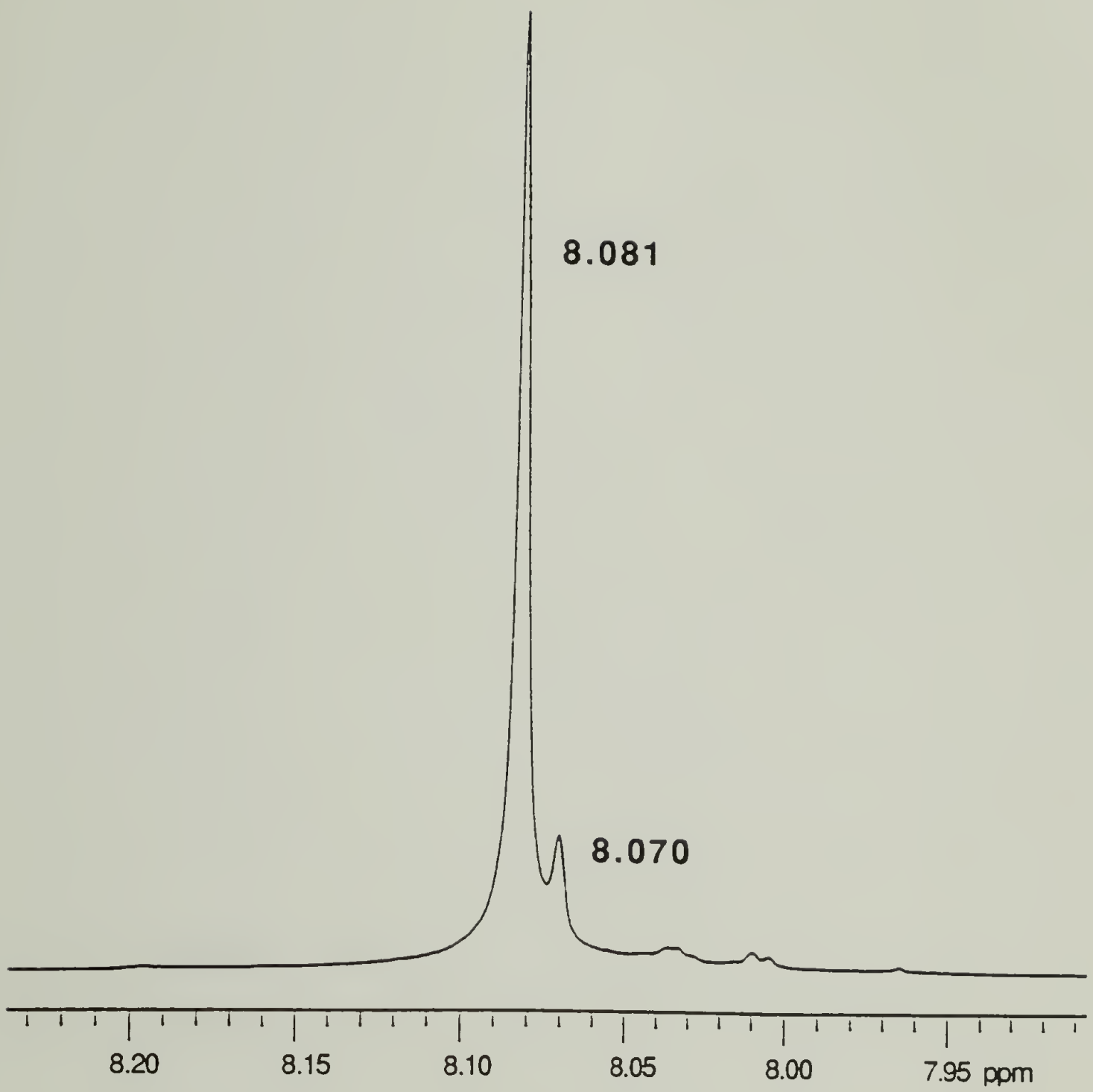

Figure 4.11 300 MHz ^{1}H NMR of PEMPT1-BNZ/PC2 50/50 wt. % blend after DSC thermal treatment. The terephthalate region of PEMPT is displayed.

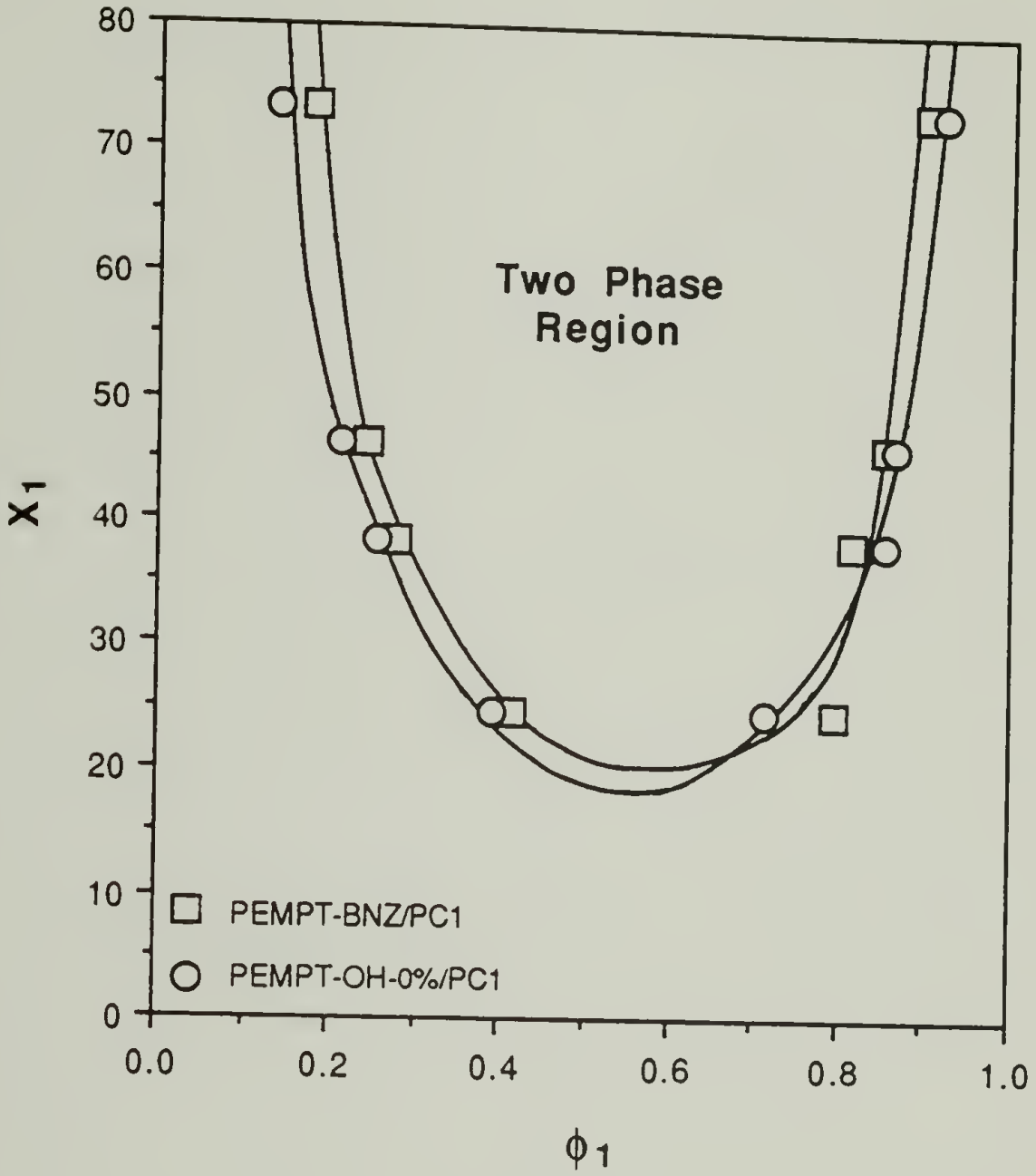

Figure 4.12 Miscibility maps of PEMPT-BNZ/PC1 and PEMPT-OH-0%/PC1 50/50 wt. % blends.

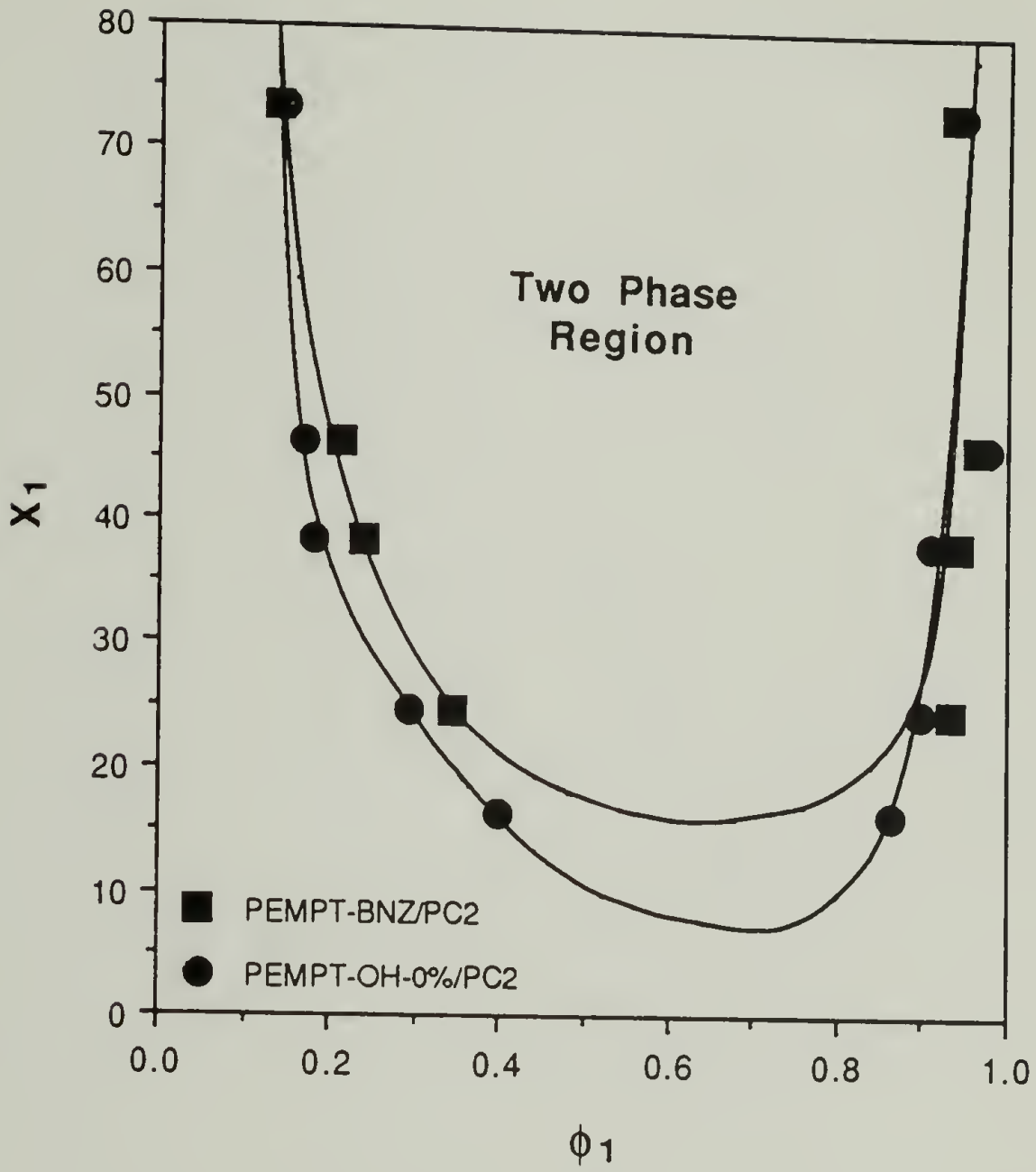

Figure 4.13 Miscibility maps of PEMPT-BNZ/PC2 and PEMPT-OH-0%/PC2 50/50 wt. % blends.

4.5.2.4 PEMPT-HFB/PC Blends

Tables 4.17 and 4.18 contains the T_g and ϕ_i data for the PEMPT-HFB/PC 50/50 wt. % blends. Figure 4.14 shows the corresponding miscibility maps. The intermixing of blend components shows little or no increase as the molecular weight of the polyester is lowered. The PC rich phase shows nearly a constant amount of intermixed PEMPT, ~ 13%, for all PEMPT and PC molecular weights studied. The PEMPT rich phase has 5-10% intermixed PC1 (PEMPT/PC1 blends) and 0-3% intermixed PC2 (PEMPT/PC2 blends) over the entire range of PEMPT molecular weights examined. These results are in stark contrast to the hydroxyl and benzylate end capped PEMPT/PC blends. Figure 4.15 and 4.16 show the miscibility maps of the heptafluorobutyrate and benzylate end capped PEMPT/PC1 and PEMPT/PC2 blends, respectively. The differences in the observed phase behavior is pronounced. In general the blends containing PEMPT-HFB show no improvement in the level of interphase mixing as the polyester molecular weight is lowered. This is in contrast to the PEMPT-BNZ systems which show considerable improvements in the degree of intermixing as both the polyester and PC molecular weights are decreased. The results on the PEMPT-HFB blends disagree entirely with entropic considerations which predict enhanced intermixing as molecular weight is lowered. The obvious conclusion is that the HFB end groups are altering the phase behavior of the blends.

For blends containing PEMPT-HFB and PEMPT-BNZ, the differences between the volume fractions, $[\phi_1'_{(HFB)} - \phi_1'_{(BNZ)}]$ and $[\phi_1''_{(BNZ)} - \phi_1''_{(HFB)}]$, were calculated (the order of subtraction was reversed for the PC rich phase so that the volume fraction differences were represented as positive values). Figure 4.17 shows the plot of these differences vs. the ratio of end groups to PEMPT midchain groups. At the low end group/midchain group ratio (high PEMPT molecular weight) there is virtually no difference between the plots. The value of the differences extrapolated to zero end/midchain ratio (infinite molecular weight) approach an identical value of ~ -0.02 volume fraction units. At infinite molecular weight, the end groups would have no effect on the blend phase behavior. Thus, the volume fraction differences are expected to be zero at a zero end group/midchain group ratio. Within experimental error, the intercept value of -0.02 volume fraction units agrees with this prediction. The greatest volume fraction differences are found at the highest end group/midchain ratio

Table 4.17 T_g and ϕ_i Data for PEMPT-HFB/PC1 50/50 Wt. % Blends

polyester	T_g' (°K)	T_g'' (°K)	ϕ_1'	ϕ_2'	ϕ_1''	ϕ_2''
PEMPT-1	324.3	393.3	0.949	0.051	0.179	0.821
PEMPT-2	331.9	396.8	0.926	0.074	0.164	0.836
PEMPT-3	336.2	401.6	0.924	0.076	0.133	0.867
PEMPT-4	339.2	401.6	0.905	0.095	0.137	0.863
PEMPT-5	340.4	404.7	0.866	0.134	0.119	0.881
PEMPT-6	342.8	403.8	0.916	0.084	0.126	0.874

Table 4.18 T_g and ϕ_i Data for PEMPT-HFB/PC2 50/50 Wt. % Blends

Polyester	T_g' (°K)	T_g'' (°K)	ϕ_1'	ϕ_2'	ϕ_1''	ϕ_2''
PEMPT-1	321.5	399.3	1.000	0.000	0.155	0.845
PEMPT-2	328.0	402.2	0.993	0.007	0.144	0.856
PEMPT-3	333.7	405.3	0.970	0.030	0.128	0.872
PEMPT-4	334.7	407.5	0.987	0.013	0.114	0.886
PEMPT-5	336.9	409.8	0.999	0.001	0.098	0.902
PEMPT-6	340.3	408.9	0.964	0.036	0.109	0.891

Single "prime" denotes PEMPT rich phase, "double prime" PC rich phase. PEMPT is designated as component 1.

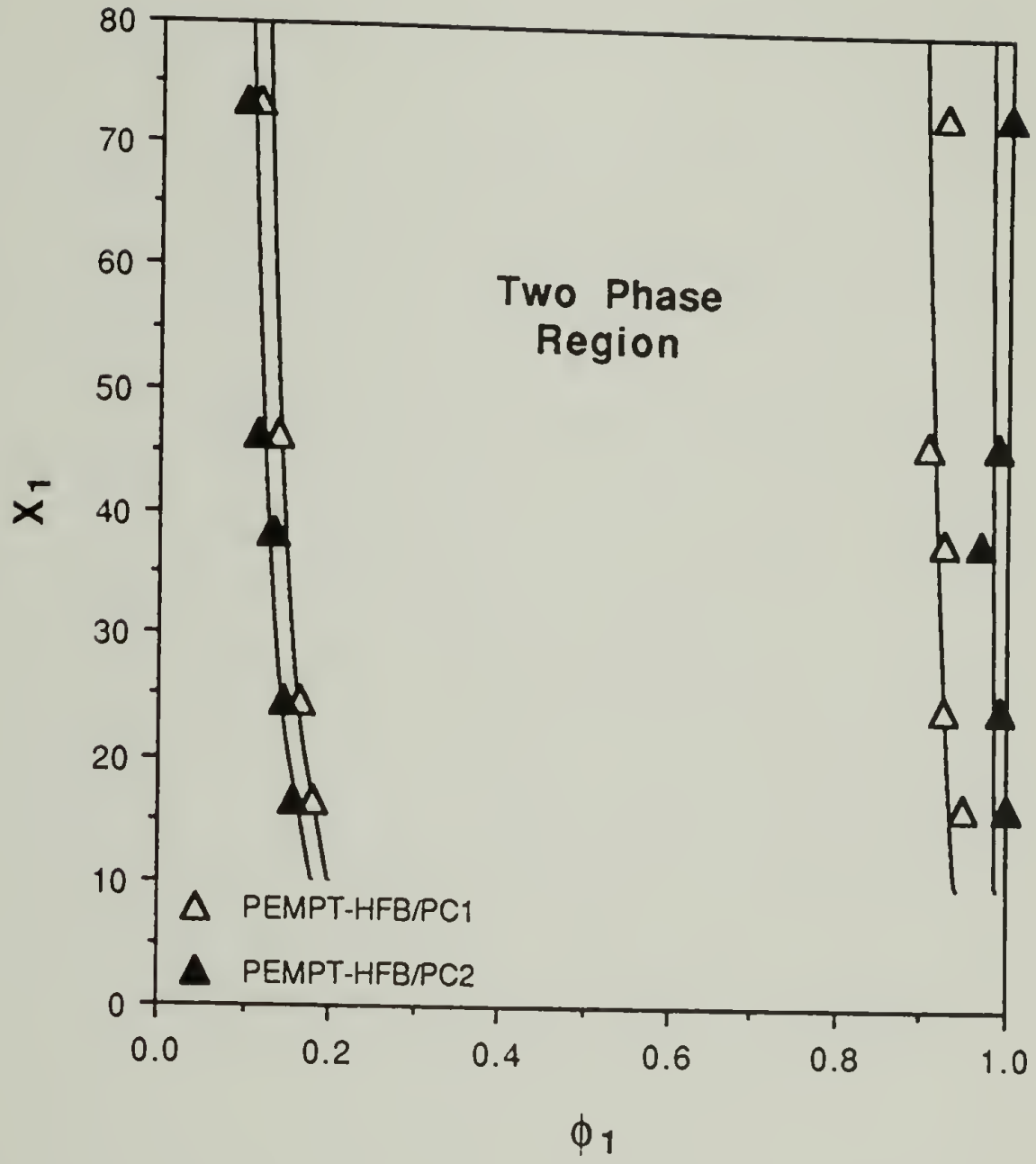

Figure 4.14 Miscibility maps of PEMPT-HFB/PC1 and PEMPT-HFB/PC2 50/50 wt. % blends.

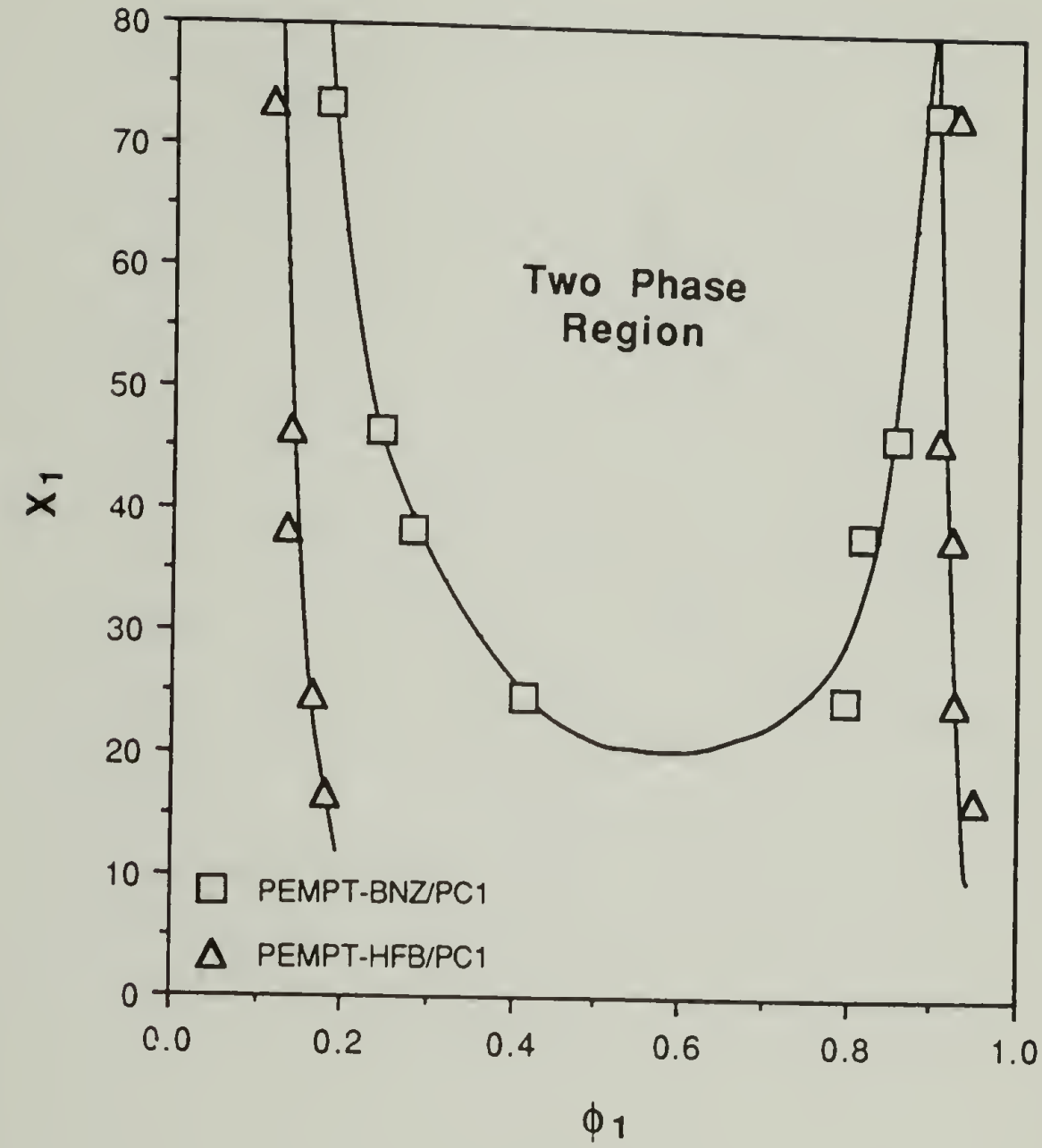

Figure 4.15 Miscibility maps of PEMPT-BNZ/PC1 and PEMPT-HFB/PC1 50/50 wt. % blends.

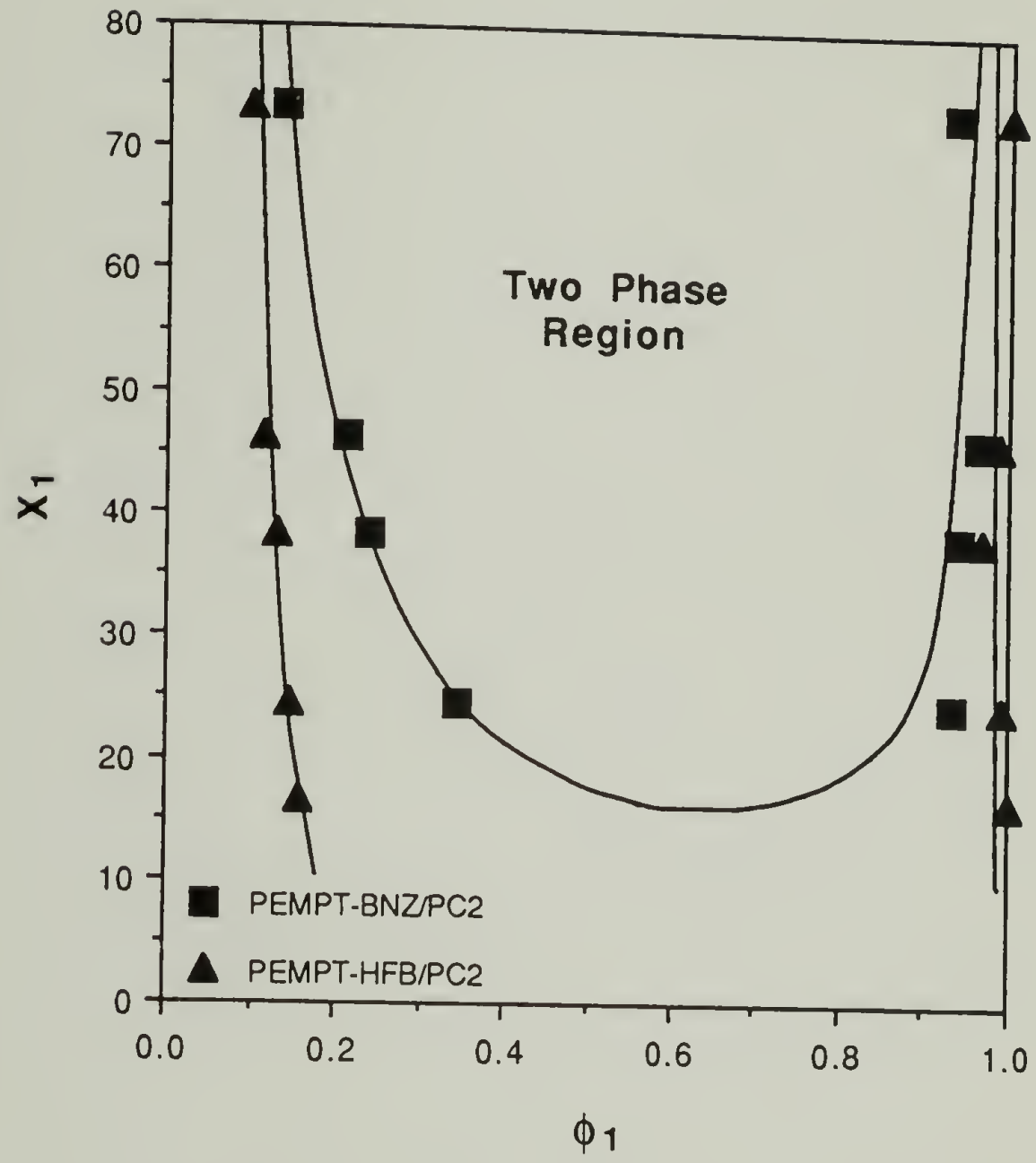

Figure 4.16 Miscibility maps of PEMPT-BNZ/PC2 and PEMPT-HFB/PC2 50/50 wt. % blends.

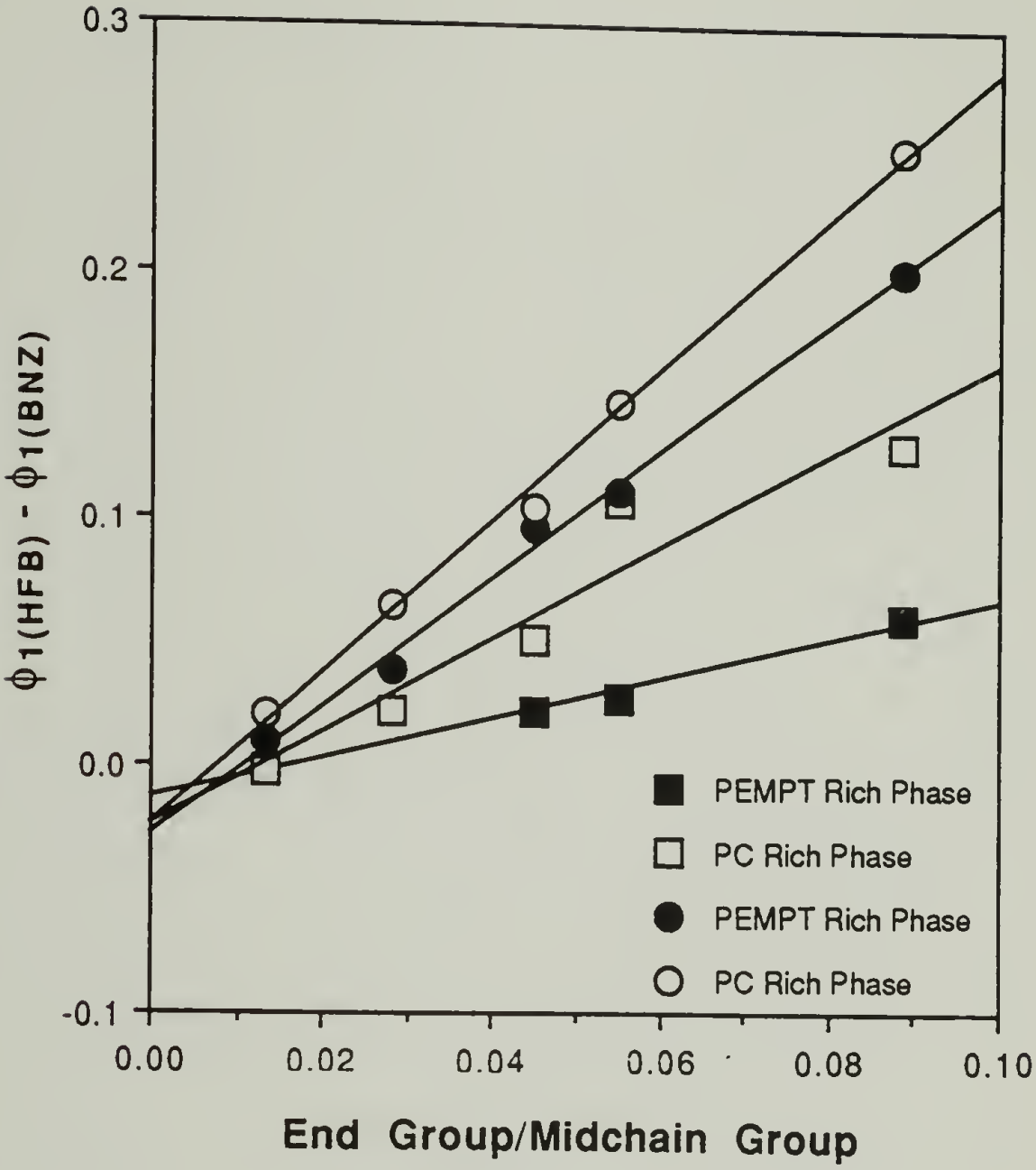

Figure 4.17 [ϕ_1(HFB)-ϕ_1(BNZ)] vs. end group/midchain group ratio for PEMPT/PC1 (circles) and PEMPT/PC2 (squares) blends.

regardless of which blend system (PEMPT/PC1 or PEMPT/PC2) or phase (PEMPT rich or PC rich) is examined. In general, the blends of PEMPT with PC1 show greater differences than those containing PC2. This is due to the increased level of intermixing associated with the lower molecular weight PC. It also suggests that the end group effect can nullify this large entropic driving force for mixing.

The linear relationship between the volume fraction differences and the end group/midchain group ratio can be explained in terms of the interaction parameter of the blend. Kennedy, Gordon and Koningsveld have generalized the Flory-Huggins treatment of polymer solutions to include end segment effects [40]. The major modification to the free energy of mixing is that two interaction parameters, one for midchain groups and one for terminal groups, are now used . With respect to a polymer-polymer blend, the enthalpic term of the free energy of mixing, ΔH_m, is rewritten as,

$$\Delta H_m = kT\left[\frac{\chi_{MC}X_{MC} + \chi_E X_E}{X_{MC} + X_E}\right]\phi_1\phi_2 \qquad (4.12)$$

χ_{MC}: Interaction parameter of midchain groups of polymers 1 and 2.
X_{MC}: Relative chain length of polymer 1.
χ_E: Interaction parameter of an end group of polymer 1 and a midchain group of polymer 2.
X_E: Relative chain length of an end group of polymer 1.

It should be mentioned that Equation 12 has been written assuming the major contribution to the enthalpy of mixing comes from polymer1-polymer2 midchain-midchain interactions and polymer1-polymer2 end group-midchain interactions. For all but the lowest molecular weights, $X_{MC} + X_E \cong X_{MC}$, and Equation 4.12 can be rewritten.

$$\Delta H_m = kT\left[\chi_{MC} + \frac{\chi_E X_E}{X_{MC}}\right]\phi_1\phi_2 \qquad (4.13)$$

The overall interaction parameter of the blend, χ_{12}, now depends on the ratio of end groups to midchain groups, Equation 4.14.

$$\chi_{12} = \left[\chi_{MC} + \frac{\chi_E X_E}{X_{MC}} \right] \qquad (4.14)$$

Qualitatively, it will be assumed that the observed volume fraction differences are, proportional to the difference in the free energy of mixing of the PEMPT-HFB/PC blends and PEMPT-BNZ/PC blends.

$$[\phi 1'_{(HFB)} - \phi 1'_{(BNZ)}] \alpha \Delta G_{m(HFB)} - \Delta G_{m(BNZ)} \qquad (4.15)$$

For each pair of blends of equivalent molecular weight, the entropic contribution to the chemical potential will cancel and the only remaining terms will be the enthalpic portion of ΔG_m. If one additional assumption is made, that the structural similarity of the benzylate end group to the terephthalate group in PEMPT allows it to be represented as a midchain group, $\chi_{E(BNZ)} \cong \chi_{MC}$, the volume fraction differences can be represented as,

$$[\phi 1'_{(HFB)} - \phi 1'_{(BNZ)}] \alpha \Delta H_{m(HFB)} - \Delta H_{m(BNZ)} = kT\left[\chi_{MC} + \frac{\chi_E X_E}{X_{MC}} - \chi_{MC}\right]\phi_1\phi_2 \qquad (4.16)$$

$$[\phi 1'_{(HFB)} - \phi 1'_{(BNZ)}] \alpha \Delta H_{m(HFB)} - \Delta H_{m(BNZ)} \alpha \frac{\chi_E X_E}{X_{MC}} \qquad (4.17)$$

Equation 4.17 predicts that the volume fraction differences are proportional to the end group/midchain group ratio in agreement with the observations of Figure 4.16. For this case, χ_E represents the HFB end group-PC midchain group interaction parameter, X_E the relative chain length of a HFB terminal group, χ_{MC} is the PEMPT midchain-PC midchain interaction parameter and X_{MC} is the relative chain length of PEMPT excluding end groups. For the calculation of X_E/X_{MC}, X_E is assumed to be 2 and X_{MC} is equal to $[X_1 - 2]$.

4.5.3 Critical Point Data and Calculation of the Interaction Parameter

4.5.3.1 Critical Point Data

Before concluding this chapter, the miscibility maps of the PEMPT-BNZ/PC blends will be used to calculate some additional thermodynamic

parameters. Examining Figure 4.10, a miscibility map represents a curve on the boundary surface similar to curve dce of Figure 4.1. Hence, each miscibility map also contains a single critical point which is of particular interest. The assumption will be made that the minimum of each miscibility map corresponds to the critical point. Within the constraints of Flory-Huggins theory, this fact is true if both blend components are monodisperse. The extent to which the above assumption is violated will be judged by the comparison between the experimentally determined critical compositions and the values derived from Equations 4.4-4.7 (F-H theory) and 4.4-4.11 (modified F-H theory accounting for polydispersity effects). Table 4.19 contains the critical chain lengths, X_{n1c}, and critical composition, ϕ_{1c}, determined from the minimums of the miscibility maps of Figure 4.10. For calculations involving Equation 4.11, the values of X_{w1} and X_{z1} corresponding to the experimentally determined X_{n1c} were determined from interpolations using the X_{n1} data of Table 4.4 and the corresponding polydispersities of PEMPT-BNZ and PC contained in Tables 3.7 and 3.3, respectively.

The experimentally determined values of ϕ_{1c} are in good agreement with the calculated values of both Equations 4.7 (F-H theory) and 4.11 (modified F-H theory). Indicating that the critical points do lie close to the minimum in the miscibility maps. The fact that values of ϕ_{1c} calculated from equations 4.7 and 4.11 are in agreement with one another is somewhat fortuitous, being associated with the observed polydispersities of the polyesters and polycarbonates. Rewriting Equation 4.11 in terms of the polydispersities, one obtains,

$$\phi_{1c} = \frac{1}{\left[\, 1 + \left(\frac{X_{n1}}{X_{n2}}\right)^{1/2} \left(\frac{X_{w1}/X_{n1}}{X_{w2}/X_{n2}}\right)^{1/2} \left(\frac{X_{z2}/X_{w2}}{X_{z1}/X_{w2}}\right)^{1/2} \right]} \qquad (4.18)$$

Using the values of M_w/M_n and M_z/M_w of Tables 3.3 and 3.7 for PC1 and PEMPT1-BNZ, the values of the 2nd and 3rd terms in the product of Equation 4.18 are calculated to be 0.975 and .0.994, respectively. Similarly for PC2 and PEMPT1-BNZ these terms are 0.999 and 0.984. With these products so nearly close to the value 1.00, the overall product in the denominator of Equation 4.18 reduces to $(X_{n1}/X_{n2})^{1/2}$ and Equation 4.18 is identical to Equation 4.7. At the low PEMPT molecular weights where the ratios described above have values

Table 4.19 Critical Point and Interaction Parameter Data

Parameter	Experimental Value	Calculated Value	
		F-H	Modified F-H
X_{n1c} (PEMPT/PC1)	21	-	-
X_{n2c} (PEMPT/PC1)	45.2	-	-
ϕ_{1c} (PEMPT/PC1)	0.56	0.59	0.60
X_{n1c} (PEMPT/PC2)	17	-	-
X_{n2c} (PEMPT/PC2)	84.8	-	-
ϕ_{1c} (PEMPT/PC2)	0.66	0.67	0.69
χ_{12s} (PEMPT/PC1)	-	0.067	0.045
χ_{12c} (PEMPT/PC1)	-	0.068	-
χ_{12s} (PEMPT/PC2)	-	0.062	0.043
χ_{12c} (PEMPT/PC2)	-	0.062	-

close to 1, the blend behaves as a monodisperse binary pair. In this case, the critical points are theoretically expected to be at the minimum in the phase diagram, as was assumed above. Results of this nature have been predicted by Koningsveld, et al [15].

4.5.3.2 Calculation of the Interaction Parameter

The miscibility maps of Figure 4.10 can also be used to calculate the interaction parameter of the blend. The critical point represents the one point on the boundary surface of Figure 4.1 where the spinodal and binodal surfaces coincide. The critical point also represents a point on the boundary surface where the interaction parameters can be easily calculated from theories such as F-H (Equation 4.4 or 4.6) or the modified F-H theory accounting for polydispersity effects (Equation 4.10). With respect to F-H theory, the interaction parameter of the blend calculated from either Equation 4.4 or Equation 4.6 should be identical, if the critical point molecular weight and volume fraction data is applied. The calculated values of χ_{12s} and χ_{12c} determined from both equations are in agreement with this statement (Table 4.19) with the interaction parameters all being ~0.065. The values calculated by applying Equation 4.10 agree with one another and have an average value of 0.044.

The interaction parameters calculated from the two different theories do not agree with one another. Unlike the equations describing ϕ_{1c}, the equations used to determine χ_{12} are not functions of the polydispersity ratios which were previously shown to be ~1. The polydispersity effects are thus expected to lead to a difference in the calculated interaction parameters. Between the two sets of calculations, the F-H theory modified to account for polydispersity effects is a better representation of the current blend system. The interaction parameter value calculated from this model, 0.044, will be designated as the interaction parameter for the PEMPT/PC blends. This value will be used later in Chapter 5 to interpret phase behavior data of the transreacting blends.

4.6 Conclusions.

The equilibrium phase behavior of PEMPT/PC blends has been studied as a function of three variables; blend composition ratio, PEMPT and PC molecular weights, and end group type. Composition effects were studied

using PEMPT-OH15/PC blends of varying molecular weight. In general, most of the blends exhibited two phase behavior with some level of intermixing between the components. Single phase blends were identified and these corresponded to blends containing the lowest molecular weights. In the phase separated blends, the amount of PC intermixed in the PEMPT rich phase showed little dependence on the blend composition. The amount of PEMPT intermixed in the PC rich phase did show a minor composition dependence with less intermixing being observed as the PEMPT/PC ratio decreased. The level of intermixing in blends containing the highest molecular weight PEMPTs were in agreement with previous phase behavior studies of PBT/PC and PET/PC blends [26,39]. In general, the miscibility maps of the blends constructed at the varying compositions exhibited the same characteristics with respect to molecular weight, i.e., improved intermixing as the molecular weight of the PEMPT or PC component is decreased. This was expected due to the decrease in ΔG_m associated with the decrease in the entropic contribution to the free energy of mixing.

Phase behavior studies examining end group type were conducted on PEMPT samples having hydroxyl, heptafluorobutyrate and benzylate end groups. These studies were also conducted as a function of varying PEMPT and PC molecular weights. The miscibility maps of the PEMPT-OH and PEMPT-BNZ blends were in fair agreement at all but the lowest molecular weight PEMPTs studied. As the molecular weight of PEMPT was lowered, the PEMPT-BNZ/PC systems showed a greater level of intermixing than the hydroxyl terminated PEMPT/PC blends. Although the phase behavior of the PEMPT-OH/PC and PEMPT-BNZ/PC displayed significant differences in blends containing the low molecular weight PEMPTs, the same general trend of improved interphase mixing with decreasing molecular weight was observed.

In contrast, the miscibility map of the PEMPT-HFB/PC blends showed little or no improvement in the level of intermixing as the molecular weight of the components were lowered. For blends containing PEMPT-HFB and PEMPT-BNZ, the volume fraction differences ($[\phi 1'_{(HFB)} - \phi 1'_{(BNZ)}]$ and $[\phi 1'_{(BNZ)} - \phi 1'_{(HFB)}]$) were calculated and found to be proportional to the end group/midchain group ratio. This behavior has been explained in terms of a two component interaction parameter, composed of χ_{MC} and χ_E. From a qualitative stand point, if it is assumed that the differences in volume fraction are proportional to the differences in the free energies of mixing, the volume fraction differences

can be theoretically shown to be proportional to the end group/midchain group ratio.

Using the miscibility maps of the PEMPT-BNZ/PC blends, critical point data and the interaction parameter were calculated. The minimums of the miscibility maps were assumed to correspond to the critical point of the blend. The critical compositions, ϕ_{1c}, and molecular weights determined experimentally were then used in conjunction with F-H theory and a modified F-H theory (accounting for polydispersity) to calculate the critical points. The agreement between the experimental and theoretical values of ϕ_{1c} was good. Unexpectedly, it was also found that the critical points calculated from F-H theory and the modified F-H theory were also in good agreement with one another. The result was fortuitous, being explained in terms of the polydispersity ratios. At the molecular weights corresponding to the critical points, these ratios were ~ 1 which allows the equation used to calculate ϕ_{1c} (accounting for polydispersity) to be reduced to that of F-H theory for monodisperse polymers. Overall, these result indicate that the miscibility maps derived from the DSC phase behavior studies are an accurate thermodynamic representation of the blend system.

Additionally, from the critical point data, the interaction parameter of the blend was calculated. At the critical point, F-H theory predicts that the the interaction parameter calculated from both the spinodal and critical point equations should be identical. This result was confirmed in the PEMPT/PC blends. Unlike ϕ_{1c}, the interaction parameter determined from F-H theory is not expected to coincide with that determined from the modified F-H theory (accounting for polydispersity). The calculated values were 0.065 (F-H) and 0.044 (modified F-H). The modified F-H theory represents a more accurate description of the current blends, hence, the interaction parameter calculated from this theory, 0.044, is taken as the interaction parameter for the PEMPT/PC system. This value was calculated from critical point data determined from the miscibility maps of the PEMPT-BNZ/PC blends. The similar structure of the benzylate end group relative to the terephthalate ring of PEMPT should minimize end group effects and allow this value to be the most accurate representation of χ_{12}.

4.7 References

1. Gibbs, J.W. *The Collected Works, Vol. I. Thermodynamics*; Yale University Press Reprint: New Haven, 1957.

2. Hildebrand, J.H.; Scott, R.L. *Regular Solutions*; Prentice-Hall, Inc.: New Jersey, 1962.

3. Hildebrand, J.H.; Scott, R.L. *The Solubility of Nonelectrolytes*; Reinhold: 1950.

4. Flory, P.J. *J. Chem. Phys.* **1941**, 9, 660.

5. Huggins, M.L. *J. Chem. Phys.* **1941**, 9, 440.

6. Flory, P.J. J. *Chem. Phys.* **1942**,10, 51.

7. Huggins, M.L. *J. Phys. Chem.* **1944**, 46, 151.

8. Flory, P.J. *J. Chem. Phys.* **1944**, 12, 425.

9. Scott, R.L.; Magat, M. *J. Chem. Phys.* **1945**, 13, 172.

10. Scott, R.L. J. *Chem. Phys.* **1949**, 17, 279.

11. Flory, P.J. *Principles of Polymer Chemistry*; Cornell University Press: Ithica, 1953.

12. Paul, D.R. *Polymer Blends*; Paul, D.R.; Newman, S. Eds., Academic Press: New York, 1978.

13. Olabisi, O.; Robeson, L.M.; Shaw, M.T. *Polymer-Polymer Miscibility*; Academic Press: New York, 1979.

14. Koningsveld, R.; Chermin, H.A.G.; Gordon, M. *Proc. Roy. Soc. Lond.* **1970**, A319, 331.

15. Koningsveld, R.; Kleintjens, L.A.; Schoffeleers, H.M. *Pure Appl. Chem.* **1974**, 39,1.

16. Warmund, D.C.; Paul, D.R.; Barlow, J.W. *J. Appl. Polym. Sci.* **1978**, 22, 2155.

17. Hanrahan, B.D.; Angeli, S.R.; Runt, J. *Polym. Bull.* **1985**, 14, 399.

18. Hobbs, S.Y.; Groshans, V.L.; Dekkers, M.E.J.; Shultz, A.R. *Polym. Bull.* **1987**, 17, 335.

19. Birley, A.W.; Chen, X.Y. *Br. Polym. J.* **1984**, 16, 77.

20. Birley, A.W.; Chen, X.Y. *Br. Polym. J.* **1985**, 17, 297.

21. Pratt, G.J.; Smith, M.J.A. *Polymer* **1989**, 30, 1113.

22. Hobbs, S.Y.; Dekkers, M.E.J.; Watkins, V.H. *J. Mat. Sci.* **1988**, 23, 1219.

23. Hobbs, S.Y.; Dekkers, M.E.J.; Watkins, V.H. *Polymer* **1988**, 29, 1598-1602.

24. Delimoy, D.; Bailly, C.; Devaux, J.; Legras, R. *Polym. Eng. Sci.* **1988**, 28, 104.

25. Hobbs, S.Y.; Watkins, V.H.; Bendler, J.T. *Polymer* **1990**, 31, 1663.

26. Kim, W.N.; Burns, C.M. *Makromol. Chem.* **1989**, 190, 661-676.

27. Nassar, T.R.; Paul, D.R,; Barlow, J.W. J. *Appl. Polym. Sci.* **1979**, 23, 85.

28. Murff, S.R.; Barlow, J.W.; Paul, D.R. *J. Appl. Polym. Sci.* **1984**, 29, 3231.

29. Huang, Z.H.; Wang, L.H. *Makromol. Chem., Rapid Commun.* **1986**, 7, 255.

30. Hanrahan, B.D.; Angeli, S.R.; Runt, J. *Polym. Bull.* **1986**, 15, 455.

31. Suzuki, T.; Tanaka, H.; Nishi, T. *Polymer* **1989**, 30, 1287.

32. Devaux, J.; Godard, P.; Mercier, P.; Touillaux, R.; Dereppe, J.M., *J. Polym. Sci., Polym. Phys. Ed.* **1982**, 20, 1881.

33. Birley, A.W.; Chen, X.Y. *Br. Polym. J.* **1984**, 16, 77

34. Huang, Z.H.; Wang L.H. *Makromol. Chem., Rapid Commun.* **1986**, 7, 255.

35. Godard, P.; Dekoninck, J.M.; Devlesaver, V.; Devaux, J. *J. Polym. Sci., Polym. Chem.* **1986**, 24, 3301.

36. Velden, G.v.d, Kolfschoten-Smitsmans, G.; Veermans, A. *Polym. Commun.* **1987**, 28, 169.

37. Henrichs, P.M.; Tribone, J.; Massa, D.J.; Hewitt, J.M. *Macromolecules* **1988**, 21, 1282.

38. Couchman, P.R. *Macromolecules* **1978**, 11, 1156.

39. Kim, W.N.; Burns, C.M. *J. Polym. Sci., Polym. Phys.* **1990**, 28, 1409.

40. Kennedy, J.W.; Gordon, M.; Koningsveld, R. *J. Polym. Sci.: Part C* **1972**, 39, 43.

CHAPTER 5

PHASE BEHAVIOR: ALCOHOLYSIS AND MIDCHAIN TRANSREACTION EFFECTS

5.1 Introduction

With the phase behavior of non-transreacted PEMPT/PC blends identified, attention will now focus on transreaction and its relation to the observed phase behavior of the blend. Similar to discussions on PBT/PC and PET/PC systems [1,2] there are four possible interchange reactions to be concerned with.

1) Direct midchain transreaction between a carbonyl of PEMPT and a carbonate of PC.
2) Alcoholysis of PC by a hydroxyl end group of PEMPT.
3) Acidolysis of PC by an acid end group of PEMPT.
4) Alcoholysis of PEMPT by a hydroxyl end group of PC.

As discussed in Chapter 1, many studies have identified transreactions either directly (NMR, IR) or indirectly from phase behavior studies (DSC, DMTA and microscopy). It is a safe conclusion that in any indirect study of exchange reaction, the separate role of midchain and end group transreactions was unidentifiable. In studies that have employed direct measures of interchange reaction, specifically ^{1}H and ^{13}C NMR [3-13], none have assigned any observed resonances to a specific end group in the polymer blend under observation. Thus, most of these studies also ignore the separate roles of the reactions. In actuality, the low level of end groups present combined with the insolubility of the polyesters studied has made indentification of these moities difficult.

In their kinetic studies of model compounds transreacting with PBT and PC [1] and in their kinetic study of a transreacting PBT/PC blend [4], Devaux, et. al., concluded that alcoholysis did not play a major role in the interchange process and that direct midchain reaction is the most likely mechanism in

PBT/PC transesterification. These conclusions could also be drawn from several other facts. With alcoholysis of PBT by PC phenol end groups not observed and with carbonate acid end groups known to be unstable (decomposing to carbon dioxide and a phenol end group [14,15]), once all of the PBT hydroxyl and acid end groups have transreacted no other end group reactions can occur. With the percentage of end groups being relatively low, less than 2-3 %, extensive randomization of the blend components could only be achieved through midchain reactions. It should be mentioned that in Devaux's studies, end group reaction was determined indirectly by molecular weight changes monitored by viscosity measurements. No direct spectroscopic identification was made.

From this information, it does appear that direct midchain reaction plays the dominant role in the extensive transesterification of polyester/PC blends, the role of alcoholysis being inconsequential. In the present studies, this may lead one to ignore alcoholysis of PC by PEMPT hydroxyl end groups, concluding that this reaction has no significant impact on this system. However, the present goal is to examine the effect of transreaction on blend phase behavior. In this case, where small amounts of diblock, triblock, etc. coplymers may lead to varying degrees of compatibilization of the blend system, end group reactions may indeed become important.

In the present study, acidolysis of PC by PEMPT acid end groups is ignored as a significant mode of interchange reaction for two reasons. First, because the carboxylic acid ends are present in extremely small quantities, less than 2% of the total end group content at M_ns less than 20,000 gm/mole, their presence in this study is immeasurable by NMR and their effect on the phase behavior of the blend will be shown to be imperceivable by DSC. Second, with the resulting carbonate acid end group known to decompose into species incapable of interchange reaction, acidolysis can not lead to extensive randomization of the blend components. Additionally, alcoholysis of PEMPT by PC hydroxyl end groups will also be ignored. Studies on model compounds has shown that this reaction does not occur [1] and evidence is presented to support that this fact is true in the PEMPT/PC system. With the proton resonances associated with the aliphatic-hydroxyl end group in PEMPT identified (Chapter 3), the PEMPT/PC blend system offers the unique opportunity to monitor the hydroxyl end groups and hence alcoholysis transreactions independent of direct midchain reaction. These two reactions,

direct midchain and alcoholysis of PC by the hydroxyl end groups of PEMPT, are the focal point of this chapter.

5.2 Experimental

5.2.1 Polyesters and Blends

The PEMPT-OH15/PC and PEMPT-OH2/PC blends of Chapter 4 are used to identify alcoholysis interchange reactions. It should be mentioned once again that these blends contain DNOP as a stabilizer to inhibit direct midchain transreaction. At the same time, DNOP may also inhibit alcoholysis reactions. This point will be discussed later in this chapter.

Blends for midchain transreaction studies were prepared by a codissolution/precipitation procedure. PEMPTB, .35 g, and PC2 (single precipitated), .35 g, were placed into a 26 ml vial. Chloroform, 17 ml (Aldrich HPLC grade), and a micro-magnetric stir bar were added. The vial was capped and the solution left overnight under moderate stirring. The solution was added dropwise to a 300 ml beaker containing 170 ml of methanol (Fisher HPLC grade) under vigorous mixing. The precipitated blend/solvent solution was filtered through a 7 cm diameter buchner funnel containing one piece of Whatman qualitative filter paper. The recovered polymer was washed with two 25 ml aloquots of fresh methanol. The blend was dried under vacuum at 76°C for several days and subsequently stored in a vacuum desiccator. This blend contained no DNOP inhibitor.

5.2.2 Alcoholysis and Midchain Transreaction

During the phase behavior studies on PEMPT-OH15/PC and PEMPT-OH2/PC blends (Chapter 4), alcoholysis transreactions occurred while the samples were annealed in the DSC-7. The annealing program and specifics on instrument set up and sample preparation are described there. It should be mentioned that no experiments were conducted to specifically promote alcoholysis interchange reactions. Quite contrary to that, these experiments were being carried out to identify equilibrium phase behavior prior to interchange reaction.

Direct midchain transesterification was conducted in a Perkin-Elmer DSC-4 under nitrogen purge at 200°C . The 6-8 mg samples of PEMPTB/PC2 blends were loaded into the DSC at 50°C, ramped at 100°C/min to 200°C, annealed specified times during which reaction occured and then cooled at 50°C/min to 50°C. The annealed blends were stored in a vacuum desiccator until thermal analysis to determine T_gs was conducted. It should be mentioned that because these samples were prepared from codissolution/precipitation, no crytallzation of the PC component was observed. Thus, the initial temperature ramp to 280°C required for the cast samples (phase behavior studies, Chapter 4) were not required for these blends.

5.2.3 Analysis

DSC was once again used to identify the T_gs and subsequently the blend phase behavior. The DSC temperature program employed is described in Chapter 4. For all the PEMPTB/PC2 blends, the temperature program was as follows. Load at 40°C, quench to 20°C, hold ~ 2 min, scan at 20°C/min to 200°C, quench to 40°C.

Proton NMR was used to quantitatively identify both midchain and alcoholysis transreactions. The samples from DSC studies were dissolved in deuterated chloroform at ~ 1% (w/v) with TMS used as an internal reference. The identical Varian 300 MHz spectrometer and operation parameters descrbed in Section 3.3.3 were employed here.

^1H-^1H correlation spetroscopy (COSY) was also conducted on the Varian 300-XL spectrometer. The spectral width was usually narrowed to the frequency region of interest. Specific scanning conditions are detailed during the discussion of the individual spectra.

Infrared spectroscopy was conducted on a IBM 38 FTIR under nitrogen at room temperature. The frequency range was 400-4000 cm^{-1} with 4 cm^{-1} resolution. One hundred scans were recorded on samples that had been cast from chloroform solution (~ 1% w/v) onto NaCl plates and annealed 24 hr under vacuum at 76°C. Samples were stored in a vacuum desiccator over calcium sulfate prior to scanning.

GPC was conducted on the identical instrument under the identical conditions described in Chapter 3. All the results present in this chapter are relative to the PS calibration standards.

5.3 Alcoholysis Transreaction in PEMPT-OH/PC Blends

5.3.1 Identification of Blend Phase Behavior

Phase behavior studies on PEMPT-OH/PC blends were conducted on polyesters that had been recovered by precipitation into methanol from a 15% w/v polyester/chloroform solution. Polyesters recovered from a 2% w/v polyester/chloroform solution were also prepared to mimic the precipitation procedure used during end capping of the PEMPT-BNZ and PEMPT-HFB polymers. Molecular weight data from GPC shows the hydroxyl terminated polyesters recovered from the 2 and 15% solutions to have similar molecular weights and distributions relative to polystyrene (Chapter 3). Equilibrium phase behavior experiments were run to identify any differences between the two polyesters and to have an accurate control for blends containing PEMPT-BNZ and PEMPT-HFB. With the nearly identical molecular weights and distributions, large deviations in the phase behavior of the two hydroxyl terminated systems were not anticipated.

As previously described, the volume fraction of PEMPT in the PEMPT rich and PC rich phases was determined by applying the Couchman equation to the observed shifts in Tgs identified by DSC. The constant in the Couchman equation, $\Delta C_{p2}/\Delta C_{p1}$, was again set equal to 0.7. Figures 5.1 and 5.2 display the phase behavior for the PEMPT-OH15 and PEMPT-OH2/PC1 and PEMPT-OH15 and PEMPT-OH2/PC2 blend systems, respectively. The miscibility maps displayed show marked differences between the PEMPT-OH15/PC and PEMPT-OH2/PC systems. The two phase region of the PEMPT-OH2/PC1 blends is decreased over that of the PEMPT-OH15/PC1 systems. The shift in the phase behavior corresponds to an increase in the volume fraction of PEMPT in the PC rich phase ranging from 0.05-0.15, depending on the degree of polymerization of the polyester. A similar increase in the volume fraction of PC in the PEMPT rich phase is seen. Additionally, the PEMPT2-OH2/PC1 blend (X_n PEMPT = 24.6) is miscible while the PEMPT2-OH15/PC1 blend displays two phases with some intermixing of the two components. The phase behavior of the PEMPT-OH2/PC2 and PEMPT-OH15/PC2 blends show similar decreases in the two phase region of the PEMPT-OH2/PC2 blends relative to the latter. The range of increase of PC in the PEMPT rich phase and the increase of

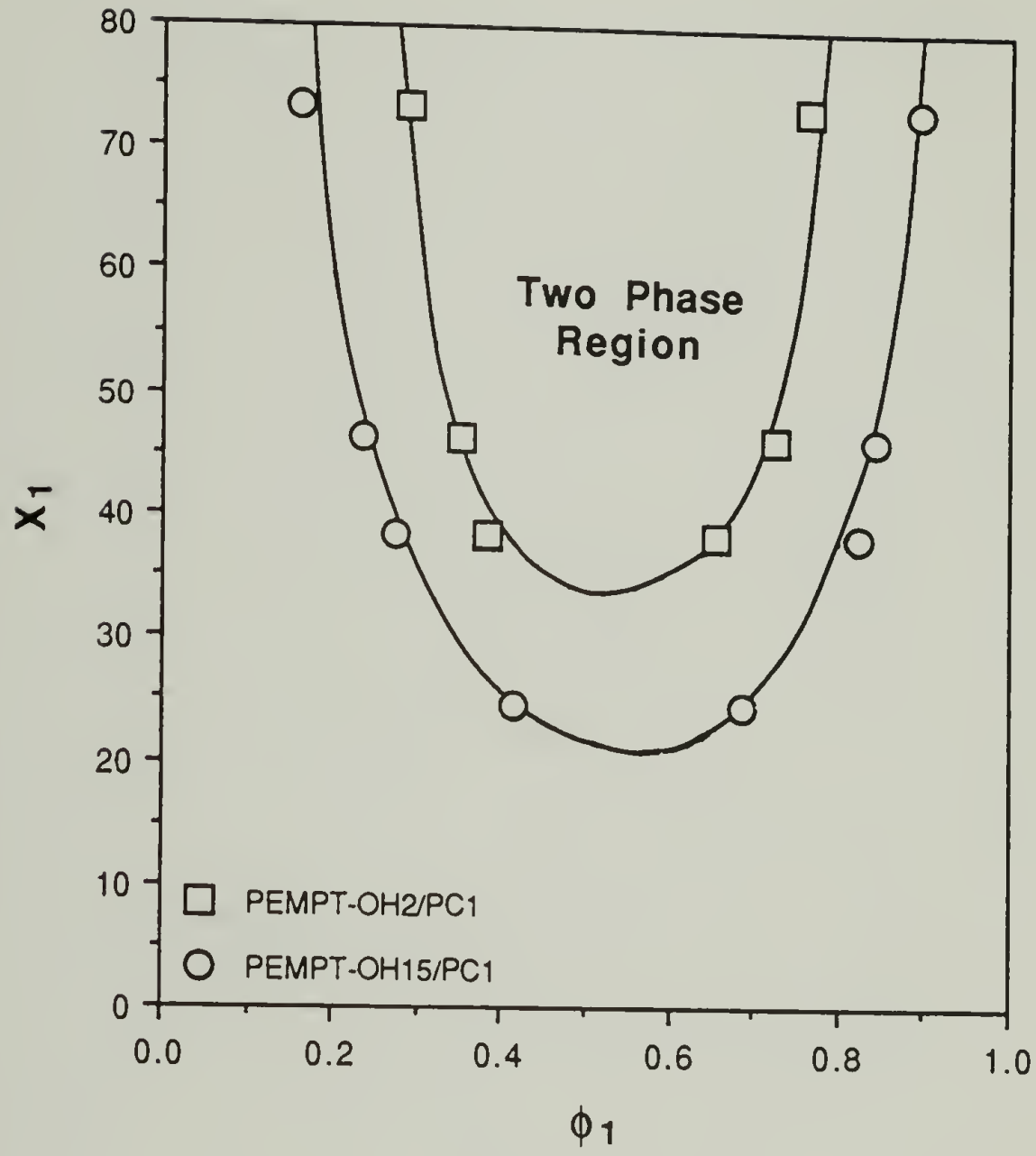

Figure 5.1 Miscibility map of PEMPT-OH2/PC1 and PEMPT-OH15/PC1 50/50 wt. % blends.

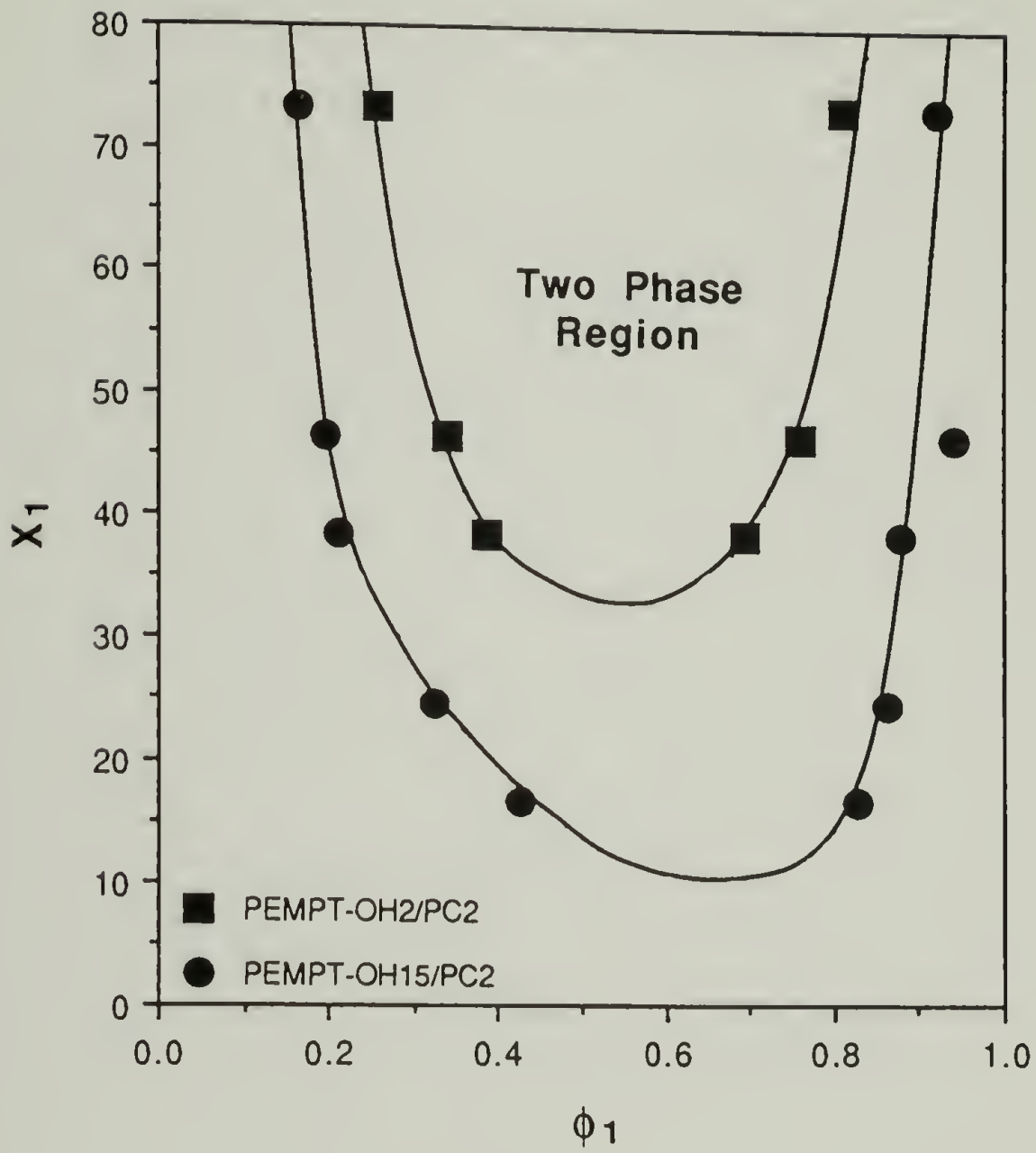

Figure 5.2 Miscibility map of PEMPT-OH2/PC2 and PEMPT-OH15/PC2 50/50 wt. % blends.

PEMPT in the PC rich phase covers a slightly larger range in volume fraction, 0.05-0.20. Additionally, the PEMPT-OH15/PC2 blends containing the two lowest molecular weight polyesters (X1 = 24.6 and 16.5) exhibit two phase behavior while these same blends prepared from PEMPT-OH2 display single phase behavior.

It seems unreasonable to believe that the minor differences in the molecular weights of the two sets of polyesters could lead to the observed changes in phase behavior. Shifts in the volume fractions of the PEMPT rich phase and PC rich phase of ~ 0.10 were observed only after the polyester molecular weights were dropped by a factor of 1/2-1/3 in the PEMPT-BNZ/PC blend studies of Chapter 4. Another possible reason for the improved miscibility of the PEMPT-OH2/PC blends is that, even in the presence of DNOP, some interchange reaction has occurred.

5.3.2 Identification of Alcoholysis Transreactions

5.3.2.1 PEMPT-OH2/PC Blends

Proton resonances associated with the aliphatic-hydroxyl end group have been identified including, a resonance at 8.065 ppm associated with the protons of the terephthalate ring adjacent to the end group and resonances at 4.231 and 3.423 ppm associated with the backbone methylene protons of the 2-ethly-2-methylpropylene hydroxyl end. Upon the occurrence of alcoholysis transreactions, any corresponding changes in the proton spectrum are expected to be observed in these resonances.

The 300 MHz ^{1}H NMR spectra of PEMPT1-OH2/PC1 blends as cast and after the DSC annealing/scanning programs are shown in Figure 5.3a and b, respectively. The region displayed corresponds to the aromatic region of PEMPT. The resonance previously assigned to the terephthalate ring adjacent to the aliphatic -hydroxyl end group, 8.065 ppm, is clearly identified in the as cast blend. However, after the thermal treatment, this peak is no longer present in the spectrum. A new resonance at 8.095 ppm is now observed. Additionally, Figure 5.4a and b displays the region of the spectrum associated with the backbone methylene protons of the aliphatic-hydroxyl end group before and after annealing. The previously identified methylene end group resonances at 4.231 and 3.423 ppm are observed in the as cast sample. These resonances

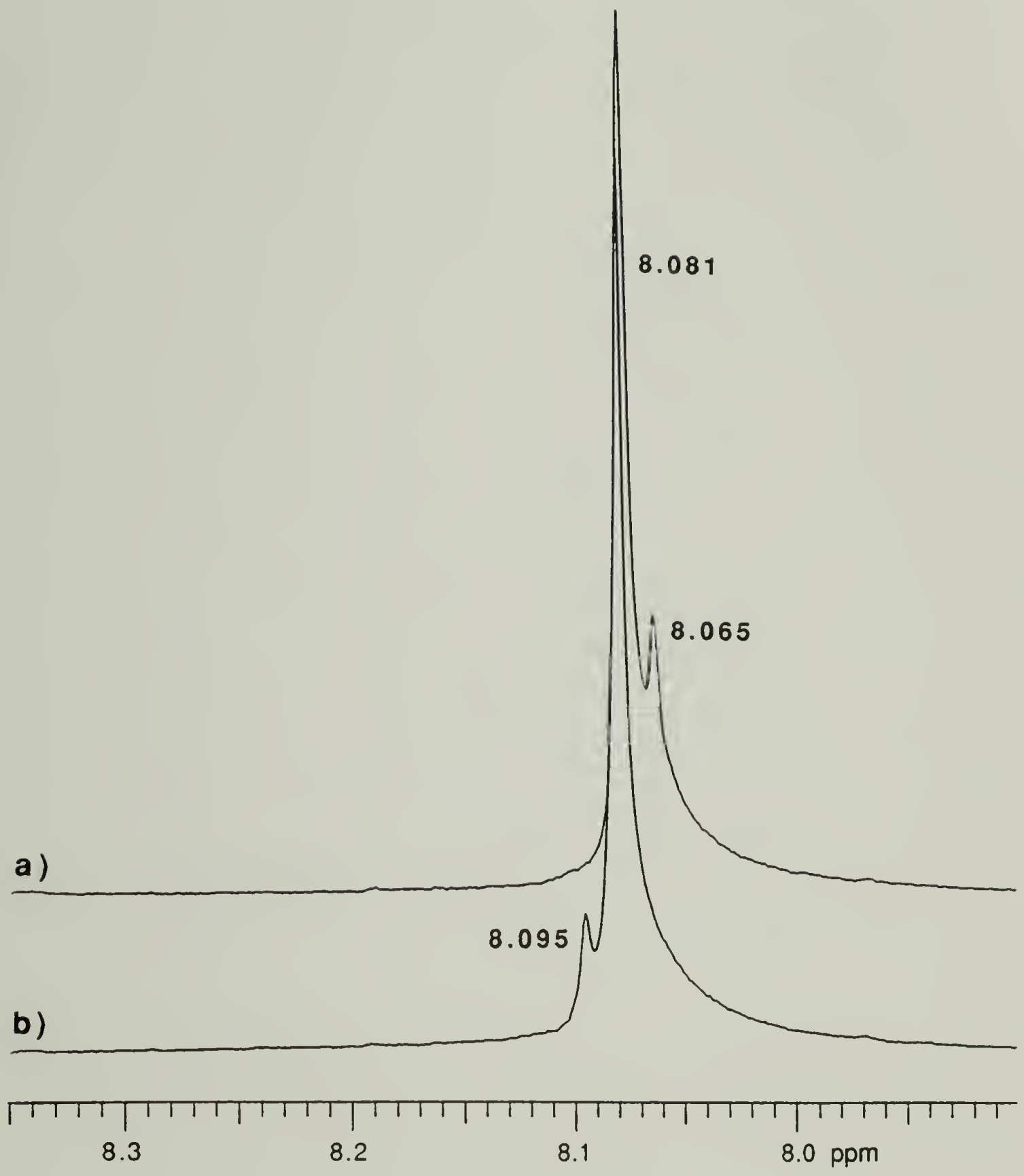

Figure 5.3 300 MHz ^{1}H NMR spectra displaying the terephthalate region of PEMPT1-OH2/PC1 50/50 wt. % blends
a) as cast b) after DSC annealing/scanning.

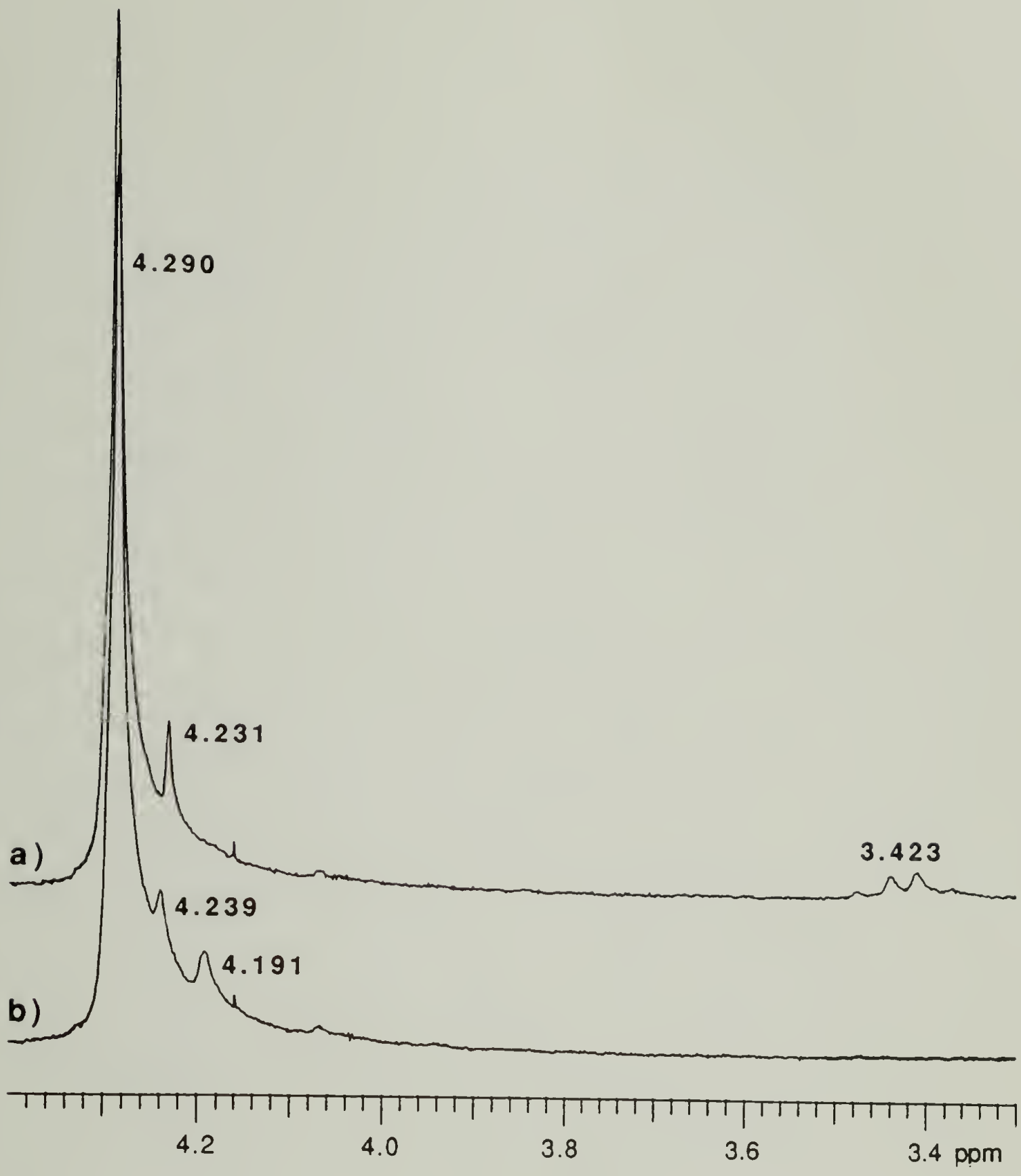

Figure 5.4 300 MHz ^{1}H NMR spectra displaying the backbone methylene region of PEMPT1-OH2/PC1 50/50 wt. % blends a) as cast b) after DSC annealing/ scanning.

have been replaced by two new peak at 4.239 and 4.192 ppm in the annealed/scanned sample. From these observations it is concluded that all of the hydroxyl end groups in the PEMPT1-OH2/PC1 blend system have reacted. New resonances at 7.035, 7.064 and 7.101 are also observed in the aromatic region associated with bisphenyl groups of PC after thermal treatment, Figure 5.5a, b. The final conclusion is that the hydroxyl end groups of PEMPT have reacted with the carbonate moieties of PC in an alcoholysis type interchange reaction.

Identical analysis was conducted on the PEMPT1-OH2/PC2 blend. Figures 5.6a, b; 5.7a, b; and 5.8a, b show the spectra of the PEMPT aromatic region, PEMPT backbone methylene region and PC aromatic region of the as cast and annealed blends, respectively. Once again the resonances associated with the aliphatic-hydroxyl end group of PEMPT have been replaced by the resonances discussed above. Further study was conducted on PEMPT-OH2/PC blends containing higher molecular weight PEMPT to see if complete alcoholysis had occured in these systems. Figures 5.9a-c and 5.10a-c show the spectra of the terephthalate region of PEMPT in PEMPT1-OH2, PEMPT2-OH2 and PEMPT6-OH2/PC1 blends and PEMPT1-OH2, PEMPT2-OH2 and PEMPT6-OH2/PC2 blends after the DSC thermal treatment. In all cases, the resonance of the terephthalate group adjacent to the aliphatic-hydroxyl chain end, 8.065 ppm, has been replaced by the resonance at 8.095 ppm. Thus, the alcoholysis reaction occurred at all PEMPT and PC molecular weights studied.

Further evidence to support alcoholysis interchange reaction is present in the GPC data of the unreacted (non-annealed) and reacted blends. Table 5.1 shows the GPC data of a PEMPT1-OH/PC1 blend before reaction, after 16% reaction (see section 5.3.2.2) and after 100% end group reaction. The extents of reaction have been determined from ^{1}H NMR. It should be mentioned that from the GPC experiments, the absorbtion coefficient for the polyester appeared to be considerably greater than than that of PC (greater intensity of peaks at equivalent concentration). The unreacted blend actually has a binodal molecular weght distribution. However, the molecular weight data on this sample resembles to a great extent the molecular weight of PEMPT1-OH2 (Note: PC1 had a M_n relative to PS standards of 24,100 gm/mole, PEMPT1-OH2 had a M_n of 3,400 gm/mole). Thus, the GPC results reflect the PEMPT mobility to a greater extent than that of PC. It is observed that as the extent of reaction increases the M_n of the blend increases. This is exactly what would be

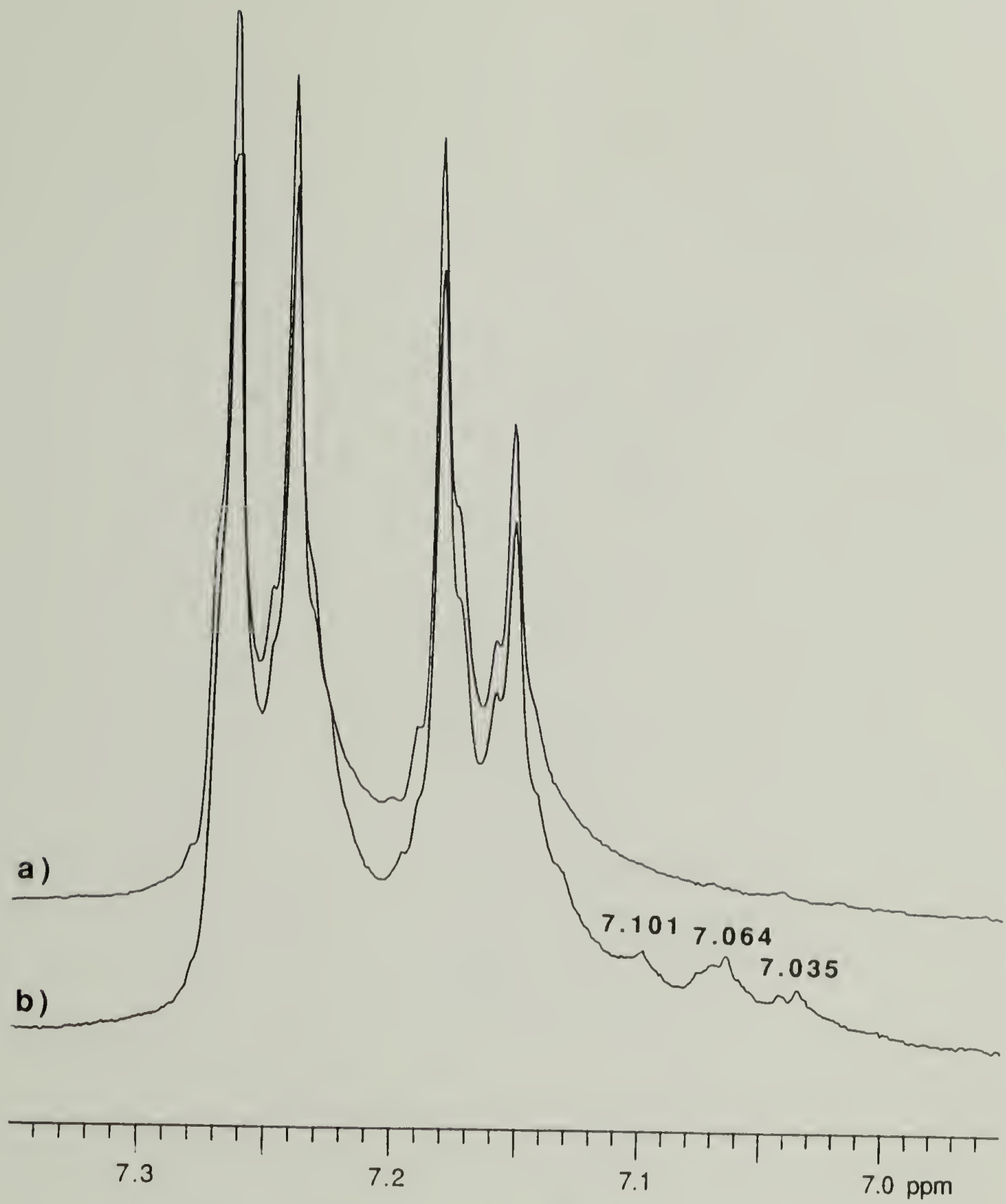

Figure 5.5 300 MHz ^{1}H NMR spectra displaying the PC aromatic region of PEMPT1-OH2/PC1 50/50 wt. % blends a) as cast b) after DSC annealing/scanning.

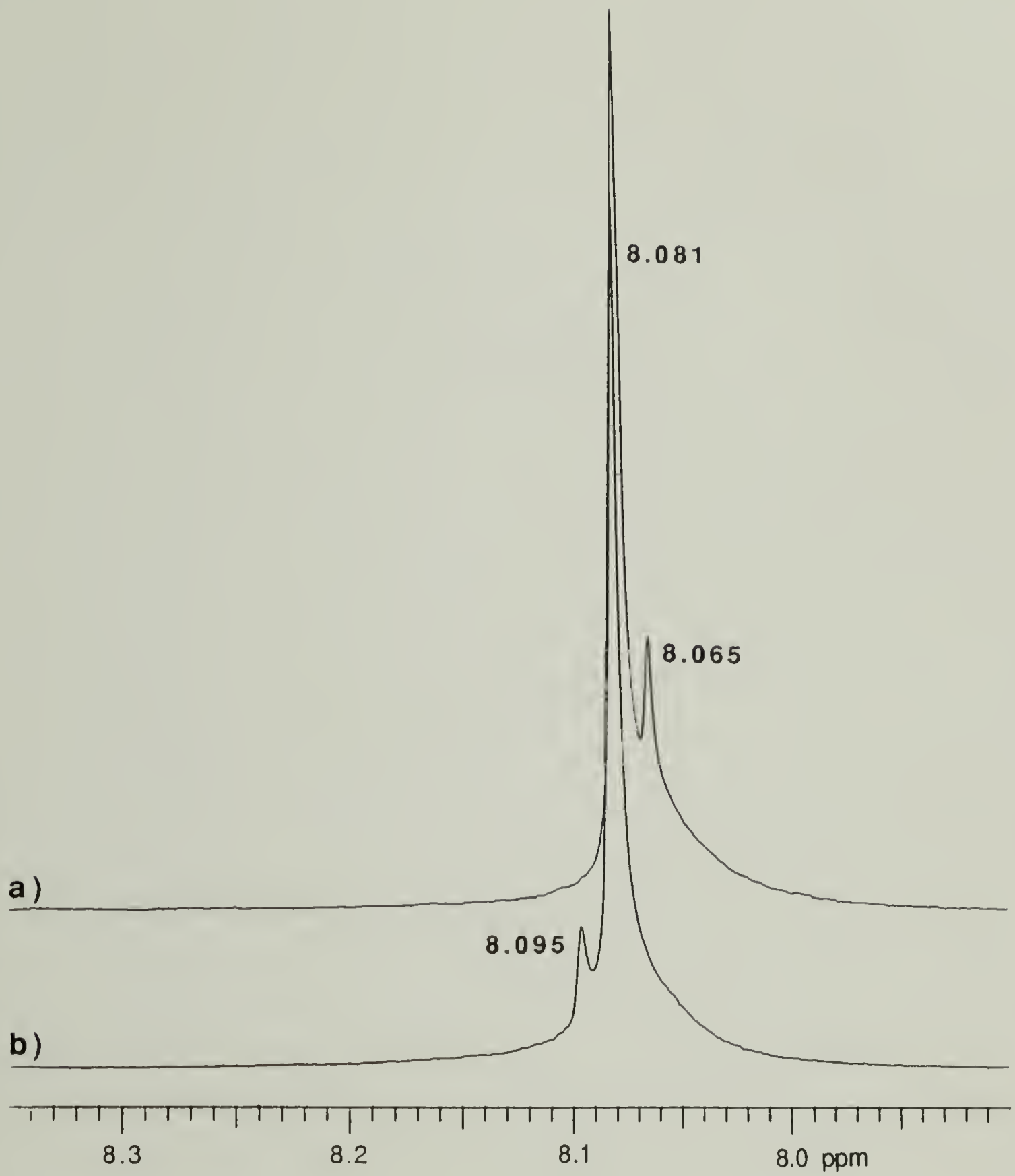

Figure 5.6 300 MHz ^{1}H NMR spectra displaying the terephthalate region of PEMPT1-OH2/PC2 50/50 wt. % blends a) as cast b) after DSC annealing/scanning.

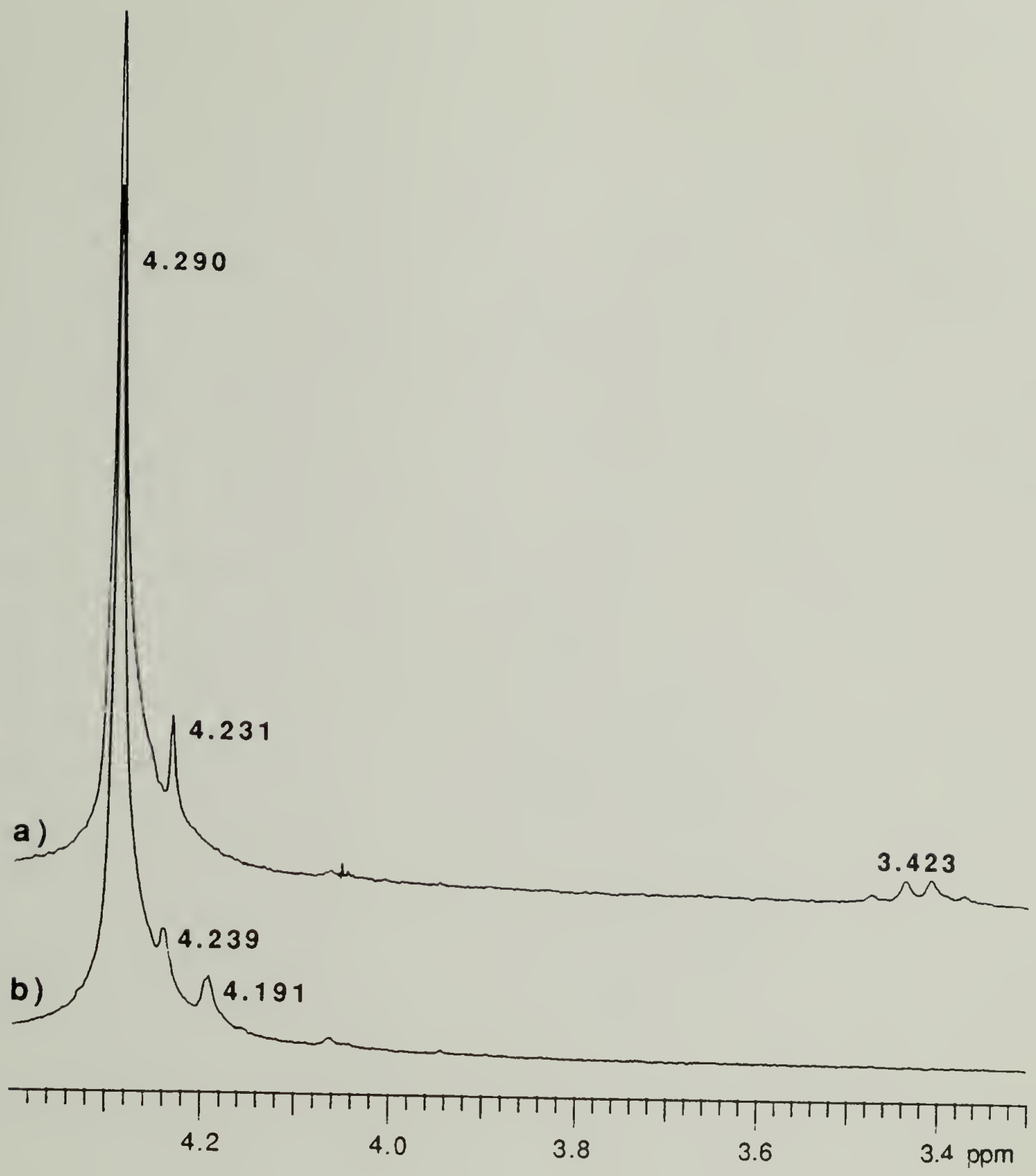

Figure 5.7 300 MHz ^{1}H NMR spectra displaying the backbone methylene region of PEMPT1-OH2/PC2 50/50 wt. % blends a) as cast b) after DSC annealing/ scanning.

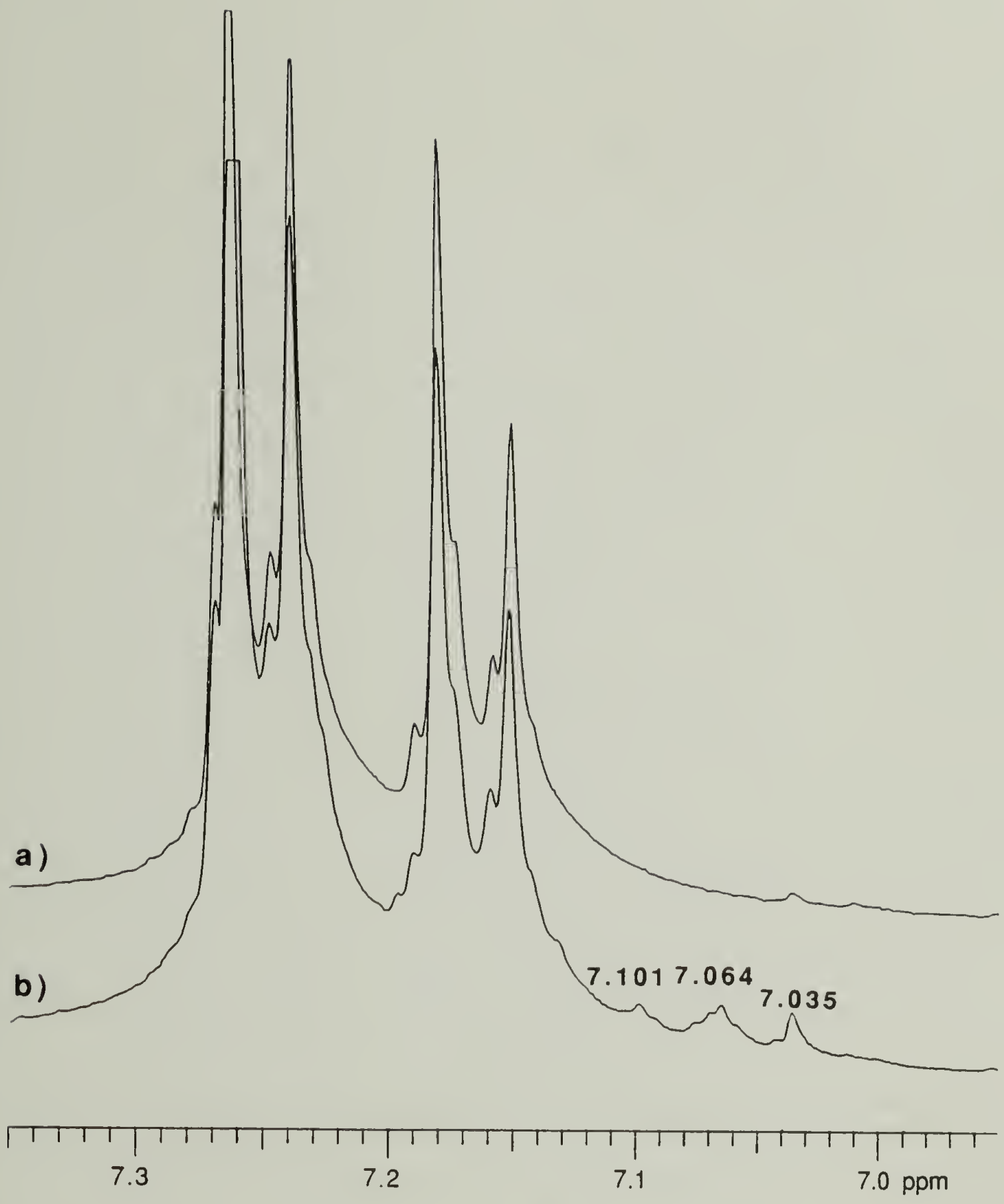

Figure 5.8 300 MHz ^{1}H NMR spectra displaying the PC aromatic region of PEMPT1-OH2/PC2 50/50 wt. % blends a) as cast b) after DSC annealing/scanning.

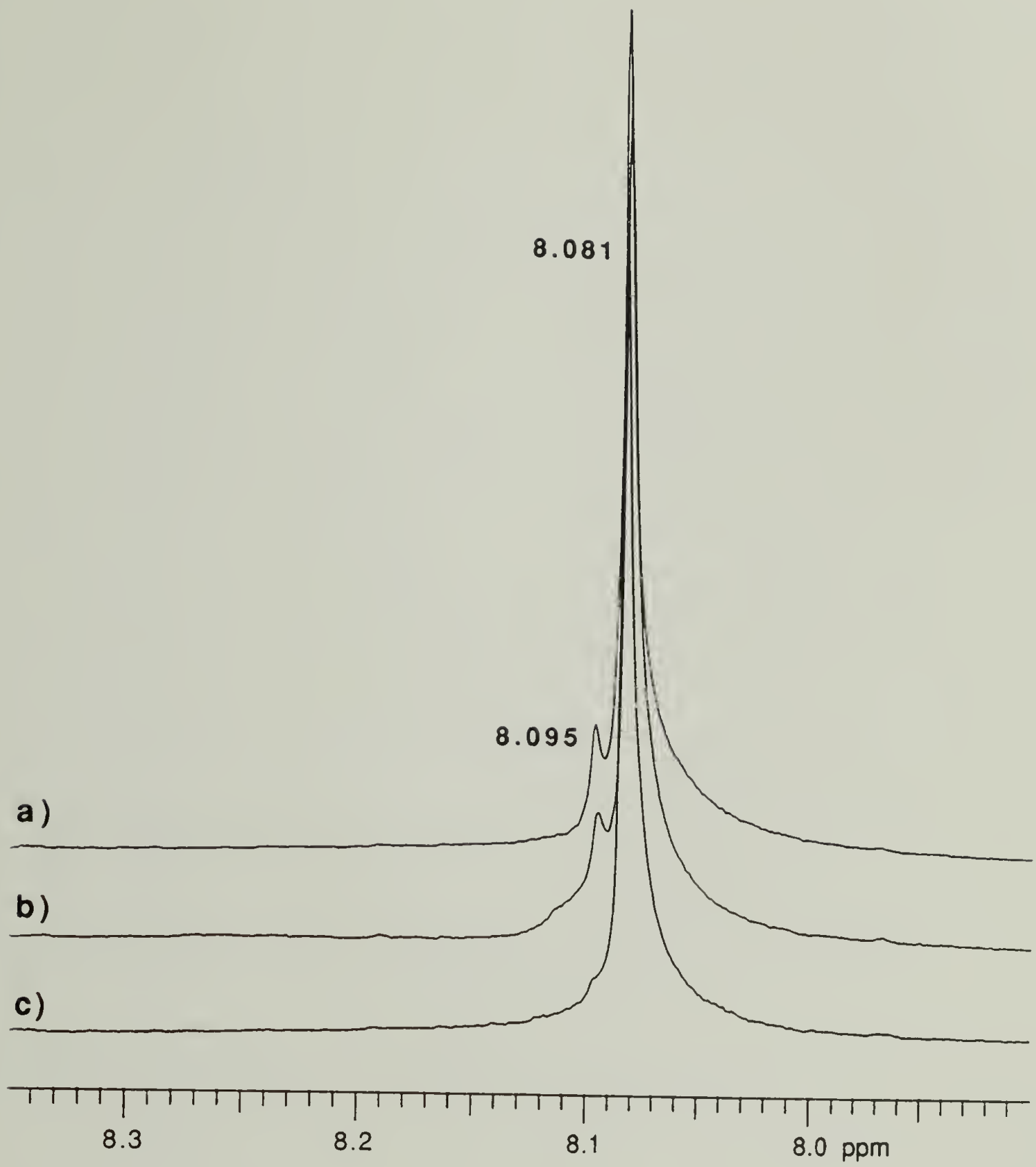

Figure 5.9 300 MHz ^{1}H NMR spectra displaying the terephthalate region of a) PEMPT1-OH2/PC1 b) PEMPT2-OH2/PC1 c) PEMPT6-OH2/PC1 50/50 wt. % blends after DSC annealing/scanning.

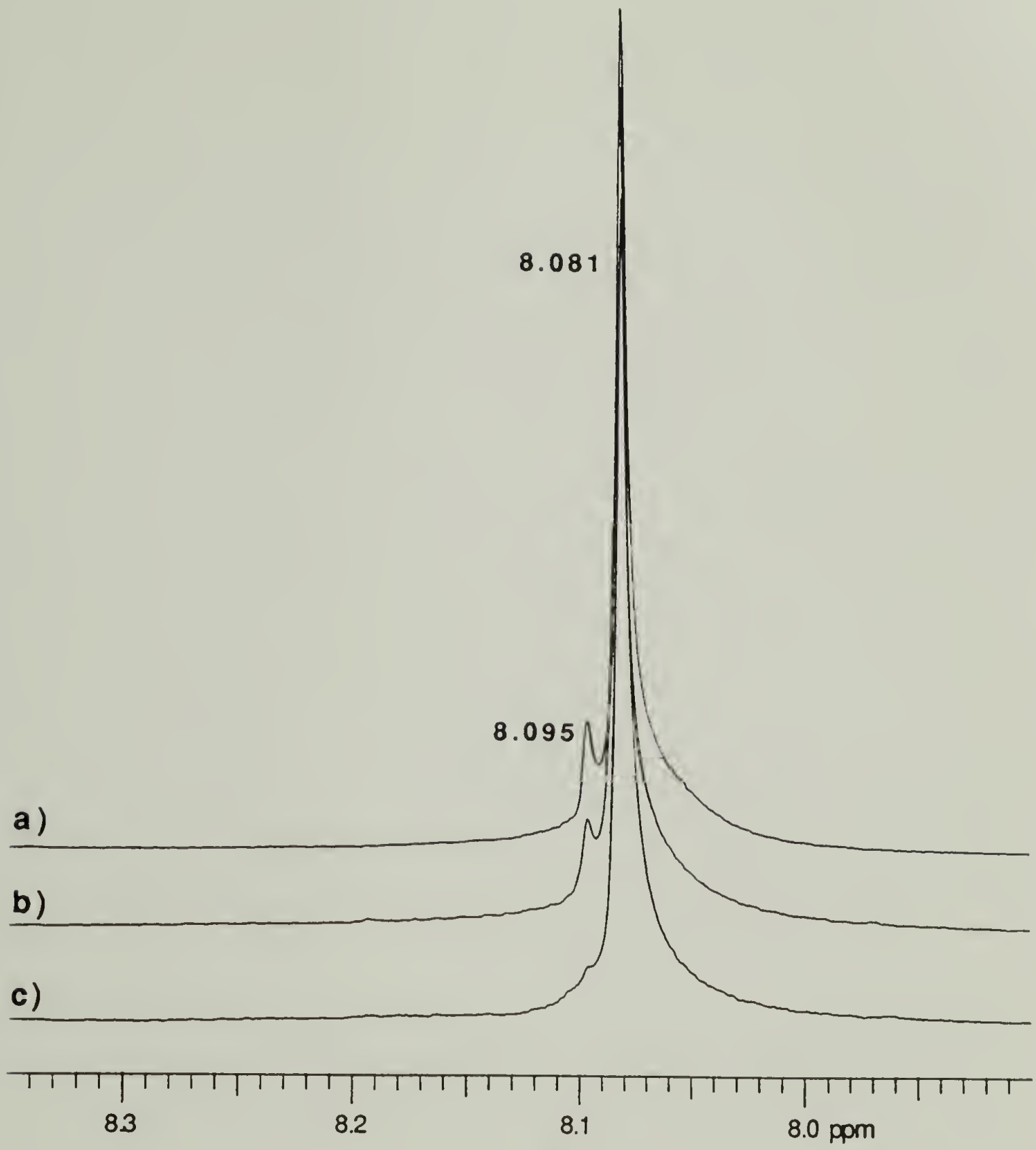

Figure 5.10 300 MHz ^{1}H NMR spectra displaying the terephthalate region of a) PEMPT1-OH2/PC2 b) PEMPT2-OH2/PC2 c) PEMPT6-OH2/PC2 50/50 wt. % blends after DSC annealing/scanning.

Table 5.1 GPC Data of PEMPT1-OH/PC1 Blends

% Transreacted Hydroxyl End Groups	M_n	M_w/M_n	M_z/M_w
0	5,900	1.63	2.23
16	7,000	1.99	1.86
100	14,500	1.90	1.54

expected if the hydroxyl end groups have reacted. The interchange reaction with PC would increase the molecular size of the PEMPT chains, leading to an observed increase in the molecular weights.

Infrared spectroscopy qualitatively supports hydroxyl end group reaction of the blends. Figure 5.11a,b shows the region of the spectrum associated with the O-H stretching vibration in the PEMPT1-OH2/PC1 50/50 as cast and annealed sample, respectively. The hydrogen bonding resonance at 3540 cm^{-1} appears to have diminished relative to resonances at 3440 and 3480 cm^{-1}. An overall shift in intensity to resonances with lower frequency is observed. No attempt was made to assign resonances to specific hydrogen bonding groups.

5.3.2.2 PEMPT-OH15/PC Blends

With alcoholysis reactions observed in the PEMPT-OH2/PC blends, similar reactions may have occurred in the PEMPT-OH15/PC systems. The differences in miscibility of the two systems would suggest that reaction had not occurred, or if it had, to a considerably lower extent in the PEMPT-OH15/PC blends. Figure 5.12a-d shows the spectra of the terephthalate region of PEMPT1-OH15/PC1, PEMPT2-OH15/PC1, PEMPT1-OH15/PC2 and PEMPT3-OH15/PC2 50/50 wt. % blends after identical annealing as the PEMPT-OH2/PC systems. All blends show a small resonance at 8.095 ppm indicating some extent of alcoholysis transreaction, as well as, a larger resonance at 8.065 associated with the unreacted end group. In this set of blends, end group reaction has not occurred completely, but has proceeded to a small extent across the range of molecular weights examined.

Additionally, from the DSC phase behavior studies of chapter 4, PEMPT-OH15/PC blends of varying PEMPT/PC ratios were examined for alcoholysis interchange reaction. Figure 5.13a-c displays the resonances of the terephthalate region of annealed PEMPT1-OH15/PC1 blends corresponding to PEMPT/PC wt. ratios of 30/70, 50/50, and 70/30, respectively. End group reaction is seen at all three compositions. Similar sets of plots for PEMPT2-OH15/PC1, PEMPT1-OH15/PC2 and PEMPT3-OH15/PC2 annealed blends are shown in Figures 5.14a-c, 5.15a-c and 5.16a-c. In the blends containing low molecular weight polyester, Figures 5.13-5.15, partial end group reaction is easily observed at all three PEMPT/PC ratios. Figure 5.16 which examines a PEMPT sample with higher molecular weight (lower end group content) shows

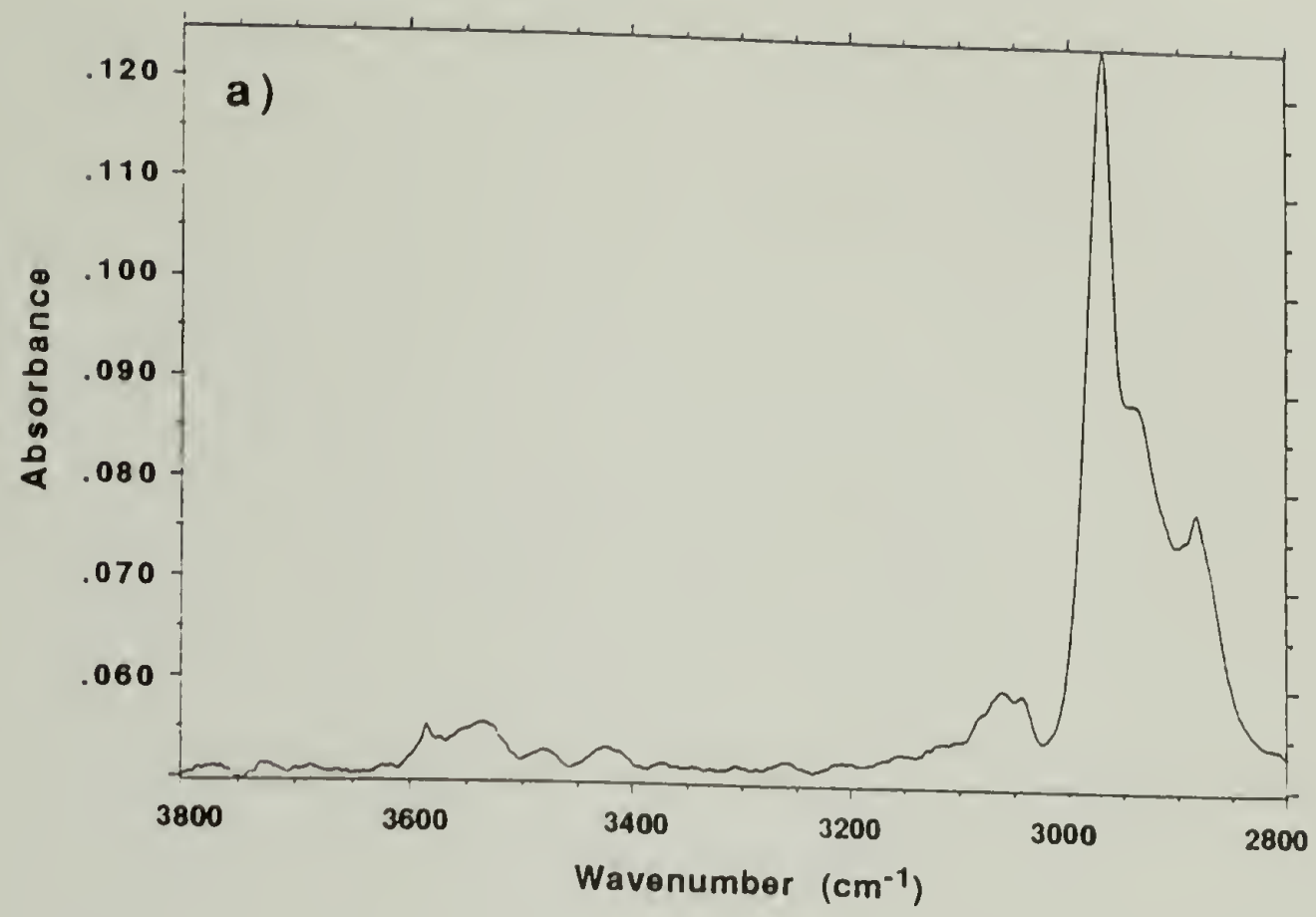

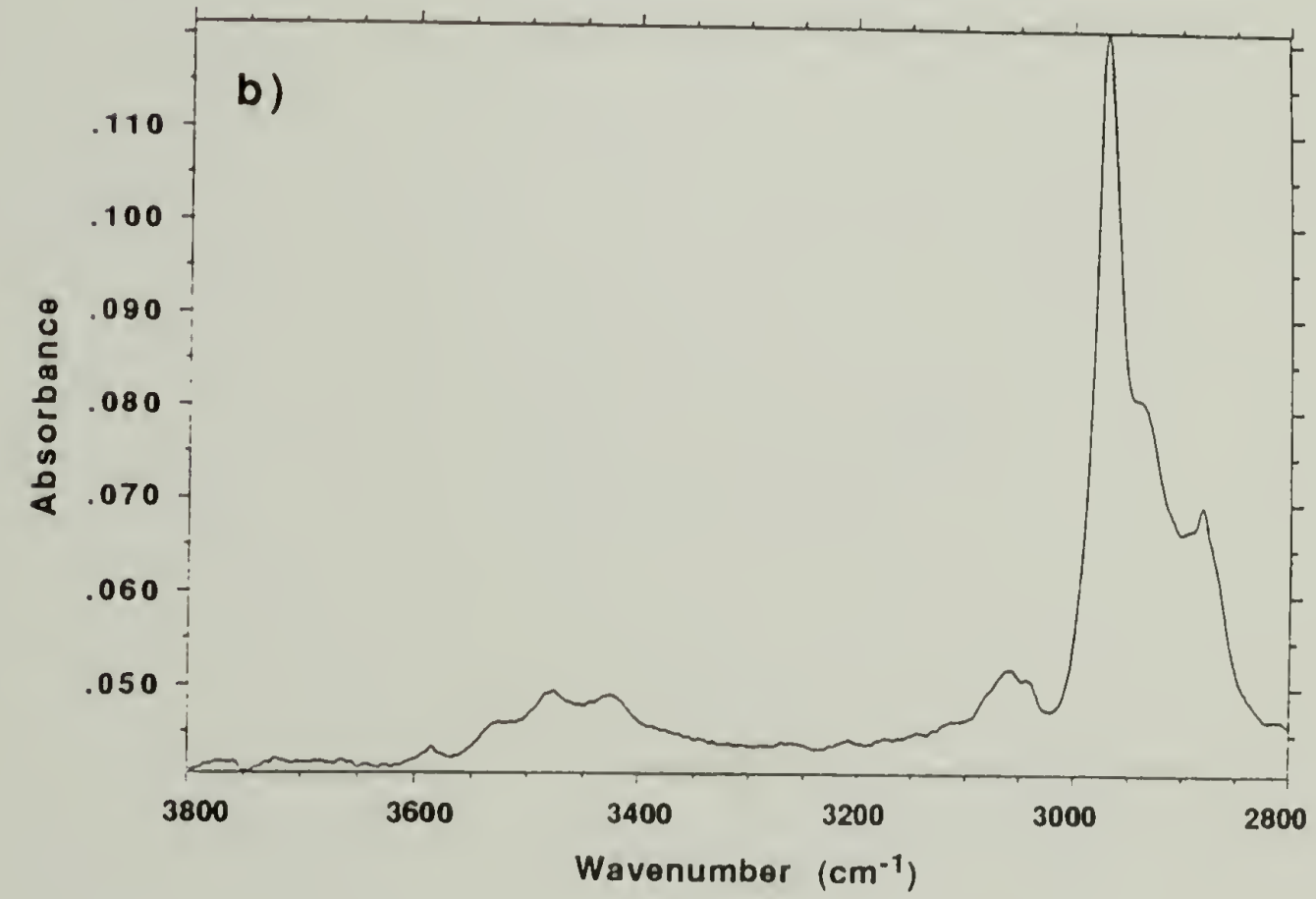

Figure 5.11 FTIR spectra displaying the hydrogen bonding region of PEMPT1-OH2/PC1 50/50 wt. % blends a) as cast b) after DSC annealing/scanning.

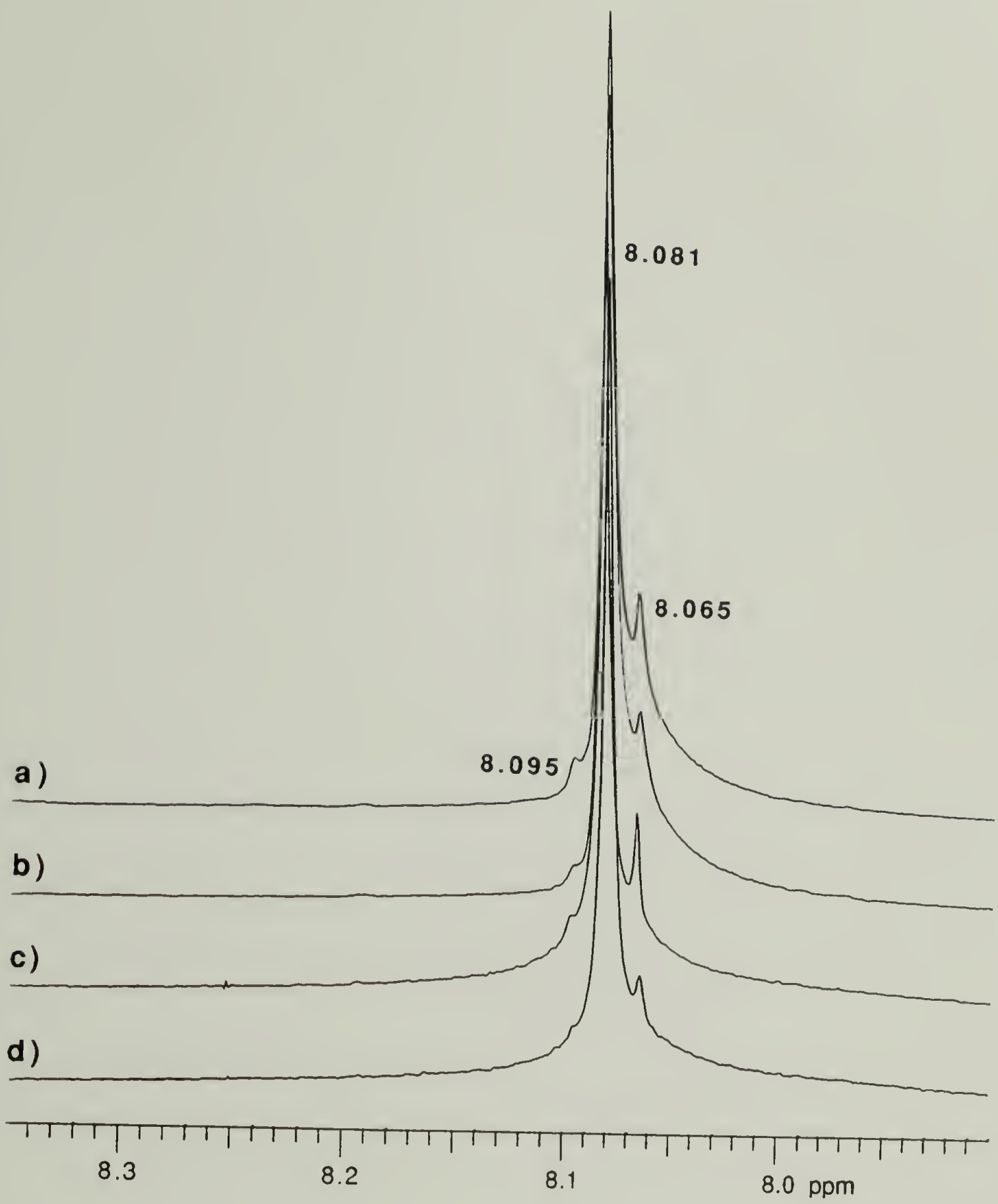

Figure 5.12 300 MHz ^{1}H NMR spectra displaying the terephthalate region of a) PEMPT1-OH15/PC1 b) PEMPT2-OH15/PC1 c) PEMPT1-OH15/PC2 d) PEMPT3-OH15/PC2 50/50 wt. % blends after DSC annealing/scanning.

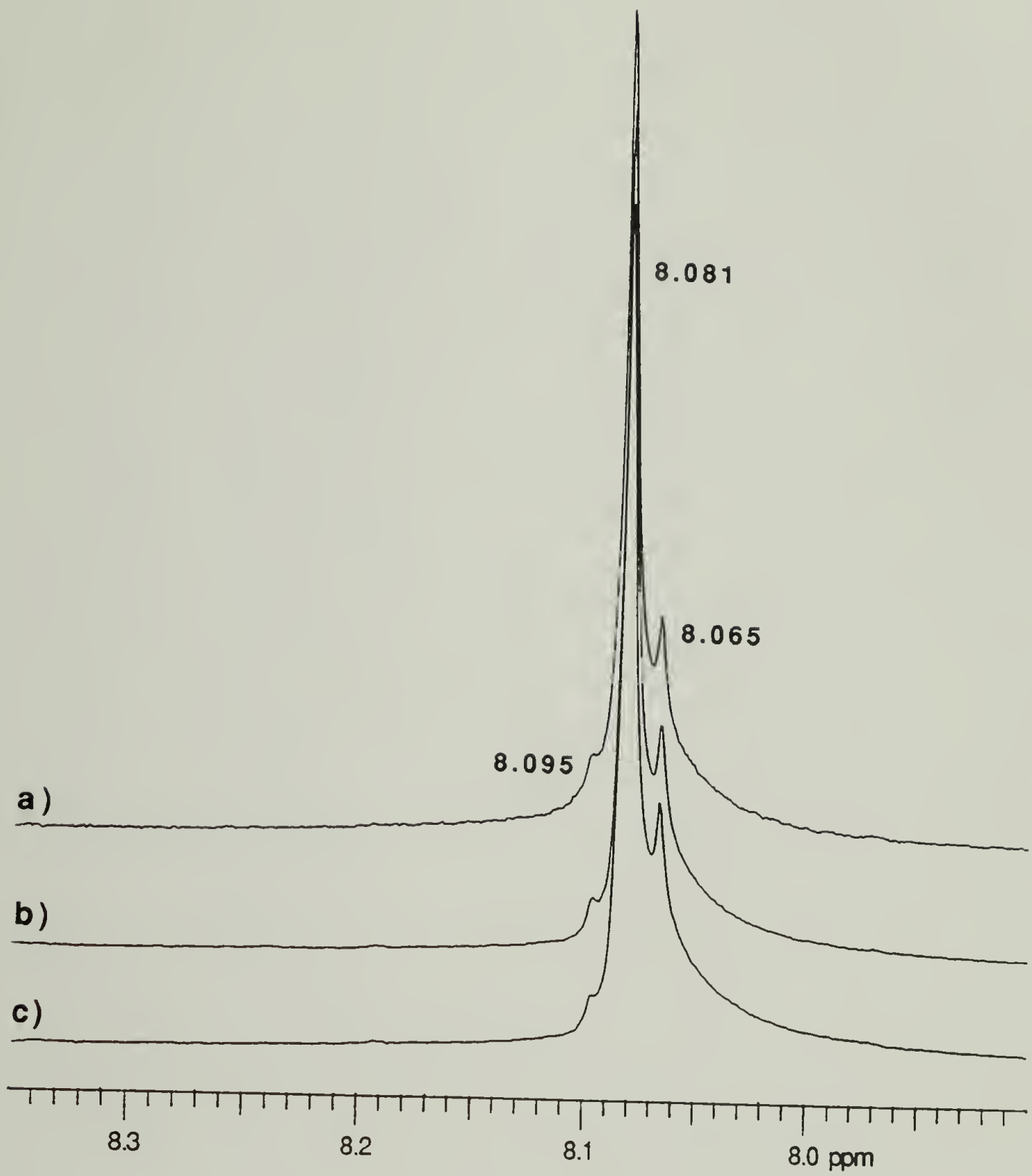

Figure 5.13 300 MHz ^{1}H NMR spectra displaying the terephthalate region of PEMPT1-OH15/PC1 blends after DSC scanning/annealing at the following compositions a) 30/70 b) 50/50 c) 70/30.

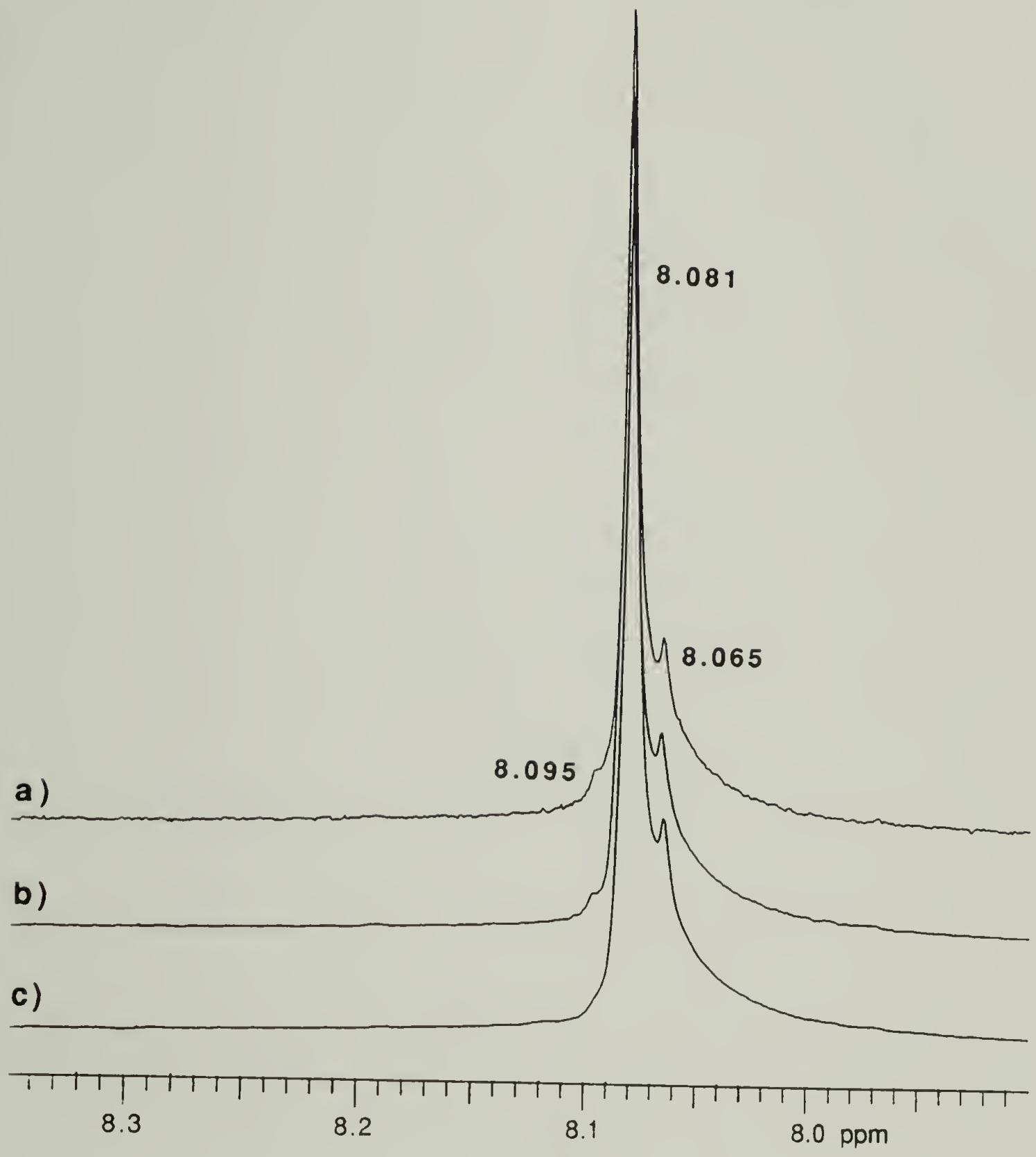

Figure 5.14 300 MHz ^{1}H NMR spectra displaying the terephthalate region of PEMPT2-OH15/PC1 blends after DSC scanning/annealing at the following compositions a) 30/70 b) 50/50 c) 70/30.

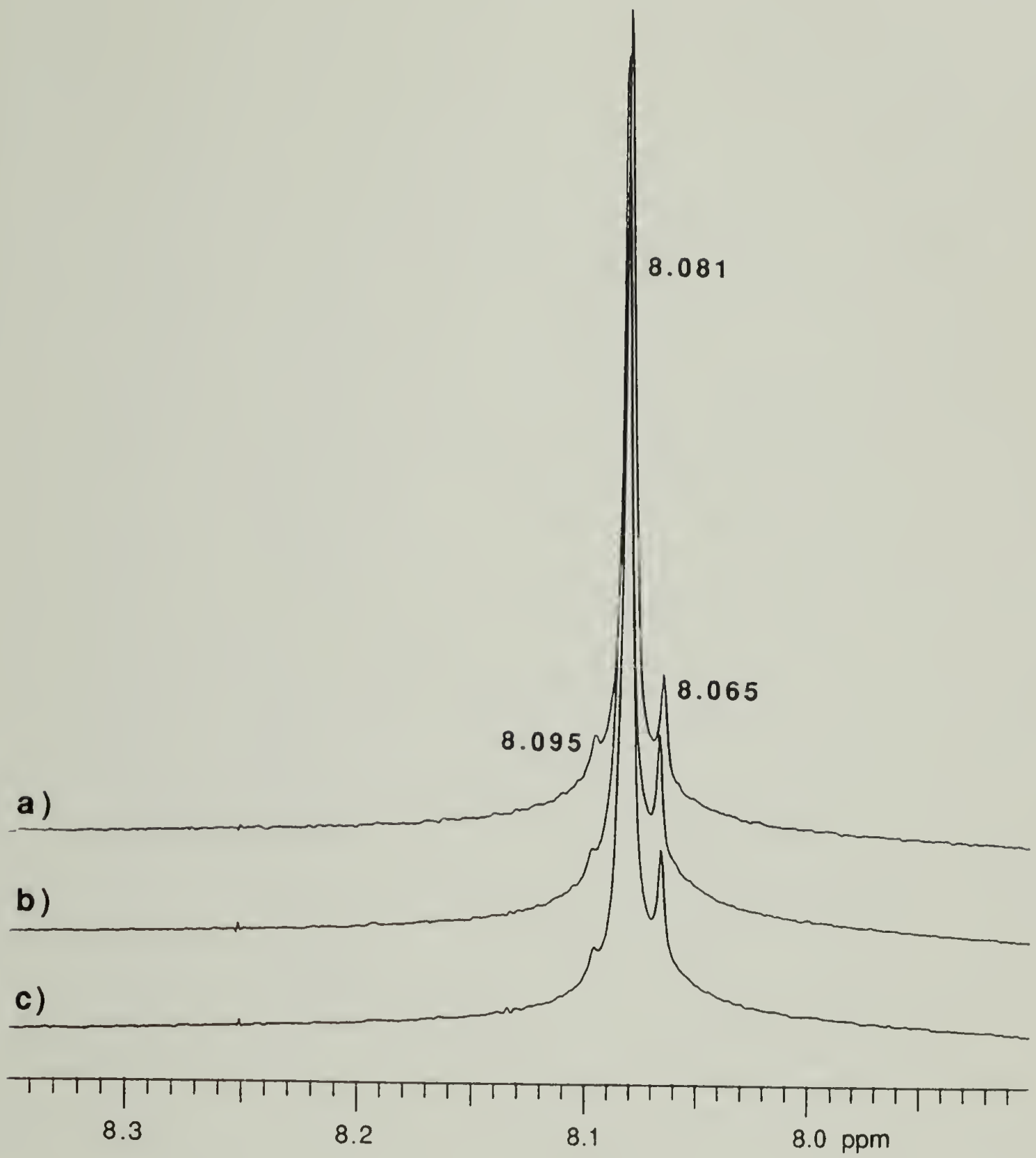

Figure 5.15 300 MHz ^{1}H NMR spectra displaying the terephthalate region of PEMPT1-OH15/PC2 blends after DSC scanning/annealing at the following compositions a) 30/70 b) 50/50 c) 70/30.

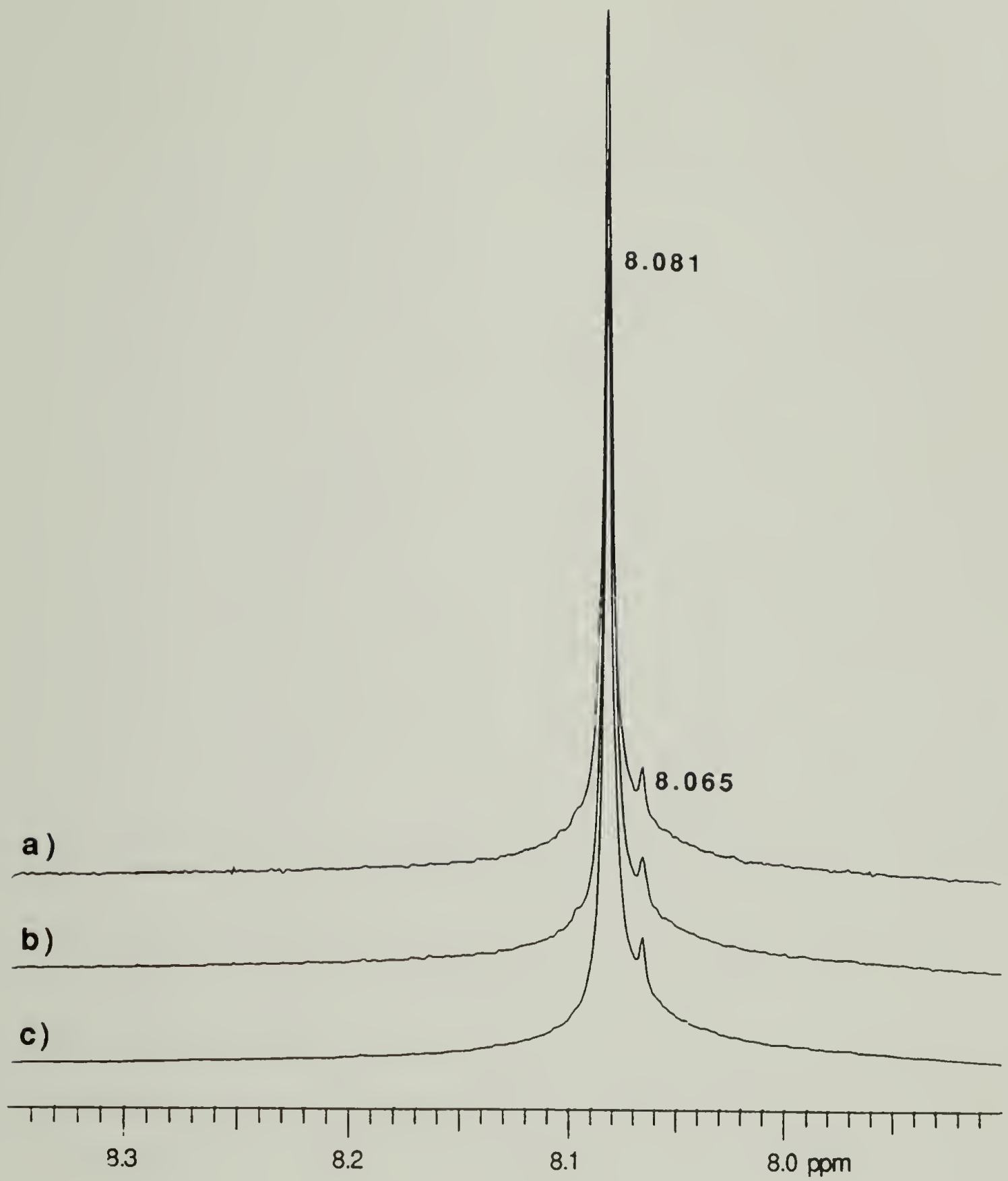

Figure 5.16 300 MHz ^{1}H NMR spectra displaying the terephthalate region of PEMPT3-OH15/PC1 blends after DSC scanning/annealing at the following compositions a) 30/70 b) 50/50 c) 70/30.

a very small peak at 8.095 ppm for the 50/50 blend, a small shoulder at 8.095 ppm in the 30/70 composition and perhaps a slight shoulder in the 70/30 blend. Although not as conclusive as the blends containing the lower molecular weight polyesters, the blends containing PEMPT3 also appear to have experienced some level of alcoholysis transreaction. It should be mentioned that PEMPT3 had a degree of polymerization of 38.3, thus the concentration of end groups in the polymer was approx. 5%. If one assumes that 20% of the hydroxyl moities transreacted, then the concentration of reacted species would be on the order of 1% which is nearing the detection limit of the spectrometer. Studies on blends containing higher molecular weight PEMPTs were not conducted for this reason.

From the area ratios of the resonances at 8.065 and 8.095 of Figures 5.13 and 5.15, the extent of interchange reaction was determined. Table 5.2 displays the calculated percent conversion of the hydroxyl end groups. The 50/50 wt % blends appear to exhibit a lower percent conversion than their 30/70 and 70/30 counterparts. However, the error in a given measurement is on the order of $\pm$ 2 % conversion, thus, there is little difference in percent conversion with blend composition. The blends containing PC1 appear to have reacted slightly less than those containing PC2, but once again the discrepancy is on the order of the experimental error in a given measurement indicating little difference between the two systems. The overall extent of reaction for the six blends was 16.3 $\pm$ 2.5%.

5.3.3 Discussion

5.3.1 Non-Transreacted PEMPT-OH/PC Blends

As shown in Figures 5.14 and 5.16 partial alcoholysis also occurred in blends containing PEMPT with higher molecular weights than those analyzed in Table 5.1. Due to the lower concentration of end groups present combined with the above mentioned resolution limits, percent conversion was not quantitatively analyzed in these blends. For all other blends composed of higher molecular weight PEMPTs, it was assumed that the extent of alcoholysis transreaction was the same as that observed for the PEMPT1-OH15/PC systems. The PEMPT-OH15/PC and the PEMPT-OH2/PC blends were

Table 5.2 Percent Conversion of Hydroxyl End Groups

Blend	% Conversion
PEMPT1-OH5/PC1 30/70	16.4
PEMPT1-OH5/PC1 50/50	13.6
PEMPT1-OH5/PC1 70/30	14.5
Average	14.8 ± 1.4
PEMPT1-OH5/PC2 30/70	19.5
PEMPT1-OH5/PC2 50/50	16.3
PEMPT1-OH5/PC2 70/30	17.5
Average	17.7 ± 2.4
Total Population Average	16.3 ± 2.5

renamed as PEMPT-OH-16%/PC and PEMPT-OH-100%/PC, the percent transreaction of the hydroxyl ends indicated.

In order to obtain an estimate of the miscibility map of non-transreacted PEMPT-OH-0%/PC systems, the volume fraction data of the 16% and 100% reacted blends was extrapolated to 0% conversion. In cases where the 100% reacted blends were miscible and no volume fraction extrapolations could be made (PEMPT1/PC1, PEMPT1/PC2 and PEMPT2/PC2), estimates of the volume fractions shifts were determined from prior extrapolations. The miscibility maps at 0, 16 and 100% hydroxyl conversion for the PEMPT/PC1 and PEMPT/PC2 blends are shown in Figures 5.17 and 5.18, respectively. It was these curves extrapolated to 0% conversion that were discussed earlier in Chapter 4.

5.3.3.2 PC-PEMPT-PC/PC Triblock/Homopolymer Blends

Complete alcoholysis results in the formation of a triblock copolymer. The resulting blend is no longer the PEMPT-OH/PC homopolymer/ homopolymer system, but instead has been transformed into a PC-PEMPT-PC/PC triblock/homopolymer system. The amount of pure homopolymer, PC, undoubtedly varies with the molecular weight of the polyester. The significance of the alcoholysis reaction and the formation of triblock copolymers is apparent in Figures 5.17 and 5.18. The PEMPT-OH-0%/PC curves represent the homopolymer/homopolymer system while the PEMPT-OH-100%/PC curves correspond to the triblock/homopolymer blends. Due to the formation of the triblock, the two phase region of the PC-PEMPT-PC/PC blends has been decreased considerably compared to that of the PEMPT/PC homopolymer system. Even at polyester molecular weights typically used for industrial applications ($X_n > 70$), shifts in the miscibility between the 0% and 100% reacted blends range from 0.10-0.15 volume fraction units along each branch of the curve. At a molecular weight equivalent to that of a homopolymer/ homopolymer blend, the improved miscibility of diblocks and triblocks, as well as, mixtures of these blocks with pure homopolymers is well documented [16-20]. The connectivity of the block and the emulsifying effect of the block copolymer in block/homopolymer blends leads to improved miscibility. These factors qualitatively explain the observed differences in the two sets of data.

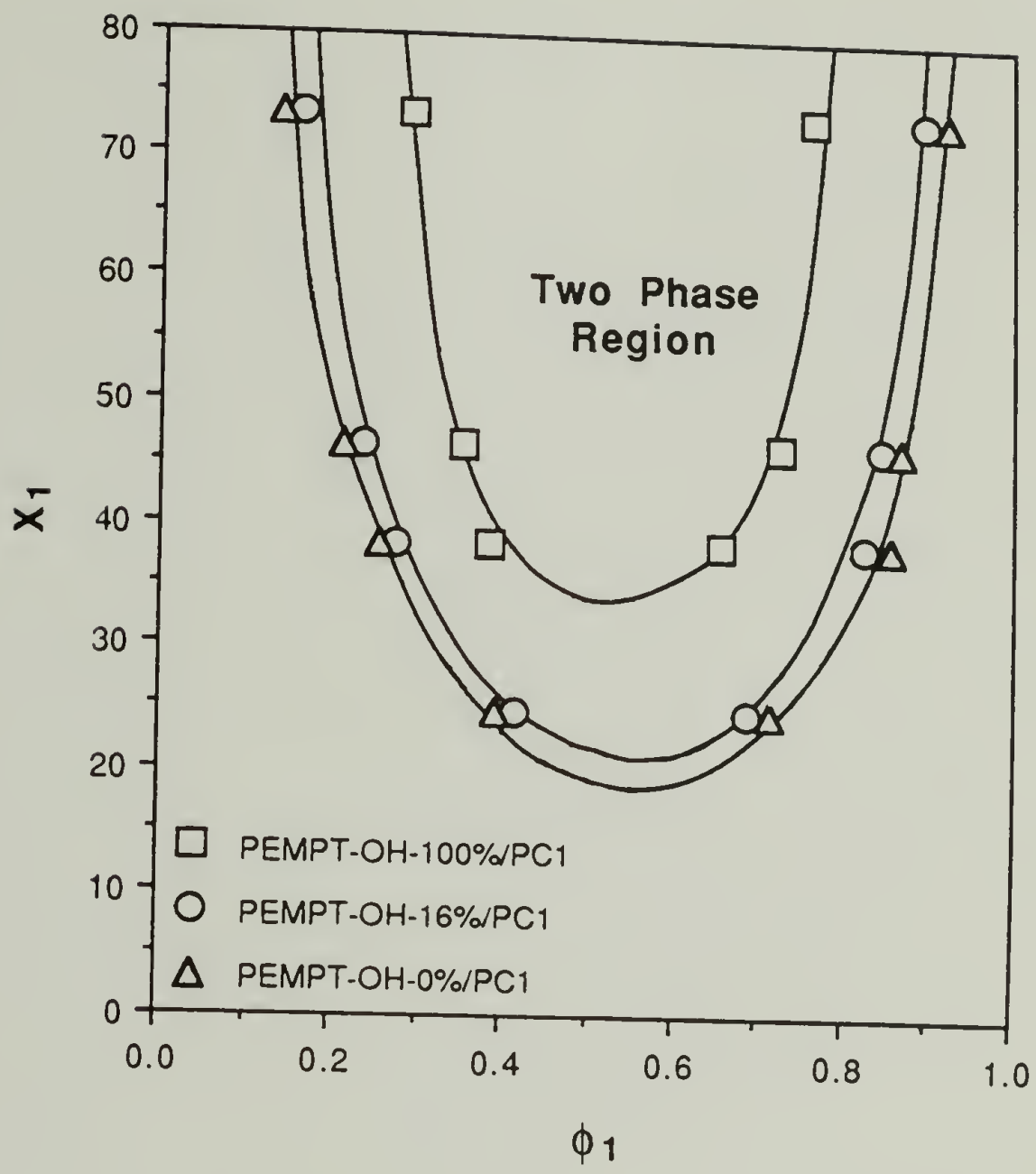

Figure 5.17 Miscibility maps of PEMPT-OH-100%/PC1, PEMPT-OH-16%/PC1 and PEMPT-OH-0%/PC1 50/50 wt. % blends.

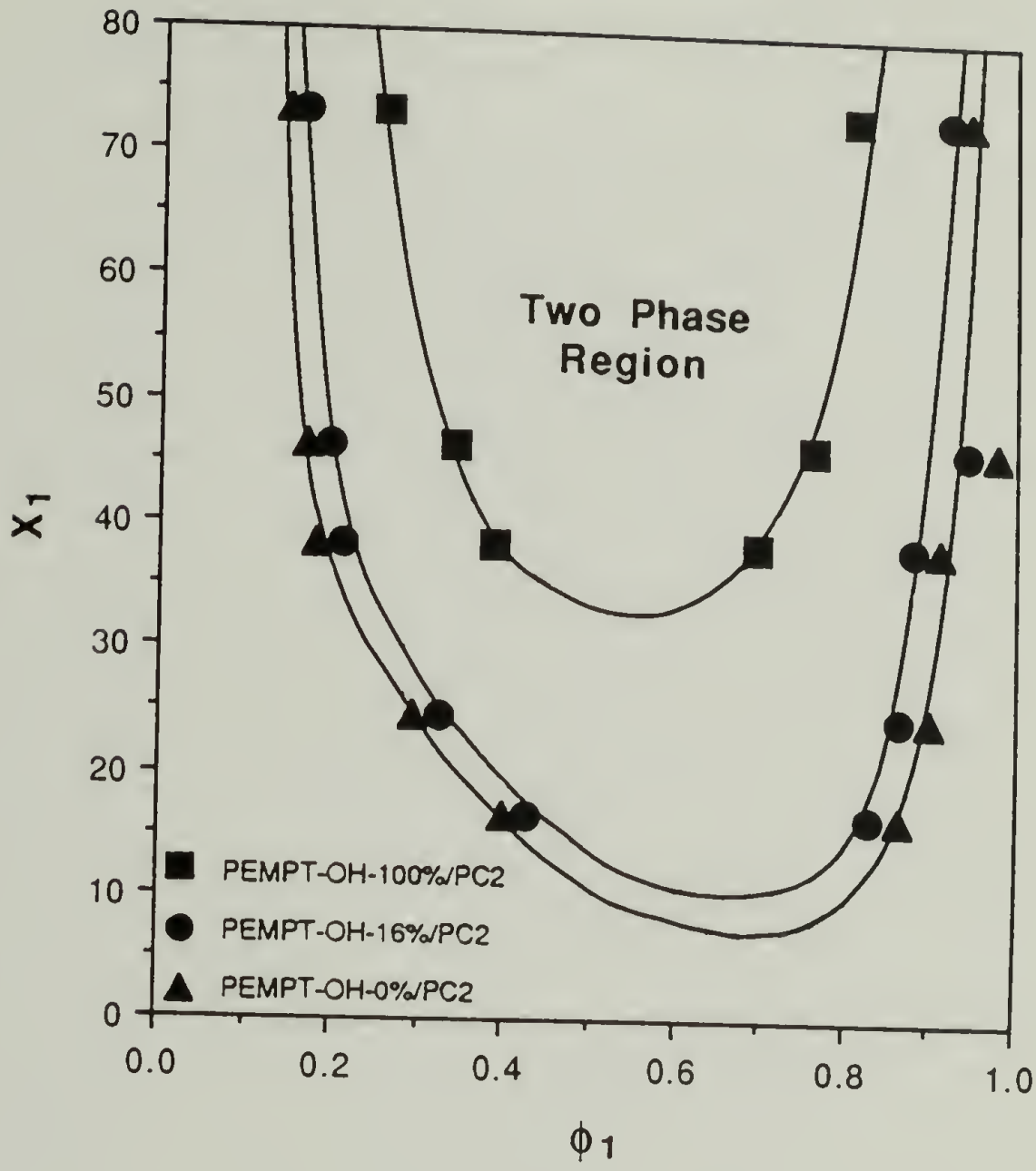

Figure 5.18 Miscibility maps of PEMPT-OH-100%/PC2, PEMPT-OH-16%/PC2 and PEMPT-OH-0%/PC2 50/50 wt. % blends.

Deviations between the PC1 and PC2 systems also warrent some discussion. Figure 5.19 shows miscibility maps corresponding to the PEMPT/PC1 and PC2 homopolymer blends (PEMPT-OH-0%), as well as, the PC-PEMPT-PC/ PC1 and PC2 triblock/homopolymer systems (PEMPT-OH-100%). The miscibility maps of the two homopolymer blends, PEMPT-OH-0%/PC1 and PEMPT-OH-0%/PC2, closely mimic the PEMPT-OH15/PC blends of Chapter 4. The point to be reiterated is that the deviation between the two curves is increased as the polyester molecular weight is lowered. This fact corresponds to the different entropic contributions to the free energy of mixing associated with the PC molecular weights. One might anticipate similar behavior in the PC-PEMPT-PC/PC1 and PC-PEMPT-PC/PC2 blends with the PC2 blends displaying a larger two phase region than the corresponding PC1 blends, especially at the lower PEMPT molecular weights. As can be observed from the Figure 5.19, this is not the case. In general, the difference between the volume fraction of the components at a given polyester degree of polymerization do not vary by more than a few percent and the gap between the two curves narrows slightly as the PEMPT molecular weight is lowered. This behavior is in complete contrast to that observed in the homopolymer blends.

5.3.3.3 Theoretical Molecular Weight Analysis

These observations can be explained in terms of the molecular weights of the components after alcoholysis. With the knowledge of exactly how many interchange reactions have occurred in the system, estimates of the number average degree of polmerization of the PC-PEMPT-PC triblock, designated X_{nBAB}, and the new DP of PC, X_{nB} can be made. The number of alcoholysis reactions will be directly proportional to the number fraction of PEMPT chains present, n_1. This value is calculated from the knowledge of the original volume fractions (50/50) and the original degrees of polymerization.

$$n_1 = \frac{\phi_1 X_{n2}}{X_{n1} - \phi_1 X_{n1} + \phi_1 X_{n2}} \qquad (5.1)$$

where,

ϕ_1 : volume fraction of PEMPT.

X_{n1} : number average degree of polymerization of PEMPT.

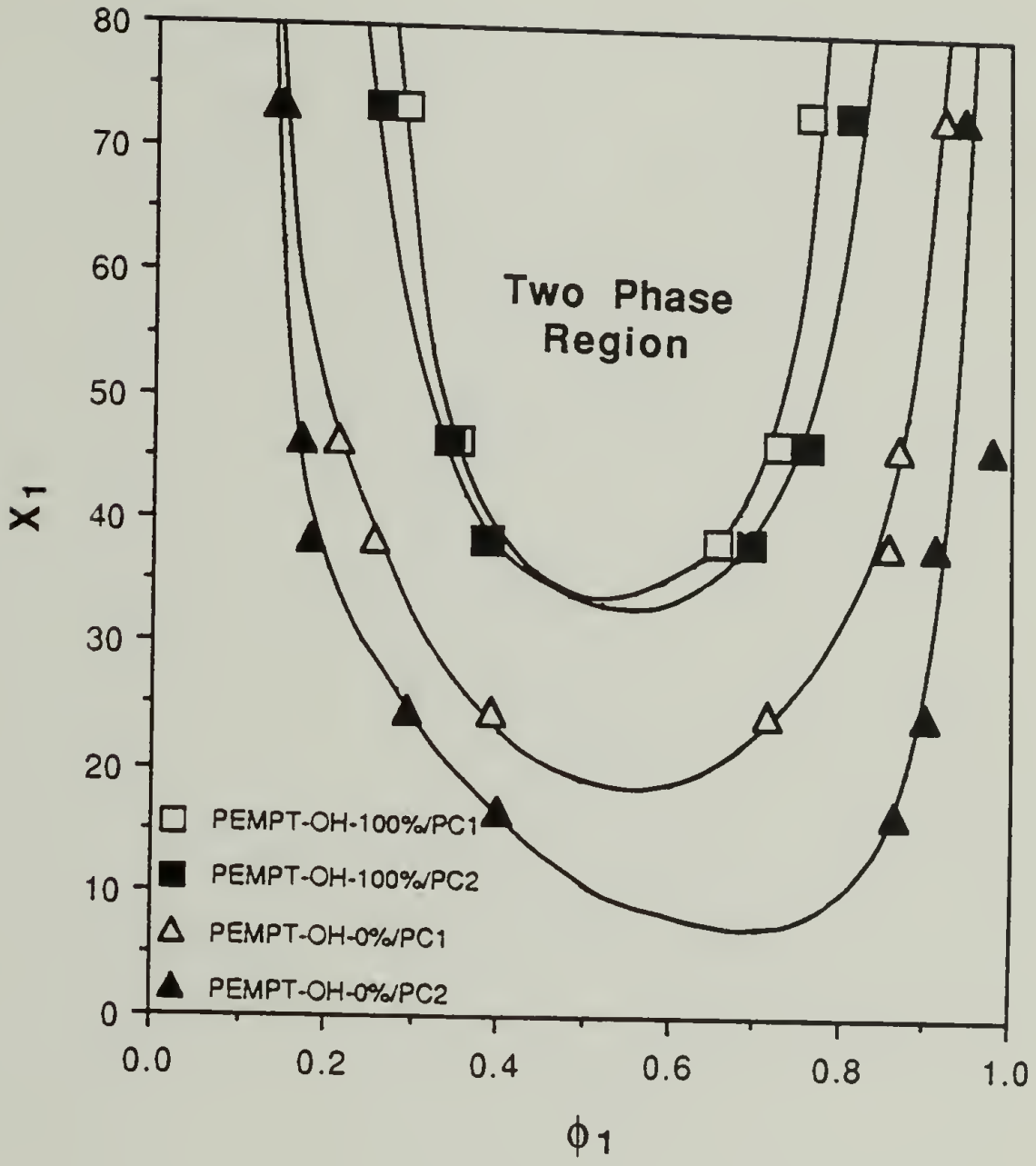

Figure 5.19 Miscibility maps of PEMPT-OH-100%/PC1, PEMPT-OH-100%/PC2 , PEMPT-OH-0%/PC1 and PEMPT-OH-0%/PC2 50/50 wt. % blends.

X_{n2} : number average degree of polymerization of PC.

What is now required is the value for the average number of alcoholysis reactions occuring per PC chain present, N_{alc}.

$$N_{alc} = \frac{2n_1}{n_2} = \frac{2n_1}{1-n_1} \qquad (5.2)$$

The number average degree of polymerization for the PC component can be calculated, ignoring the connectivity of the PC blocks to the polyester.

$$X_{nB} = \frac{x_{n2}}{1+N_{alc}} \qquad (5.3)$$

An estimate of the triblock DP will be based on this calculated value for the new DP of the polycarbonate component.

$$X_{nBAB} = X_{n1} + 2X_{nB} \qquad (5.4)$$

Using equations 5.1-5.4 above, values for N_{alc}, X_{nB} and X_{nBAB} were calculated. Table 5.3 contains these values for the PEMPT/PC1 and PC2 blends.

Examining Table 5.3, one notices that N_{alc} increases as the starting degree of polymerization of the original polyester decreases (PEMPT6, X_{1n} = 151; PEMPT1, X_{1n} = 16.5). This is expected, due to the increase in the number of end groups as molecular weight is lowered. What is more interesting is that as N_{alc} increases, x_{nBAB} and x_{nB} decrease considerably, the values originating from the PC2 blend quickly approach the values of that of the PC1 system. The alcoholysis reaction thus acts to equalize the molecular weights of the original PEMPT/PC1 and PC2 blends. At DPs of the original polyester of 46 or less (PEMPT4 through PEMPT1), the triblock/homopolymer blends have nearly identical number average moleclar weights after alcoholysis. The final result of this equivalence of molecular weights is the observation of nearly identical phase behavior as shown in Figure 5.19. Little deviation between the PEMPT-OH-100%/PC1 and PC2 miscibility maps is observed as the PEMPT molecular weight is lowered, in contrast to the unreacted blends.

Before closing this discussion on the effects of alcoholysis on blend phase behavior, several additional points should be made. In all of the NMR

Table 5.3 Triblock/Homopolymer Blend Characterization Data

Original Blend	Triblock/Homopolymer		
	N_{alc}	x_{nBAB}	x_{nB}
PEMPT1-OH2/PC1	5.49	30.5	7.0
PEMPT2-OH2/PC1	3.68	43.9	9.7
PEMPT3-OH2/PC1	2.37	65.2	13.5
PEMPT4-OH2/PC1	1.95	77.1	15.3
PEMPT5-OH2/PC1	1.23	113	20.3
PEMPT6-OH2/PC1	0.60	208	28.3
PEMPT1-OH2/PC2	10.3	31.5	7.5
PEMPT2-OH2/PC2	6.89	46.1	10.7
PEMPT3-OH2/PC2	4.43	69.5	15.6
PEMPT4-OH2/PC2	3.66	82.8	18.2
PEMPT5-OH2/PC2	2.31	125	25.6
PEMPT6-OH2/PC2	1.12	231	40.0

spectra of PEMPT/PC blends, in no instance is any evidence of direct midchain transreaction observed. Direct midchain reactions result in additional proton resonances between 8.1 and 8.3 ppm (as will be shown in section 5.4). The DNOP stabilizer appears to inhibit the direct midchain transreaction, however, it is not successful in preventing alcoholysis. The Ti catalyst used in the polymerization of PEMPT is known to be both an alcoholysis interchange reaction catalyst and a direct midchain transreaction catalyst. It seems reasonable to believe that the Ti catalyst could enhance the rate of alcoholysis of the carbonate group in PC. However, with no evidence of direct midchain reaction, it appears that the catalyst has been rendered inactive, and that the alcoholysis reaction has proceeded by an alternate mechanism, perhaps being catalyzed by the small concentration of acid end groups present from the original polyester synthesis. Pilati, et.al., during a PBT synthesis study using low molecular weight model compounds, has shown that addition of catalytic amounts of benzoic acid leads to an increase in the rate of alcoholysis [21]. It should be mentioned that Pilati also observed alcoholysis reactions in non-catalyzed systems.

In addition, their is no evidence of a back alcoholysis reaction, i.e, upon initial alcoholysis of PC, the resulting phenol end groups do not appear to react with PEMPT carbonyls. Figures 5.3a, 5.6a, 5.9 and 5.10, show complete reaction of the PEMPT hydroxyl groups. If the resulting phenol end groups were reacting with the carbonyl groups of PEMPT, an equilibrium between the two reactions should be achieved and a stable resonances associated with the PEMPT hydroxyl group should be observed. This is not the case. The lack of alcoholysis of PEMPT by phenol end groups of PC is consistent with the study of model compounds by Devaux, et. al. [1].

The difference in the alcoholysis reaction rate between the PEMPT-OH2/PC and PEMPT-OH15/PC blends also needs to be addressed. The DSC annealing and scanning treatments for both blend systems were identical (the only exception being previously mentioned). One would thus expect similar reaction rates and similar extents of hydrolysis in each set of blends. The NMR data presented above shows considerably different extents of reaction. Presently, their is no experimentally varified reason for this descrepancy. Identification would most likely require a detailed kinetic study of the two systems and, more specifically, a detailed kinetic study of alcoholysis reactions

examining catalyst, acid end group and stabilizer concentration effects. This was not done during the course of this dissertation.

Offsetting this disquieting fact is the knowledge that alcoholysis reactions in a polyester/PC blend have been quantitatively identified and the resulting effects on blend miscibility elucidated. Prior to this work, direct identification of end group reactions were not reported in systems of this type. Also, the overall effect of hydrolysis should not be completely manifestated in the observed blend phase behavior. Granted, the shifts in the miscibility windows between the PEMPT-OH-0%/PC and PEMPT-OH-100%/PC systems are significant. However, the transformation of the homopolymer/homopolymer blend to a triblock/homopolymer system will have profound effects on a variety of other properties, specifically those which depend on the interfacial behavior of the two components, e.g., fraction toughness. This important point should not be overlooked, as it may apply equally well to the the random block copolymers formed through direct midchain transreaction discussed below.

5.4 Direct Midchain and Alcoholysis Transreactions in PEMPTB/PC Blends

5.4.1 Spectroscopy of Transreacted Blend

The overall goal of this study is to quantitatively identify the extent of transreaction required to shift the blend phase behavior from two phase to single phase. In order to achieve this, a direct measure of the extent of transreaction occuring in the blend system is required. Proton NMR will be used for this measurement, however, before this can be done specific resonances consistent with the expected structures after interchange reaction has occurred must be identified and assigned. Alcoholysis transreactions have already been observed by ^{1}H NMR (Section 5.3.2), although no attempt was made to associate the new resonances with the chemical structure changes occuring in the blend. This will now be done for both alcoholysis and direct midchain reactions.

5.4.1.1 Expected Structures After Transreaction

Previous studies on transreacting polyester and polyester/PC blends have used predominantly dyad and to a lesser extent triad analysis to correlate

the observed spectra to the structures expected after interchange reaction [2,3,10,12,13,22]. Proton NMR of PEMPT (Chapter 3) has revealed that the protons of the terephthalate ring adjacent to the aliphatic-hydroxyl end are not magnetically equivalent to the corresponding dual aliphatic-aromatic substituted ring (Figure 3.14). Due to this fact, complete structure identification of PEMPT in the transreacting system can not be adequately represented by dyad or triad analysis and pentads should be examined. Designating A_1 as the terephthalate ring of PEMPT, B_1 as the aliphatic sequence of PEMPT, A_2 as the carbonate moiety of PC and B_2 as the aromatic-aliphatic portion of PC, the polymer repeat units can be represented as follows:

PEMPT	$-(A_1B_1)-$
PC	$-(A_2B_2)-$

The expected pentads in a transreacting PEMPT/PC blend can be represented using similar notation. Centering the pentad on a terephthalate ring of PEMPT (A_1), 16 different combinations are documented. However, 6 pairs of these are degenerate, thus, there are 10 chemically non-equivalent pentads. Table 5.4 list these pentads along with the corresponding number of transreactions required to form the sequence. Pentad 1 corresponds to the structure of PEMPT while 2-7 are the six degenerate pairs.

Due to NMR instrument resolution limitations, assigning all the possible resonances associated with these 10 structures would at present be an impossible task. To circumvent this problem, relatively low levels of transreaction will be examined. If this restraint is applied, only the statistically most probable pentads will be of importance, i.e., the pentads formed from the minimum number of interchange reactions. The statistically most probable pentads are pentads 2 and 3 (Table 5.4). Combining this with the fact that they represent a degenerate pair, the resonances of these pentads should be the most dominant in the observed spectra of transreacted blends. These two sequences will be rewritten as a quartad and a triad which both focus on the connecting point between the two blocks.

$$A_1B_1A_1B_1A_2 \equiv A_1B_1A_2B_2$$

$$A_1B_1A_1B_2A_2 \equiv B_1A_1B_2$$

Table 5.4 Pentads Centered on the PEMPT Terephthalate Ring

Pentad		Number of Transreactions
1)	$A_1B_1A_1B_1A_1$	0
2)	$A_1B_1A_1B_1A_2$	1
3)	$A_1B_1A_1B_2A_2$	1
4)	$A_1B_1A_1B_2A_1$	2
5)	$A_2B_1A_1B_2A_2$	2
6)	$A_2B_1A_1B_2A_1$	3
7)	$A_1B_2A_1B_2A_2$	3
8)	$A_2B_1A_1B_1A_2$	2
9)	$A_2B_2A_1B_2A_2$	2
10)	$A_1B_2A_1B_2A_1$	4

These two structures correspond to the block sequences after a single midchain reaction between a carbonyl of PEMPT and a carbonate group of PC. The midchain transreaction and the resulting quartad and triad with alphabetically coded hydrogens are shown in Figure 5.20a (reactants) and 5.20b (products). Figure 5.21a,b displays the alcoholysis reaction and the resulting sequences. It is the hydrogen resonances of these products that require identification and assignment in the transreacting blend. It should be noted that direct midchain and alcoholysis interchange reaction lead to the identical quartad, reducing the number of resonances to be assigned.

The proton resonances for unreacted PEMPT, protons **a**, **b**, **c**, **d** and **e** of Figures 5.20a and 5.21a have been assigned in Chapter 3. The proton resonances of the unreacted PC will now be briefly discussed. The proton spectrum of PC is straight forward with three main resonances, Figure 5.22. A singlet at 1.678 ppm associated with the methyl groups and a pair of doublets centered at 7.164 and 7.253 ppm corresponding to the aromatic ring protons are observed (protons **f** in Figures 5.20 and 5.21). Expanding the aromatic portion of the spectrum, Figure 5.23, finer splitting of this original pair of doublets is observed. Eleven resonances are seen and an additional resonance is most likely hidden by the chloroform peak at 7.261 ppm. Aromatic rings with different electron withdrawing groups in the para position fall into spin system known as an AA'BB' system [23,24]. These spin systems may exhibit up to 24 lines in their spectra, however, resolution limitations often prevent observation of all resonances. The importance of this spin system lies in the fact that upon direct midchain reaction, the $B_1A_1B_2$ triad (Figure 5.20, protons **d"**) represents this spin system, thus, it can be used as a indication for midchain transreaction.

The bisphenol-A sequence of PC will be used as a model for the 2-dimensional ^1H-^1H COSY pattern for the AA'BB' spin system. Figure 5.24 shows the 300 MHz COSY spectrum of the aromatic region of PC. The pulse width was 9.3 µsec, the spectral width was 6.950-7.376 ppm with 64 intervals and 16 scans per interval being run. The resulting spectrum which corresponds to proton correlations in the aromatic ring exhibits a four lobe pattern. This pattern will be used as conformation of direct midchain transreaction between PEMPT and PC.

a)

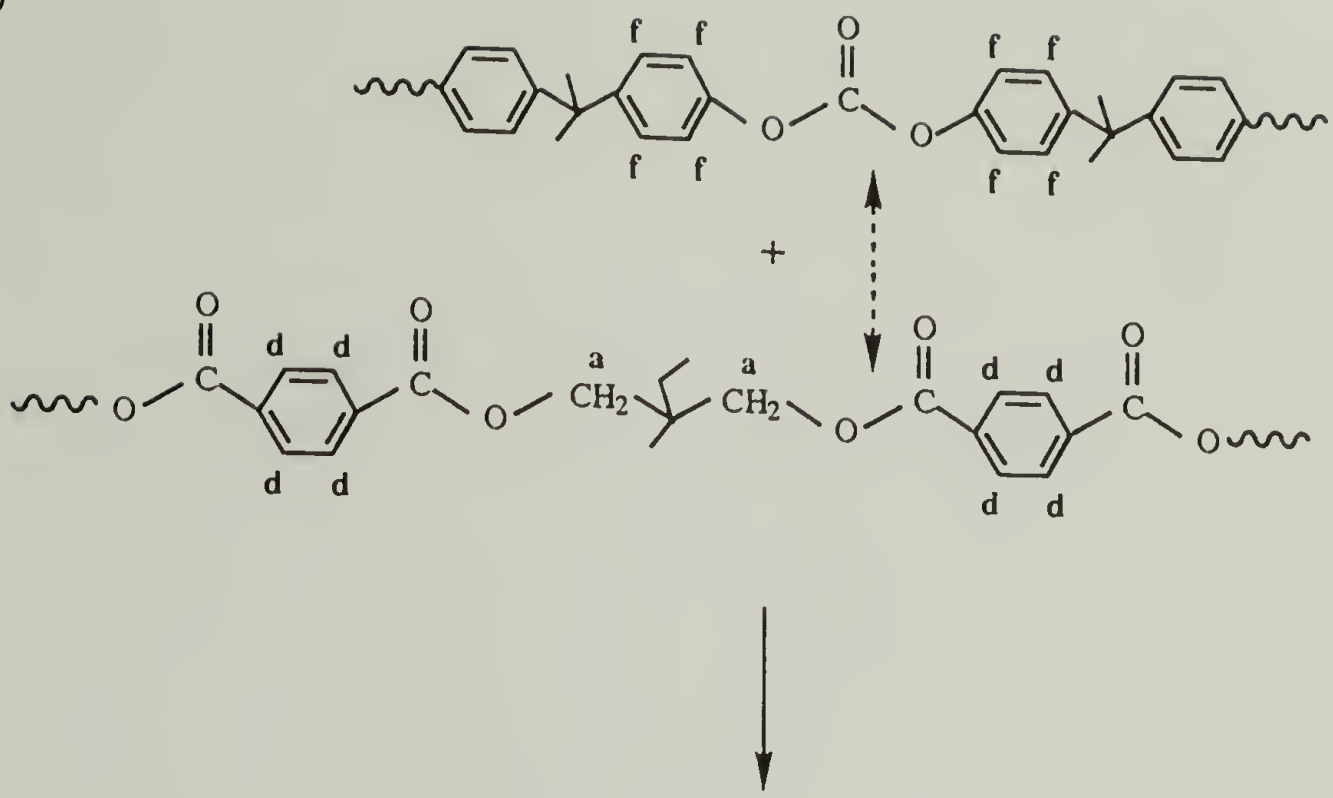

b)

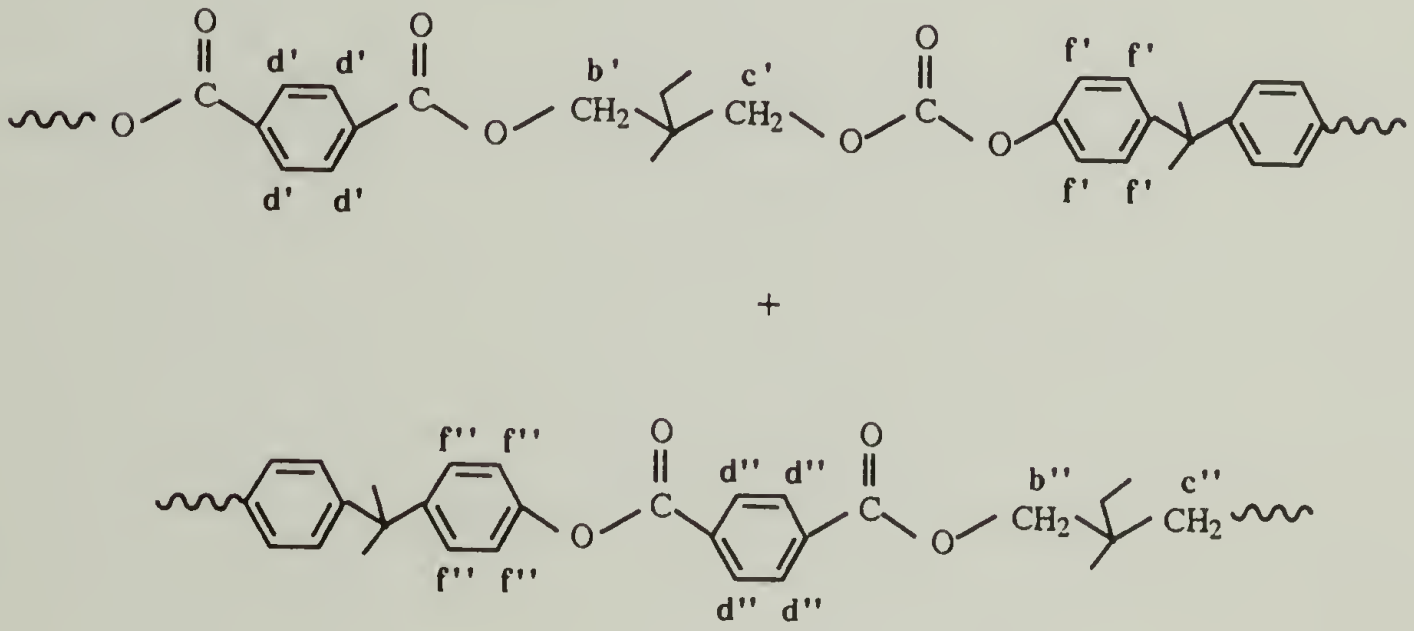

Figure 5.20 Direct midchain transreaction a) reactants b) products.

a)

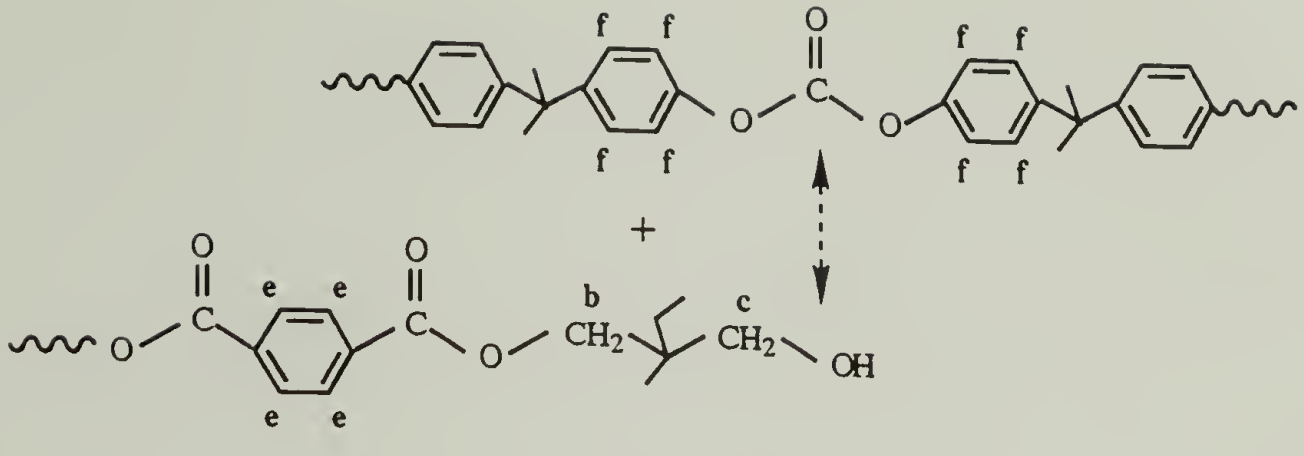

b)

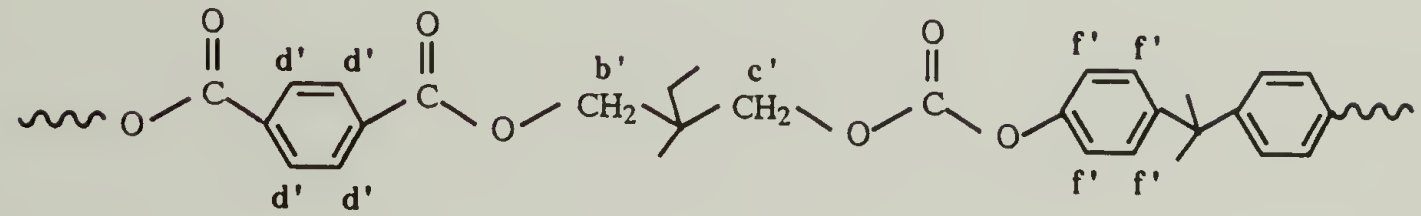

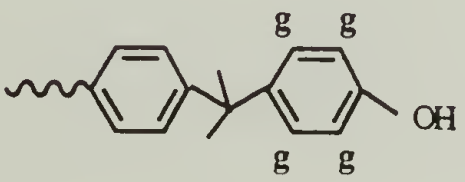

Figure 5.21 Alcoholysis transreaction a) products b) reactants.

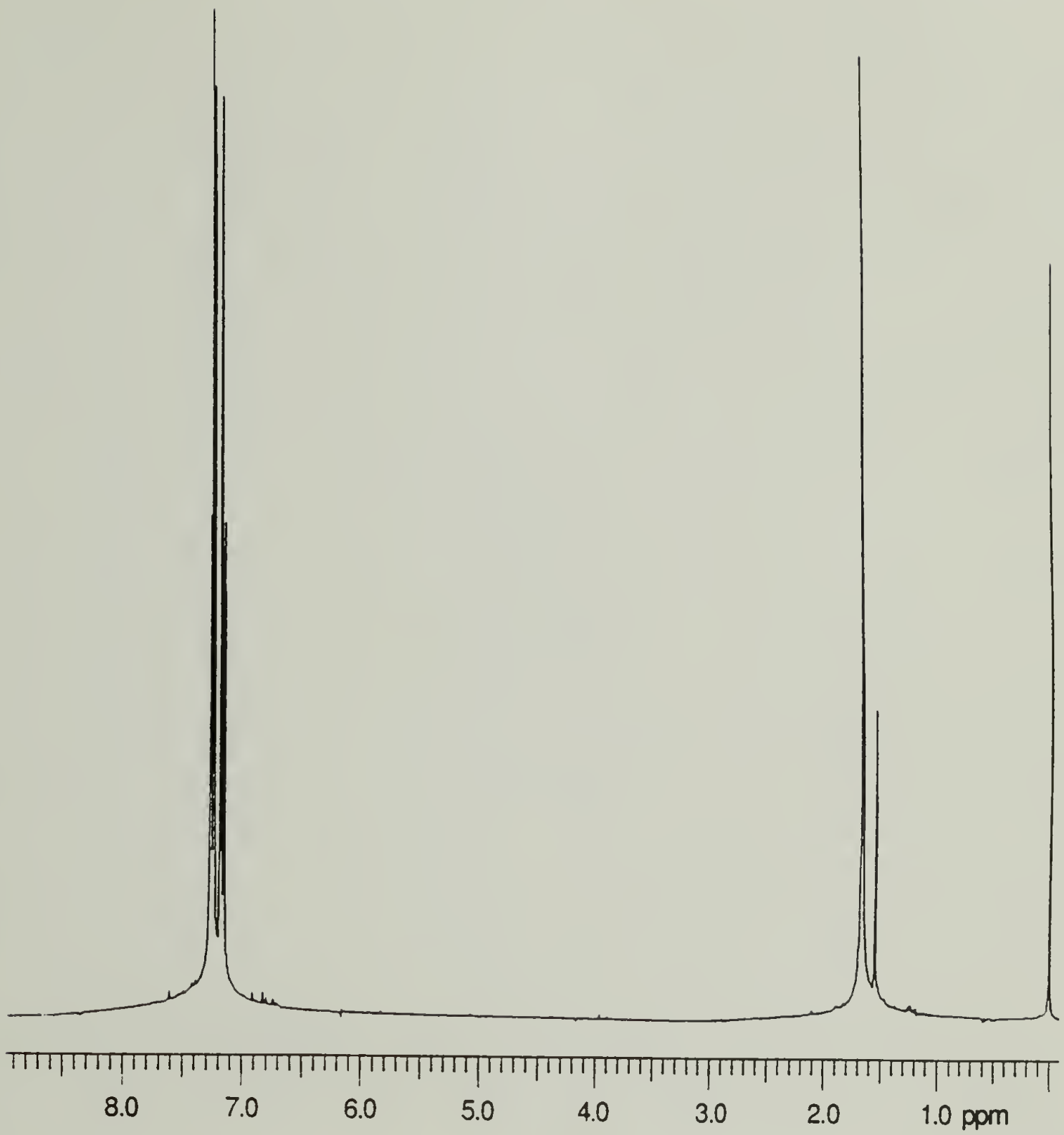

Figure 5.22 300 MHz ^{1}H NMR spectrum of PC2.

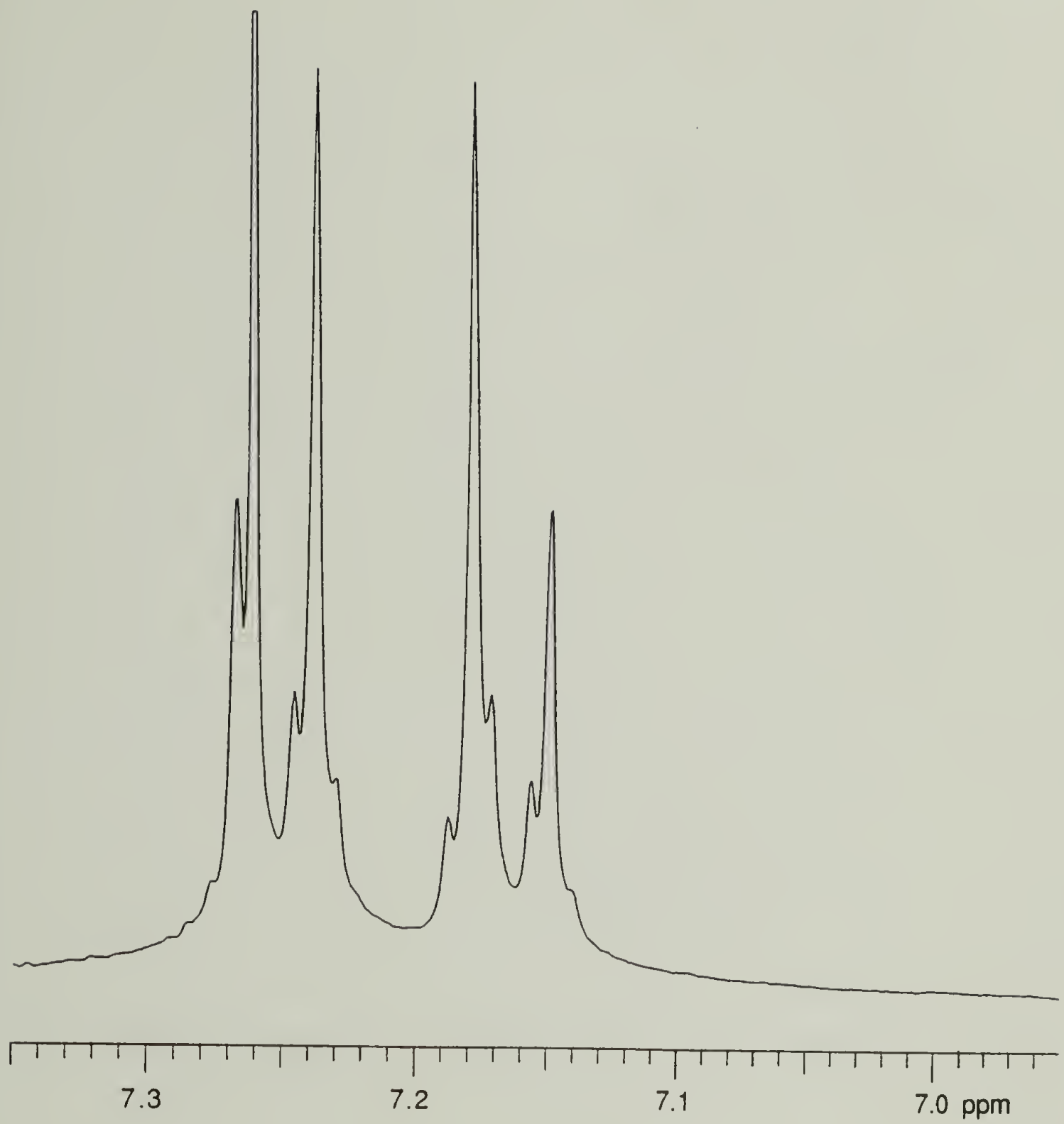

Figure 5.23 300 MHz ^{1}H NMR spectrum displaying the aromatic region of PC2.

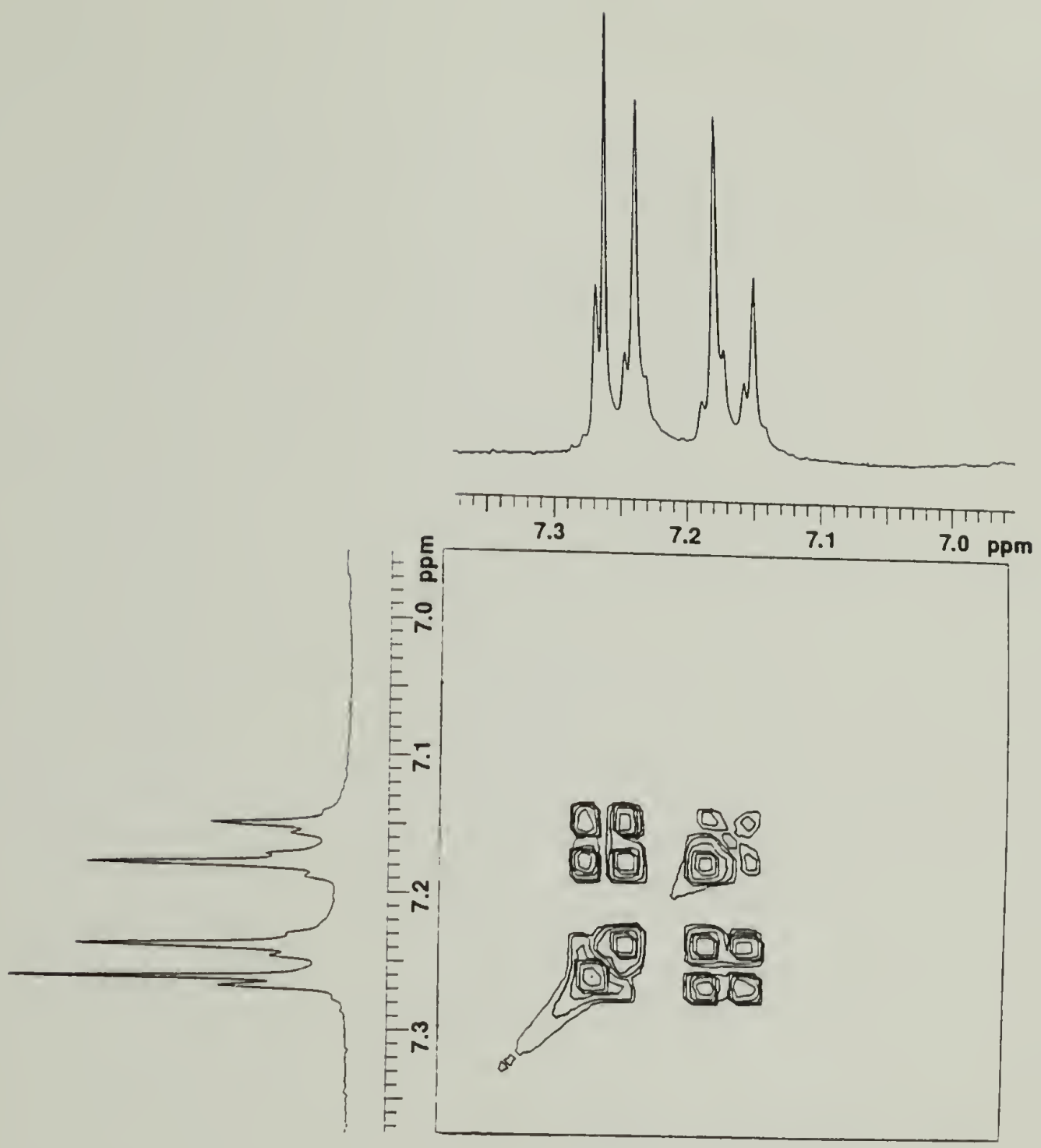

Figure 5.24 300 MHz ^{1}H-^{1}H NMR COSY spectrum displaying the aromatic region of PC2.

5.4.1.2 Identification and Assignment of Proton Resonances

Previous ^1H NMR studies have identified new resonances in both the aromatic (terephthalate group) and aliphatic (methylene group) regions of the spectra during transreaction in polyester and polyester/PC blends [3,4,10,11,13]. It is anticipated that the PEMPT/PC system will exhibit analogous changes in these regions, as well as, that of the aromatic frequency range associated with the bisphenol group. Spectroscopic examination will thus focus on these three portions of the spectrum, ignoring the aliphatic region corresponding to the side chain substitution in PEMPT. This does not imply that shifts in these aliphatic regions are not observed, but the close proximity of the peaks combined with splitting leads to a more ambiguous identification and assignment of resonances.

Figures 5.25 shows the ^1H NMR spectra of a PEMPTB/PC2 blend after annealing for 128 min. at 240°C. The annealed sample displays numerous additional resonances associated with structure changes caused by interchange reaction. Expansions of the transreacted sample's spectrum corresponding to the backbone methylene, terephthalate and PC aromatic proton regions are shown in Figures 5.26, 5.27 and 5.28, respectfully. The chemical shifts of the most prominent new resonances are labeled in each diagram. ^1H-^1H COSY experiments were also run on the annealed sample.

Figure 5.29 shows the 300 MHz COSY spectrum of the terephthalate region. The spectral width was narrowed to 7.902-8.423 ppm and was divided into 64 intervals. Thirty-two scans per interval were run with a pulse widths of 9.3 µsec. Examining Figure 5.29 we see off diagonals indicating that both of the protons resonating at 8.121 and 8.150 ppm are coupled with the protons at 8.227 and 8.255 ppm. The coupling pattern is extremely similar to that observed for the PC model AA'BB' spin system and indicates that this pair of protons belong to a para substituted aromatic ring with different electron withdrawing groups. Similarly, a COSY experiment was conducted encompassing the aromatic region corresponding to the aromatic PC groups. In this case, the spectral window was 7.381-6.948 ppm which was again divided into 64 intervals. Thirty-two scans were recorded per interval with the same pulse width used above. This spectrum is shown in Figure 5.30. One new AA'BB' coupling pattern is clearly present, corresponding to coupling of both the protons resonating 7.035 and 7.064 ppm with two protons at 7.198 and

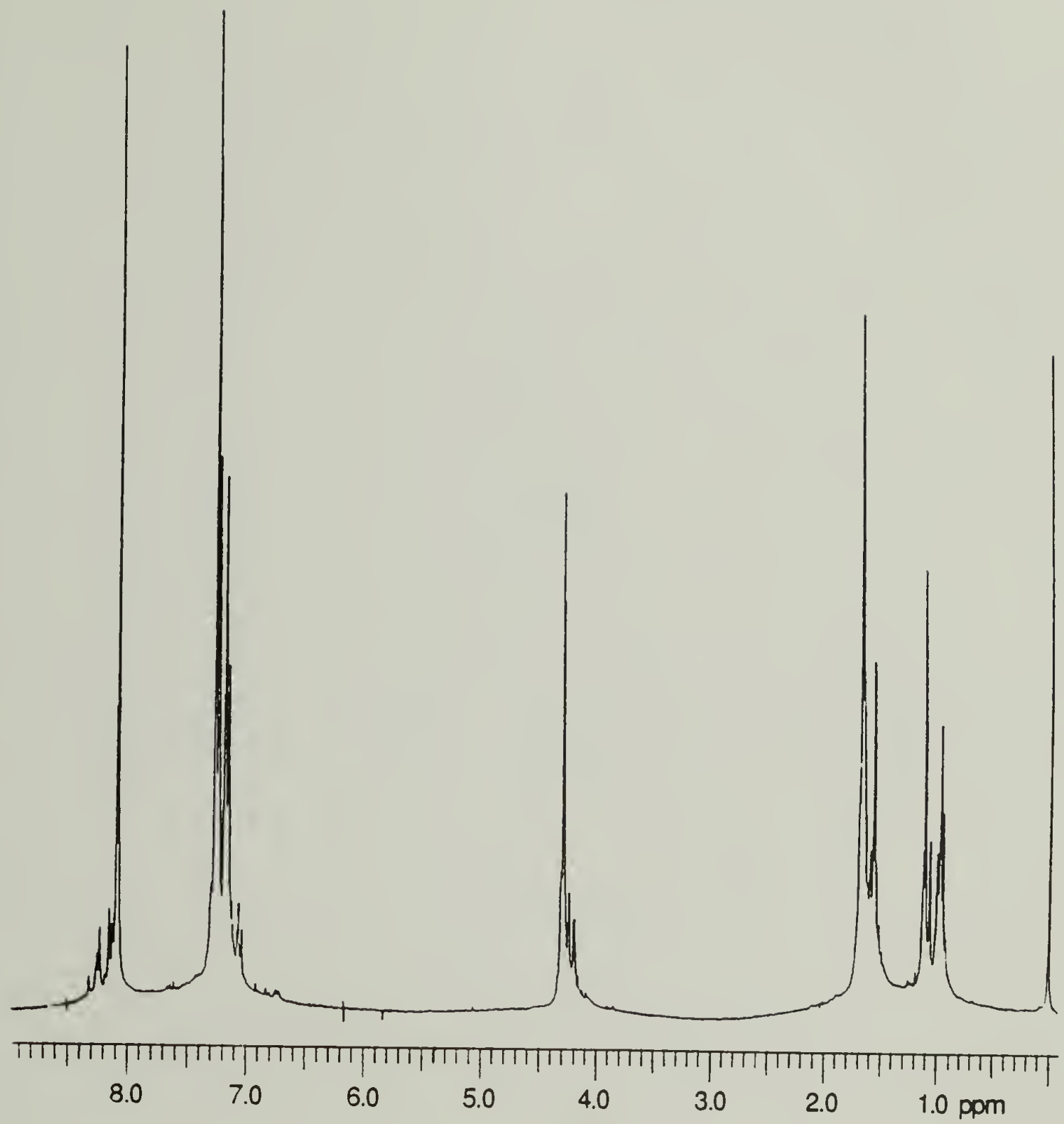

Figure 5.25 300 MHz ^{1}H NMR of PEMPTB/PC2 50/50 wt. % blend annealed 128 min @ 240°C.

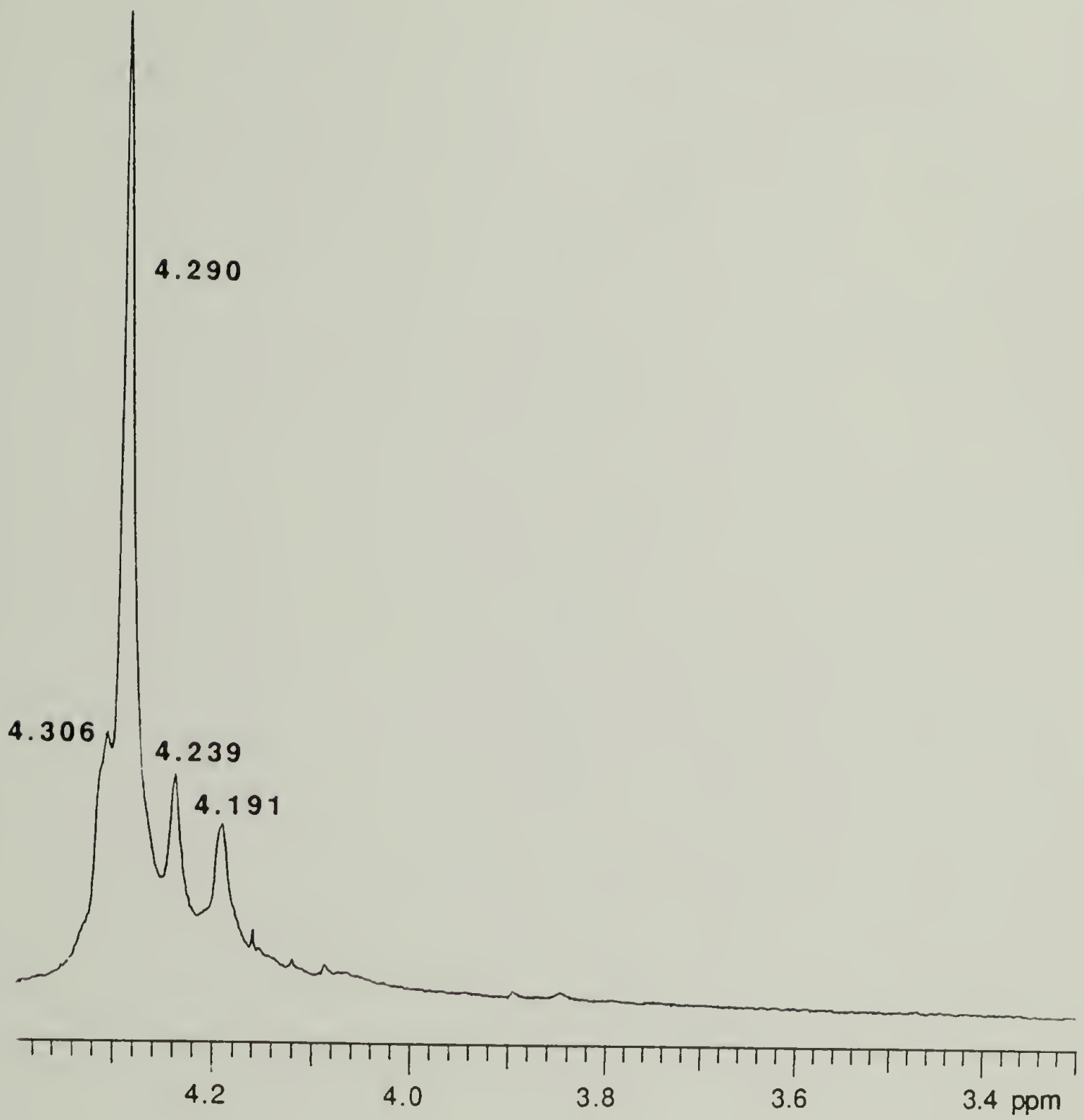

Figure 5.26 300 MHz ^{1}H NMR spectrum displaying the methylene backbone region of a PEMPTB/PC2 50/50 wt. % blend annealed 128 min @ 240°C.

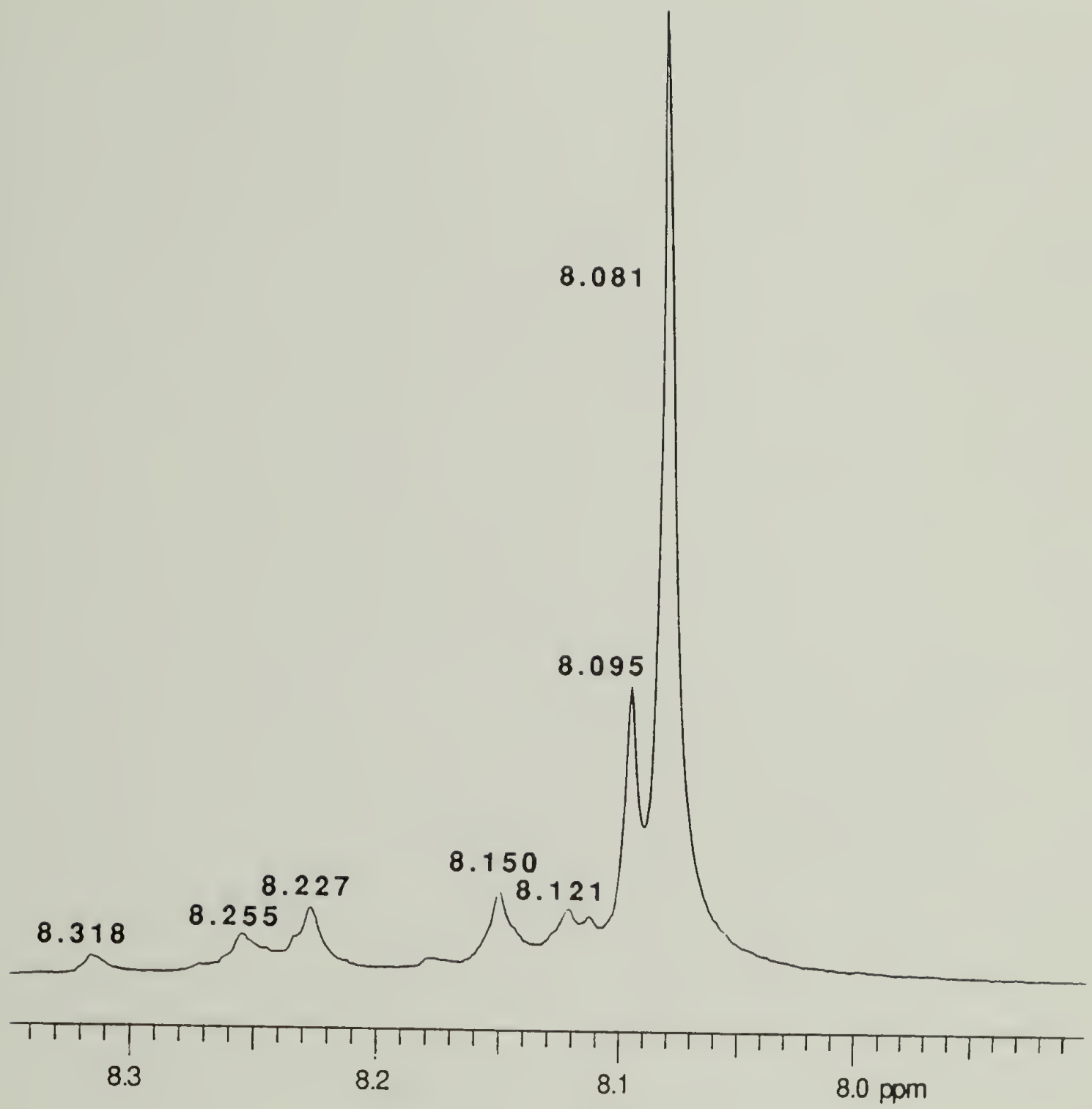

Figure 5.27 300 MHz ^{1}H NMR spectrum displaying the terephthalate region of a PEMPTB/PC2 50/50 wt. % blend annealed 128 min @ 240°C.

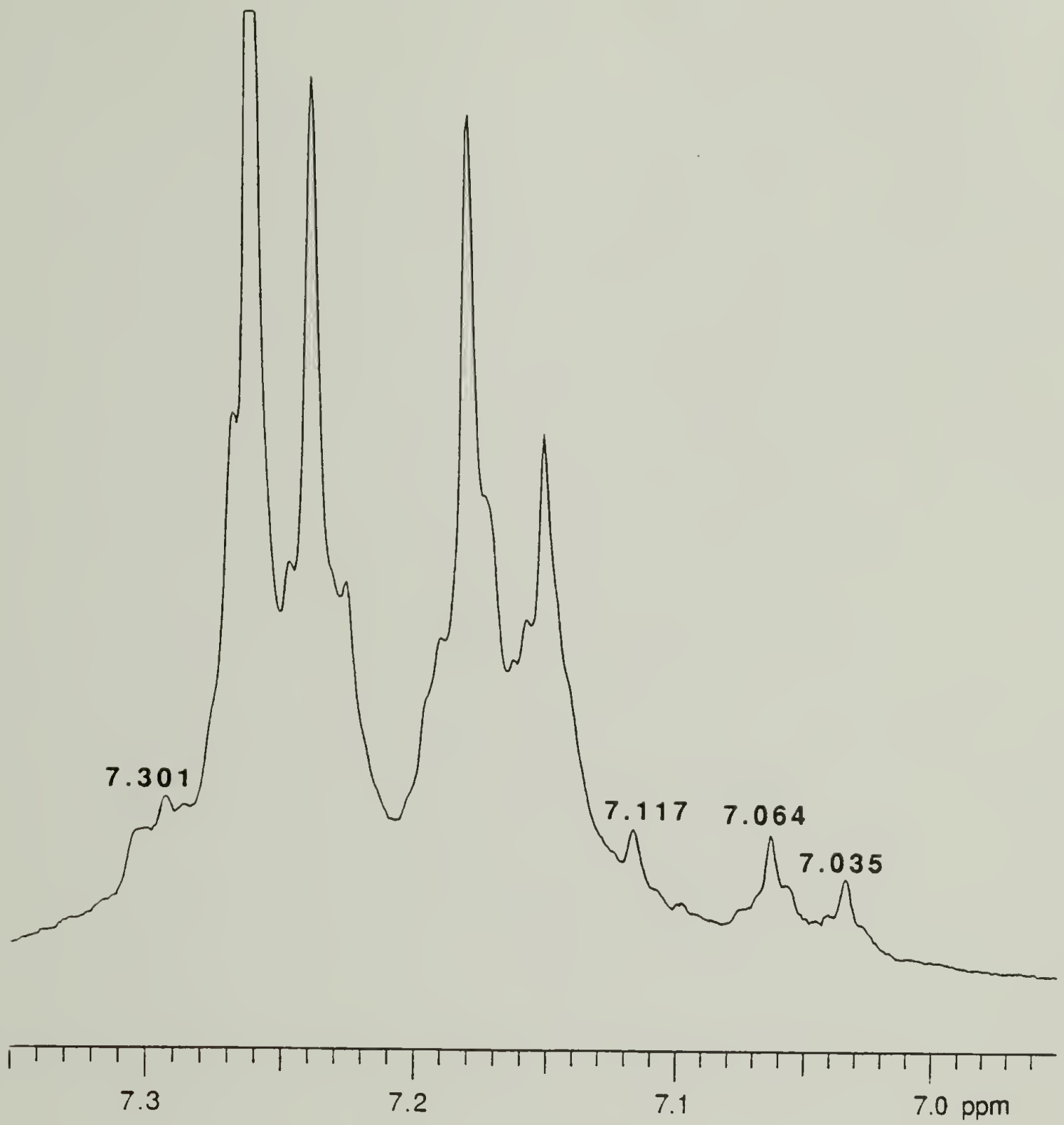

Figure 5.28 300 MHz ^{1}H NMR spectrum displaying the PC aromatic region of a PEMPTB/PC2 50/50 wt. % blend annealed 128 min @ 240°C.

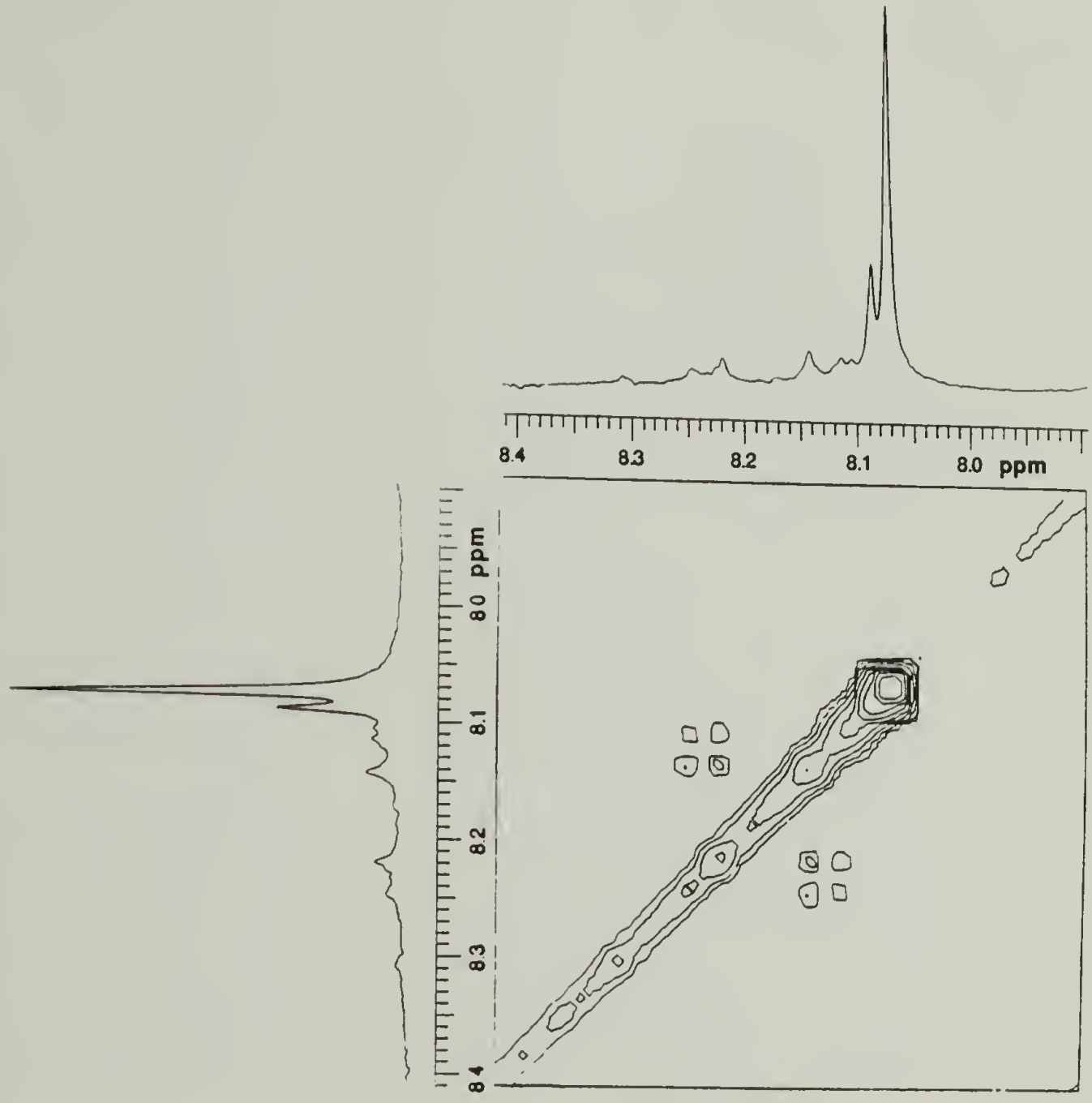

Figure 5.29 300 MHz ^{1}H-^{1}H NMR COSY spectrum displaying the terephthalate region of a PEMPTB/PC2 50/50 wt. % blend annealed 128 min @ 240°C.

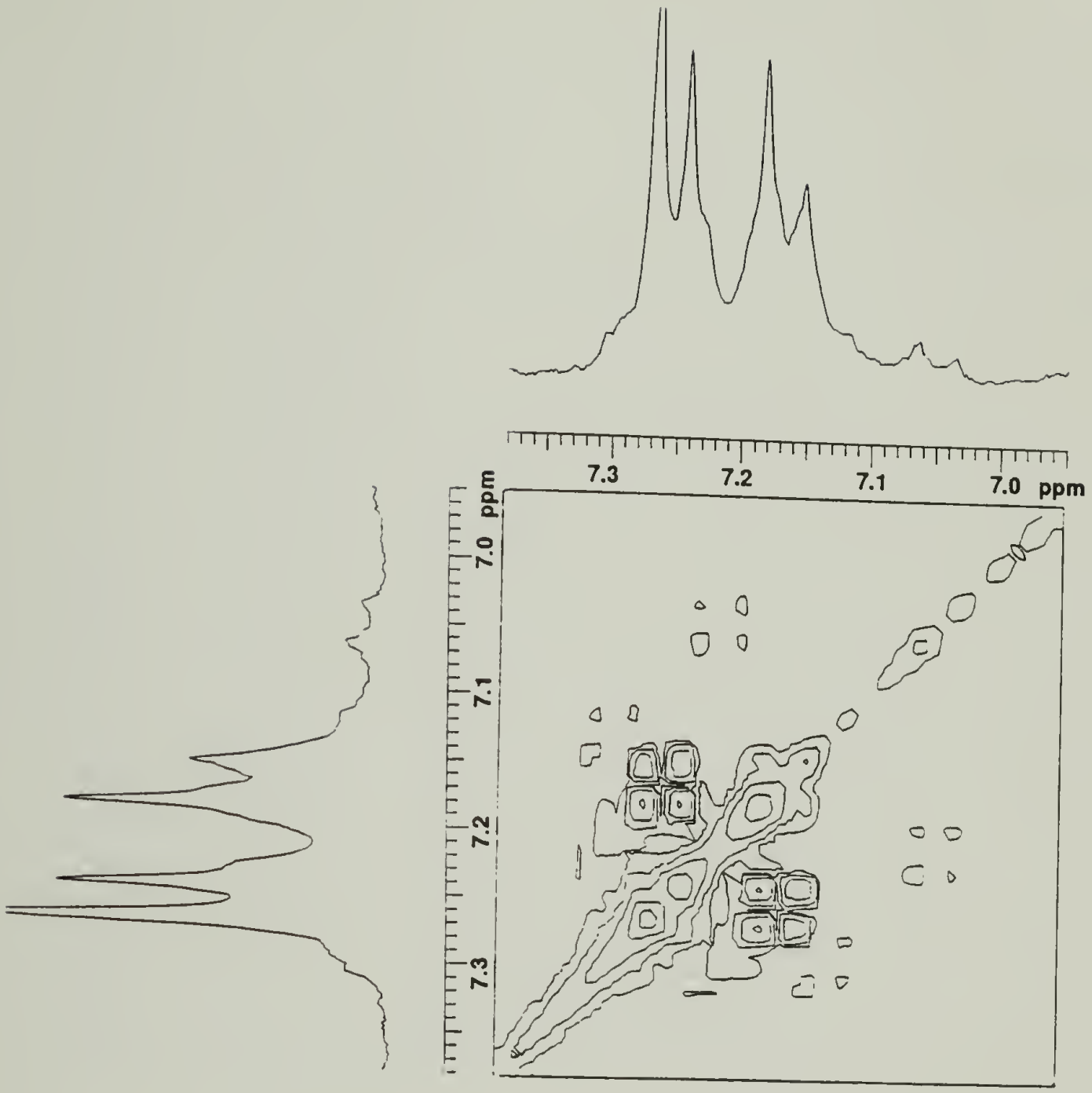

Figure 5.30 300 MHz ^{1}H-^{1}H NMR COSY spectrum displaying the PC aromatic region of a PEMPTB/PC2 50/50 wt. % blend annealed 128 min @ 240°C.

7.230 ppm. These last two resonances, 7.198 and 7.230 ppm, were previously undetected in the one dimensional ^{1}H NMR, being overlapped by the original pair of doublets of the aromatic rings. Additionally, what appears to be another AA'BB' coupling pattern is also observed in this spectrum. This off diagonal pattern slightly overlaps the coupling pattern of the original aromatic protons. Coupling between both peaks at 7.117 and 7.145 ppm with resonances at 7.274 and 7.301 can be deduced. In this case, two additional resonances have been determined from the COSY experiment, 7.145 and 7.274 ppm. These coupling patterns are once again very similar to the original model pattern and indicate that different electron withdrawing groups are now present in the para position of the PC aromatic ring. It should be noted that the error in determining the resonance frequencies from the COSY spectra is on the order of ± 0.005 ppm. The error in the determined frequencies from the standard ^{1}H NMR is on the order of ± 0.002 ppm.

With the most prominent new frequencies in the transreacted blend identified, it is now necessary to assign these frequencies to the expected structures after transreaction. Table 5.5 list all these assignments and, for convience, the corresponding stuctures (from Figures 5.20 and 5.21) below it. Discussion will now focus on these assignments. Beginning with the quartet sequence (identical in Figures 5.20b and 5.21b), the resonances at 4.239 and 4.191 ppm are asigned to protons **b'** and **c'**, respectively. The upfield shift from the main methylene backbone resonance is expected upon replacement of the aromatic ester by the less deshielding aromatic carbonate group. The nonsymmetric substitution on the propylene group should also lead to the appearance of two resonances, as is observed. These assignments are confirmed by the earlier spectroscopy conducted on the blends undergoing alcoholysis transreaction. Upon alcoholysis which leads to this same quartet sequence, these identical two resonances were observed (Figures. 5.4 and 5.7). Similar upfield shifts have been noted in a model study of oligomers synthesized from phthalic anhydride and 1,2-propanediol, where the methylene backbone resonances were dependent on triad sequence (midchain vs end group) [25].

Continuing to the aromatic resonances of PC, replacement of a bisphenol-A group by the less deshielding propylene group is expected to produce an upfield shift on the remaining adjacent aromatic ring of the triad, protons **f'**. The four resonances shifted upfield from the original resonances

Table 5.5 Proton Asignments After Transreaction

Backbone Methylene	Proton Assign. (ppm)	Aromatic Bisphenol-A	Proton Assign. (ppm)	Aromatic Terephthalate	Proton Assign. (ppm)
b'	4.239	f'	7.035	d'	8.095
c'	4.191	f'	7.064		
		f'	7.198		
		f'	7.230		
b''	4.306	f''	7.117	d''	8.150
		f''	7.145	d''	8.121
		f''	7.274	d''	8.227
		f''	7.301	d''	8.255

and confirmed by the COSY experiment to have the coupling of an AA'BB' spin system; 7.035, 7.064, 7.198, and 7.230 ppm; are assigned to protons **f'**.

Perhaps the most interesting assignment of this quartet sequence are protons **d'** assigned to the resonance at 8.095 ppm. Originally, this peak appeared to be completely inconsistent with the dyad analysis commonly used for peak assignments in these systems [3,5]. End capping experiments (Chapter 3) identified a resonance associated with the terephthalate group adjacent to hydroxyl end group indicating that dyad analysis was insufficient to describe all the observed resonances. Confirmation that the resonance at 8.095 ppm was indeed associated with protons **d'** came again from the NMR studies of the alcoholysis transreaction. Upon complete alcoholysis, the resonance at 8.065 ppm was replaced by the 8.095 ppm peak. One may question whether this resonance, 8.095 ppm, corresponds to all four protons of the terephthalate ring or the two most adjacent to the bisphenol-A group. The molecular weight data of Chapter 3 derived from the corresponding 8.065 ppm peak is consistent with this resonance representing all four ring protons. The appearance of this resonance also appears dependent on the aliphatic sequence length. Figure 5.31 shows the terphthalate region of the 300 MHz ^{1}H NMR of a PHT/PC2 blend (from the screening study of Chapter 2) annealed 120 min at 240°C. No singlet shifted slightly downfield from the original terephthalate resonance is observed, however, the pair of doublets previously observed in the PEMPT/PC system are also seen here, indicating that transreaction has occurred in this blend.

The assignment of the proton resonances associated with the triad of Figure 5.20b will now be discussed. Beginning with terephthalate region of the spectum, the four new resonances confirmed to be an AA'BB' spin system; 8.150, 8.121, 8.227, and 8.255 ppm; are assigned to protons **d"**. This splitting pattern has been noted in a transreacting PBT/PAr blend [11]. Next, the remaining observed AA'BB' spin system in the bisphenol-A aromatic region, resonances 7.117, 7.145, 7.274, and 7.301 ppm, are assigned to the protons **f"**. The final assignment is the resonance at 4.306 ppm to protons **b"**. This assignment is somewhat tenitive and represents another instance in this system where dyads can not sufficiently describe all the observed resonances.

Several observed resonances have not been assigned. They include peaks at 8.318, 8.179, and 8.113 ppm. A resonance at 8.28 ppm has been associated with a symetrically substituted terephthate ring in a transreacting

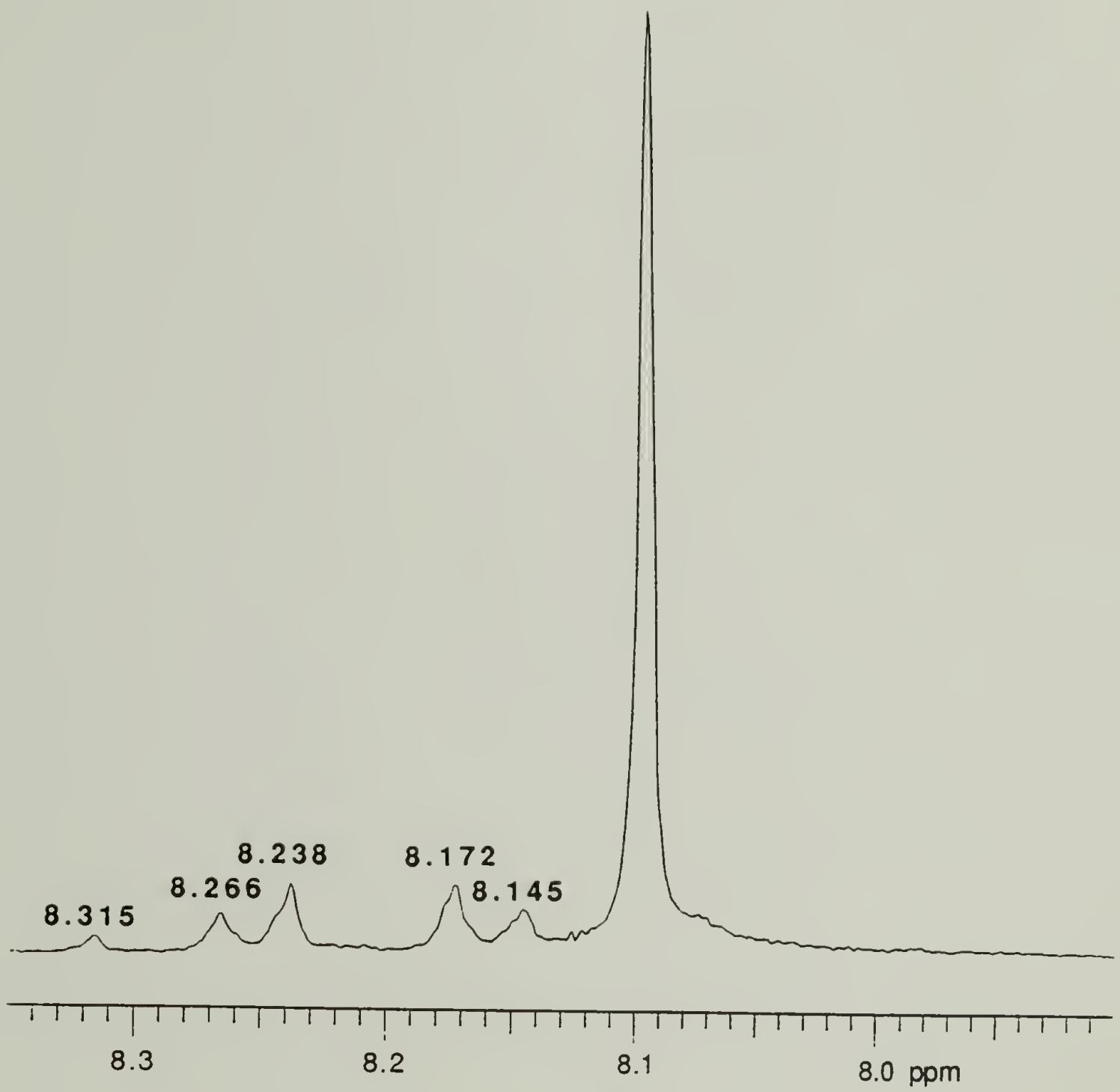

Figure 5.31 300 MHz ^{1}H NMR spectrum displaying the terephthalate region of a PHT/PC2 blend annealed 120 min @ 240°C.

PBT/PC system [3]. In the PEMPT/PC system, the corresponding terephthalate protons of an $A_2B_2A_1B_2A_2$ sequence are thus assigned to the 8.318 ppm resonance. Note that this resonance is observed in the PHT/PC spectrum of Figure 5.31 and is consistent with the formation of the identical sequence in this blend. The two other unassigned resonances, 8.179 and 8.113 ppm, are not observed in the PHT/PC spectrum. It is presumed that they correspond to pentad effects. One possible assignment of the resonance at 8.113 ppm is to the terephthalate protons with the symmetric substitution $A_2B_1A_1B_1A_2$. The shift is consistent with that observed for the formation of a $A_1B_1A_1B_1A_2$ pentad decribed above (8.095 ppm resonance).

A final point should be made about end group reaction in this blend. In neither the terephthalate aromatic region nor the backbone methylene region (Figures 5.28 and 5.29) are any resonances associated with the original end sequence present. Once again all of the hydroxyl groups have reacted during the annealing process. It is important to note that we can now spectroscopically differentiate end group and direct midchain reaction. End group reaction can be identified by the disappearence of the 8.065 ppm resonance while direct midchain transreaction leads to the appearence of the AA'BB' terephthalate doublets. With the resonances of both midchain and alcoholysis interchange reaction identified, a study correlating the extent of transreaction to the observed phase transition in the blend can be conducted.

5.4.2 Quantitative Phase Behavior Study

5.4.2.1 Phase Behavior-Interchange Reaction Correlations

Figure 5.32 shows the DSC traces of PEMPTB/PC2 non-stabilized blends, except for the one indicated scan, annealed for times varying from 0-128 min. By 32 min, there has been a large shift in the T_gs of both the upper and lower T_g phases. After 128 min of annealing, the single sharp T_g indicates a single phase blend has been formed. The improvement in miscibility could be caused by several factors including, solvent/preparation effects, molecular weight reduction (due to hydrolysis), or interchange reaction. The DSC trace of the DNOP stabilized PEMPTB/PC2 blend annealed 128 min at 200°C is shown to indicate the two phase nature of the blend at equilibrium. From this and the extensive phase behavior studies of Chapter 4, solvent/preparation effects can

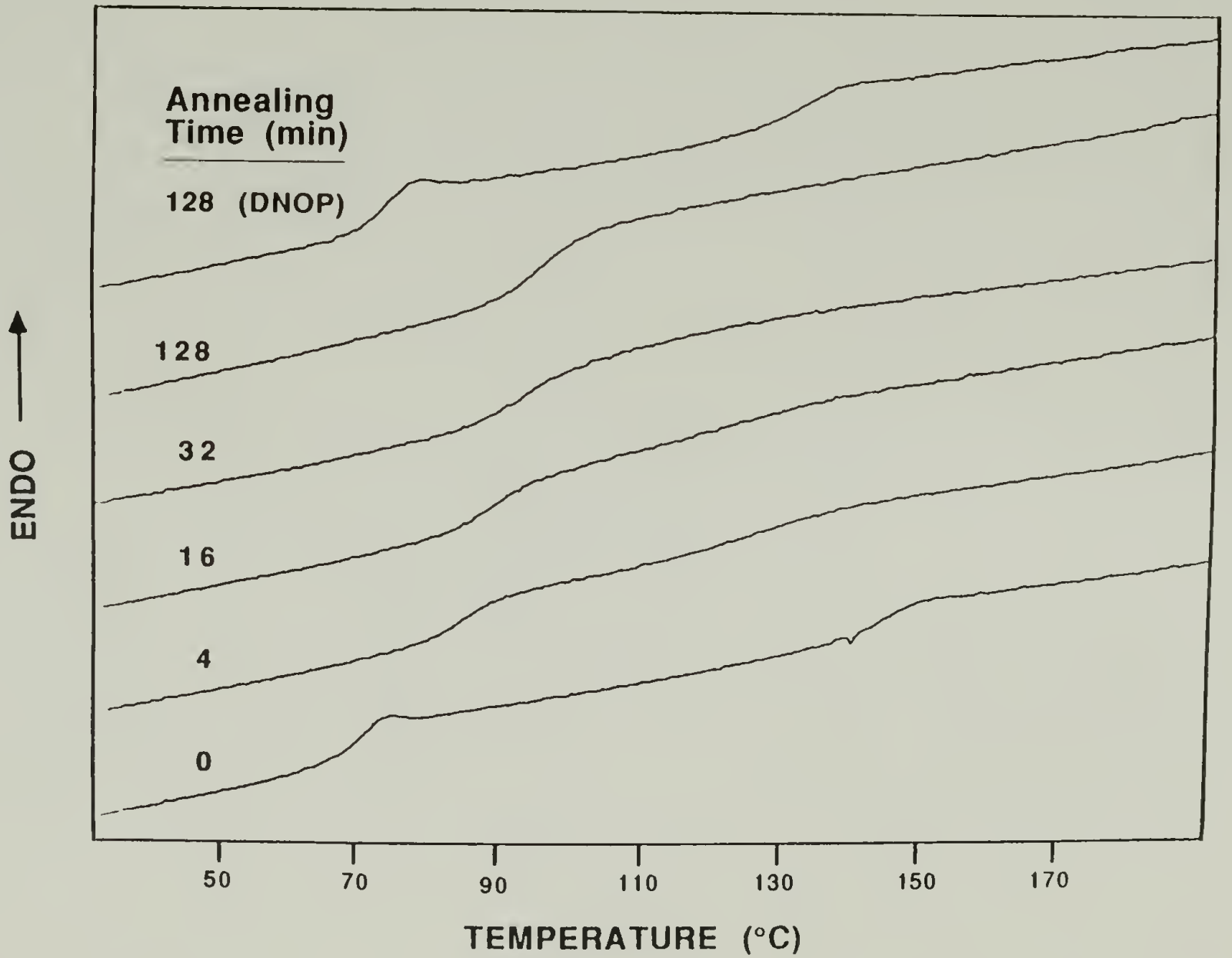

Figure 5.32 DSC heating scans of PEMPTB/PC2 blends annealed @ 200°C for the indicated times.

not be the cause of the observed phase change. Decreases in molecular weight due to hydrolysis could be another reason for the observed increase in miscibility. However, GPC results of samples annealed for 8, 32 and 128 mins. show a considerable increase in M_n compared to an as precipitated sample, Table 5.6. From the studies of Chapter 4, a decrease in molecular weight of PEMPT by at least a factor of 2 (easily identifiable by GPC) would be required to justify the observed improvement in miscibility. Combining these facts, one must conclude that the change in the phase behavior of the system with annealing time is due to reaction between blend components.

Proton NMR of the terephthalate and backbone methylene regions of DSC samples annealed 0, 4 and 8 min are shown in Figure 5.33a-c and 5.34a-c. From Figure 5.33, it is immediately apparent that the resonance associated with the terminal terephthalate ring, 8.065 ppm, is present in the sample annealed for 0 min, but it is replaced with a resonance (shoulder) at 8.095 ppm in the samples annealed for 4 and 8 min. This indicates alcoholysis exchange reaction has occurred and has occurred in a very short time in these mildly annealed samples. The methylene backbone region of the spectrum, Figure 5.34, confirms these results, with the disappearence of the 4.231 singlet and 3.423 multiplet (multiplet is barely visible in Figure 5.34a). The GPC results of Table 5.6 also confirm these results with a large jump in the M_n between the as precipitated sample and the sample annealed 8 mins. Once again this reflects the increase in the molecular size of the PEMPT chains as PC blocks are added to their ends.

Continuing to longer annealing times, Figure 5.35 shows the terephthalate region of the ^1H NMR spectra, at equal intensities, for samples annealed for 32, 64, and 128 min. The resonance at 8.095 ppm is increasing with increasing annealing time, corresponding to the formation of the quartad of Figure 4.20b. The sample annealed for 128 min also shows the faint appearence of the pair of doublets (8.255, 8.227, 8.121 and 8.150 ppm) previously associated with direct midchain transreaction. These results are confirmed by the increase in intesity of the methylene proton resonances, 4.239 and 4.191 ppm, of Figure 5.36. Comparing the DSC scans of Figure 5.32 to the ^1H NMR spectra of Figures 5.35 and 5.36, it is obvious that a very small amount of interchage reaction has lead to the transition from a two phase to a single phase blend.

Table 5.6 GPC Data of PEMPTB/PC2 Blends

Annealing Time @ 200°C (mins.)	M_n	M_w/M_n	M_z/M_w
0	20,300	2.10	1.61
8	38,000	2.25	1.55
32	40,200	2.26	1.55
128	35,300	2.28	1.73

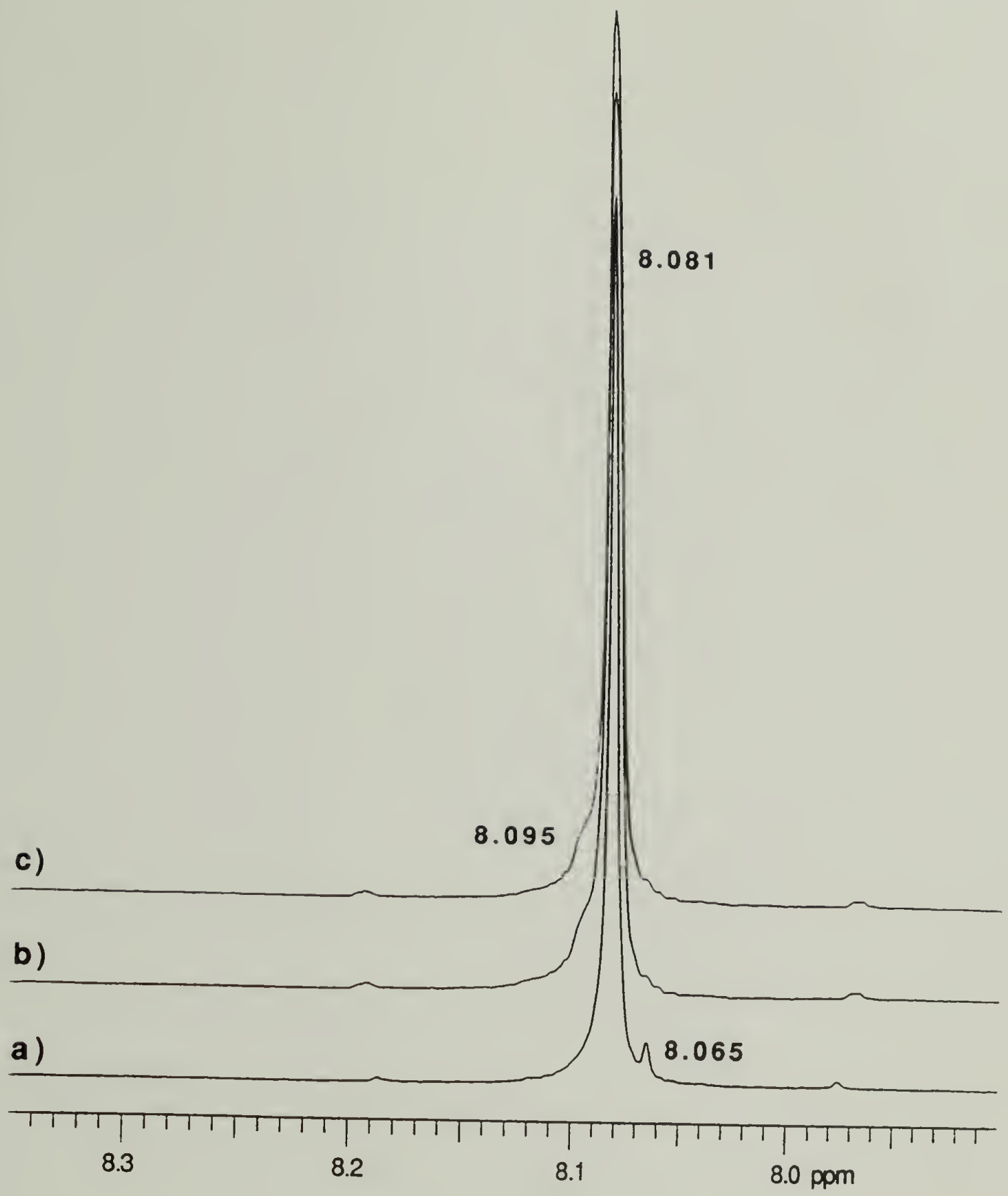

Figure 5.33 300 MHz ^{1}H NMR spectra displaying the terephthalate region of PEMPTB/PC2 blends annealed @ 200°C for a) 0 b) 4 c) 8 min.

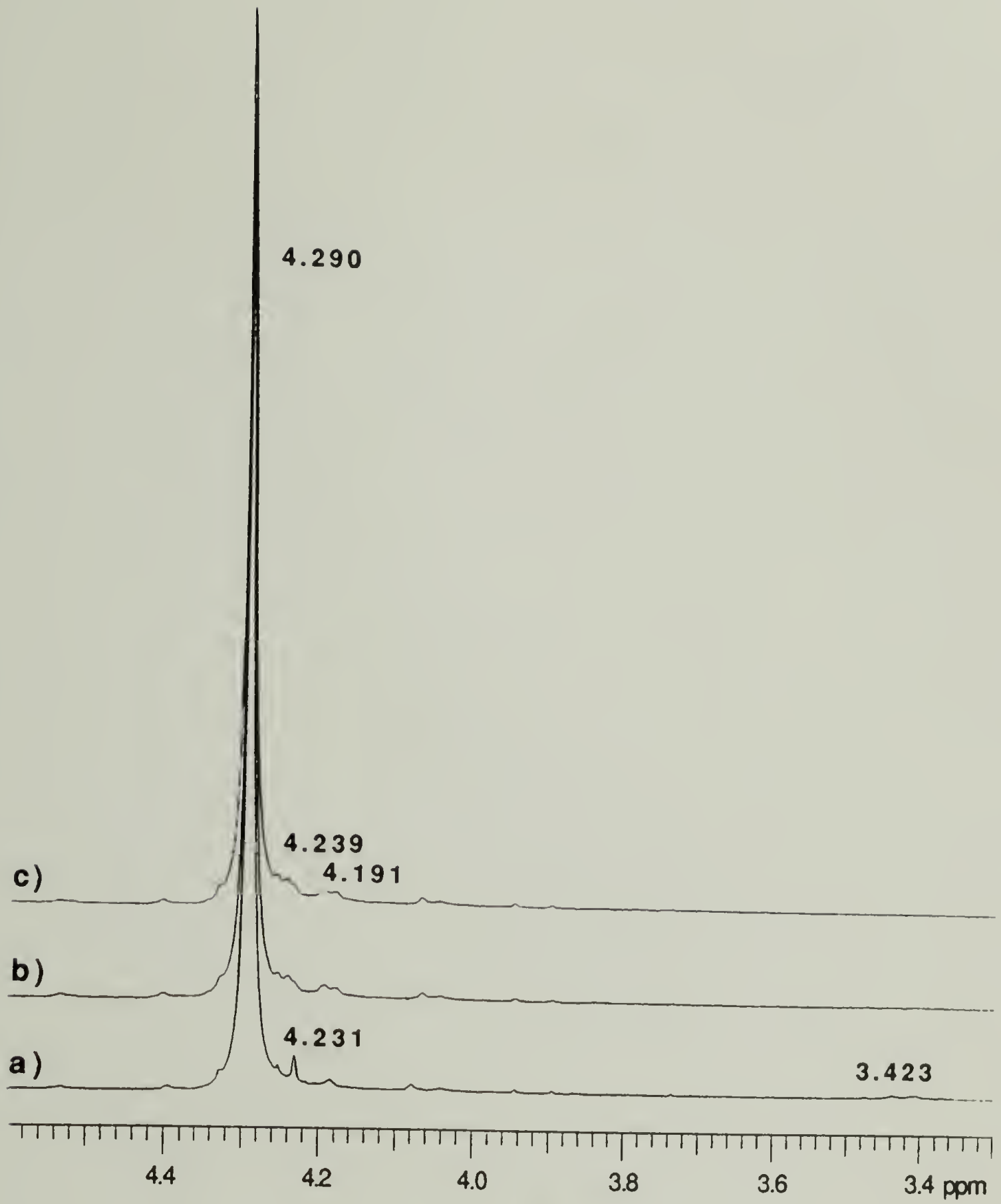

Figure 5.34 300 MHz ^{1}H NMR spectra displaying the methylene backbone region of PEMPTB/PC2 blends annealed @ 200°C for a) 0 b) 4 c) 8 min.

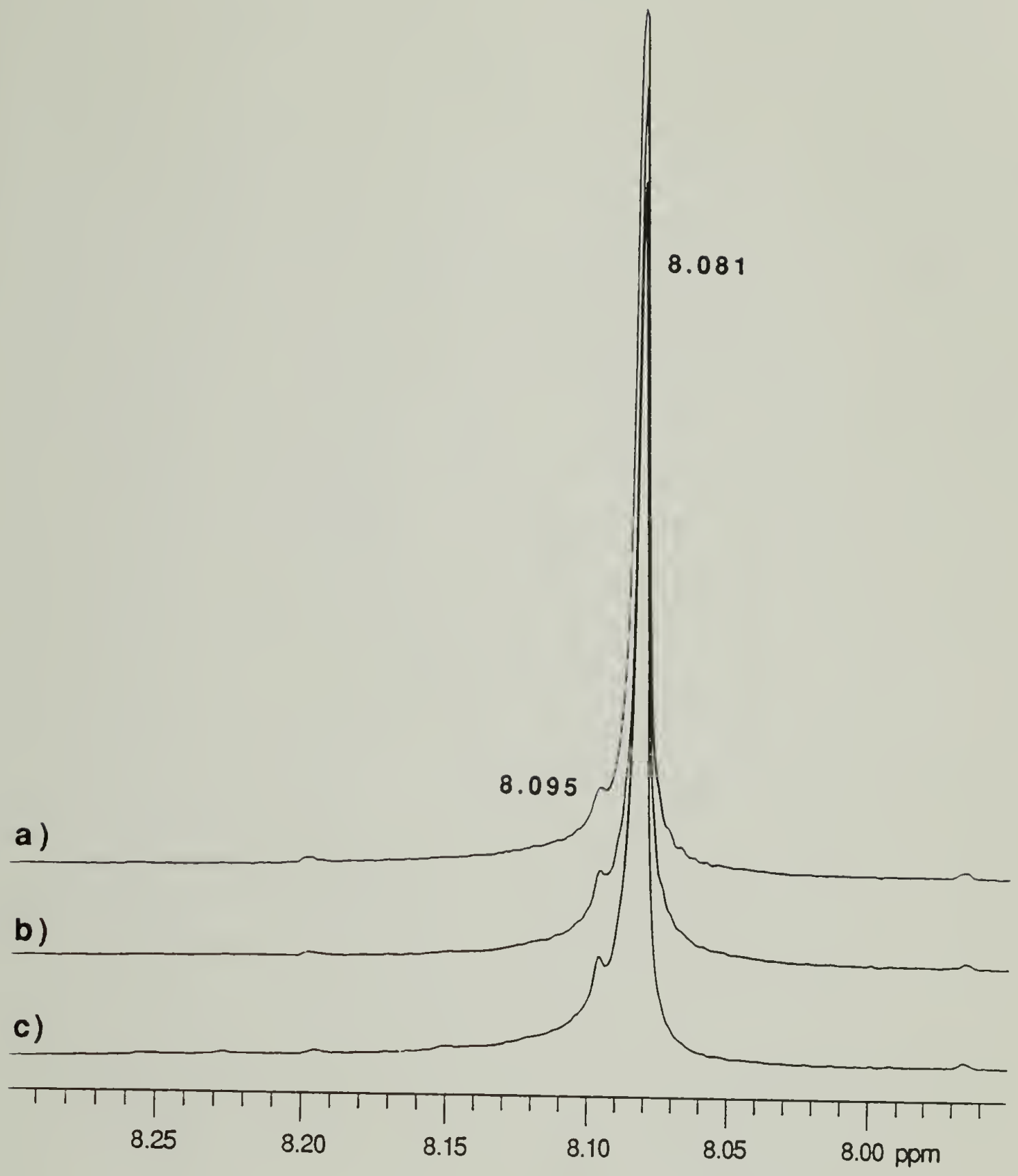

Figure 5.35 300 MHz ^{1}H NMR spectra displaying the terephthalate region of PEMPTB/PC2 blends annealed @ 200°C for a) 32 b) 64 c) 128 min.

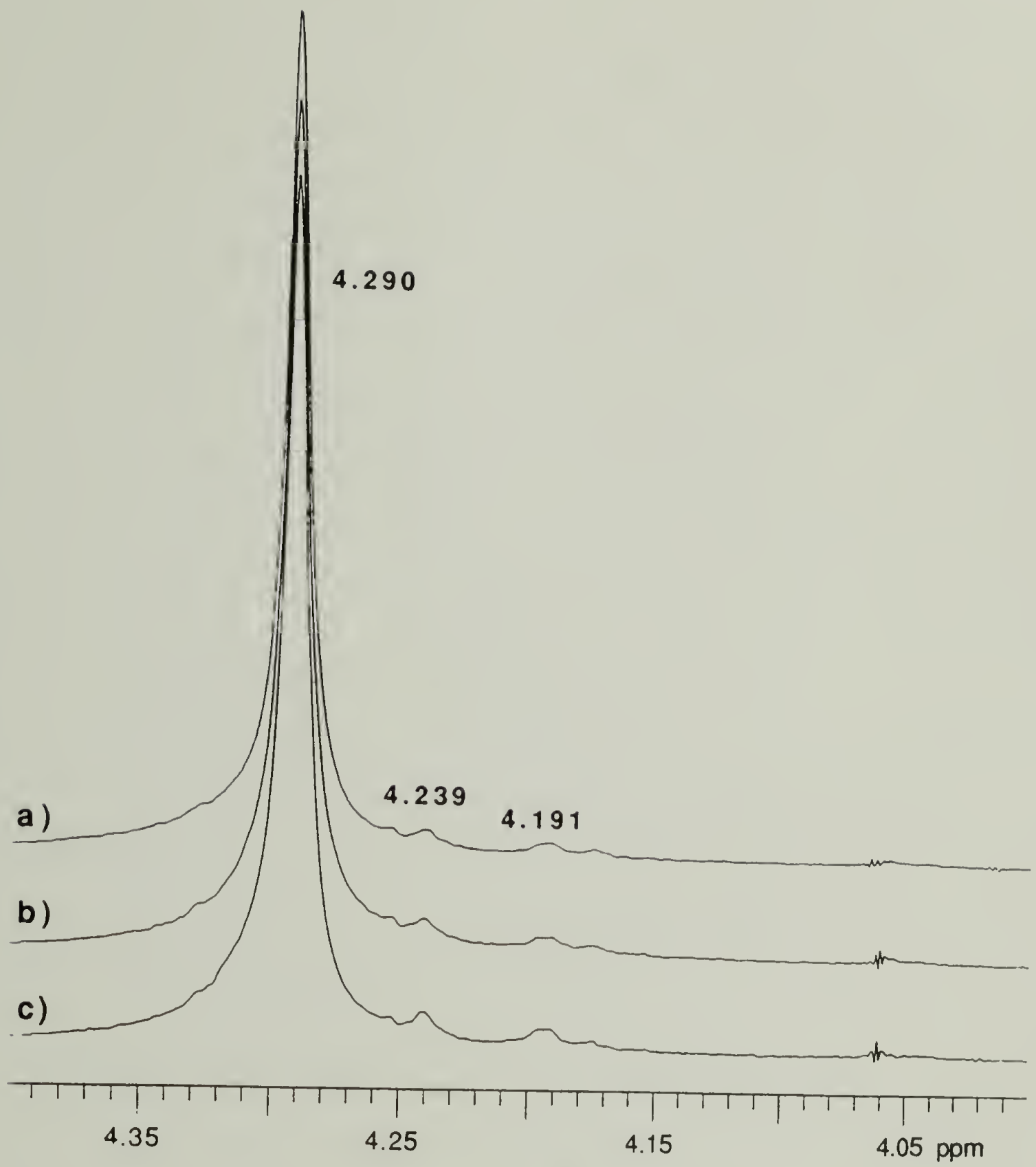

Figure 5.36 300 MHz ^{1}H NMR spectra displaying the methylene backbone region of a PEMPTB/PC2 blends annealed @ 200°C for a) 32 b) 64 c) 128 min.

A quantitative measure of the amount of interchange reaction leading to the phase transition can be made from the area ratios of the 8.095 and 8.081 and 4.239, 4.191 and 4.290 ppm resonances. From these ratios, it is determined that ~ 4% of the terephthalate groups have undergone transreaction. This value can be divided into the amount of alcoholysis and direct midchain exchange reaction. With all the hydroxyl groups having reacted, the percentage of terephthalate groups that reacted through alcoholysis can be determined from the number average molecular weight of the polyester. The M_n of PEMPTB is 17,700 gm/mole which corresponds to a DP of 71. The percentage of end groups in the polymer is 2.8, thus, ~ 2.8% of the interchange reactions are alcoholysis and 1.2 % correspond to direct midchain reaction. From a theoretical standpoint, it is not intuitively obvious that an extent of transreaction of 4% should cause the observed phase transition. Theoretical interpretation of these results is conducted employing the results of the phase behavior studies of Chapter 4 along with aspects of diblock copolymer phase behavior theory.

5.4.2.2 Interpretation of Phase Transition Data

The improvement in miscibility caused by interchange reaction is associated with two factors, the decrease in the molecular weight of the component polymers as transreaction occurs and the connectivity effect associated with the formation of block copolymers. With this as a basis, two approaches will be taken to analyze the above results.The first approach is to assume that transreaction only leads to a decrease in the molecular weight of the polyester. The decrease in the molecular weight of PC and the connectivity effects will be ignored. With this assumption, the phase behavior studies of Chapter 4 examining molecular weight effects can be used to determine the extent of interchange reaction required to cause the phase transition. From Table 4.5, the critical degree of polymerization of a PEMPT/PC2 blend is 17. This implies that if the molecular weight of the polyester is lowered from the original DP of 71 to a value of 17, a single phase blend will result. To lower the DP of PEMPTB from 71 to 17 would require 3-4 reactions per molecule (if the reactions are assumed to occur in the middle of the chain and the subsequent chain segments). This corresponds to ~ 4-6% interchange reaction. The molecular weight reduction of PC and the connectivity effects are both expected

to improve the blend miscibility, lowering this value. The fact that interchange reaction occurs randomly along the chains and not selectively in the middle, as assumed, is expected to raise this value.

The second approach used to interpret this data comes from the diblock copolymer theories developed over the past two decades[16-20,26-37]. From these theories, the dominant parameter used to correlate the microphase separation transition to physical characteristics of the polymer is (χN), where χ is the interaction parameter and N is the number average degree of polymerization of the block copolymer. In this approach, the transreacting blend will be treated as a ideal block copolymer. It is assumed that each chain has undergone one interchange reaction exactly in the middle of both molecules to produce a perfect diblock. Polydispersity effects will also be ignored. PEMPTB and PC2 have degrees of polymerization of 71 and 85, respectively. This leads to a block copolymer with a DP of 78. The interaction parameter of the PEMPT/PC blend was previously calculated to be 0.044. With these two values, (χN) for the model PEMPT/PC2 diblock is 3.4. For a given block composition, Leibler [17] has determined the values for the above product at the microphase separation transition point, $(\chi N)_s$. A block copolymer is predicted to be miscible if $(\chi N) < (\chi N)_s$. For the current model system, $(\chi N)_s$, is ~12 [17]. Thus, the model PEMPTB/PC block copolymer would be expected to form a single phase blend. This model diblock system was based on a single transraction per chain, corresponding to an extent of reaction of ~ 1.5%. Once again the assumption of interchange reaction occuring exactly in the middle of the chains is two restrictive. The exchange reaction will proceed randomly along the chains and this fact is expected to increase the level of reaction required to form a miscible blend over the value predicted here. Additionally, kinetic and diffusion factors are also expected to increase the extent of transreaction required for the phase transition.

Although the two interpretations given above represent an over simplified version of the transreacting blend, the analysis is useful in that it defines a range where the true value is expected to lie. The experimentally detemined value for extent of transreaction required to cause the phase transition, 4%, falls between the values calculated from these model systems, adding theoretical support to the experimental findings.

5.5 Conclusions

Alcoholysis interchange reaction was identifed by ^{1}H NMR in PEMPT-OH15/PC and PEMPT-OH2/PC blends. These blends contained DNOP as an inhibitor which adequately stopped direct midchain transreaction, but appeared to be unable to inhibit alcoholysis. Infrared spectroscopy and GPC results supported the NMR data. In the PEMPT-OH2/PC blends, the extent of interchange reaction was determined to be 100% regardless of blend composition or molecular weight. The hydroxyl groups of the PEMPT-OH15/PC blends exhibited only 16% reaction. Within experimental error, this value was constant at the blend compositions and molecular weights studied. Due to their varying extents of alcoholysis, the miscibility maps of the PEMPT-OH2/PC and PEMPT-OH15/PC blends were considerably different. The 100% reacted blends had a greater degree of interphase mixing compared to the 16% reacted blends. The improved miscibility was associated with the formation of a triblock/homopolymer (PC-PEMPT-PC/PC) blend. The miscibility maps of the PEMPT-OH-100%/PC1 and PEMPT-OH-16%/PC2 blends converged as DP of PEMPT decreased. The miscibility maps of the extrapolated PEMPT-OH-0%/PC1 and PEMPT-OH-0%/PC2 blends diverged as X_1 was lowered. The results on the PEMPT-OH-0%/PC blends follow the trends anticipated from entropic considerations. The deviations from this behavior exhibited by the PEMPT-OH-100%/PC blends was associated with the equalization of the M_ns of the two blends cause by the alcoholysis reactions.

^{1}H NMR and ^{1}H-^{1}H COSY spectroscopy of the transreacting blend revealed a wealth of information. ^{1}H NMR enabled identification of both alcoholysis and direct midchain transreaction independent of one another. Complete identification and assignmet of the observed resonances in the transreacting blend required examination of the two statistically most probable pentads. Analysis was simplified by reducing these pentads to the correspondng quartad and a triad. Using these structures as a guide, nearly all the resonances in the PEMPT terephthalate, PC aromatic and methylene backbone region of the spectras were assigned. Additionally separate resonances associated with direct midchain and alcoholysis transreactions were identified and assigned. Additional, COSY experiments were run to confirm AA'BB' spin system assignments. These spectra also proved useful in elucidating hidden resconances in the PC aromatic portion of the spectrum.

The COSY experiments proved that substitutions were occurring at the para position of the aromatic rings.

Quantitative studies relating transreaction to the observed phase behavior of the blend showed that transreaction of ~ 4% of the terephthalate groups was sufficient to cause the shift from two phase to single phase. This result was supported by theoretical predictions based on simplified models of the transreacting blend. The value of 4% corresponded to ~ 2.8% alcoholysis and 1.2% direct midchain transreaction. Additionally, it was observed that complete reaction of the hydroxyl end groups in PEMPT occured in 4 min or less in this non-DNOP stabilized blend. This result was confirmed by GPC which showed a jump in the molecular weight as the polyester was transformed to a triblock copolymer. Additionally no evidence of back alcoholysis reaction was observed in any of the blends examined. Overall, this study has shown that only a relatively small amount of interchange reaction is needed to shift the blend from two phase to single phase. Also, the formation of block copolymers at extremely short times via alcoholysis transreactions alters the blends molecular weight and distribution. These triblocks will likely alter other material properties, particularly those dependent on interfacial adhesion.

5.6 References

1. Devaux, J.; Godard, P.; Mercier, P. *J. Polym. Sci., Polym. Phys. Ed.* **1982**, 20, 1895.

2. Pilati, F.; Marianucci, E.; Berti, C. *J. Appl. Polym. Sci.* **1985**, 30, 1267.

3. Devaux, J.; Godard, P.; Mercier, P.; Touillaux, R.; Dereppe, J.M. *J. Polym. Sci., Polym. Phys. Ed.* **1982**, 20, 1881.

4. Devaux, J.; Godard, P.; Mercier, P. *J. Polym. Sci., Polym. Phys. Ed.* **1982**, 20, 1901.

5. Godard, P.; Dekoninck, J.M.; Devlesaver, V.; Devaux, J. *J. Polym. Sci., Polym. Chem.* **1986**, 24, 3301.

6. Godard, P.; Dekoninck, J.M.; Devlesaver, V.; Devaux, J. *J. Polym. Sci., Polym. Chem.* **1986**, 24, 3315.

7. Velden, G.v.d, Kolfschoten-Smitsmans, G.; Veermans, A. *Polym. Commun.* **1987**, 28, 169.

8. Henrichs, P.M.; Tribone, J.; Massa, D.J.; Hewitt, J.M. *Macromolecules* **1988**, 21, 1282.

9. Li, H.M; Wong, A.H. *MMI Press Symp., Ser. 2* **1982**, 395.

10. Murano, M; Yamadera, R. *Polymer J.* **1971**, 2, 8.

11. Valero, M.; Iruin, J.J.; Espinosa, E.; Fernandez-Berridi, M.J. *Polym. Commun.* **1990**, 31, 127.

12. Gouinlock, E.V.; Wolfe, R.A.; Rosenfeld, J.C *J. Appl. Polym. Sci.* **1976**, 20, 949.

13. Yamadera, R.; Murano, M. *J. Polym. Sci.: A-1* **1967**, 5, 2259.

14. Ritchie, P.D. *J. Chem. Soc.* **1935**, 1054.

15. Devaux, J.; Godard, P.; Mercier, J.P. *Polym. Eng. Sci.* **1982**, 22, 229.

16. Helfand, E. *Polymer Interfaces* **1975**, 8, 295.

17. Leibler, L., *Macromolecules* **1980**, 13, 1602.

18. Olvera De La Cruz, M.; Sanchez, I.C. *Macromolecules* **1987**, 20, 440.

19. Mayes, A.M.; Olvera De La Cruz, M. *J. Chem. Phys.* **1989**, 91(11), 7228.

20. Kinning, D.J. Ph.D. Thesis, University of Massachusetts at Amherst, 1986.

21. Pilati, F.; Manaresi, P.; Fortunato, B.; Munari, A.; Passalacqua, V., *Polymer* **1981**, 22, 799.

22. Devaux, J.; Godard, P.; Mercier, P. *J. Polym. Sci., Polym. Phys. Ed.* **1982**, 20, 1875.

23. Martin, J. and Dailey, B.P. *J. Chem. Phys.* **1962**, 37(11), 2594.

24. Bovey, F.A.; Jelinski, L; and Mirau, P.A. *Nuclear Magnetic Resonance Spectroscopy*; Academic Press, Inc.: San Diego, California, 1988.

25. Judas, D.; Fradet, A.; Marechal, E. *Makromol Chem.* **1983**, 184, 1129.

26. Helfand, E; Wasserman, Z.R. *Macromolecuels* **1976**, 9, 879.

27. Helfand, E.; Wasserman, Z.R. *Polym. Eng. Sci.* **1977**, 17, 582.

28. Helfand, E.; Wasserman, Z.R. *Macromolecules* **1978**, 11, 960.

29. Leibler, L.; Benoit, H. *Polymer* **1981**, 22, 195.

30. Leibller, L.; Orland, H.; Wheeler, J.C. *J. Chem. Phys.* **1983**, 79, 3550.

31. Whitmore, M.D.; Noolandi, J. *Polym. Eng. Sci.* **1985**, 25, 1120.

32. Hong, K.M.; Noolandi, J. *Polym. Commun.* **1984**, 25, 265.

33. Whitmore, M.D.; Noolandi, J. *Macromolecules* **1985**, 18, 657.

34. Whitmore, M.D.; Noolandi, J. *Macromolecules* **1985**, 18, 2486.

35. Whitmore, M.D.; Noolandi, J. *Polym. Commun.* **1985**, 26, 267.

36. Tanaka, H; Hashimoto, T. *Polym. Commun.* **1988**, 29, 212.

37. Shull, K.R.; Kramer, E.J. *Macromolecules* **1990**, 23, 4769.

CHAPTER 6

CONCLUSIONS AND FUTURE WORK

6.1 Conclusions

Shifts in the phase behavior of a model polyester/bisphenol-A-polycarbonate blend have been quantitatively correlated to the extent of interchange reaction. The extent of reaction required to cause the shift from two phase to single phase is ~ 4% (4% of the terephthalate groups previously belonging to a midchain group or end group in PEMPT now belong to the $A_1B_1A_2B_2$ quartad). The reaction extent can be divided between alcoholysis and direct midchain transreaction which corresponded to 2.8 and 1.2%, respectively. These results were in agreement with calculations based on simplified models of the transreacting blends. Although no detailed kinetic studies were conducted, the rate of alcoholysis exchange reaction was much greater than that of direct midchain reaction in a non-stabilized PEMPTB/PC2 blend. Complete alcoholysis occurred rapidly, within 4 min @ 200°C. In this same blend, 2 h. of annealing @ 200°C resulted in only 1.2% midchain reaction. This information implies that the mechanism of alcoholysis most likely follows a different scheme than that of direct midchain reaction. Alcoholysis perhaps being catalyzed by the small concentration of acid end groups present.

In DNOP stabilized blends, no evidence of direct midchain reaction was observed. However, alcoholysis transreaction still occurred in these blends. PEMPT/PC blends prepared with PEMPT samples recovered by slightly different precipitation procedures exhibited considerably different extents of alcoholysis following identical thermal treatments. GPC showed these polyesters to have nearly identical M_ns and distributions, thus, this was not the cause of the discrepancy. At this time, the cause for the differences are not known. Alcoholysis leads to the formation of diblock and triblock copolymers which also cause a shift in the observe phase behavior. At the two lowest molecular weight PEMPTs studied, complete alcoholysis lead to the formation of single phase blends in PEMPT1-OH15/PC2, PEMPT2-OH15/PC2 and PEMPT2-OH15/PC1 blends. The phase behavior of these

triblock/homopolymer blends were relatively insensitive to the PC molecular weight. Estimates of the molecular weights of the blends after reaction indicate that the component M_ns of blends containing PC1 and PC2 became more identical as the amount of alcoholysis reaction increased, promoting similar phase behavior. Additionally, no evidence of back reaction, i.e., alcoholysis of PEMPT by PC was observed in any of the blends studied.

The selection of the model polyester, PEMPT, has allowed detailed spectroscopic studies to be carried out on PEMPT and the transreacting PEMPT/PC blends. Spectroscopic studies of PEMPT have identify all the expected midchain resonances, as well as, additional resonances associated with the chain ends. Based on these results, a complete ^1H NMR spectroscopic study of the transreacting blend required analysis of pentads. However, at low levels of interchange reaction, the two statistically most probable pentads were a good representation of the blend. Under these conditions, the corresponding quartad and triad of these two pentads adequately represented the transreacting blend. Nearly all the new proton resonances observed in the PEMPT aromatic, PC aromatic and PEMPT methylene backbone region of the spectrum were assigned to the quartad and triad structures. Confirmation of para substitution of both the PEMPT and PC aromatic rings and the identification of obscured resonances in the aromatic PC region of the ^1H NMR spectra were achieved with ^1H-^1H COSY experiments.

The equilibrium phase behavior of PEMPT/PC blends was studied as a function of composition, varying component molecular weights, and end group type. Compositional effects were apparent in the PC rich phase with the level of intermixing of PEMPT in the PC phase decreasing with decreasing PEMPT/PC ratio. In general, the phase behavior of all PEMPT-OH15/PC blends followed similar trends with respect to varying component molecular weights, independent of composition. For blends with hydroxyl or benzylate PEMPT end groups, molecular weight effects followed the general characteristics of F-H theory. Hydrogen bonding in the PEMPT/PC blends did not significantly alter blend phase behavior until PEMPT M_ns of less than ~ 7,500 were reached. Blends containing hyptafluorobutyrate end groups did not follow the molecular weight functionality of F-H theory. The phase behavior was altered considerably compared to PEMPTs with OH and BNZ ends, with little or no improvement in intermixing as the M_n of PEMPT in the blend was lowered. These results were shown to be in agreement with a two component interaction

parameter model. Critical point data was in good agreement with theoretical values. The interaction parameter, calculated from critical point data, was 0.044.

The model polyester, PEMPT, was conveniently synthesized using standard two stage polycondensation techniques with titanium (IV) isopropoxide as catalyst. PEMPT is amorphous with improved thermal stability and solubility compared to other linear aliphatic-aromatic polyesters. These properties facilitated the characterization of PEMPT, as well as, preparation, characterization and analysis of PEMPT/PC blends. End group modification was carried out using a nucleophillic substitution reaction of the appropriate acid chlorides. Molecular weights of PEMPT were determined by weight analysis fluorine of HFB end capped PEMPTs. This procedure should be applicable to other polyesters or polymers capable of reacting by this mechanism.

6.2 Future Work

With the identification of proton NMR resonances corresponding to the end groups of PEMPT, it is now possible to follow alcoholysis and direct midchain reaction separately. This fact alone should open the door to new research in this area. Specifically, kinetic studies examining the role of various catalyst systems on alcoholysis reactions relative to direct interchange reaction could be studied. The role of acid end groups on the rate of alcoholysis could also be studied by the addition of catalytic amounts of acid to the blend or by preparing PEMPTs with acid end groups and blending them with hydroxyl terminated PEMPTs. The role of stabilizing agents relative to alcoholysis transreaction is also an area needing future investigation. The current studies revealed large differences in the extent of alcoholysis transreaction between blends composed of PEMPTs recovered from a 2% and 15% solutions. The amount of Ti catalyst remaining in the blends may have varied due to this fact. However, these blends also contained a large amount of DNOP stabilizing agent to inhibit this catalyst. The complex relationships between the inhibitor and the catalyst relative to alcoholysis is not known.

The formation of the triblock/homopolymer blends due to complete alcoholysis was shown to modify the blend phase behavior. However, the importance of this fact is not only manifested in the observed changes in phase behavior, but perhaps more importantly in the mechanical properties of the

blend. The compatibilizing effect of the triblock copolymers will improve the interfacial properties of the blend and lead to changes in mechanical properties that are sensitive to interfacial phenomena. Variation in the mechanical properties as a function of extent of alcoholysis and extent of direct midchain reaction seems to be an appropriate extension of the present work.

In the present study, two amorphous polymers were the focus. Future studies could quantitatively examine the relationship between crystallinity and transreaction. In the screening study (Chapter 2), PPT, PHT and PNT were all shown to crystallize when quenched from the melt. These polyesters all are more readily soluble compared to PET and PBT, which would facilitate studies on these polymers. In addition, the detailed spectroscopic analysis of the PEMPT/PC blends should enable quick identification of resonances corresponding to interchange reaction in blends of these polyesters with PC. Anyone of these polyesters blended with PC should provide a model semi-crystalline/amorphous blend for investigation.

The transreaction studies presented here were all conducted on PEMPTs with hydroxyl end groups. The role of end group type on the rate of transreaction is another possible extension of this work. In particular, studies on PEMPT-BNZ/PC blends would be an excellent way to study the individual role of direct midchain reaction on blend phase behavior and exhibited mechanical properties. Later this could be compared to a hydroxyl terminated PEMPT/PC blend where end groups are capable of reaction.

Additional studies on phase behavior modifications due to interchange reaction could be conducted on blends containing PEMPT and another polymer capable of interchange reaction. Some initial studies were carried out on PEMPT/PAr blends. This system appears to be another excellent model blend system. The complexity of the aromatic region of PAr does make the spectroscopic characterization more complicated. However, the aromatic region corresponding to the terephthalate group in PEMPT is relatively clear of other aromatic resonances, allowing a measure of the extent of interchange reaction.

BIBLIOGRAPHY

Addleman, R.L.; Zichy, V.J.I. "Accurate Measurement of Carboxyl and Hydroxyl End-Group Concentrations in Poly(ethylene terephthalate) Film by Infrared Spectroscopy", *Polymer* **1972**, 13, 391-398.

Allan, R.J.; Iengar, H.V.R.; Ritchie, P.D. "Studies in Pyrolysis IX. The Pyrolysis of the Model Systems 2-Benzoyloxyethyl and 2-p-Chlorobenzoyloxyethyl Terephthalate, and Poly(ethylene terephthalate)", *J. Chem. Soc.* **1957**, 2107-2113.

Billmeyer Jr., F.W. *Textbook of Polymer Science*; Wiley-Interscience, New York, 1971.

Birley, A.W.; Chen, X.Y. " Further Studies of Polycarbonate-Poly(butylene terephthalate) Blends", *Br. Polym. J.* **1985**, 17, 297-305.

Birley, A.W.; Chen, X.Y. "Studies of Polycarbonate-Poly(butylene terephthalate) Blends", *Br. Polym. J.* **1984**, 16, 77-82.

Boreman, W.F.H. "Molecular Weight-Viscosity Relationships for Poly(1,4-butylene terephthalate)", *J. Appl. Polym. Sci.* **1978**, 22, 2119-2126.

Bovey, F.A.; Jelinski, L; and Mirau, P.A. *Nuclear Magnetic Resonance Spectroscopy*; Academic Press, Inc.: San Diego, California, 1988.

Bovey, F.A.; Winslow, F.H., Eds. *Macromolecules, An Introduction to Polymer Science*, Academic Press; New York, 1979.

Carduner, K.R.; Carter III, R.O.; Cheung, M.-F.; Golovoy, A. "Studies on the Role of Organophosphites in Polyester Blends: I. ^{31}P Nuclear Magnetic Resonance Spectroscopy", *J. Appl. Polym. Sci.* **1990**, 40, 963-975.

Challa, G. "The Formation of Polyethylene Terephthalate by Ester Interchange I. The Polycondensation Equilibrium", *Makromol. Chem.* **1960**, 38, 105-122.

Chen, M.S.; Chang, S.J.; Chang, R.S.; Kuo, W.F.; Tsai, H.B. "Copolyester. I. Sequence Distribution of Poly(Butylene Terephthalate-co-Adipate) Copolyesters Determined by 400 MHz NMR", *J. Appl. Polym. Sci.* **1990**, 40, 1053-1057.

Cheung, M.-F.; Carduner, K.R.; Golovoy, A.; Van Oene, H. "Studies on the Role of Organophosphites in Polyester Blends: II. The Inhibition of Ester Exchange Reactions", *J. Appl. Polym. Sci.* **1990**, 40, 977-987.

Coleman, M.; Painter, P.C. "Fourier Transform Infrared Spectroscopy: Probing the Structure of Multicomponent Blends", *Appl. Spectr. Rev.* **1984**, 20, 255-346.

Couchman, P.R. "Compositional Variations of the Glass-Transition Temperatures. 2. Application of the Thermodynamic Theory to Compatible Polymer Blends", *Macromolecules* **1978**, 11, 1156-1161.

Delimoy, D.; Bailly, C.; Devaux, J.; Legras, R. "Morphological Studies of Polycarbonate-Poly(butylene terephthalate) Blends by Transmission Electron Microscopy", *Polym. Eng. Sci.* **1988**, 28, 104-112.

Devaux, J.; Godard, P.; Mercier, J.P. "The Transesterification of Bisphenol-A-Polycarbonate (PC) and Polybutylene Terephthalate (PBTP): A New Route to Block Copolycondensates", *Polym. Eng. Sci.* **1982**, 22, 229-233.

Devaux, J.; Godard, P.; Mercier, P. "Bisphenol-A-Polycarbonate-Poly(butylene terephthalate) Transesterification. I. Theoretical Study of the Structure and of the Degree of Randomness in Four-Component Copolyesters", *J. Polym. Sci., Polym. Phys. Ed.* **1982**, 20, 1875-1880.

Devaux, J.; Godard, P.; Mercier, P. "Bisphenol-A-Polycarbonate-Poly(butylene terephthalate) Transesterification. III. Study of Model Reactions", *J. Polym. Sci., Polym. Phys. Ed.* **1982**, 20, 1895-1900.

Devaux, J.; Godard, P.; Mercier, P. "Bisphenol-A-Polycarbonate-Poly(butylene terephthalate) Transesterification. IV. "Kinetics and Mechanism of the Exchange Reaction", *J. Polym. Sci., Polym. Phys. Ed.* **1982**, 20, 1901-1907.

Devaux, J.; Godard, P.; Mercier, P.; Touillaux, R.; Dereppe, J.M. "Bisphenol-A-Polycarbonate-Poly(butylene terephtalate) Transesterification. II. Structure and Analysis of the Reaction Products by IR and ^{1}H and ^{13}C NMR", *J. Polym. Sci., Polym. Phys. Ed.* **1982**, 20, 1881-1894 .

Droscher, M.; Wagner, G. "Poly(ethylene terephthalate): a Solid State Condensation Process", *Polymer* **1978**, 19, 43-47.

Edgerton, H.E "Electrode for Sensing Fluoride Ion Activity in Solution", *Science* **1966**, 154, 1553-1555.

Fagerburg, D.R. "Synthesis and Some Properties of a Series of Polyterephthalates Having Side-Chain Branching", *J. Appl. Polym. Sci.* **1985**, 30, 889-896.

Flory, P.J. *Principles of Polymer Chemistry*; Cornell University Press: Ithica, 1953.

Flory, P.J. "The Thermodynamics of High Polymer Solutions", *J. Chem. Phys.* **1941**, 9, 660-661.

Flory, P.J. "Thermodynamics of Heterogenous Polymers and Their Solutions", *J. Chem. Phys.* **1944**, 12, 425-438.

Flory, P.J. "Thermodynamics of High Polymer Solutions", *J. Chem. Phys.* **1942**,10, 51-61.

Fontana, C.M. "Polycondensation Equilibrium and the Kinetics of the Catalyzed Transesterification in the Formation of Polyethylene Terephthalate", *J. Polym. Sci.: A-1* **1968**, 6, 2343-2358.

Fortunato, B.; Pilati, F.; Manaresi, P. "Solid State Polycondensation of Poly(butylene terephthalate)", *Polymer* **1981**, 22 655-657.

Fox Jr., T.G.; Flory, P.J. "Second Order Transition Temperatures and Related Properties of Polystyrene. I. Influence of Molecular Weight", *J. Appl. Phys.* **1950**, 21, 581-591.

Fox Jr., T.G.; Flory, P.J. "The Glass Transition and Related Properties of Polystyrene. Influence of Molecular Weight", *J. Polym. Sci.* **1954**, 14, 315-319.

Freitag, D.; Grigo, U.; Muller, P.R.; Nouvertne, W. *Encyclopedia of Polymer Science and Engineering, Vol. 11, Second Ed.*; Wiley, New York, 1988.

Gardon, J.L. "The Influence of Polarity Upon the Solubility Parameter Concept", *J. Paint Technol.* **1966**, 38, 43-57.

Gibbs, J.W. *The Collected Works, Vol. I. Thermodynamics*; Yale University Press Reprint: New Haven, 1957.

Godard, P.; Dekoninck, J.M.; Devlesaver, V.; Devaux, J. "Molten Bisphenol A Polycarbonate-Poly(ethylene terephthalate) Blends. II. Kinetics of the Exchange Reaction", *J. Polym. Sci., Polym. Chem.* **1986**, 24, 3315-3324.

Godard, P.; Dekoninck, J.M.; Devlesaver, V.; Devaux, J. "Molten Bisphenol-A Polycarbonate-Poly(Ethylene Terephthalate) Blends. I. Identification of the Reactions", *J. Polym. Sci., Polym. Chem.* **1986**, 24, 3301-3314.

Golovoy, A.; Cheung, M.-F.; Carduner, K.R.; Rokosz, M.J. "Control of Transesterification in Polyester Blends", *Polym. Eng. Sci.* **1989**, 29, 1226-1231.

Golovoy, A.; Cheung, M.-F.; Van Oene, H. "The Phase Behavior and Mechanical Properties of Polyarylate and Polycarbonate Blends", *Polym. Eng. Sci.* **1987**, 27, 1642-1648.

Goodman, I. in *The Encyclopedia of Polymer Science and Engineering, Vol. 12, 2nd Ed.*; Wiley: New York,1988.

Gouinlock, E.V.; Wolfe, R.A.; Rosenfeld, J.C "Copolyester Sequence Distribution by 60, 100, and 220 MHz NMR", *J. Appl. Polym. Sci.* **1976**, 20, 949-958.

Hanrahan, B.D.; Angeli, S.R.; Runt, J. "Miscibility and Melting in Poly(butylene terephthalate/Poly(Bisphenol A-Carbonate) Blends" *Polym. Bull.* **1985**, 14, 399-406.

Hanrahan, B.D.; Angeli, S.R.; Runt, J. "Miscibility and Melting in Poly(ethylene terephthalate)/Polycarbonate Blends", *Polym. Bull.* **1986**, 15, 455-463.

Helfand, E. "Block Copolymers, Polymer-Polymer Interfaces, and the Theory of Inhomogeneous Polymers", *Polymer Interfaces* **1975**, 8, 295-299.

Helfand, E.; Wasserman, Z.R. "Block Copolymer Theory. 5. Spherical Domains", *Macromolecules* **1978**, 11, 960-966.

Helfand, E.; Wasserman, Z.R. "Statistical Thermodynamics of Microdomain Structures in Block Copolymer Systems", *Polym. Eng. Sci.* **1977**, 17, 582-586.

Helfand, E; Wasserman, Z.R. "Block Coplymer Theory. 4. Narrow Interphase Approximation", *Macromolecuels* **1976**, 9, 879-888.

Henrichs, P.M.; Tribone, J.; Massa, D.J.; Hewitt, J.M "Blend Miscibility of Bisphenol A Polycarbonate and Poly(ethylene terephthalate) As Studied by High-Resolution ^{13}C NMR Spectroscopy", *Macromolecules* **1988**, 21, 1282-1291.

Hildebrand, J.H.; Scott, R.L. *Regular Solutions*; Prentice-Hall, Inc.: New Jersey, 1962.

Hildebrand, J.H.; Scott, R.L. *The Solubility of Nonelectrolytes*; Reinhold: 1950.

Hobbs, S.Y.; Dekkers, M.E.J.; Watkins, V.H. "Effect of Interfacial Forces on Polymer Blend Morphologies", *Polymer* **1988**, 29, 1598-1602.

Hobbs, S.Y.; Dekkers, M.E.J.; Watkins, V.H. "Toughened Blends of Poly(butylene terephthalate) and BPA Polycarbonate", *J. Mat. Sci.* **1988**, 23, 1219-1224.

Hobbs, S.Y.; Groshans, V.L.; Dekkers, M.E.J.; Shultz, A.R. "Partial Miscibility of Poly(Butylene Terephthalate)/BPA Polycarbonate Blends", *Polym. Bull.* **1987**, 17, 335-339.

Hobbs, S.Y.; Watkins, V.H.; Bendler, J.T. "Diffusion Bonding between BPA Polycarbonate and Poly(butylene terephthalate)", *Polymer* **1990**, 31, 1663-1668.

Hong, K.M.; Noolandi, J. "The Effect of Polydispersities on the Microphase Separation of a Block opolymer System", *Polym. Commun.* **1984**, 25, 265-268.

Hovenkamp, S.G. "Kinetic Aspects of Catalyzed Reactions in the Formation of Poly(ethylene terephthalate)", J. *Polym. Sci.: A-1* **1971**, 9, 3617-3625.

Huang, Z.H.; Wang L.H. "Infrared Studies of Transreaction in Poly(ethylene terephthalate)/Polycarbonate Blends", *Makromol. Chem., Rapid Commun.* **1986**, 7, 255-259.

Huggins, M.L. "Solutions of Long Chain Compounds", *J. Chem. Phys.* **1941**, 9, 440.

Huggins, M.L. "Some Properties of Solutions of Long Chain Compounds", J. *Phys. Chem.* **1944**, 46, 151-158.

Hurd, C.D.; Blunk, F.H. "The Pyrolysis of Esters", *J. Amer. Chem Soc.* **1938**, 60, 419-2425.

Iengar, H.V.R.; Ritchie, P.D. "Studies in Pyrolysis VII. Model Systems for the Pyrolysis of Poly(ethylene terephthalate): 2:2'-Dibenzoyloxydiethyl Ether, 2-Benzoyloxyethyl Vinyl Ether, and Certain related Vinyl Ethers", *J. Chem. Soc.* **1956**, 3563-3570.

Jonza, J.M."Bisphenol-A-Polycarbonate/Polycaprolactone Blends", Ph. D. Dissertation, University of Massachusetts, 1985.

Judas, D.; Fradet, A.; Marechal, E. "Characterization of Polyesters Resulting from 1,2-Propanediol and Phthalic Anhydride and Their Model Compounds by ^{1}H and ^{13}C NMR Spectroscopy", *Makromol Chem.* **1983**, 184, 1129-1142.

Kennedy, J.W.; Gordon, M.; Koningsveld, R. "Generalization of the Flory Huggins Treatment of Polymer Solutions", *J. Polym. Sci.: Part C* **1972**, 39, 43-69.

Kim, W.N.; Burns, C.M. "Compatibility Studies of Blends of Polycarbonate and Poly(ethylene terephthalate)", *J. Polym. Sci., Polym. Phys.* **1990**, 28, 1409-1429.

Kim, W.N.; Burns, C.M. "Thermal Behavior, Morphology and the Determination of the Polymer-Polymer Interaction Parameter of Polycarbonate Poly(butylene terephthalate) Blends", *Makromol. Chem.* **1989**, 190, 661-676.

Kimura, M.; Porter, R.S. "Blends of Poly(butylene terephthalate) and a Polyarylate Before and After Transesterification", *J. Polym. Sci., Polym. Phys. Ed.* **1983**, 21, 367-378.

Kimura, M.; Porter, R.S. in *Analytical Calorimetry*; edited by P. Gill and J.F. Johnson, Plenum Press: New York, 1984.

Kimura, M.; Salee, G.; Porter, R.S. "Blends of Poly(ethylene terephthalate) and a Polyarylate Before and After Transesterification", J. *Appl. Polym. Sci.* **1984**, 29, 1629-1638.

Kinning, D.J. "Micelle Formation in Block Copolymer/Homopolymer Blends", Ph.D. Thesis, University of Massachusetts at Amherst, 1986.

Koningsveld, R.; Chermin, H.A.G.; Gordon, M. "Liquid-Liquid Phase Separation in Multicomponent Polymer Solutions VIII. Stability Limits and Consolute States in Quasi-Ternary Mixtures", *Proc. Roy. Soc. Lond.* **1970**, A319, 331-349.

Koningsveld, R.; Kleintjens, L.A.; Schoffeleers, H.M. "Thermodynamic Aspects of Polymer Compatibility", *Pure Appl. Chem.* **1974**, 39,1-32.

Kotliar, A.M. "Interchange Reactions Involving Condensation Polymers", *J. Polym. Sci., Macromol. Rev.* **1981**, 16, 367-395.

Kurashiki Rayon Kabushiki Kaisha, "Method of Manufacturing Stable Block Copolyesters and Polyester Mixtures" Japanese Patent 1,060,401.

Leibler, L. "Theory of Microphase Separation in Block Copolymers", *Macromolecules* **1980**, 13, 1602-1617.

Leibler, L.; Benoit, H. "Theory of Correlations in Partially Labelled Homopolymer Melts", *Polymer* **1981**, 22, 195-201.

Leibller, L.; Orland, H.; Wheeler, J.C. "Theory of Critical Micelle Concentration for Solutions of Block Copolymers", *J. Chem. Phys.* **1983**, 79, 3550-3557.

Li, H.M; Wong, A.H. "Characterization of Extruded Films Based on Blends of Poly(ethylene terephthalate) and Poly(tetramethylene terephthalate)", *MMI Press Symp., Ser. 2* **1982**, 395-411.

Macdonald, A.M.G. "The Microdetermination of Fluorine in Organic Compounds", *Org. Microchem. Appl.* **1971**, 8, 12-13.

Martin, J. and Dailey, B.P. "Proton NMR Spectra of Disubstituted Benzenes", *J. Chem. Phys.* **1962**, 37(11), 2594-2602.

Mayes, A.M.; Olvera De La Cruz, M. "Microphase Separation in Multiblock Copolymer Melts", *J. Chem. Phys.* **1989**, 91(11), 7228-7235 .

Mondragon, I. "Control of Interchange Reactions of Polycarbonate/Polyarylate Blends and Their Influence on Physical Behavior", *J. Appl. Polym. Sci.* **1986**, 32, 6191-6207.

Murano, M.; Yamadera, R. "Kinetic Studies on the Transesterification Reactions Between Poly(Ethylene Terephthalate) and Poly(Ethylene Sebacate), *Polymer J.* **1971**, 2, 8-12.

Murff, S.R.; Barlow, J.W.; Paul, D.R. "Thermal Mechanical Behavior of Polycarbonate-Poly(ethylene terephthalate) Blends", *J. Appl. Polym. Sci.* **1984**, 29, 3231-3240.

Nassar, T.R.; Paul, D.R,; Barlow, J.W. "Polyester-Polycarbonate Blends. II. Poly(ethylene terephthalate)", *J. Appl. Polym. Sci.* **1979**, 23, 85-99.

O'Connor, G.L; Nace, H.R. "Chemical and Kinetic studies on the Chugaev Reaction", *J. Amer. Chem Soc.* **1952**, 74, 5454-5459.

O'Connor, G.L; Nace, H.R. "Further Studies on the Chugaev Reaction and Related Reactions", *J. Amer. Chem Soc.* **1953**, 75, 2118-2123.

Odian, G. *Principles of Polymerization*; Wiley-Interscience, New York, 1981.

Olabisi, O.; Robeson, L.M.; Shaw, M.T. *Polymer-Polymer Miscibility*; Academic Press: New York, 1979.

Olvera De La Cruz, M.; Sanchez, I.C., "Microphase Separation in Block Copolymer/Homopolymer Blends", *Macromolecules* **1987**, 20, 440-443.

Passalacqua, V.; Pilati, F.; Zamboni, V.; Fortunato, B.; Manaresi,P. "Thermal Degradation of poly(butylene terephthalate)", *Polymer* **1976**, 17, 1044-1048.

Paul, D.R. *Polymer Blends*; Paul, D.R.; Newman, S. Eds., Academic Press: New York, 1978.

Pavel, J.; Kuebler, R.; Wagner, H. "Microdetermination of Fluorine in Organic Compounds by Direct Measurement with a Fluoride Electrode", *Microchem. J.* **1970**, 15, 192-198.

Peebles, L.H.; Wagner, W.S. "The Kinetic Analysis of a Distilling System and Its Application to Preliminary Data on the Transesterification of Dimethyl Terephthalate by Ethylene Glycol", *J. Phys. Chem.* **1959**, 63, 1206-1212.

Pilati, F.; Manaresi, P.; Fortunato, B.; Munari, A.; Passalacqua, V. "Formation of Poly(butylene terephthalate): Growing Reactions Studied by Model Molecules", *Polymer* **1981**, 22, 799-803.

Pilati, F.; Manaresi, P.; Fortunato, B.; Munari, A.; Passalacqua, V. "Formation of Poly(butylene terephthalate): Secondary Reactions Studied by Model Molecules", *Polymer* **1981**, 22, 1566-1570.

Pilati, F.; Manaresi, P.; Fortunato, B.; Munari, A.; Passalacqua, V. "Formation of Poly(butylene terephthalate): Growing Reactions Studied by Model Molecules", *Polymer* **1981**, 22, 799-803.

Pilati, F.; Marianucci, E.; Berti, C. "Study of the Reactions Occurring During Mixing of Poly(ethylene Terephthalate) and Polycarbonate", J. *Appl. Polym. Sci.* **1985**, 30, 1267-1275.

Pilati, F.; Munari, A.; Manaresi, P.; Milani, G.; Bonora, V. "Linear and Branched Poly(Butylene Isophthalate): Synthesis and Molecular Characterization", *Eur. Polym. J.* **1987**, 23, 265-271.

Pohl, H.A. "Determination of Carboxyl End Groups in a Polyester, Polyethylene Terephthalate", *Analyt. Chem.* **1954**, 26, 1614-1616.

Pratt, G.J.; Smith, M.J.A. "The Dielectric Response of a Polycarbonate/ Poly(butylene terephthalate) Blend", *Polymer* **1989**, 30, 1113-1116.

Reimschuessel, H.K. "Poly(ethylene terephthalate) Formation, Mechanistic and Kinetic Aspects of the Direct Esterification Process", *Ind. Chem. Res. Dev.* **1980**, 19, 117-125.

Ritchie, P.D. "Studies in Pyrolysis. Part III. The Pyrolysis of Carbonic and Sulphurous Esters", J. *Chem. Soc.* **1935**, 1054-1061.

Robeson, L.M. "Phase Behavior of Polyarylate Blends" J. *Appl. Polym. Sci.* **1985**, 30, 4081-4098.

Scott, R.L.; Magat, M. "The Thermodynamics of High-Polymer Solutions: I. The Free Energy of Mixing of Solvents and Polymers of Heterogeneous Distribution", *J. Chem. Phys.* **1945**, 13, 172-177.

Scott, R.L.; "The Thermodynamics of High-Polymer Solutions: V. Phase Equilibria in the Ternary System: Polymer 1-Polymer 2-Solvent", *J. Chem. Phys.* **1949**, 17, 279-284.

Shearer, D.A.; Morris, G.F. "Microdetermination of Fluorine in Organic Compounds with a Fluoride Ion Electrode Following an Oxygen Flask Combustion", *Microchem. J.* **1970**, 15, 199-204.

Shull, K.R.; Kramer, E.J. "Mean-Field Theory of Polymer Interfaces in the Presence of Block Copolymers", *Macromolecules* **1990**, 23, 4769-4779.

Sivaram, S.; Upadhyay, V.K.; Bhardwaj, I.S. "Synthesis, Characterization and Polycondensation of Bis-(4-Hydroxybutyl) Terephthalate", *Polym. Bull.* **1981**, 5, 159-166.

Smith, J.G; Kibler, C.J.; Sublett, B.J. "Preparation and Properties of Poly(methylene terephthalates), *J. Polym. Sci.: A-1* **1966**, 4, 1851-1859.

Sommers, E.E.; Crowell, T.I. "The Rate of Pyrolysis of Di-(2-ethylhexyl) sebacate", *J. Chem. Soc.* **1955**, 5443-5444.

Stokr, J.; Schneider, B.; Doskocilova, D.; Lovy, J.; Sedlacek, P. "Conformational Structure of Poly(ethylene terephthalate). Infra-red, Raman and N.M.R. Spectra", *Polymer* **1982**, 23, 714-721.

Streitwiesser Jr., A.; Heathcock, C.H. *Introduction to Organic Chemistry Second Edition*; Macmillian Publishing Co., Inc.: New York, 1981

Suzuki, T.; Tanaka, H.; Nishi, T. "Miscibility and Transesterification in Bisphenol A Polycarbonate/Poly(ethylene terephthalate) Blends", *Polymer* **1989**, 30, 1287-1297.

Tanaka, H; Hashimoto, T. "Stability Limits for Macro- and Microphase Transitions and Compatibilizing Effects in Mixtures of A-B Block Polymers with Corresponding Homopolymers", *Polym. Commun.* **1988**, 29, 212-216.

Tomita, K.; Hiroaki, I. "Studies on the Formation of Poly(ethylene terephthalate); 2. Rate of Transesterification of Dimethyl Terephthalate with Ethylene Glycol", *Polymer* **1973**, 14, 55-60.

Tomita, K.; Hiroaki, I. "Studies on the Formation of Poly(ethylene terephthalate); 3. Catalytic Activity of Metal Compounds in Transesterification of Dimethyl Terephthalate with Ethylene Glycol", *Polymer* **1975**, 16, 185-190.

Valero, M.; Iruin, J.J.; Espinosa, E.; Fernandez-Berridi, M.J. "N.M.R. Evidence of Interchange Reaction in a Polyarylate/Poly(butylene terephthalate) Blend", *Polym. Commun.* **1990**, 31, 127-129.

Van Krevelen, D.W. *Properties of Polymers Their Estimation and Correlation with Chemical Structure*; Elsevier/North Holland, Inc.: New York, 1972.

Velden, G.v.d, Kolfschoten-Smitsmans, G.; Veermans, A.; "^{13}C CP/MAS N.M.R., DRIFT, and ATR/FT I.R. Study of a Solid Polycarbonate Poly(butylene terephthalate) Blend: Evidence for Transesterification", *Polym. Commun.* **1987**, 28, 169-171.

Wang, L.H.; Huang, Z.; Hong, T.; Porter, R.S. "The Compatibility and Transesterification for Blends of Poly(ethylene terephthalate)/ Poly(bisphenol-A-carbonate)" *J. Macromol. Sci. Phys.* **1990**, B29, 155-169.

Wang, L.H.; Lu, M.; Yang, X.; Porter, R.S. "Thin Layer Chromatography of Copolyesters from Blends of Poly(ethylene terephthalate)/Polycarbonate", *J. Macromol. Sci. Phys.* **1990**, B29, 171-183.

Ward, I.M.; Wilding, M.A. "Infra-red and Raman Spectra of Poly(n-methylene terephthalate) Polymers", *Polymer* **1977**, 18, 327-335.

Warmund, D.C.; Paul, D.R.; Barlow, J.W. "Polyester-Polycarbonate Blends. I. Poly(butylene terephthalate", *J. Appl. Polym. Sci.* **1978**, 22, 2155-2164.

Whitmore, M.D.; Noolandi, J. "Theory of Block Copolymer-Homopolymer Blends: Suggested Measurements", *Polym. Commun.* **1985**, 26, 267-270.

Whitmore, M.D.; Noolandi, J. "Theory of Micelle Formation in Block Copolymer-Homopolymer Blends", *Macromolecules* **1985**, 18, 657-665.

Whitmore, M.D.; Noolandi, J. "Theory of Phase Equilibria in Block Copolymer Homopolymer Blends", *Macromolecules* **1985**, 18, 2486-2497.

Whitmore, M.D.; Noolandi, J. "Theory of Phase Equilibria in Block Copolymer-Homopolymer Mixtures", *Polym. Eng. Sci.* **1985**, 25, 1120-1121.

Wick, G.; Zeitler, H. "Cyclische Oligomere in Polyestern aus Diolen und Aromatischen Dicarbonsauren", *Die Angew. Macromol. Chem.* **1983**, 112, 59-94.

Yamadera, R.; Murano, M. "The Determination of Randomness in Copolyester by High Resolution Nuclear Magnetic Resonance", J. *Polym.: Part A-1* **1967**, 5, 2259-2268.

Young, R.J. *Introduction to Polymers*; Chapman and Hall, Ltd.: New York, 1981.

Yu, T.-Y.; Fu, S.-K.; J, C.-Y.; Cheng, W.-Z.; Xu, R.-Y. "Polycondensation Kinetics of Poly(ethylene terephthalate) and Poly(butylene terephthalate)", *Polymer* **1986**, 27, 1111-1114.

Yuan, L.; Williams, H.L. "A Dynamic-Mechanical Study of Polycarbonate Polyester Blends", *J. Appl. Polym. Sci.* **1990**, 40, 1891-1902.

Zimmerman, H.; Kim, N.T. "Investigations on Thermal and Hydrolytic Degradation of Poly(ethylene terephthalate)", *Polym. Eng. Sci.* **1980**, 20, 680-683.